Faculty of Sciences
Department of Analytical Chemistry

Characterisation and optimisation of mobile Raman spectroscopy for art analysis

Thesis submitted in fulfillment of the requirements for the
degree of Doctor of Science: Chemistry

By

Debbie Lauwers

Supervisor: Prof. Dr. Luc Moens
Co-supervisor: Prof. Dr. Peter Vandenabeele

January 26, 2017

Contents

Abbreviations and acronyms

MA-XRF	Macro X-ray fluorescence spectroscopy
IRR	Infrared reflectography
PIXE	particle-induced X-ray emission spectroscopy
XRF	X-ray fluorescence spectroscopy
XRD	X-ray diffraction spectroscopy
SEM	Scanning electron microscopy
TXRF	Total-reflection X-ray fluorescence spectroscopy
ICP-MS	Inductively coupled plasma mass spectrometry
AES	Atomic emission spectroscopy
STD	Standard
LWD	Long working distance
HiNA	High numerical aperture
CCD	Charge-coupled-device
SERS	Surface-enhanced Raman Spectroscopy
MArtA	Mobile Art Analyser
ASTM	American Society for Testing and Materials
LOD	Limit of detection
LOI	Limit of identification
SNR	Signal-to-noise ratio
μ-XRF	Micro X-ray fluorescence spectroscopy
hXRF	Handheld X-ray fluorescence spectroscopy
SDD	silicon-drift detector
f	Focal length

List of Tables

List of Figures

Chapter 1

Introduction and aims

In recent years, scientific research on art historical and archaeological objects for the interpretation of our cultural heritage has received much attention [1–3]. The study of these materials helps to support restoration/conservation processes and, at the same time, historical and visual examination can assist in the interpretation of scientific data. Close collaboration between multidisciplinary domains contributes in different ways to conservation studies as conservators need to assess and recover the damage that artworks have undergone during many years, due to exposure to different environments. This cooperation assists materially in deciding on treatment options and in the identification of materials and techniques (production processes) etc. [4,5].

The subject of this PhD thesis is directed towards this interdisciplinary context. It is part of a larger and unique project funded by the concerted research actions (GOA) program, called the Archaeometrical Study of the Ghent Altarpiece. This overall project comprises of members of different disciplines including art historians, conservators and scientists. The scientific studies performed by the Raman spectroscopy research group are strongly related to analytical chemistry/spectroscopy. Spectroscopic investigations deliver information about the composition of a historical sample. This type of research has an important role in the support of conservators or art historians who have sometimes the difficult job to date a piece of art and link an artist to it. Additionally, information can be obtained about old trading routes and the sociocultural and political interactions between societies.

The Raman spectroscopy research group contributes in different ways to the GOA project: (i) conservation study of the exposed silver foils of the frames; (ii) optimisation of XRF techniques for the study of oil paintings and (iii) optimisation of mobile Raman

spectroscopy for the study of art objects. The latter objective forms the core study of this PhD thesis.

1.1 Composition of paint

To completely understand the problems and research questions surrounding the history of art works, one needs to be informed about the basic principles of paint manufacturing. Fresh paint is a solution, suspension or colloid, and consists of 3 components: a colourant, a binder and a solvent [6–8]. The colour of paint is determined by the colourant, which can be a dye, pigment or lake. A dye is an animal or vegetable colour-providing substance that is soluble in the binding agent. It is often used in textile dyeing and its application in oil paintings is often limited due to its low refractive index and tendency to migrate [9]. Pigments, on the contrary, are not soluble and generally more stable, i.e. chemically inert. They are derived from a wide variety of sources: (i) naturally occurring minerals (such as e.g. cinnabar, lapis lazuli, azurite, malachite, and earths); (ii) synthetic pigments, manufactured by chemical processes (e.g. lead white, lead tin yellow); (iii) organic plant (e.g. indigo, carbon) and animal products (Kermes). The latter is a special case of a pigment source as it is obtained by precipitating a soluble dye upon a base substrate (i.e. a so-called lake) which is an usually insoluble, finely divided, inorganic inert substance such as aluminum hydrate or calcium sulphate [10,11].

To be able to dissolve or suspend the colourant, a combination of a binder and a solvent is used. This solvent must possess the appropriate viscosity and the ability to evaporate during drying [12]. Sometimes, it acts also as a thinner for the binder [6]. The binder is an organic material that is responsible for the good attachment of the colourant on the support. After application, the chemical drying process (curing) can commence, such as crosslinking by oxidation of a polymer network [13,14]. Different types of binding medium exist, such as drying oil, egg yolk, egg white, gum, etc. [15].

1.2 Structure of painted objects

Through history, many artists have used paint as a medium for expressing their ideas which can be practiced in different application methods on a range of substrates. For instance, wall paintings can be constructed with several techniques such as *fresco* and *secco* [16]. During the *fresco* technique, paint is applied on a wet background. In contrast, the *secco* technique involves painting onto a dry substrate. Whereas wall paintings are an important part of painted cultural heritage, illuminated manuscripts are intrinsically objects. Manuscripts were mainly produced in the Middle Ages where parchment, and in later stages paper, was used as a support [17,18]. The illuminations in manuscripts are generally characterised by a simple multilayered structure of the paint decoration.
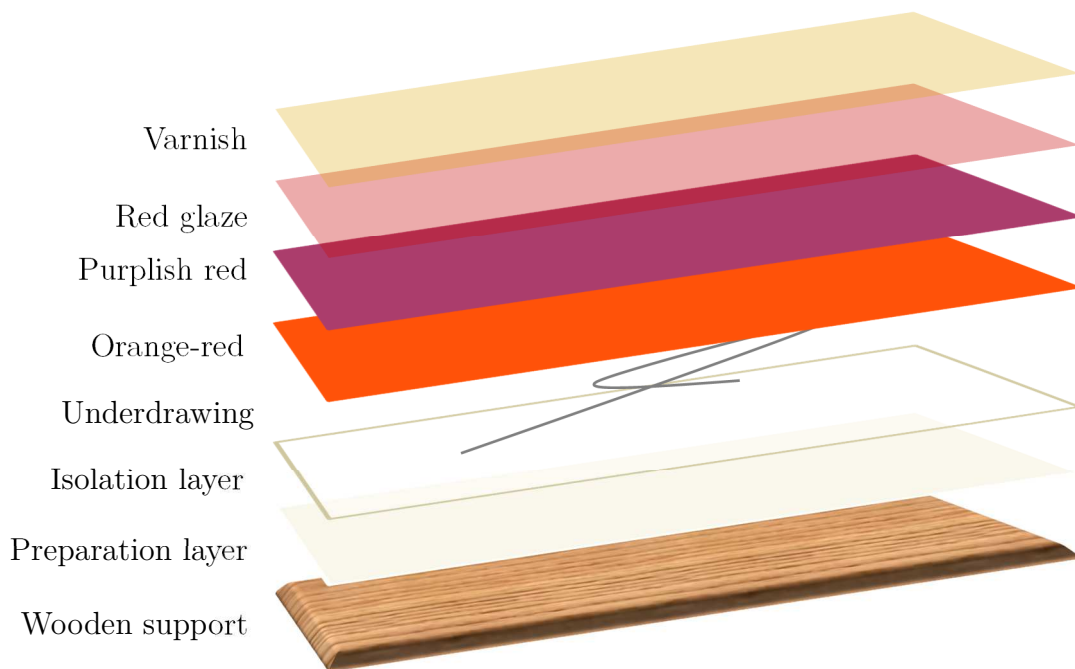
Figure 1.1 Stratigraphy of an oil painting on wooden support, based on a cross section from the Ghent Altarpiece, panel IV - Deity Enthroned, red mantle [20].

The stratigraphy of an easel painting, however, is much more complex [19]. A complete description of the painting materials and techniques is beyond the scope of this work. So here, a general description is given of the stratigraphy. The support of an oil

painting can be canvas or wooden panels. In this thesis, only oil paintings with wooden supports will be analysed and their composition is illustrated in Figure 1.1, based on a cross-section from the Ghent Altarpiece panel IV - Deity Enthroned, red mantle [20]. Traditionally, the wooden support is covered with a preparation layer, which is a mixture of animal glue with pigment, often gypsum or calcite. This layer is coated with an extra layer, the *imprimatura*, which reduces the permeability of the ground layer. This serves as an isolation layer and provides an overall homogeneous, optical effect in the painting. Then an underdrawing (employing charcoal, metal point, ink, etc.) is applied, followed by superimposed paint layers. The pictural layers are painted witth varying degrees of transparency. Different thin layers of glaze create subtle changes or small nuances in tone, such as shadow representations [21]. A glaze is a paint that is diluted with extra binder, giving a translucent effect. The oil painting is finished with a varnish layer, which has both a protective and aesthetic purpose.

1.3 The analysis of art objects

Preservation of cultural heritage is an important aspect in modern society as it reflects the culture and history of the past and present. Cultural objects are composed of a wide variety of materials and are of different sizes ranging from historical sites, to monuments, and to samples of fine craft or art. Their conservation is mainly dependent on the materials of which they are composed.

Application of scientific research to artworks dates back to the 18th century, when in 1888 the first specialised laboratory, namely the *Chemical Laboratory of the Royal Museums of Berlin*, dedicated to scientific examination of cultural goods was established [22]. Currently, scientific disciplines play an essential role in the material characterisation of art objects. The analytical approach can be considered two-fold: the focus can be on material identification or on diagnostic analysis [22–24]. Material identification gives information about the artistic techniques and production techniques, which can be related to provenance, authentication and dating. So, analytical data provide useful information concerning the object's history, conservation and restoration conditions.

Cultural goods are unique and often irreplaceable, and as such, they deserve to be preserved as intact as possible. This imposes restrictions for applying analytical techniques. An analytical analysis can be divided into 4 steps: sampling, sample preparation, selection of the analytical method and data processing [22]. The first step is to determine the sampling strategy of which location of sampling, sampling method, number and size of the samples are important parameters. In general, research methods can be divided into direct techniques and analysis including sampling procedures [25–28]. The investigation of the entire object is the most desirable approach. In this case, sampling is not needed so the object can stay intact. Direct investigation of art objects is assumed to be non-destructive and does not require sampling. However, it has the disadvantage that either the analytical equipment or piece of art has to be transported. Direct approaches can be divided into imaging methods, point analyses and surface techniques. Unfortunately, direct analysis is not always possible or is deemed to be not the best approach to apply. The method of approach is dependent upon the research question: if for example information about stratigraphy or in-depth knowledge has to be obtained, the art object should be sampled. When sampling is needed, it should be kept to a minimum and the locations and number of samples should be well-planned. Reedy and Reedy [29] propose four possible sampling strategies for the analysis of a single art object: (i) take randomly located samples to estimate the composition of the entire object; (ii) perform sampling at regular intervals across an object; (iii) select positions which are restricted by aesthetic and preservation reasons and (iv) intentionally choose areas to gain information about specific alterations or the characterisation of the artist's palette. These strategies all have a risk of obtaining biased results and are not totally representative for the total object. Techniques for which sampling is requested, can be divided into destructive and non-destructive methods. An overview of the different approaches, including several important analytical techniques in archaeometry, is given in Table 1.1.

Analytical methods can deliver molecular (e.g. XRD, Raman spectroscopy) or elemental information (e.g. XRF, PIXE, SEM) and can be executed in a qualitative or quantitative manner. Qualitative techniques determine whether or not a compound or element is present. In many cases, this approach is sufficient to answer the conservator's

question. Sometimes, a more extensive investigation is required which can be supported by quantitative analysis. An estimation is made of the concentration of components or elements and is often applied in, for example, provenance studies, dating purposes or for the development of conservation strategies for storage condition [30,31].

Table 1.1 Several important analytical techniques for the analysis of art objects. This overview is just a selection of methods; more techniques exist on the market [25–28].

Direct analytical methods	Imaging	Infrared reflectography (IRR)
		X-ray radiography
		Raking light photography
		High resolution microscopy
	Point analysis	*In situ* particle-induced X-ray emission spectroscopy (PIXE)
		In situ X-ray fluorescence spectroscopy (XRF)
		Direct Raman spectroscopy
		Portable X-ray diffraction (pXRD)
Methods after sampling and, when needed, sample preparation	Non-destructive	Micro-Raman spectroscopy
		Micro-X-ray fluorescence spectroscopy (μ-XRF)
		Scanning electron microscopy (SEM)
		Total-reflection X-ray fluorescence spectroscopy (TXRF)
		X-ray diffraction (XRD)
	Destructive	Separation methods (e.g. High-performance liquid chromatography)
		Inductively coupled plasma mass spectrometry (ICP-MS)
		Atomic absorption spectroscopy (AAS)

A broad range of analytical techniques for art analysis is available on the commercial market. The ideal method for the examination of ancient artefacts is dependent upon the research question and needs to fulfil several requirements: it is preferable to apply a technique ideally that is sensitive, fast, non-destructive, universal, non-intrusive and, if possible, mobile. Hence, it is impossible to meet all these demands for one specific analytical technique. Therefore, to characterise analytically cultural artefact as completely as possible, multiple methods are preferred [24,32,33].

The Raman research group (Ghent University) mainly specialises in Raman spectroscopy and XRF. Both methods are valuable techniques for art analysis because they fulfil almost all conditions mentioned above. As the demand for mobile, non-destructive methods in art analysis is increasing, this provides the focal point for the current PhD research.

It is, however, noteworthy that XRF is not the only complementary method that is used alongside Raman spectroscopy in art analysis. Several other non-invasive methods exist such as optical microscopy, XRD, fibre optic reflectance spectroscopy (FORS), SEM-EDS and imaging micro-FTIR spectroscopy. Often as a first approach, macro photography and optical microscopy are used to observe the region of interest in order to understand the potential analytical problems [34]. These observations can help in deciding which complementary techniques can be of use. If sampling is not allowed, *in situ*, molecular methods like FORS and p-XRD are suitable techniques to use, along with Raman spectroscopy, as not every molecule is Raman active. FORS is user friendly, yet, it is difficult to interpret as a reflectance spectrum is influenced by the reflectivity, roughness and composition of the materials [35]. p-XRD, on the other hand, can give additional information to the Raman results as in Raman spectroscopy no distinction can be made between different crystalline phases of a molecular structure. Notwithstanding this, the positioning and the penetrating character of X-rays cause some difficulties during the measurements.

When no restrictions concerning sampling need to be taken into account, techniques such as SEM-EDS and imaging micro-FTIR can be used in addition. Using SEM-EDS, information on the morphology (for example, to investigate alterations or degradation), with high magnification, and the elemental distribution is obtained. Unfortunately, measurements are expensive and samples need to be coated to increase the conductivity [36]. It is well-known that FTIR is a good complementary technique to Raman spectroscopy. Imaging micro-FTIR is an ideal tool to represent the molecular distribution in a sample of products which are not Raman active or which are masked by interferences (i.e. fluorescence, absorption).

1.4 Goals and outline

As described above, many analytical techniques exist for the investigation of cultural heritage. In this work, we concentrate on the application of mobile Raman spectroscopy for the investigation of art objects. The main aim is to explore the possibilities of a new mobile Raman spectrometer, the EZRaman-I-Dual Raman system (TSI Inc., Irvine CA, USA) in these applications. As a starting point, an approach is developed to evaluate the quality and applicability of mobile Raman instrumentation in archaeometry, which is illustrated by demonstrating it using the EZRaman-I-Dual Raman system. Furthermore, it is necessary to demonstrate the improvements in mobile Raman spectroscopy and their application for art analysis, compatible with the increasing use of Raman spectroscopy in this field. The theoretical background of Raman spectroscopy and X-ray fluorescence spectroscopy, required to understand the different approaches in this thesis is described in Chapter 2.

In the first step of this study, the aspects which need to be considered when selecting a mobile Raman spectrometer for *in situ* art analysis are discussed. Chapter 3 provides an approach to evaluate these parameters and to apply this to the commercially available Raman instrument discussed. This involves a twofold characterisation that includes the investigation of spectroscopic characteristics and the evaluation of specific properties that are useful for mobile studies in archaeometry. The research is completed with field tests by studying the pigments used in a mediaeval wall painting. In the subsequent chapters, the spectrometer's beneficial use for different art applications is illustrated.

Among the objects studied, pigments are very attractive targets for scientific analysis, because of their coloured appearance. Analysis can provide information about the artist's palette and reveal information about the painter's technique. Chapter 4 illustrates the possibilities of the mobile Raman spectrometer for pigment analysis based on the investigation of an important mediaeval manuscript, *De Civitate Dei* (from the Cultural Heritage Library in Bruges, Belgium). By reason of their simple composition, mediaeval handwriting is ideal objects for the demonstration of the capabilities of the

instrument. This includes the description of its essential characteristics: the availability of two lasers and performance of the equipment.

As pigment analysis is not the only application of Raman spectroscopy in archaeometry, the benefit of two excitation sources is also shown by the investigation of a set of glyptics (chapter 5) belonging to the collection of the museum 'Quinta das Cruzes' in Funchal (Madeira, Portugal). Thus far, a single method, Raman spectroscopy, has been applied. But often, the use of several complementary techniques results in a more complete documentation of the object. Therefore, chapter 5 also demonstrates the advantage of the complementary use of Raman spectroscopy and X-ray fluorescence spectroscopy for this type of sample. Additionally, the gemmological identification is confirmed and extra information about the glass composition is provided.

Chapters 4 and 5 illustrate the excellent performance of the chosen Raman spectrometer in these studies. However, this instrument is not the only one available on the market. Chapter 6 describes the comparison between the EZRaman-I-Dual Raman system (785 and 532 nm laser) and an i-Raman® EX (1064 nm) to evaluate if our chosen equipment was a good choice out of the broad selection of the many commercially available Raman spectrometers. For this research, the mediaeval wall paintings from Sala Vaccarini are used as a case. It is shown that both mobile Raman spectrometers are useful for pigment analysis. However, the EZRaman-I-Dual Raman system is preferred when inorganic compounds need to be investigated due to the low Raman wavenumber detection range (down to 100 cm^{-1}).

Up to this point, painted materials with a simple paint structure (manuscripts, wall paintings) have been examined. Oil paintings are more complex in structure, which makes *in situ* measurements more complicated. Therefore, chapter 7 is concerned with the optimisation of the examination of mediaeval oil paintings towards *in situ* investigation. The opportunity was given to upgrade the use of *in situ* XRF and Raman spectroscopy based on the analysis of the Ghent Altarpiece, a magnificent piece of art, created by Jan and Hubert Van Eyck. As a result, it was possible to support the restoration campaign

by introducing Hirox microscopy investigations for the selection of the regions of interest prior to the spectroscopic analysis.

Even though the approaches were successful, the application of mobile Raman spectroscopy can still be improved. Because, only point measurements were performed, causing the method to fail in the reconstruction of the chemical distribution of particular compounds. Chapter 8 discusses a first step towards a chemical imaging concept for *in situ* Raman spectroscopy. Challenges of the development are explained with its focus mainly on the data-treatment, which is important for the creation of a Raman map. Also hard- and software modifications were considered, as a suitable set-up and software are essential for the development of an *in situ* Raman mapping system.

A second improvement can be made towards an optimal, mobile Raman mapping system. Chapter 9 explains the first steps towards the direct coupling of a microscopic image with the molecular image. A methodology was devised for the combination of the Hirox microscope with the mobile Raman spectrometer for the successful recording of reasonable Raman spectra.

Finally, the results obtained throughout this work are summarized in chapters 10 (Eng) and 11 (NL), along with the conclusions and future perspectives.

1.5 References

[1] I. Nakai, Y. Abe, Portable X-ray powder diffractometer for the analysis of art and archaeological materials, Appl. Phys. A. 106 (2011) 279–293. doi:10.1007/s00339-011-6694-4.

[2] A. Deneckere, B. Vekemans, L. Van de Voorde, P. Paepe, L. Vincze, L. Moens, et al., Feasibility study of the application of micro-Raman imaging as complement to micro-XRF imaging, Appl. Phys. A. 106 (2011) 363–376. doi:10.1007/s00339-011-6693-5.

[3] K. Fukunaga, I. Hosako, Y. Kohdzuma, T. Koezuka, M.-J. Kim, T. Ikari, et al., Terahertz analysis of an East Asian historical mural painting, J. Eur. Opt. Soc. Rapid Publ. 5 (2010) 1–4. doi:10.2971/jeos.2010.10024.

[4] C. Vazquez-Calvo, S. Martinez-Ramirez, M.A. de Buergo, R. Fort, The Use of Portable Raman Spectroscopy to Identify Conservation Treatments Applied to Heritage Stone, Spectrosc. Lett. 45 (2012) 146–150. doi:10.1080/00387010.2011.627526.

[5] J.-F. Huang, Data and interpretation: enhancing conservation of art and cultural heritage through collaboration between scientist, conservator, and art historian., IOP Conf. Ser. Mater. Sci. Eng. 37 (2012) 1–7. doi:10.1088/1757-899X/37/1/012003.

[6] F.A. Henglein, Chemcial technology, Pergamon press, Oxford, 1989.

[7] R. Hughes, Painting and decorating: Basic coatings, Routledge, 2005.

[8] H.V. Orna, T. Pamer, Artists' colors, in: B. Elvers, J.F. Rounsaville, G. Schulz (Eds.), Ullmann's Encycl. Ind. Chem., 3th editio, VCH Verlagsgesellschaft, Weinheim, 1990.

[9] G. Booth, H. Zollinger, K. McLaren, W.G. Sharpless, A. Westfell, Dyes, general survey, in: J.F. Rounsaville, G. Schulz (Eds.), Ullmann's Emcyclopedia Ind. Chem., 3th edition, VCH Verlagsgesellschaft, Weinheim, 1990.

[10] A. Albus, The art of arts: Rediscovering painting, Alfred A. Knopf, New York, 2000.

[11] P. Ball, Bright earth: The invention of colour, Pengiun, London, 2001.

[12] G.W.R. Ward, The Grove Encyclopedia of Materials and Techniques in Art, Oxford university press, 2008.

[13] B.R. Greenberg, D. Patterson, Art in chemistry; chemistry in art (second edition), Techers ideas press, 2009.

[14] S. Higuchi, T. Hamada, Y. Gohshi, Examination of the Photochemical Curing and Degradation of Oil Paints by Laser Raman Spectroscopy, Appl. Spectrosc. 51 (1997) 1218–1223.

[15] D.V. Thompson, The materials and techniques of medieval painting, Dover Publications, Inc., New York, 1956.

[16] R.J. Gettens, G.L. Stout, Painting materials: A short encyclopaedia, Dover Publications, Inc., New York, 1966.

[17] R. Clemens, T. Graham, Introduction to manuscript studies, Cornell University Press, 2007.

[18] C. De Hamel, Medieval craftsmen - Scribes and illuminators, British Museum Press, London, 1992.

[19] K. Nicolaus, Handbuch der Gemälderestaurierung, Könemann, 2001.

[20] P. Coremans, Les Primitifs Flamands: III. Contributions a L'etude Des Primitifs Flamands, No. 2: L'Agneau Mystique Au Laboratoire, Examen et Traitemant, De Sikkel, 1953.

[21] P. Vandenabeele, L. Moens, Overview: Raman spectroscopy of pigments and dyes, in: H.G.M. Edwards, J.M. Chalmers (Eds.), Raman Spectrosc. Archaeol. Art Hist., The Royal Society of Chemistry, 2005.

[22] A. Domenech-Carbo, M.T. Domenech-Carbo, V. Costa, Application of Instrumental Methods in the Analysis of Historic, Artistic and archaeological objects, in: Electrochem. Methods Archaeom. Conserv. Restor., Springer-Verlag Berlin Heidelberg, 2009: pp. 1–32. doi:10.1007/978-3-540-92868-3_1.

[23] K. Janssens, G. Vittiglio, I. Deraedt, A. Aerts, B. Vekemans, L. Vincze, et al., Use of microscopic XRF for non-destructive analysis in art and archaeometry, X-Ray Spectrom. 29 (2000) 73–91.

[24] K. Janssens, R. Van Grieken, Non-destructive micro analysis of cultural heritage materials, Elsevier, 2004.

[25] F. Settle, ed., Handbook of instrumental techniques for analytical chemistry, Prentice-Hall, Inc., New Jersey, 1997.

[26] E.A. Varella, ed., Conservation science for the cutural heritage: Applications of instrumental analysis, Springer-Verlag Berlin Heidelberg, 2013. doi:10.1007/978-3-642-30985-4.

[27] I.N.M. Wainwright, Examination of paintings by physical and chemical methods, in: B.A. Ramsay-Jolicoeur, I.N.W. Wainwright (Eds.), Shar. Responsib. Proc. a Semin. Curators Conserv., Ottawa, 1990: pp. 79–102.

[28] M.W. Alfeld, Development of scanning macro-XRF, University of Antwerp and University of Hamburg, 2013.

[29] T.J. Reedy, C.L. Reedy, Statistical Analysis in Art Conservation Research, The Getty conservation institute, USA, 1988.

[30] M. Pollard, C. Batt, B. Stern, S.M.M. Young, Analytical chemistry in archaeology, Cambridge University Press, 2007.

[31] M. Montagnari Kokelj, M. Budinich, C. Tuniz, eds., science for cultural heritage: technological innovation and case studies in marine and land archaeology in the Adriatic region and inland, World Scientific Publishing Co. Pte. Ltd., 2010.

[32] M.L. Young, Archaeometallurgy using synchrotron radiation: a review, Reports Prog. Phys. 75 (2012) 036504. doi:10.1088/0034-4885/75/3/036504.

[33] C. Lahanier, G. Amsel, C. Heitz, M. Menu, H.H. Andersen, International workshop devoted to ion beam analysis in the arts and archeology, Nucl. Instruments Methods B. 14 (1986) 1–168.

[34] H.G.M. Edwards and J.M. Chalmers, Raman spectroscopy in archaeology and Art history, Royal Society of Chemistry, 2005.

[35] R. Ploeger, O. Chiantore, D. Scalarone, T. Poli, Appl. Spectrosc. 65 (4) (2011) 429-435. doi: 10.1366/10-06059.

[36] H.G.M. Edwards and P. Vandenabeele, analytical Archaeometry: selected topics, Royal Society of Chemistry, 2012.

Chapter 2

Analytical techniques

This chapter presents briefly some theoretical aspects of Raman spectroscopy and X-ray fluorescence spectroscopy. The theoretical backgrounds are discussed along with the instrumental properties of the applied Raman spectrometer.

2.1 Raman spectroscopy: theory

2.1.1. Introduction

Vibrational spectroscopy is the general term that covers Raman spectroscopy and infrared (IR) spectroscopy. These methods are often applied for vibrational studies of molecules present on the surface of art objects [1]. Molecular vibrations are measured either by the absorption of radiation (IR spectroscopy) or by the inelastic scattering of photons (Raman spectroscopy) [2]. In order for a vibration to be infrared active the molecular dipole moment must vary during the vibration. The Raman effect occurs when there is a change in polarizability. Because some vibrations can be active in the Raman but inactive in infrared (and vice versa), these techniques can be used in a complementary way [3]. Moreover, since IR spectroscopy is more sensitive to functional groups and asymmetric, polar bonds Raman spectroscopy can be very useful in determining backbone structures and symmetric, electron rich moieties [4].

In this thesis, we shall concentrate on the application of Raman spectroscopy for art analysis. Raman spectroscopy is a non-destructive spectroscopic technique that is used to study low-frequency modes in a system. The Raman effect was discovered by Sir C.V. Raman in 1928 and ever since the technique has been widely developed and has

many applications, for example in archaeometry (e.g. pigment identification), solid state physics, and in the detection of counterfeit drugs, etc. [5-7].

Here, a brief introduction to Raman spectroscopy is given. For a more in-depth study of the Raman effect, we refer to the literature [8-12].

2.1.2. The Raman effect

In a classical approach, the fundamental condition for the Raman effect to occur is described by a change in polarizability. This reflects how easy an electron cloud of a molecule can be distorted by an electric field [1].
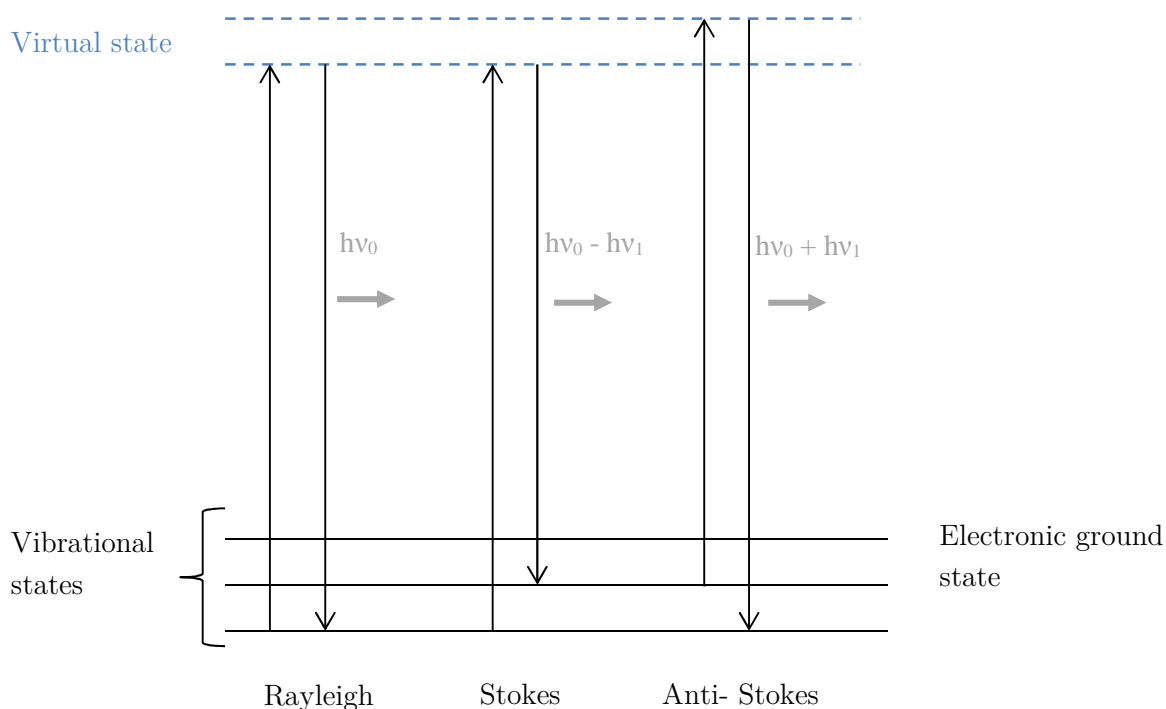
Figure 2.1 Energy level diagram that illustrates the origin of Rayleigh and Raman Scattering (Stokes and Anti-Stokes scattering).

The Raman effect can also be explained as a light scattering phenomenon in which the mechanism can be described in terms of energy transfer between monochromatic incident radiation (laser) and the scattering molecules. The energy level diagram of Figure 2.1 provides a qualitative view of the origin of Rayleigh and Raman scattering [3].

One can consider that before the incident radiation interacts with the sample, the molecule is found in the ground state (E_0). When the radiation with an energy $h\nu_0$ (with h, Planck's constant and ν_0, the frequency of the incident monochromatic radiation) interacts with a molecule, the molecule can be excited to a virtual state. This situation is not stable and relaxes with the emission of a photon. Three different scattering processes can occur:

1) More than 99% of the incident photons undergo Rayleigh scattering (i.e. an elastic effect). In this case, a photon excites the molecule from the vibrational ground state to a virtual state, which in his turn relaxes back to the vibrational ground state, releasing a photon with the same energy as the incident beam.

2) If the scattered photon has a different energy in comparison with the incident beam, the collision is said to be inelastic (there is an energy transfer between the molecule and the photon) and this is called Raman scattering. Given this case, there are two possible phenomena:

- If the molecule is promoted from the vibrational ground state to a virtual state, but relaxes to the first excited vibrational state, we can talk about Stokes Raman scattering. In this case the emitted photon has a lower energy than the incident photon.
- If the molecule is transferred from the first vibrational excited state to the virtual state and relaxes to the ground state, then the scattered photon has more energy than the initial monochromatic light. This process is known as Anti-Stokes Raman scattering.

2.1.3. The Raman spectrum

Raman spectroscopy is based on focusing an intense, monochromatic electromagnetic beam on a sample. After interaction, the intensity of the scattered radiation is measured as a function of the frequency. A Raman spectrum plots these intensities against the corresponding Raman wavenumbers (expressed in cm^{-1}) which represent the frequency difference between the scattered and incoming radiation. The

most intense band detected at 0 cm^{-1} is related to the inelastic scattering, the Rayleigh scattering. In many Raman spectrometers, this signal is suppressed using a holographic filter. Additionally, a Raman spectrum consists of inelastic scattering: Stokes and Anti-Stokes lines. Raman bands are observed at positive and negative Raman wavenumbers, respectively, and have a symmetric pattern around 0 cm^{-1}. According to the Boltzmann distribution, the number of molecules at thermal equilibrium in a lower vibrational state is always higher than those in a higher vibrational state. Therefore, the Stokes intensity is usually higher than the Anti-Stokes intensity and is thus only represented in a Raman spectrum.

2.1.4. Advantages and disadvantages

Raman spectroscopy has several advantageous properties: it is a non-destructive technique, there is almost no sample preparation needed, it is a relatively fast method and *in situ* measurements can be performed. Nevertheless, Raman spectroscopy is not a perfect technique and has some disadvantages as well. Absorption (i.e. reduction of the intensity of the scattering) and fluorescence are the two most important interferences that can occur [8]. Because the Raman effect is very weak, these phenomena interfere and cause a decrease in the quality of the Raman spectrum. In this work, Raman spectra are often presented after baseline correction: a polynomial is manually fitted to the spectra, and then substracted to eliminate the fluorescence background.

2.2 Raman mapping and imaging

In this thesis, an attempt will be made to improve *in situ* Raman spectroscopy towards an *in situ* Raman mapping system. It is important to understand the fundamentals of this method in order to follow the development phases. The principle of Raman mapping is quite simple: the laser spot is stepwise moved relative to the sample over a defined region. At every position, a full Raman spectrum is recorded. Afterwards a map is created, based on the stored spectra with specific coordinates [11].

This is not the only option to create a chemical image in Raman spectroscopy, as imaging exists. The main difference with Raman mapping lies in the way a chemical image is obtained. A larger area is illuminated with a defocused beam and, in its turn, the scattered radiation is filtered to image a specific Raman band. Typically a liquid crystal tunable filter is used which has a spatial resolution of 250 nm and spectral resolution of ~ 7 cm^{-1} [13]. Raman imaging is a fast method but due to its low spectral resolution, it is difficult to discriminate between single Raman bands. In addition, during an imaging experiment no discrimination is made between characteristic Raman signals and fluorescence photons with a similar wavelength. Moreover, the focus only relies on the detection of one compound whereas for Raman mapping one must decide what parameter to map such as intensity ratios, band positions, bandwidths, etc. Due to these limitations, Raman mapping is preferred.

2.3 Raman instrumentation

All measurements in this PhD thesis were performed using a new portable EZRaman-I-Dual Raman system (TSI Inc., Irvine CA, USA). The fiber-optic-based spectrometer is equipped with two lasers, a red diode laser (785 nm) and a green Nd:YAG laser (532 nm). For each wavelength there are three interchangeable lenses: a standard lens (STD), a long working distance lens (LWD) and a high numerical aperture lens (HiNA). The Raman spectrometer is also equipped with an adjustable power controller for each laser (maximum output power 400 mW and 100 mW for 785 nm and 532 nm laser, respectively) and has a Charge-Coupled-Device (CCD) detector. Depending upon the selected laser, a different grating is used in the spectrometer and hence a different spectral range is obtained. When using the 785 nm laser the signals are recorded between 100 and 2350 cm^{-1}, while, when using the green 532 nm laser, the spectral range lies between 100 and 3200 cm^{-1}. Consequently, the spectral resolutions are different, namely 6 or 7 cm^{-1}, for the 785 and 532 nm lasers, respectively (as reported by the manufacturer). The spectrometer can be powered by using 230 V AC or by using an internal or external Li-battery, allowing for larger autonomy of usage. A schematic overview of the internal composition of the portable Raman spectrometer is given in Figure 2.2.
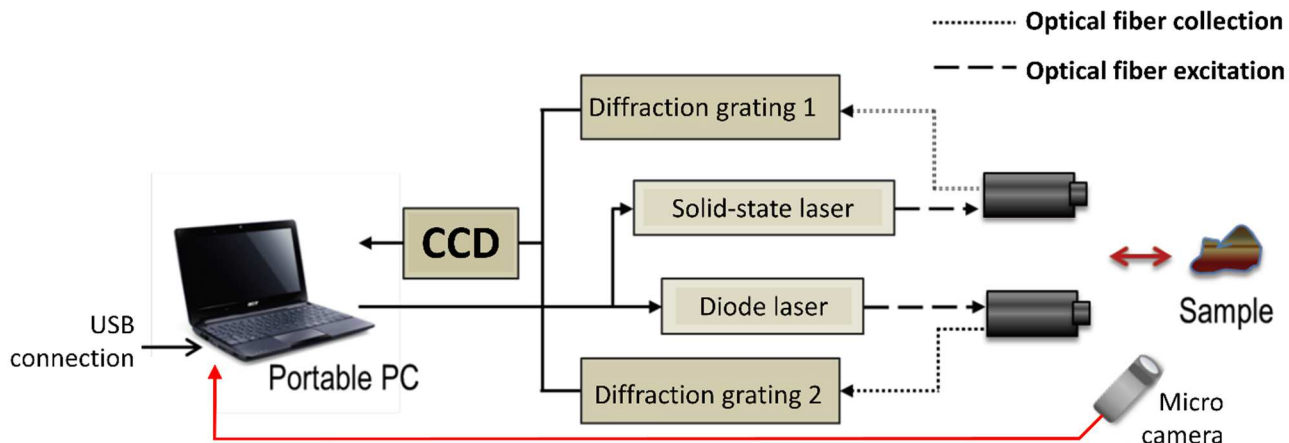
Figure 2.2 Schematic overview of the composition of the portable EZRAMAN-I-DUAL Raman spectrometer.

2.4 X-ray fluorescence spectroscopy

2.4.1. Introduction

X-rays were discovered by Wilhelm Conrad Röntgen in 1895, during his experiments with Crookes tubes (discharge tubes), observing a green glow that was emitted by a fluorescent screen painted with $BaPt(CN)_4$, positioned close to an operational tube. X-ray fluorescence spectroscopy is applied in many archaeometrical studies due to its non-destructive character. Via this method qualitative and semi-quantitative information on the elemental composition of materials of which art objects are made can be obtained. The basic principle of this technique relies on the detection of induced X-rays with a wavelength between 0.01 and 10 nm which corresponds to an energy range of approximately 0.1 to 100 keV [14]. The penetrating property of X-rays is dependent on their energy: high energy X-rays have a larger penetration depth than low energy X-rays.

In general, when an incident X-ray photon interacts with a sample, three main phenomena can occur: Rayleigh scattering, Compton scattering and the photoelectric effect. [15] These interactions are explained in the next section.

2.4.2. Interaction of X-rays

Two types of X-ray photon scattering can occur: Rayleigh and Compton scattering. Rayleigh scattering, also known as elastic scattering, is an interaction where no energy exchange occurs (**Figure** *2.3*). The scattering is a result of the interaction between an incoming photon and a tightly bound inner shell electron.[16-18] Compton scattering, on the other hand, is a type of inelastic scattering (**Figure** *2.3*). During this effect, an incoming X-ray interacts with a loosely bound atomic electron. Part of the photon energy is transferred to the bounded electron and is ejected in its turn with a kinetic energy equal to the energy difference between the incoming and scattered X-ray beam [19]. This energy difference depends on the scattering angle (θ) and is defined by the Compton equation (Equation (1)): larger scattering angles cause larger shifts in the energy of the Compton scattered photons.

$$E_{compton} = \frac{E_0}{1 + \frac{E_0}{m_e c^2}(1 - \cos\theta)} \tag{1}$$

With E_0: the energy of the initial photon; m_e the mass of the electron; c: the speed of light.

Next to these scattering interactions a third and the most important phenomenon can occur, called the photoelectric effect. **Figure** *2.4* illustrates the basic principle of the effect: an incoming X-ray is fully absorbed by the atom and causes the ejection of an electron of the inner shell. This vacancy is subsequently filled with an electron from one of the higher shells. This transition releases energy by the emission of a secondary photon that is characteristic for every element. It is noteworthy that this interaction is in competition with the Auger effect, which has a higher probability to occur with lower Z elements.
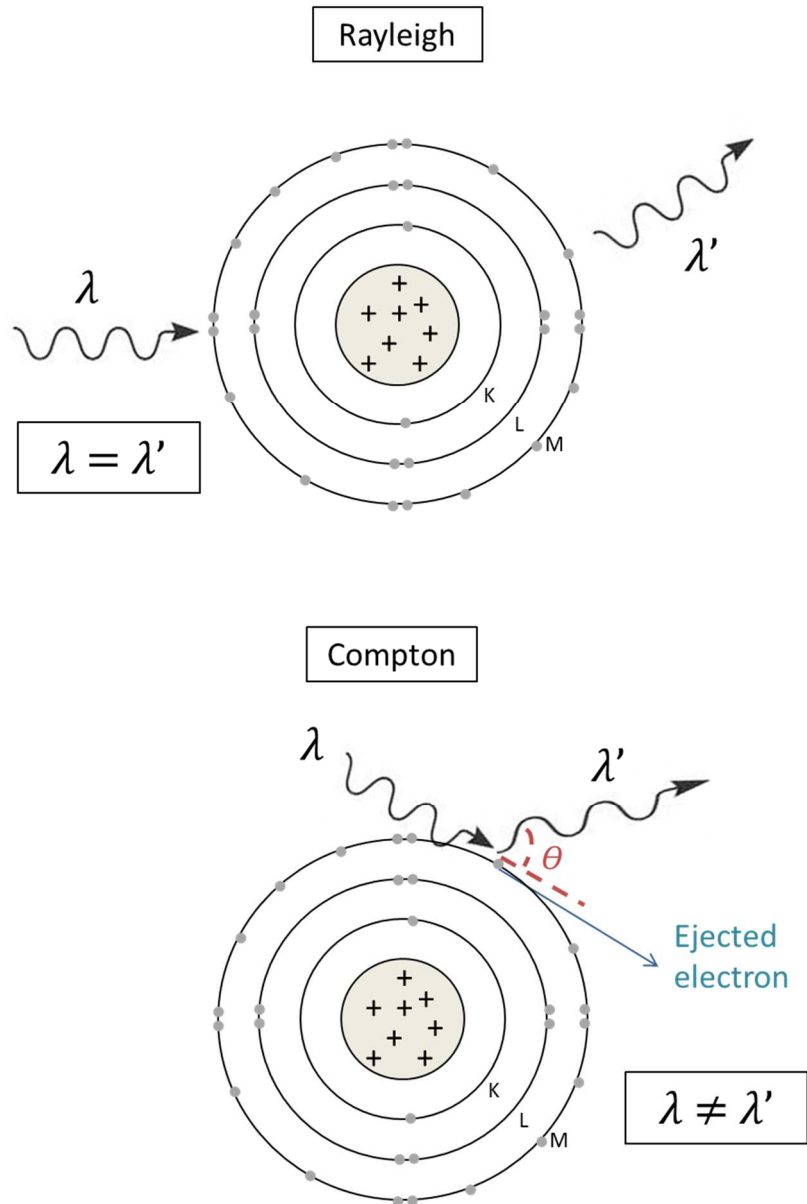
Figure 2.3. Schematic overview of the two types of X-ray photon scattering: Rayleigh (top) and Compton (bottom) scattering; with λ= initial wavelength, λ'= emitted wavelength, and θ = scattered angle.
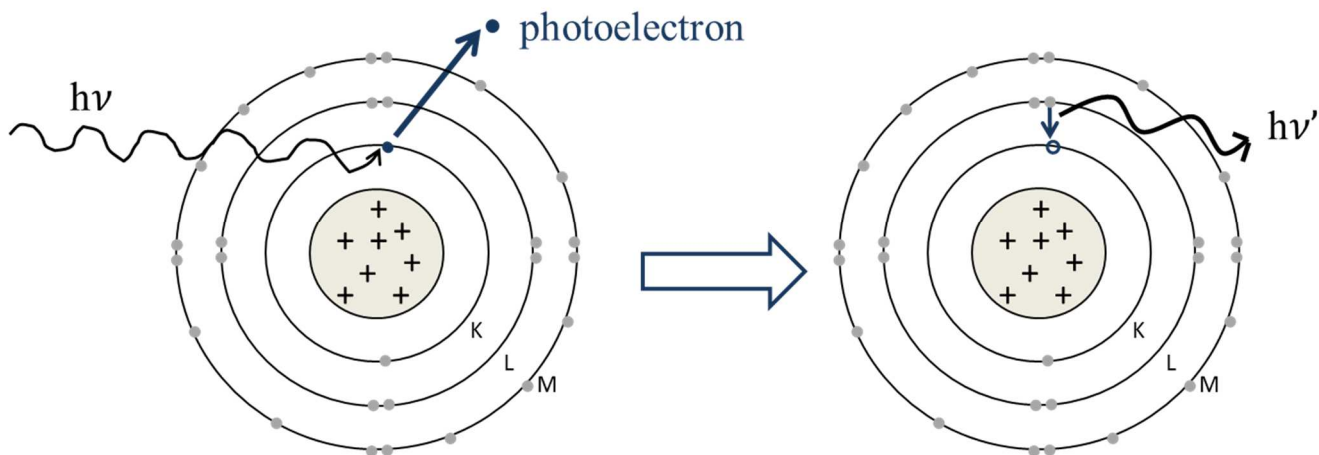
Figure 2.4 The photoelectric effect with hν, the energy emitted by the source and hν' the energy of the secondary X-ray.

2.4.3. The X-ray spectrum

In X-ray fluorescence spectra, different contributions can be distinguished. Every spectrum is defined by a continuous background signal, i.e. Bremsstrahlung (Figure 2.5). The continuum X-rays are produced when electrons lose a part of their energy when interacting with the nucleus of an atom [14,20]. Next to this continuous contribution, characteristic X-rays for each atom are detected (as a result of the photoelectric effect) which are shown as sharp peaks as illustrated in Figure 2.5. Additionally, the two types of scattered radiation (Compton and Rayleigh scattering) can be observed. The Rayleigh peak corresponds to the highest X-ray energy in case of an incoming monochromatic X-ray beam.

2.4.4. Advantages and disadvantages

As for every analytical technique, X-ray fluorescence has its advantages and limitations. The method is widely used as a complementary technique due to its non-destructive character, *in situ* applicability, cheapness and its simplicity of use. It can be applied without any sample preparation to determine a large set of elements (main group and side) of the periodic system. However, the penetration depth of X-rays and matrix effects of untreated samples can influence the accuracy of a qualitative analysis.
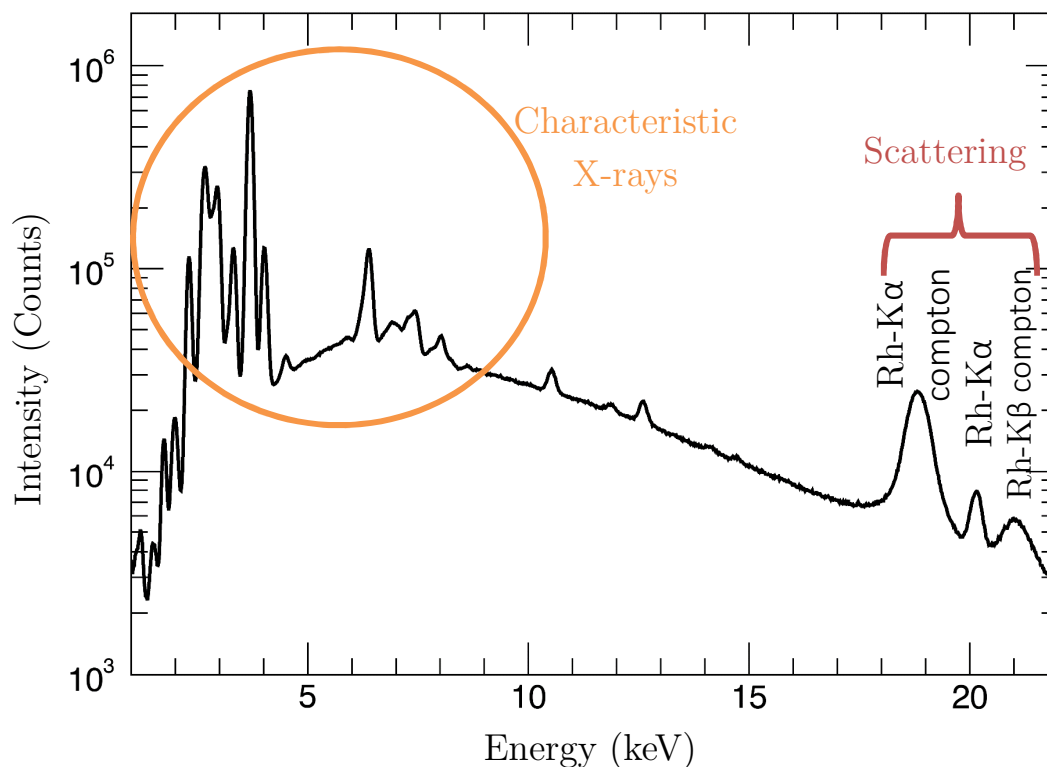
Figure 2.5 Example of an X-ray spectrum to illustrate the different contributions.

2.5 Conclusion

In this chapter, a brief introduction is made of the analytical techniques. Theoretical aspects of Raman and XRF spectroscopy are discussed which are of importance for understanding the approaches considered in the thesis. In addition, since all measurements are performed with one Raman instrument, its parameters are also explained.

In a first step to explore the possibilities and applicability of mobile Raman instrumentation for art analyses, a protocol will be presented in the next chapter on the characterisation of a mobile Raman spectrometer by applying it to a specific Raman system.

2.6 References

[1] J.L. Koening, Infrared and Raman spectroscopy of polymers, Smithers Rapra Publishing, 2000:12(2).

[2] S.M. Ali, F. Bonnier, H. Lambkinm K.Flynn, V. MC Donagh, C. Healy, T.C. Lee, F.M. Lyng and H.J. Byrne, A comparison of Raman, FTIR and ATR-FTIR micro spectroscopy for imaging human skin tissue sections, Anal. Methods 5 (2013) 2281-2291. Doi 10.1039/C3AY40185E.

[3] B.Sivasanskar, Engineering chemistry, Tata McGraw-Hill Publishing company limited, 2008.

[4] N. Kumar and S. Kumbhat, Essentials in Nanoscience and Nanotechnology, John Wiley & Sons, 2016.

[5] H.G.M. Edwards, P. Vandenabeele, Vibrational spectroscopy: theoritical basis relevant to archaeometry and archaeological applications, in: H.G.M. Edwards, P. Vandenabeele (Eds.), Analytical Archaeometry: Selected Topics, The Royal Society of Chemistry, Cambridge, 2012: 49–58.

[6] J.M. Chalmers, H.G.M. Edwards, M.D. Hargreaves, Introduction and scope, in: Infrared Raman Spectrosc. Forensic Sci., John Wiley & Sons Ltd, 2012: 3–7.

[7] E.C. Le Ru, P.G. Etchegoin, Principles of Surface-Enhanced Raman Spectroscopy: and related plasmonic effects, Elsevier B.V., 2008.

[8] M.J. Pelletier, Introduction to applied Raman spectroscopy., in: Anal. Appl. Raman Spectrosc., Blackwell Science Ltd., Oxford, 1999: 1–52.

[9] E. Smith, G. Dent, Modern Raman spectroscopy: a practical approach, John Wiley & Sons, 2005.

[10] R.L. McCreery, Raman spectroscopy for chemical analysis, John Wiley & Sons, 2000.

[11] P. Vandenabeele, Practical Raman spectrosopy, John Wiley & Sons, Ltd, 2013.

[12] J.R. Ferraro, K. Nakamoto, C.W. Brown, Introductory Raman spectroscopy, Academic Press, 2003.

[13] W.H. Weber and R. merlin, Raman scattering in material science, Springer-Verlag Berlin Heidelberg, 2000.

[14] R. Schlotz, S. Uhling, Introduction of X-ray fluorescence analysis, Karlruhe: Bruker AXS GmbH, 2000.

[15] http://www.kollewin.com/blog/electromagnetic-spectrum.

[16] B. Beckhoff, B. Kanngieβer, N. Langhoff, R. Wedell, and H. Wolff, Handbook of Practical X-Ray Fluorescence Analysis. Springer Berlin Heidelberg, 2006.

[17] R. Van Grieken and A. Markowicz, Handbook of X-Ray Spectrometry, CRC Press; 2nd edition, 2001.

[18] A. Thompson, D. Attwood, E. Gullikson, M. Howells, K.-J. Kim, J. Kirz, J. Kortright, I. Lindau, Y. Liu, P. Pianetta, A. Robinson, J. Sco_eld, J. Underwood, G. Williams, and H. Winick, X-ray data booklet. Berkely: Center for X-ray Optics and Advanced Light Source: University of California, 2009.

[19] L. Vincze, K. Tsuji, J. Injuk, and R. Van Grieken, Chapter 6: New computerisation Methods, in X-Ray Spectrometry: Recent Technological Advances, Wiley, 2004.

[20] J. Beutel, Handbook of medical imaging: Physics and psychophysics, Washington: SPIE, 2000.

Chapter 3

Characterisation of mobile Raman instrumentation for archaeometric research

Based on the paper: D. Lauwers, A.G. Hutado, V. Tanevska, L. Moens, D. Bersani and P. Vandenabeele (2014). Characterisation of a portable Raman spectrometer for *in situ* analysis of art objects. Spectrochimica Acta A, 118:294-301.

In the previous chapter theoretical considerations of Raman spectroscopy are discussed and a mobile Raman spectrometer, EZRaman-I-Dual Raman system, is introduced. In this chapter, the aim is to point out several aspects that need to be considered when selecting a mobile Raman spectrometer for in situ archaeometrical studies. A protocol has been drawn up that involves a twofold characterisation of mobile Raman instrumentation for art analysis. It includes the investigation of spectroscopic characteristics and the evaluation of specific properties that are useful for mobile studies in archaeometry. Finally, the research is completed with field tests by studying the pigments of a mediaeval wall painting.

3.1 Introduction

During the last few decades, Raman spectroscopy has grown to be an established analytical technique in archaeometry, art analysis and conservation science [1]. Indeed, the technique is well appreciated for its non-destructive character, its speed of analysis and for its ability to obtain molecular spectra of micrometer-sized particles of an organic or inorganic nature. In this research field, the technique has successfully been applied for the study of, amongst others, oil paintings [2-4], mediaeval manuscripts [5-7], ceramics [8-11], stained glass [12], wall paintings [13,14], rock art [15], gemstones [16,17] or for the analysis of archaeological objects [18]. Surface-enhanced Raman Spectroscopy (SERS) is frequently used for the analysis of dyes [19]. Moreover, Raman spectroscopy

is not only a favourable technique for the analysis of artists' materials but it is also used for investigating degradation processes [20,21].

In archaeometrical research, often precious and brittle artefacts are examined. A typical request is to maximise the information that is obtained, while minimising the (risk of) damage to the artwork. Raman spectroscopy, being a non-destructive spectroscopic technique, is a favourable approach as, when a sample was taken, this sample remains available for further investigation. However, the method can also be used for non-destructive direct analysis of small objects by using laboratory instrumentation [22]. Mobile Raman instrumentation was developed, allowing to investigate art objects directly *in situ*, eliminating the need to transport the artefacts to the laboratory. Fiber optic probeheads have been shown to be successful to investigate pigments of paintings [23]. Dedicated instruments were developed to meet specific needs in art analysis. An important contribution was the creation of the in-house mobile art analyser (MArtA) by P. Vandenabeele [24]. The first instruments were used under many different conditions, such as museum environments [25–27], but also to investigate wall paintings [28]. Increasingly, more mobile instruments came available on the commercial market and they were also used in different applications, such as the analysis of stained glass windows [29], porcelain [30,31] or rock art [32,33]. Mobile instrumentation was also used to investigate the degradation effects *in situ* due to environmental pollution on historical buildings [34,35].

In 2007, a brief test to evaluate mobile Raman instrumentation in different laboratories around Europe was published [36]. The aim of this paper was to evaluate the quality of these instruments for their applicability towards art analysis. The evolution of mobile Raman instrumentation for applications in art and archaeology and other related fields of research has been extensively reviewed [37,38]. When characterising mobile Raman instrumentation, different types of mobile equipment have to be distinguished. Ph. Colomban [38] classifies instruments based on their weight: a mobile instrument weights less than 30 kg, whereas the instrument or probehead of an ultramobile or hands-on instruments weighs less than 2 kg. Smith [39] distinguished between transportable (by 4 men) and portable (by 1 man) instruments. We propose to

discriminate between transportable, mobile, portable, handheld and palm instruments, as described in Table 3.1

Table 3.1 Overview of the distinction between transportable, mobile, portable, handheld and palm instruments.

Type of instrumentation	Definition
Transportable	- Can be carried from one site to another - On site, some alignments have to be made to ensure optimal performances - Not designed to be moved frequently, although it is possible - Most laboratory Raman instruments are transportable
Mobile	- General term for all the Raman spectrometers, designed for mobile use - The engineers took into account the requirements for a stable spectrometer - User does not have to make any adjustments inside the spectrometer
Portable	- Mobile instrument that can be carried and brought at the field by a single person - Typically battery operated
Handheld	- Can be operated while held in one hand of the operator - Battery operated
Palm	- Spectrometer size reduced to very small dimensions - Fit into the palm of one's hand - Battery operated

During the recent years, an increasing number of mobile Raman spectrometers have become available on the market. These spectrometers are generally designed for a broad range of applications. Evaluating and selecting a suitable portable instrument for applications in archaeometry is not always straightforward. Indeed, different parameters need to be taken into account. The aims of this research are multiple: (i) Selection of the characteristics of mobile Raman spectrometers that are of importance for Raman spectroscopic analysis of art objects; (ii) Suggested approaches that can be used to evaluate these parameters; (iii) Illustration of the method, by applying this approach to an EZRaman-I-Dual Raman spectro-meter and demonstration of the use of this instrument during the analysis of a wall painting.

3.2 Experimental

All measurements were performed using a portable EZRaman-I-Dual Raman system (TSI Inc., Irvine CA, USA). Specification of the instrument can be found in Chapter 2.

3.2.1. Reagents

A selection of products was used for wavelength calibration purposes: sulphur (UCB), epsilon-caprolactone (Acros Organics), cyclohexane (Kaiser), polystyrene pellets (Aldrich) and acetonnitrile/toluene (mixed in 50/50 volume%), obtained from Panreac and UCB respectively [24,40]. Lead tin yellow type I (Pb_2SnO_4) and vermilion (HgS) were obtained from Kremer, Aichstetten, Germany. NaCl from E. Merck (Germany) was used as a matrix for the measurement of the limit of detection (LOD) of the approach.

3.2.2. Neon spectra

Full spectral calibration was performed by analysing the atomic emission lines of a standard neon lamp (230 V AC, Gentronics, Belgium). Neon spectra were collected by placing the neon lamp in front of the objective. They were recorded for 1 s to acquire the intense neon emission lines and 30 s to collect also the weaker lines. During the measurements, the neon lamp was moved relative to the lens to ensure complete and reproducible filling of the aperture of the objective [40].

3.2.3. Software

Data processing was performed by using Thermo Grams/AI 8.0_suite software (Thermo Galactic). For the study on the stability of the Raman instrument, the spectra were processed with ACD/SpecManager (ACD/Labs, Berks, England).

3.3 Results and discussion

Different portable Raman instruments are available on the commercial market. To select the most suitable instrumentation for *in situ* art analysis, some critical requirements need to be examined. In general, the characteristics that should be evaluated can be divided in two groups. On the one hand, there are typical spectroscopic characteristics such as (amongst others) spectral resolution, spectral window, signal to noise ratio and limit of detection. On the other hand, there are a number of instrumental characteristics that are specifically of practical importance when performing art analysis. These include options for easy positioning and focusing, the ability to reduce laser power on the surface of the art object and the working distance between the probehead and the artefact. Although we present these characteristics here as two groups, in practice, the distinction is not so strict.

3.3.1. Spectroscopic characteristics

Spectral resolution and spectral window

In contrast to to Fourier-transform (FT-) Raman spectrometers, in dispersive instruments, for a given detector, there is a trade-off between the spectral resolution and the spectral window: the higher the spectral resolution, the smaller the spectral window. Thus, when selecting a mobile Raman spectrometer, it is important to evaluate these properties. It has to be taken into account that the highest spectral resolution is not always the most desirable, as high resolution also means that few photons hit each pixel of the CCD detector – hence lower sensitivity is obtained.

Instrument manufacturers typically state one number for the spectral resolution of an instrument. However, it is not always clear how this was determined. Sometimes there is confusion between the spectrometer resolution and the detector resolution (i.e. the numbers of pixels per wavenumber unit). However, the latter disregards the influence of the spectrometer grating, the spectrometer entrance slit, etc. Spectral resolution can be determined by measuring the full bandwidth at half maximum

(Lorentzian) of an atomic emission line of a neon lamp. It should be noted that the spectral resolution is typically not constant over the whole spectrum.

When selecting the spectral window of an instrument, different aspects have to be taken into account. First of all, in art analysis it is often very useful to be able to detect Raman bands at relatively low wavenumbers. For example, the most intense Raman band of anatase (TiO_2) is observed at 142 cm^{-1} [41]. On the other hand, the cut-off of the spectral window is not only determined by the (positioning of the) grating and detector, but the cut-off values of the Rayleigh filter also determine the lowest band position on which a Raman band can be detected. Similarly, the spectrometer response as a function of the wavenumber has to be taken into account when selecting the spectral window. As CCD detectors typically lack sensitivity in the infrared region it should be considered whether it is worthwhile to cover also the high wavenumber range (e.g. around 3000 cm^{-1}) when using a 785 nm laser. In our case, the spectral range of the EZRaman-I-Dual instrument was selected to be 100–2350 cm^{-1} and 100–3200 cm^{-1} for the 785 nm and 532 nm laser, respectively. Corresponding spectral resolutions are presented in Table 3.2

Table 3.2 Overview of the spectral range and the corresponding spectral resolution of the EZRAMAN-I-DUAL Raman system for the 785 nm and 532 nm laser.

Laser wavelength	Range	Ne-emission band	Full-width-half maximum	
785 nm	100-2350 cm^{-1}	849.41 nm	0.41 nm	5.67 cm^{-1}
532 nm	100-3200 cm^{-1}	537.03 nm	0.20 nm	6.94 cm^{-1}

Raman wavenumber calibration

When selecting a portable Raman instrument for art analysis, the wavenumber stability has to be considered. Although wavenumber calibration might be time consuming, it is often of vital importance to obtain reliable results. Some mineral pigments have only slightly different band positions [9,10]. A typical example is the Raman band position of the $\nu(CO_3)$ symmetrical stretching vibration in calcite

(CaCO$_3$, 1086 cm^{-1}), aragonite (CaCO$_3$, 1086 cm^{-1}), dolomite (CaMg(CO$_3$)$_2$, 1098 cm^{-1}) and magnesite (MgCO$_3$, 1094 cm^{-1}). Due to the same Raman band position of calcite and aragonite at 1086 cm^{-1}, one has to make a distinction based on the band position at 713 or 704 cm^{-1}, respectively. The identification of the correct pigment is of importance to understand production processes and the origin of materials, as aragonite is often linked with a marine origin of the chalk (e.g. sea shells) [42].

For the calculation of the Raman shift axis [40], five standards were selected and were compared to their reference values which have been examined under the Authority of the American Society for Testing and Materials (ASTM) [43]. This set of wavenumbers has the advantage of being independent of the laser wavelength and covering a spectral region from 153.8 to 2292.6 cm^{-1} [44]. The linear interpolation of the recorded Raman wavenumbers as a function of the certified Raman band positions indicates a significant shift, especially at the low wavenumber range. Therefore, when it is necessary to determine precise band positions, two different calibrations need to be performed: one for the region below 500 cm^{-1} and a second one for the region above 500 cm^{-1} (Figure 3.1).

Another parameter of interest is the wavenumber stability of the spectrometer. This is its ability to retain its wavenumber calibration over a period of time [45]. Different aspects should be distinguished, such as:

- The wavenumber stability over a relative short time span (several hours)
- The stability of the laser wavelength
- The influence of changing lasers (and thus changing the grating position)
- The influence of moving the instrument (e.g. vibrations)
- The wavenumber stability over a longer period (several days)
- The influence of temperature fluctuations (e.g. when performing outdoor measurements).
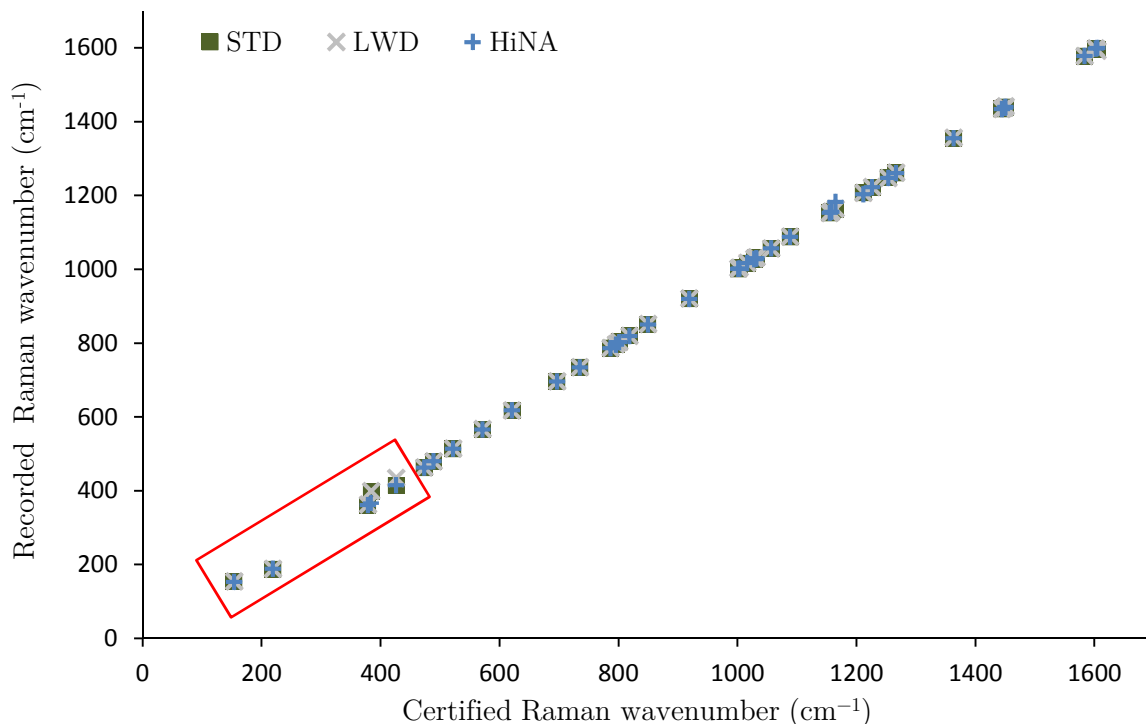
Figure 3.1 Relation between the recorded Raman wavenumbers (cm^{-1}) of standards used during calibration and the certified Raman band positions for the 785 nm laser, illustrating the interesting spectral window between 158 and 1605 cm^{-1}.

In practice, due to the instrument use, it is not always possible to discriminate between all of these aspects. On the one hand, the stability of the spectrometer should be examined, whereas on the other hand reasons for possible instability should be evaluated. Therefore, the overall stability of the instrument was studied by measuring the possible drift of the Raman band positions of reference products. These variations can be caused by changes in the optics (e.g. grating position) as well as changes in the laser wavelength.

To evaluate the short-term reproducibility, spectra of polystyrene pellets were recorded every 6 min over a period of 22 h 30 min, resulting in 226 spectra. The spectra were recorded for 30 s each, using maximum laser power. The procedure was repeated for each laser. Comparing the position of the most intense band (ring breathing vibration, 1001 cm^{-1}) of all the spectra, no significant changes are observed: an average band position of polystyrene at 1001.10 $\pm$ 0.04 cm^{-1} and 1001.99 $\pm$ 0.07 cm^{-1} for the 785 nm

and 532 nm laser, respectively. The long-term instrument stability was evaluated by measuring the same Raman band position of the polystyrene spectrum at the start of each working day, over a period of ca. 2 months. Raman band positions are highly reproducible, within a standard deviation that is lower than 0.5 cm^{-1}.

Mode-hopping of the lasers was evaluated by calibrating the spectrometer [46] based on the emission lines of a neon lamp and Equation (2). The laser wavelengths were, over a 3 month period, considered as stable: 784.89 ± 0.05 nm and 531.80 ± 0.04 nm for the red and green laser, respectively.

$$\text{Raman shift (cm}^{-1}) = \left(\frac{1}{\lambda_{\text{inc}}(\text{nm})} - \frac{1}{\lambda_{\text{stokes}}(\text{nm})} \right) \times 10^7 \qquad (2)$$

Sensitivity of the spectrometer

It is obvious that the Raman spectrometer used for archaeometrical purposes should be as sensitive as possible. As discussed before, spectrometer sensitivity is related to the spectral resolution. Apart from the instrumental factors, the measured limits of detection [47] are dependent on laser intensity, measurement times and the analyte molecule in a specific matrix.

To enhance the sensitivity, it is favourable to work at high laser power. However, when working with brittle artefacts, it is of the outmost importance to avoid any possible laser damage. The EZRaman-I-Dual Raman system is programmed so that the laser is only on during the measurements, thus limiting the time of exposure to laser radiation. Moreover, the laser can be adjusted according to the needs, by using a power control button. One thing that required testing is the correctness of this scale at the buttons. The correlation between the set laser power and the corresponding laser output power at the sample was measured with a Nova laser power monitor (Ophir Optronics ®). This study proved that the scale on the power control button (assigned by the company) does not correspond to the measured power reduction at the sample. Both lasers show a similar trend: from a minimum set laser power, 33% for the red laser and 55% for the green laser,

a linear relation was found (Figure 3.2). When recording spectra at a laser power lower than this critical value, no Raman signal was detected. Also from this approach, the same linearity was observed between the Raman signal intensity and the set laser power reduction.
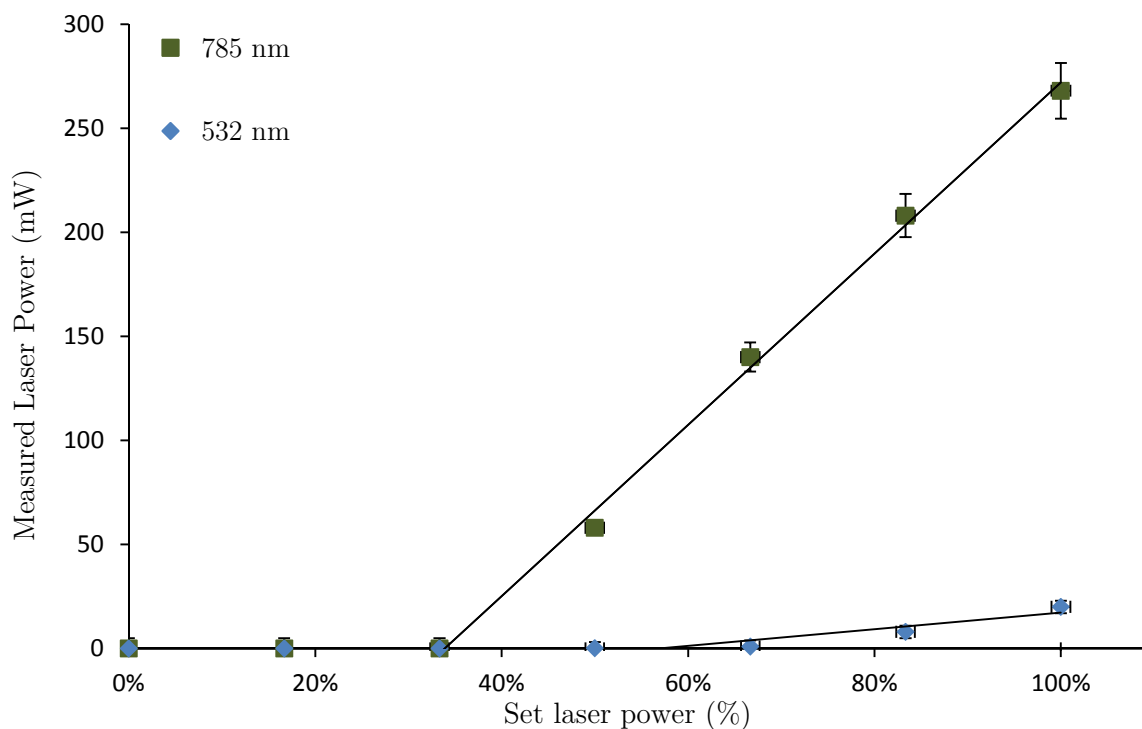
Figure 3.2 Relation between the set laser power (%) and the corresponding laser output power at the sample (mW) for the 785 nm and the 532 nm lasers.

The measured power at the sample surface is influenced by several factors, such as absorption by the particular objective lens used. As the intensity of the Raman effect is proportional to the power density at the sample, the effect of different lenses on the sensitivity of the Raman spectrometer should be evaluated. Moreover, the different objective lenses have different working distances and solid angles and hence different collection efficiencies. When performing *in situ* measurements it is, because of safety issues, interesting to have a long working distance, but this has to be balanced against the sensitivity.

To measure the optimal working distance for all the lenses and both lasers, the fiber-optic probehead was placed on a millimeter metal bar, moving it over a distance of

25 mm in steps of 1 mm. For each step a spectrum of polystyrene pellets was recorded for 20 s at maximum power. At the same time, the laser spot size was determined at each distance.
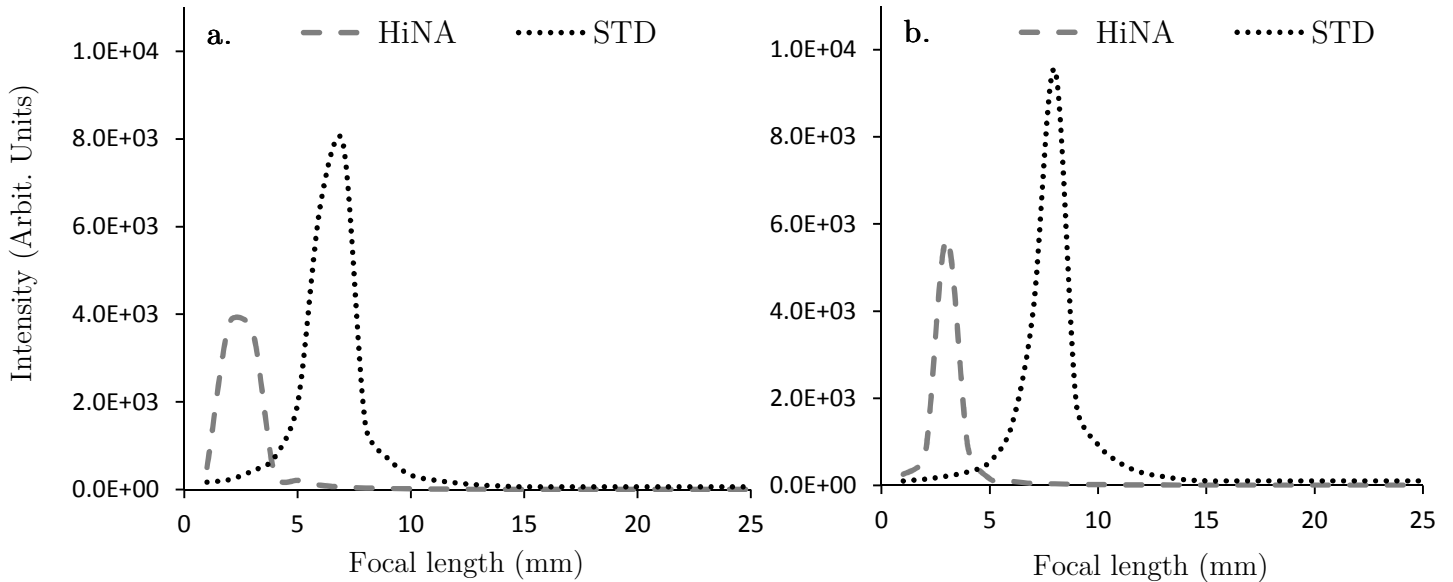
Figure 3.3 Relation between the Raman band intensity (Arbit. Units) of polystyrene, at 1001 cm^{-1}, and the working distance (mm) for the 785 nm laser (a) and the 532 nm laser (b), for the HiNa and STD lenses.

Figure 3.3 gives a graphical representation of the Raman band signal intensity, at 1001 cm^{-1}, as a function of the focal length. One can conclude that the optimal working distance is independent of the type of laser, except for the STD lens, and corresponds to a distance of 3 mm for the HiNA lens, <1 mm for the LWD lens. The STD lens has an optimal focal length at 7 mm and 8 mm for the 785 nm and 532 nm laser, respectively. The estimated optimal working distances of the HiNA and STD lenses are in agreement with the data given by the company. In contrast to this, the specified working distance for the LWD lens (13 mm) is totally different from that which has been experimentally determined. The LWD lens is equipped with a plastic tube, changing the LWD lens into a contact lens. In addition, the Raman band intensity at the focal distance is five times lower than in the case of the STD and HiNA lens. For the other lenses, other properties, such as spot size and differences in Raman signal intensity, also were examined at optimal focal distance. The STD and the HiNA lenses of both lasers have a similar circular spot size of 0.074 ± 0.002 mm and 0.088 ± 0.002 mm, respectively. Opposite to what is

expected, when comparing the Raman signal intensity one can see that the intensity obtained with the STD lens is ca. double to what is obtained with the HiNA lens. This results in a lower efficiency for the latter lens.

The sensitivity of a Raman spectrometer is an important spectroscopic characteristic of the instrument. Not only does a sensitive spectrometer allow us to reduce the measuring time at the artefact (hence, more spectra at different positions can be recorded in the same time), but also degradation products that may be present in low concentrations can be examined. Studying degradation processes of artists' materials is highly important as this helps us to understand the phenomena that can be initiated by light, relative humidity, atmospheric pollutants (e.g. ozone, NO_x, SO_4^{2-}, acetic acid, etc.) or temperature [48,49]. The limit of detection (LOD) expresses the sensitivity of an instrument, as measured on known samples; when analysing samples with unknown composition, the limit of identification (LOI) should be considered [47]. The LOD, expressed as a concentration or quantity, is the lowest concentration of a sample in a given matrix that can be detected. The concentration of a product is related to the detection of its most intense Raman band. Therefore, the LOD can be determined at which the most intense Raman band of that product is still detectable. It can be defined as the concentration where the Raman signal intensity equals three times the spectral noise (Equation (3)):

$$\text{LOD} \sim I_{\text{raman}} > 3 \times \sqrt{I_{\text{Raman}} + I_{\text{background}}} \qquad (3)$$

The total Raman intensity equals the sum of the Raman signal (I_{Raman}) and the background signal ($I_{\text{background}}$). When determining the LOD of a sample, several factors that influence the LOD have to be considered: it is a function of the laser intensity and laser wavelength, experimental conditions, sample matrix and the studied analyte [47,50]. Here, two pigments (lead tin yellow type I (Pb_2SnO_4) and vermilion (HgS)) were chosen to calculate the LOD of each sample. These pigments were selected, as these are commonly encountered in antique art objects, they are stable and can relatively easily

be purchased (e.g. for comparative experiments between laboratories). Moreover, these pigments are strong Raman scatterers. A series of well-known pigment concentrations was made by mixing them with a NaCl-matix. A NaCl matrix was selected, as this material is relatively transparent for the light and it is not Raman active. Moreover, it is easy to handle and the mixtures are easily made by weighing. For each concentration and pigment a Raman spectrum was recorded for 20 s at 50% laser power (70 mW) with the red laser. When determining the limit concentration, one has to consider the lowest intensity of the most intense Raman band (band position at 129 cm^{-1} and 252 cm^{-1} for lead tin yellow type I and vermilion, respectively), which is still detectable. As a result, the detection limits are determined, for the specified experimental conditions, to be 9.8 mg g^{-1} for lead tin yellow type I and 43.8 mg g^{-1} for vermilion.

3.3.2. Characteristics of particular importance to archaeometrical research

Apart from the spectroscopic characteristics, some features of a mobile instrument are of particular importance when analysing art objects on site. In many cases, when bringing a mobile Raman instrument to a cultural heritage site (e.g. museum, cathedral, or archaeological site), weight and access to electrical power are important aspects, which may lead to some restrictions. The portable Raman spectrometer used in this work is 43 x 33 x 18 cm and weighs ca. 17 kg. It works on 220 V AC, but is also supplied with an internal battery. Moreover, also an external lithium battery can be connected to the instrument and has an effective operational live time of ca. 6 h 30 min, although this time is reduced when often changing between two lasers. It should be noted that the laser output power decreases slightly with usage and thus leads to a decrease in Raman signal intensity, and that this reaches a constant power output of 230 mW after 2 h, until the battery is flat. The spectrometer is equipped with two 5 m long fibre optic cables, which allow one to record spectra from a distance. Each probehead has a trigger, which is useful when recording spectra in hand-accessible areas. The instrument is controlled by a built-in laptop, making it possible to visualise the spectra on a reasonably sized screen (opposite to palm-sized or handheld spectrometers). Although weight and electrical power constraints can be of importance, as archaeometrical research is often performed in museums, this is usually not a major problem for these studies.

As the Raman effect is relatively weak, and as the spectrometer is stray light sensitive, the experiment is also sensitive to interference from ambient light. Therefore, special attention should be given to blocking all ambient light. When working in a museum or a church it is not always possible to work in a darkened room. Therefore, it is advisable to work during the night or to use a shelter to avoid direct background illumination. If these two options are not applicable, one can use a light blocker (e.g. a piece of foam or metal) that can be applied over the lens so that no stray light can reach the objective.

An important aspect when investigating art objects is the positioning of the probehead relative to the artefact. On the one hand, positioning equipment should be sufficient flexible, so that the set-up can be modified depending on the situation. On the other hand, the positioning equipment should be sufficiently stable and allow the focusing of the laser beam on the object. During the time of measurement the object should remain in focus. If the laser beam is not stable, band broadening occurs and a weaker spectrum is observed. In previous studies, different combinations of macro-positioning and micro-positioning systems were examined [24]. A similar set-up is possible with the Enwave spectrometer; the probehead can be mounted on the existing stages. A clamp (Figure 3.4) was developed that is able to hold both probeheads simultaneously, thus facilitating an easy switch between the laser wavelengths. Moreover, the same clamp can also hold a digital microscope camera (dyno-lite), which is connected to the USB port of the laptop that is incorporated into the spectrometer. This digital microscope is also equipped with LED-lights, allowing the illuminate the whole area under study.

Apart from the positioning equipment described hitherto [51], new positioning equipment was developed based on perpendicular optical rails with slides. This can easily be mounted on a tripod, thus allowing for an enhanced mobility, compared to more heavy positioning systems. The main advantage of using sliders over a simple tripod with clamp, is that this approach allows for easier positioning, hence, the time for positioning is reduced. Finally, thanks to the triggers that are present on the probeheads and provided that the measurements do not last too long, it is possible to hold the (light) probehead manually, during measurement.
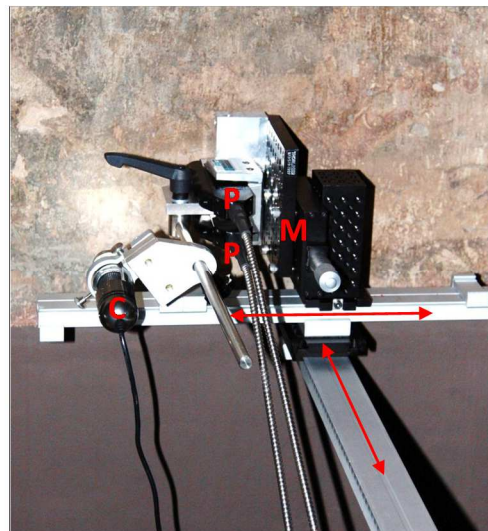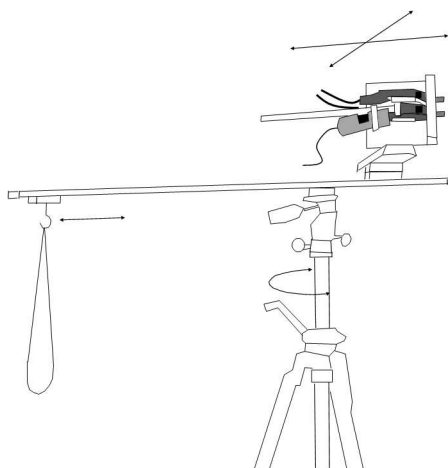
Figure 3.4 System for positioning the probeheads (P) of the portable Enwave dual laser Raman system. The system is based on two orthogonal rails that are mounted on a tripod and allow for easy positioning by sliding the probehead clamping system over the rails. A micrometer translation stage (M) is mounted for focusing, while a USB-microscope camera (C) allows for visualisation and illumination. On the drawing, a counterweight is shown to balance the system on the tripod.

3.3.3. Field test: analysis of the mediaeval wall painting "San Cristoforo" (1495), Pianazzola, Italy

The possibilities of the Enwave Raman spectrometer were tested by analysing some pigments from the mediaeval wall painting of San Cristoforo on the outside walls of the church of the village of Pianazzola (Prov. Di Sondrio, LO, Italy). This large painting was probably painted by Andrea Passeris di Torno (Como) in 1495, and was restored in 1892. To test the abilities of the instrument, spectra were recorded under bad conditions: bright sunlight and positioning the probehead by hand, in some cases standing on ladders to reach the highest zones (Figure 3.5) During the experiment, it was requested that we explain the work to the people living in the small village. To avoid as much as possible interference from ambient sunlight, a copper tube was slid over the objective lens tube. However, focusing was difficult and still some sunlight interfered with the spectral acquisition.

Figure 3.5 Evaluation of the portable Raman spectrometer by analysing the pigments of the mediaeval wall painting of S. Cristoforo at the church of Pianazzola (a). During the analysis the research was explained to the inhabitants of the village (b). During the analysis the probehead was manually positioned (c-d) and the sunlight was blocked out by sliding a copper tube over the objective lens (c').

From this experience we shall propose the manufacture of small plastic or foam caps that effectively block all interferences from the sunlight. Nevertheless, it was possible to identify the pigments in this artwork. This was especially successful as we had access to two different lasers: where some pigments yield weak spectra with one of the lasers (or the signal is overwhelmed by fluorescence), it was possible to obtain better results when using the other laser. As an example of our approach, Figure 3.6a, we present two Raman spectra as recorded from a blue area, by using the green 532 nm laser. These spectra are recorded with only 10 s of accumulation time. Although the spectra are noisy, clear features from ultramarine ($Na_{8-10}(Al_6Si_6O_{24})S_{2-4}$) and calcite ($CaCO_3$) can be
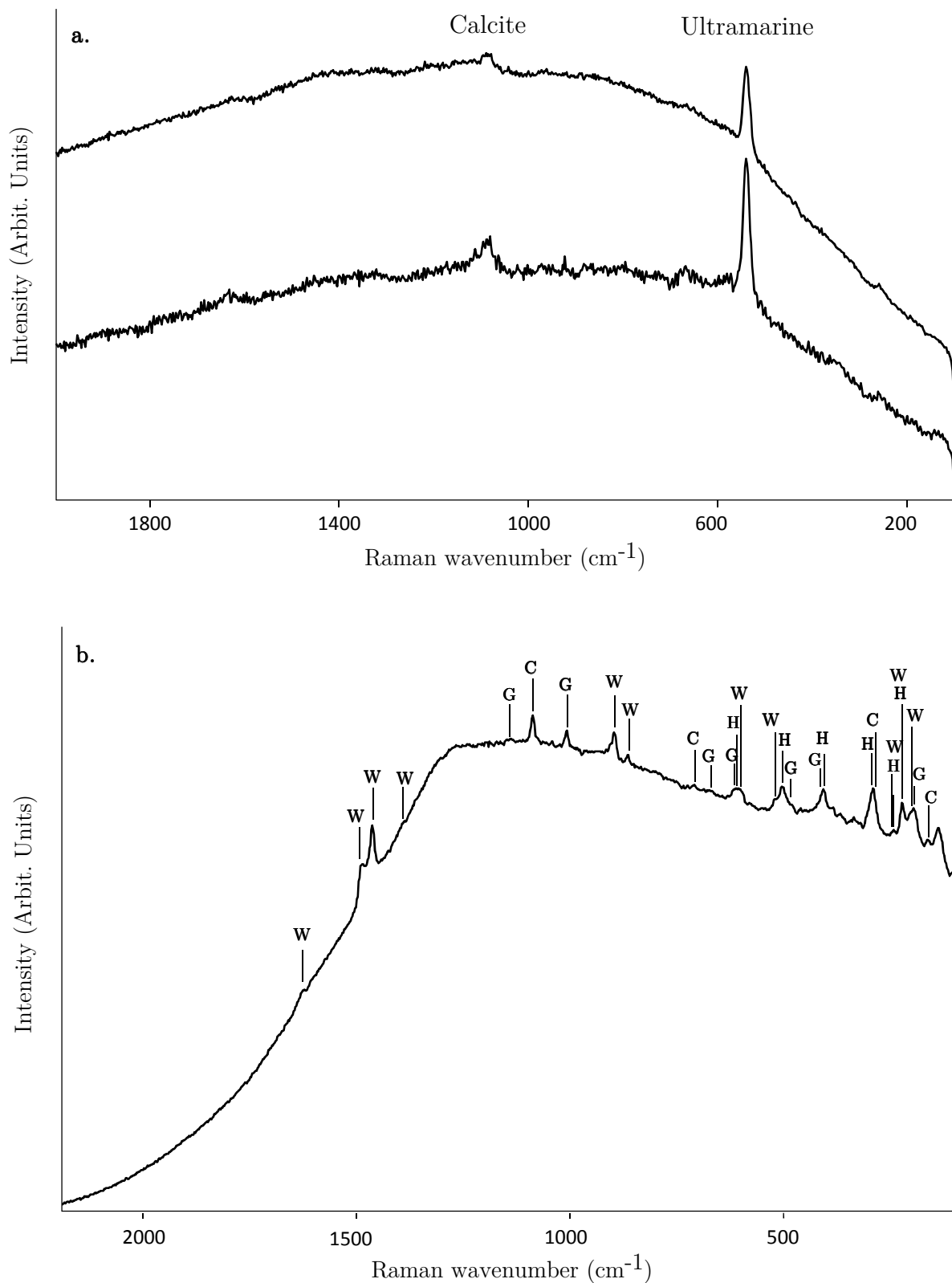
Figure 3.6 Raman spectra as recorded from the wall painting of S. Cristoforo at the church of Pianazzola. (a) Two spectra from a blue area, recorded with the 532 nm laser, 10 s of measuring time. Features from ultramarine and calcite can be recognised. (b) Spectrum from a red area, recorded with the 785 nm laser, 60 s of measuring time. Spectral features from haematite (H), calcite (C), gypsum (G) and whewellite (W) are observed.

distinguished. The intense band from ultramarine at 545 cm^{-1} can be assigned to the stretching vibration of the $[S–S]^-$ ion [52]. It should be noted that we cannot discriminate between the natural lapis lazuli and the synthetic ultramarine, which could result from a previous restoration. The symmetrical stretching vibration of the CO_3^{2-} ion in chalk is observed at 1086 cm^{-1}. This material is formed during the drying process of the wall, whereby the calcium-hydroxide $(Ca(OH)_2)$ of the plaster reacts with carbon dioxide in the atmosphere. The Raman spectrum as presented in Figure 3.6b, is recorded by using the 785 nm laser, and was recorded for 60 s. Although a large fluorescence background is present, a number of spectral features can be observed. The colouring agent present is haematite (α-Fe$_2$O$_3$). Next to this, distinct feature of calcite (CaCO$_3$), gypsum (CaSO$_4$.2H$_2$O) and whewellite (CaC$_2$O$_4$.H$_2$O) can be identified [34,53]. It is interesting to see that, in this spectrum recorded with a mobile instrument, different types of possible degradation can be observed: the presence of gypsum could be caused by reaction of the calcite with atmospheric SO$_2$, H$_2$S or SO$_4^{2-}$ pollutants, while the presence of an oxalate tends to indicate some microbiological degradation processes.

3.4 Conclusions

An overview of different features that are of importance when selecting a mobile Raman instrument for *in situ* art analysis, are provided. These comprise spectroscopic characteristics as well as specific topics that are of practical importance during archaeometrical studies. It is discussed how these characteristics can be evaluated and a standardised procedure is proposed for the evaluation of mobile Raman spectrometers. This approach is illustrated by using a dual laser portable Raman instrument. Finally, the research was completed with field tests by studying the pigments in a mediaeval wall painting. It is clear that, when selecting a mobile Raman spectrometer for archaeometrical research, a balance has to be found between different parameters, such as practical limitations (e.g. cost, weight, positioning, etc.), spectroscopic characteristics (e.g. spectral resolution, sensitivity, etc.), and the specific range of cultural heritage objects that forms the focus of the research group.

The present work is novel research on a micro-scale as well as in a broader perspective. On a micro-scale we are the first scientists to publish a full characterisation of the EZRaman-I-Dual spectrometer and use it for the first examination and report on the analysis of the Pianazzola church wall painting. In a broader view, it can be said that for the first time a protocol has now been established that describes how a mobile Raman instrument can be fully characterised and what characteristics are important or should be compensated. We have indicated the different options with advantages and disadvantages. Moreover, from time to time critical notes to common practices are made (e.g. saying that laboratory instrumentation is mobile, as it can be transported (while not designed for mobile use).

As all the important characteristics of the EZRaman-I-Dual Raman spectrometer are evaluated, the suitability of the instrument for different art applications can be examined. In the coming chapters, its beneficial use for different art applications, including pigment analysis and gemstones, will be pointed out. In the next chapter, the capabilities for pigment analysis will be illustrated based on the investigation of an important mediaeval manuscript, *De Civitate Dei*.

3.5 References

[1]   P. Vandenabeele, H.G.M. Edwards, L. Moens, A decade of Raman spectroscopy in art and archaeology, Chem. Rev. 107 (2007) 675–686. doi:10.1021/cr068036i.

[2]   P. Vandenabeele, B. Wehling, L. Moens, H.G.M. Edwards, M. De Reu, G. Van Hooydonk, Analysis with micro-Raman spectroscopy of natural organic binding media and varnishes used in art, Anal. Chim. Acta. 407 (2000) 261–274. ISI:000085377900030.

[3]   E. Cazzanelli, E. Platania, G. De Santo, A. Fasanella, M. Castriota, Micro-spectroscopic Raman investigation on the canvas oil painting "Rebecca at the well" of Neapolitan anonymous, J. Raman Spectrosc. 43 (2012) 1694–1698. doi:10.1002/jrs.4174.

[4]   L. Vančo, M. Kadlečíková, J. Breza, Ľ. Čaplovič, M. Gregor, Examining the ground layer of St. Anthony from Padua 19th century oil painting by Raman spectroscopy, scanning electron microscopy and X-ray diffraction, Appl. Surf. Sci. 264 (2013) 692–698. doi:10.1016/j.apsusc.2012.10.099.

[5]   D. Bersani, P. Lottici, F. Vignali, G. Zanichelli, A study of medieval illuminated manuscripts by means of portable Raman equipments, J. Raman Spectrosc. 37 (2006) 1012–1018. ISI:000241209500008.

[6]   P. Vandenabeele, B. Wehling, L. Moens, B. Dekeyzer, Pigment investigation of a late-medieval manuscript with total-reflection X-ray fluorescence and micro-Raman spectroscopy, Analyst. 124 (1999) 169–172.

[7]   B. Wehling, P. Vandenabeele, L. Moens, R. Klockenkiimper, A. von Bohlen, G. Van Hooydonk, et al., Investigation of pigments in medieval manuscripts by micro Raman spectroscopy and total-reflection X-ray fluorescence spectrometry, Mikrochim. Acta. 130 (1999) 253–260. ISI:000079727500005.

[8]   P. Colomban, V. Milande, H. Lucas, On-site Raman analysis of Medici porcelain, (2004) 68–72. doi:10.1002/jrs.1085.

[9]   N.Q. Liem, N.T. Thanh, P. Colomban, Reliability of Raman micro-spectroscopy in analysing ancient ceramics: the case of ancient Vietnamese porcelain and celadon glazes, J. Raman Spectrosc. 33 (2002) 287–294. doi:10.1002/jrs.854.

[10]   P. Colomban, G. Sagon, X. Faurel, Differentiation of antique ceramics from the Raman spectra of their coloured glazes and paintings, J. Raman Spectrosc. 32 (2001) 351–360. doi:10.1002/jrs.704.

[11]   P. Colomban, A. Tournie, L. Bellot-Gurlet, Raman identification of glassy silicates used in ceramics, glass and jewellery: a tentative differentiation guide, J. Raman Spectrosc. 37 (2006) 841–852. doi:10.1002/jrs.1515.

[12]   P. Colomban, M.-P. Etcheverry, M. Asquier, M. Bounichou, A. Tournié, Raman identification of ancient stained glasses and their degree of deterioration, J. Raman Spectrosc. 37 (2006) 614–626. doi:10.1002/jrs.1495.

[13]   P. Vandenabeele, S. Bodé, A. Alonso, L. Moens, Raman spectroscopic analysis of the Maya wall paintings in Ek'Balam, Mexico, Spectrochim. Acta. A. Mol. Biomol. Spectrosc. 61 (2005) 2349–56. doi:10.1016/j.saa.2005.02.034.

[14]   I. Aliatis, D. Bersani, E. Campani, A. Casoli, P.P. Lottici, S. Mantovan, et al., Green pigments of the Pompeian artists' palette., Spectrochim. Acta. A. Mol. Biomol. Spectrosc. 73 (2009) 532–538. doi:10.1016/j.saa.2008.11.009.

[15]   H.G.M. Edwards, L. Drummond, J. Russ, Fourier-transform Raman spectroscopic study of pigments in native American Indian rock art: Seminole Canyon, Spectrochim. Acta Part A-Molecular Biomol. Spectrosc. 54 (1998) 1849–1856. ISI:000076909700008.

[16]   D. Bersani, P.P. Lottici, Applications of Raman spectroscopy to gemology, Anal. Bioanal. Chem. 397 (2010) 2631–2646. doi:10.1007/s00216-010-3700-1.

[17]   I. Reiche, S. Pages-Camagna, L. Lambacha, *In situ* Raman spectroscopic investigations of the adorning gemstones on the reliquary Heinrich's Cross from the treasury of Basel Cathedral, J. Raman Spectrosc. 35 (n.d.) 719–725. ISI:000223113600019.

[18] D. Bersani, J.M. Madariaga, Applications of Raman spectroscopy in art and archaeology, J. Raman Spectrosc. 43 (2012) 1523–1528. doi:10.1002/jrs.4219.

[19] A. Whitney, R.P. Van Duyne, F. Casadio, An innovative surface-enhanced Raman spectroscopy (SERS) method for the identification of six historical red lakes and dyestuffs, J. Raman Spectrosc. 37 (2006) 993–1002. ISI:000241209500006.

[20] M.J. Pérez-Alonso M., Castro K., Investigation of degradation mechanisms by portable Raman spectroscopy and thermodynamic speciation: The wall painting of Santa Maria de Lemoniz (Basque Country, North of Spain), Anal. Chim. Acta. 571 (2006) 121–128. ISI:000238720100019.

[21] D. Bersani, E. Campani, A. Casoli, P.P. Lottici, I.-G. Marino, Spectroscopic study of the degradation products in the holy water fonts in Santa Maria della Steccata Church in Parma (Italy)., Anal. Chim. Acta. 610 (2008) 74–79. doi:10.1016/j.aca.2008.01.041.

[22] P. Vandenabeele, P. De Paepe, L. Moens, Study of the 19th century porcelain cards with direct Raman analysis, J. Raman Spectrosc. 39 (2008) 1099–1103. doi:10.1002/jrs.

[23] P. Vandenabeele, F. Verpoort, L. Moens, Non-destructive analysis of paintings using FT-Raman with Fibre-optics, J. Raman Spectrosc. 32 (2001) 263–269.

[24] P. Vandenabeele, T.L. Weis, E.R. Grant, L.G. Moens, A new instrument adapted to *in situ* Raman analysis of objects of art, Anal. Bioanal. Chem. 379 (2004) 137–142. ISI:000221116300025.

[25] P. Vandenabeele, J. Tate, L. Moens, Non-destructive analysis of museum objects by fibre-optic Raman spectroscopy., Anal. Bioanal. Chem. 387 (2007) 813–819. doi:10.1007/s00216-006-0758-x.

[26] P. Vandenabeele, M.C. Christiansen, L. Moens, Analysis of South-Asian Shaman paintings at the national museum of Denmark, J. Raman Spectrosc. 39 (2008) 1030–1034. ISI:000259242100011.

[27] A. Deneckere, M. Leeflang, M. Bloem, C. Chavannes-Mazel, B. Vekemans, L. Vincze, et al., The use of mobile Raman spectroscopy to compare three full-page miniatures from the Breviary of Arnold of Egmond., Spectrochim. Acta. A. Mol. Biomol. Spectrosc. 83 (2011) 194–9. doi:10.1016/j.saa.2011.08.016.

[28] P. Vandenabeele, K. Lambert, S. Matthys, W. Schudel, A. Bergmans, L. Moens, *In situ* analysis of mediaeval wall paintings: a challenge for mobile Raman spectroscopy, Anal. Bioanal. Chem. 383 (2005) 707–712. ISI:000233457900022.

[29] P. Colomban, A. Tournié, On-site Raman identification and dating of ancient/modern stained glasses at the Sainte-Chapelle, Paris, J. Cult. Herit. 8 (2007) 242–256. doi:10.1016/j.culher.2007.04.002.

[30] H.G.M. Edwards, P. Colomban, B. Bowden, Raman spectroscopic analysis of an English soft-paste porcelain plaque-mounted table, J. Raman Spectrosc. 35 (2004) 656–661. doi:10.1002/jrs.1211.

[31] P. Colomban, F. Treppoz, Identification and differentiation of ancient and modern European porcelains by Raman macro- and micro-spectroscopy, J. Raman Spectrosc. 32 (2001) 93–102. doi:10.1002/jrs.678.

[32] A. Tournié, L.C. Prinsloo, C. Paris, P. Colomban, B. Smith, The first *in situ* Raman spectroscopic study of San rock art in South Africa: procedures and preliminary results, J. Raman Spectrosc. 42 (2011) 399–406. doi:10.1002/jrs.2682.

[33] L.C. Prinsloo, A. Tournié, P. Colomban, C. Paris, S.T. Bassett, In search of the optimum Raman/IR signatures of potential ingredients used in San/Bushman rock art paint, J. Archaeol. Sci. 40 (2013) 2981–2990. doi:10.1016/j.jas.2013.02.010.

[34] I. Martínez-Arkarazo, D.C. Smith, O. Zuloaga, M.A. Olazabal, J.M. Madariaga, Evaluation of three different mobile Raman microscopes employed to study deteriorated civil building stones, J. Raman Spectrosc. 39 (2008) 1018–1029. ISI:000259242100010.

[35] N. Prieto-Taboada, I. Ibarrondo, O. Gómez-Laserna, I. Martinez-Arkarazo, M.A. Olazabal, J.M. Madariaga, Buildings as repositories of hazardous pollutants of anthropogenic origin., J. Hazard. Mater. (2013) 451–460. doi:10.1016/j.jhazmat.2013.01.008.

[36] P. Vandenabeele, K. Castro, M. M.Hargreaves, L. Moens, J.. Madariaga, H.G.M. Edwards, Comparative study of mobile Raman instrumentation for art analysis, Anal. Chim. Acta. (2007).

[37] P. Vandenabeele, H.G.M. Edwards, J. Jehlicka, The role of mobile instrumentation in novel applications of Raman spectroscopy: archaeometry, geosciences, and forensics, Chem. Rev. (2013).

[38] P. Colomban, The on-site/remote Raman analysis with mobile instruments: a review of drawbacks and success in cultural heritage studies and other associated fields, J. Raman Spectrosc. 43 (2012) 1529–1535. doi:10.1002/jrs.4042.

[39] D.C. Smith, *In situ* mobile subaquatic archaeometry evaluated by non-destructive Raman microscopy of gemstones lying under impure waters, Spectrochim. Acta Part A Mol. Biomol. Spectrosc. 59 (2003) 2353–2369. doi:10.1016/S1386-1425(03)00078-7.

[40] D. Hutsebaut, P. Vandenabeele, L. Moens, Evaluation of an accurate calibration and spectral standardization procedure for Raman spectroscopy., Analyst. 130 (2005) 1204–14. doi:10.1039/b503624k.

[41] H.G.M. Edwards, N. Hassan, P. Middleton, Anatase - a pigment in ancient artwork or a modern usurper?, Anal. Bioanal. Chem. 384 (2006) 1356–1365. ISI:000236031600013.

[42] H.G.M. Edwards, S. Villar, J. Jehlicka, T. Munshi, FT-Raman spectroscopic study of calcium-rich and magnesium-rich carbonate minerals, Spectrochim. Acta Part A-Molecular Biomol. Spectrosc. 61 (2005) 2273–2280. ISI:000231027600002.

[43] R.L. McCreery, Raman spectroscopy for Chemical Analysis, John Wiley & Sons inc, Canada, 2000.

[44] J. Laserna, ed., Modern Techniques in Raman Spectroscopy, John Wiley & Sons, 1996.

[45] J. Planelles, I. Climente, J. Gabriel Díaz, Espectroscòpia, Universidad Jaume I, 2002.

[46] Hamaguchi H., Calibrating multichannel Raman spectrometers, Appl. Spectrosc. Rev. 24 (1988) 137–174.

[47] P. Vandenabeele, L. Moens, Some ideas on the definition of Raman spectroscopic detection limits for the analysis of art and archaeological objects, J. Raman Spectrosc. 43 (2012) 1545–1550. doi:10.1002/jrs.4055.

[48] N. De Laet, S. Lycke, J. Van Pevenage, L. Moens, P. Vandenabeele, Investigation of pigment degradation due to acetic acid vapours: Raman spectroscopic analysis, Eur. J. Mineral. (2012).

[49] G.D. Smith, R.J.H. Clark, The role of H_2S in pigment blackening, J. Cult. Herit. 3 (2002) 101–105. doi:10.1016/S1296-2074(02)01173-1.

[50] P. Vandenabeele, J. Jehlička, P. Vítek, H.G.M. Edwards, On the definition of Raman spectroscopic detection limits for the analysis of biomarkers in solid matrices, Planet. Space Sci. 62 (2012) 48–54. doi:10.1016/j.pss.2011.12.006.

[51] F. Settle, ed., Handbook of instrumental techniques for analytical chemistry, Prentice-Hall, Inc., New Jersey, 1997.

[52] K. Nakamoto, Infrared and Raman spectra of inorganic and coordination compounds, Wiley (New York), 1986.

[53] M. Perez-Alonso, K. Castro, I. Martinez-Arkarazo, M. Angulo, M.A. Olazabal, J.M. Madariaga, Analysis of bulk and inorganic degradation products of stones, mortars and wall paintings by portable Raman microprobe spectroscopy, Anal. Bioanal. Chem. 379 (2004) 42–50. ISI:000221116300009.

.

Chapter 4

Pigment identification of an illuminated mediaeval manuscript De Civitate Dei by means of portable Raman equipment

In the previous chapter, the characteristics of the EZRaman-I-Dual spectrometer were extensively evaluated. This is a good starting point for checking the suitability of the instrument. Mobile Raman spectrometers should be versatile: the method should be applicable for various type of art objects with different shapes, sizes and composition. For this reason, it is important to check the applicability of the instrument in different case studies and optimise it where needed. In this next part, the possibilities of the portable Raman spectrometer for pigment analysis of an important mediaeval manuscript De Civitate Dei (cultural heritage library in Bruges, Belgium) are illustrated. Pigments are the most attractive targets for scientific studies, because of their colourful appearance. It can provide information of the artist's palette and reveal information about the painter's technique.

The study of mediaeval handwriting was one of the first applications of Raman spectroscopy in art analysis as these are ideal objects to illustrate the capabilities of the instrument for pigment analysis, due to the simple paint composition (in comparison to oil paintings). Miniatures are usually painted in a tempera technique with arabic gum. The focus of this chapter mainly lays on the discussion of the characteristics important for in situ pigment analysis. The advantage of the availability of two lasers, which are an integral part of the equipment, are pointed out. Also, good performance of the Raman spectrometer to allow pigment identification in a short time is proven. At the same time,

information about the artists' palette is obtained, which gives information about the working practice and the materials used by the illuminator.

4.1 Introduction

Direct identification of pigments in mediaeval illuminated manuscripts was one of the first applications of Raman spectroscopy in art and archaeology [1–3]. The analytical investigation of pigments is an important aspect of the technical characterisation of (art) historical objects [4,5]. It can reveal important information relevant to dating and authentication, conservation or restoration of art [4,6]. Micro-Raman spectroscopy is well known for its non-destructive character, molecular specificity, spatial resolution and its suitability for *in situ* characterisation of illuminated manuscripts [7–11]. Direct analysis can be performed in the lab or in the field, depending on the size of the artefact and the ability to transport the object [12–17]. If transportation of the book is not allowed, analytical approaches are available: (i) sampling via the Q-tip method as previously reported [18] or (ii) direct analysis with a mobile instrument. Often, despite the possible interference of fluorescence from support and binders [14,19], on-site analysis is preferred over sampling (Q-tip) due to the limited, thin paint layers used in miniature art (which can impede the sampling) [15,20].

In previous *in situ* analysis campaigns of manuscripts, the equipment was typically provided with a single excitation source [21–23]. Nevertheless, the ability to switch between different lasers is extremely useful, as absorption of the scattered light by the sample may result in a reduced spectral quality of the Raman spectrum [24,25]. Moreover, in some cases, wavelength-dependent fluorescence can be overcome by using a different excitation laser. Therefore, in this work, a portable Raman spectrometer (cf. definition formulated elsewhere [26,27]), equipped with two lasers, is introduced to characterise the pigments present in the mediaeval *De Civitate Dei* manuscript from the cultural heritage library in Bruges. The pigment identification will contribute to the enrichment of information of the working practice and materials used by the illuminator.

4.2 Experimental

In situ Raman spectroscopy was performed on a selection of illuminated folios in the manuscript *De Civitate Dei* using the EZRaman-I-Dual Raman system. The recorded Raman data were processed using Thermo Grams/AI 8.0 ® suite software (Thermo Galactic).

On folio 1 (recto,r) the decorative fleuronnée initial of the letter 'A' was examined. The miniature on folio 22r was also a region of great interest, since it was attributed to the illuminator Willem Vrelant (or his workshop) by F. Lyna and G. Bousmanne [28,29]. The folios studied and the examined areas are shown in Figure 4.1. A digital version of the manuscript can be found on the website of the cultural heritage library in Bruges [30].

Figure 4.1 (a) Ms.106, f1r, Litterae duplex; (b) Ms.106, f22r, Litterae duplex and border decoration; (c) Ms.106, f22r, Detailed picture of the decorated initial; (d) Ms.106, f22r, Miniature of Saint Augustine who is teaching the audience.

4.2.1. Reagents

Lead white ($2PbCO_3 \cdot Pb(OH)_2$), atacamite ($Cu_2Cl(OH)_3$), cobalt blue ($CoAl_2O_4$) and red lead (Pb_3O_4) were obtained from Kremer, Aichstetten, Germany.

4.2.2. The mediaeval manuscript De Civitate Dei (Ms.106)

Since the original version of the *De Civitate Dei* was written in the 5th century, by the early theologian and philosopher Aurelius Augustine, this 22 chapter Latin-written manuscript has been very influential for Western Christian societies throughout the middle ages. Proof of its popularity can be found in the fact that almost 450 copies of this work are still preserved to date [31].

In this research, an important copy of the *De Civitate Dei*, which is preserved at the public library Biekorf in Bruges, is examined. It was produced in the second half of the 15th century and ended-up in Bruges in the 17th century, foreseen of a so called *Campmansstrap* (after Bernard Campmans, the 40th abbot of the abbey *Ten Duinen*) and a cross of *Ten Duinen*. This indicates that the manuscript was once part of the Cistercian libraries. Although the cross of *Ten Duinen* denotes the provenance of the manuscript from the abbey *Ten Duinen* (Koksijde, Belgium), the book can also come from the abbey *Ter Doest* (a daughter foundation of *Ten Duinen*), due to the fusion of the abbeys. Codicological research (i.e. systematic study of all material aspects of a codex, including folio gathering,binding, etc.) with the focus on a microscopic study of the parchment support,supported the estimation of the manuscript production during the 15th century. It showed that a high density of hair follicles are uniformly distributed throughout the parchment surface, which are representative for parchment made from calf skin. It is known that the use of this skin was widespread for this region throughout the 15th century [32].

The content of the manuscript focuses on Christian philosophy, more specific on the dualism between good and evil. The book is decorated with some colourful illuminations and can be attributed to Willem Vrelant, who was an active member of the Saint John the Evangelist Guild [18,28]. The latter was exclusively reserved for

craftsmen that were related to production and trade of manuscripts. Vrelant was most active during the third quarter of the 15th century and is considered as one of the most influential and commercially successful illuminators of his time. His distinctive technique and pictorial vocabulary can be described as rather conservative for the time. Most recognisable in his oeuvre are the static figures, oval faces, straight and slender noses, high and wide foreheads and the figures lacking personality [29].

4.3 Results and discussion

Technical aspects of miniature art can be studied via sampling and via direct analysis. Due to the limited materials, the preciousness and fragility of the manuscript, non-destructive investigation was chosen, more specific *in situ* Raman analysis.

When analysing art objects directly, good quality positioning (i.e. focusing) of the equipment is of utmost importance to obtain high quality results [33]. It is required to have stable equipment and the way the instrument is mounted must be safe. Apart from the requirement for stable positioning equipment, it should also allow easy macro and micro-positioning. The set-up used for direct analysis is shown in Figure 4.2. The probeheads were mounted on an articulating arm [34], using the in-house developed clam that is introduced in chapter 3. Correct and easy positioning is made possible due to the presence of micrometer translation stages, which can be operated manually. This set-up also provides the advantage of allowing switching easily between both lasers, 785 and 532 nm lasers, to use the preferred laser wavelength for a coloured area [19]. Switching is done rather quickly (200 s) and easily: the spectrometer is equipped with a switch button and is also provided with two operation software's, one for each laser. To exchange between lasers, the software of the one laser has to be closed, and the cooling system needs to be turned off, using a central key. Next, the switch button has to be turned to the preferred laser, and the cooling system can be turned on again, together with starting up the software of the corresponding laser. To avoid damage to the manuscript (e.g. crumbling of the leather or parchment, peeling off the back or cover of the manuscript, but mainly to avoid cracking of the binding), book pillows and V-shaped foam were used to open it. If needed also, lead laces were applied to keep manuscript

folios in place. In the next part, we will discuss some features that are of importance to direct analysis, applied to the investigation of the *De Civitate Dei* manuscript.
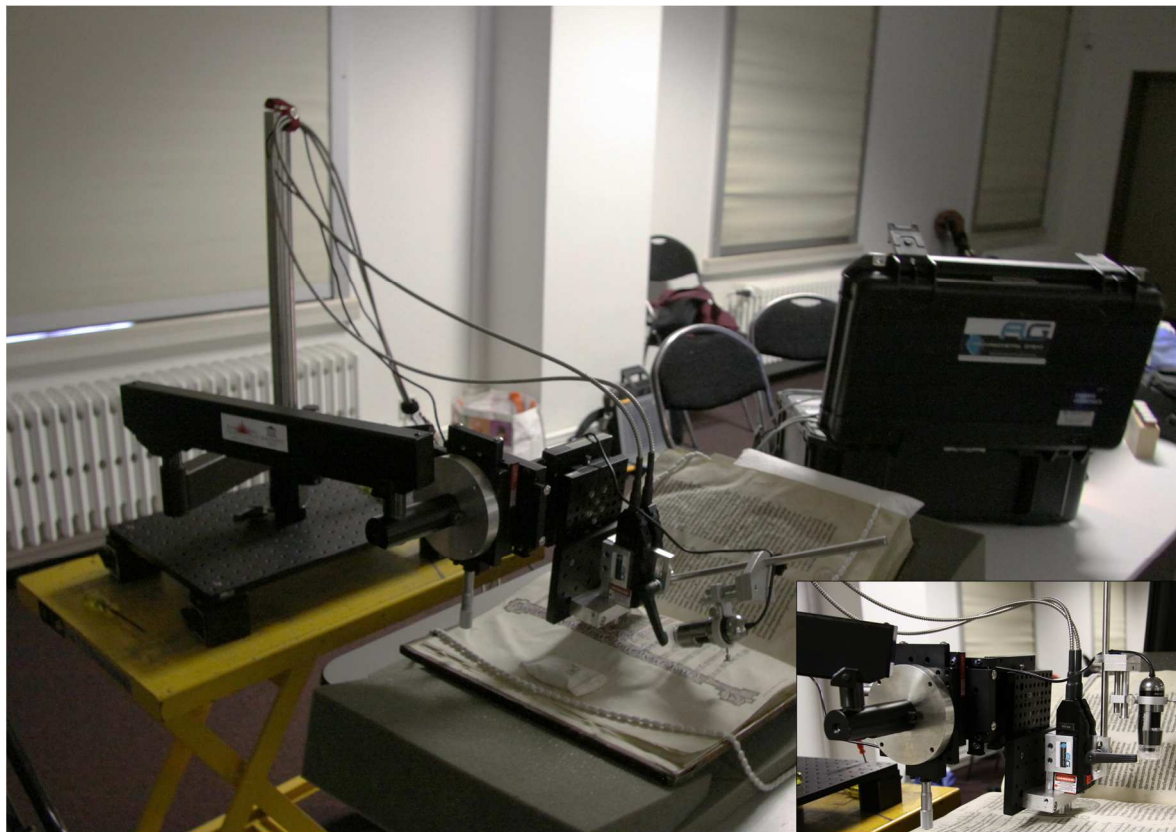
Figure 4.2 General overview of the set-up for the pigment analysis of the *De Civitate Dei*.

4.3.1. Characteristics important for in situ analysis

When performing analysis in museums, libraries, etc., the availability of the object is often limited in time. This means that the analyst has to plan well, in order to execute a complete characterisation of the object quickly. In this project, two approaches were taken into account: (i) obtain excellent quality spectra of a selection of paint colours and (ii) characterise as much as possible, i.e. record one spectrum (max. three) of each paint colour with a relatively good spectral quality (reasonable signal-to-noise ratio, SNR), in a short time. The selection of one of the approaches depends on the intended purpose. When the analyst wants to compare the composition of similar colours or identify degradation products (results in weak Raman bands), it is better to obtain excellent quality spectra. If he wants to obtain information about the total used artist's palette,

the second perspective is preferred. The latter approach was selected for the analysis of this mediaeval manuscript. Note that in this case, the Raman spectra (within short measuring time) are obtained probably at the expense of the spectral quality. Figure 4.3 represents some of the Raman spectra that were recorded in only 30 s. As one can see, clear bands could be detected in a short time, with a good SNR. This proves that the introduced Raman spectrometer is highly performant to allow pigment identification in a short time, with reasonable spectral quality. As a result, all the paint colours at the selected regions (28 points), present in the folios, could be examined. As mentioned, two lasers (785 and 532 nm) can be used during the analysis of the *De Civitate Dei* manuscript, between which we can switch. This can lead to successful identification of pigments: as some pigments yield weak spectra with one of the lasers (i.e. low SNR), better results can be obtained with the other one.

Some measurements were performed in the lab to point out the benefit of dual laser excitation. Raman spectra were recorded of several reference pigments with both lasers. In this paper, we selected four pigments (labelled by Kremer pigmente as lead white, atacamite, cobalt blue and red lead) for which the need of two lasers becomes clear. Figure 4.4 represents the Raman spectra recorded of the four pigments with both excitation sources. Cobalt blue and red lead prove to be good scatterers for the red laser but show clear absorption interference for the 532 nm laser, resulting in weak Raman bands. The green pigment labelled atacamite, on the other hand, strongly absorbs the red laser and can burn even with a low laser power. In this case, the green laser is the optimal laser to use; this is true for most blue and green pigments. Note, when taking a closer look to the recorded spectrum of atacamite (Kremer), it was clear that it does not correspond to the spectrum of this compound. Comparing this spectrum with reference spectra of malachite and atacamite from the database of RRUFF [35], it was found that we are dealing with malachite instead of atacamite. On the basis of the findings in the preceding text, it is clear that the presence of two lasers can lead to more successful identification of materials. Not every pigment is only Raman active for a certain laser wavelength: lead white for example results in a good Raman spectrum for both excitation wavelengths (Figure 4.4).
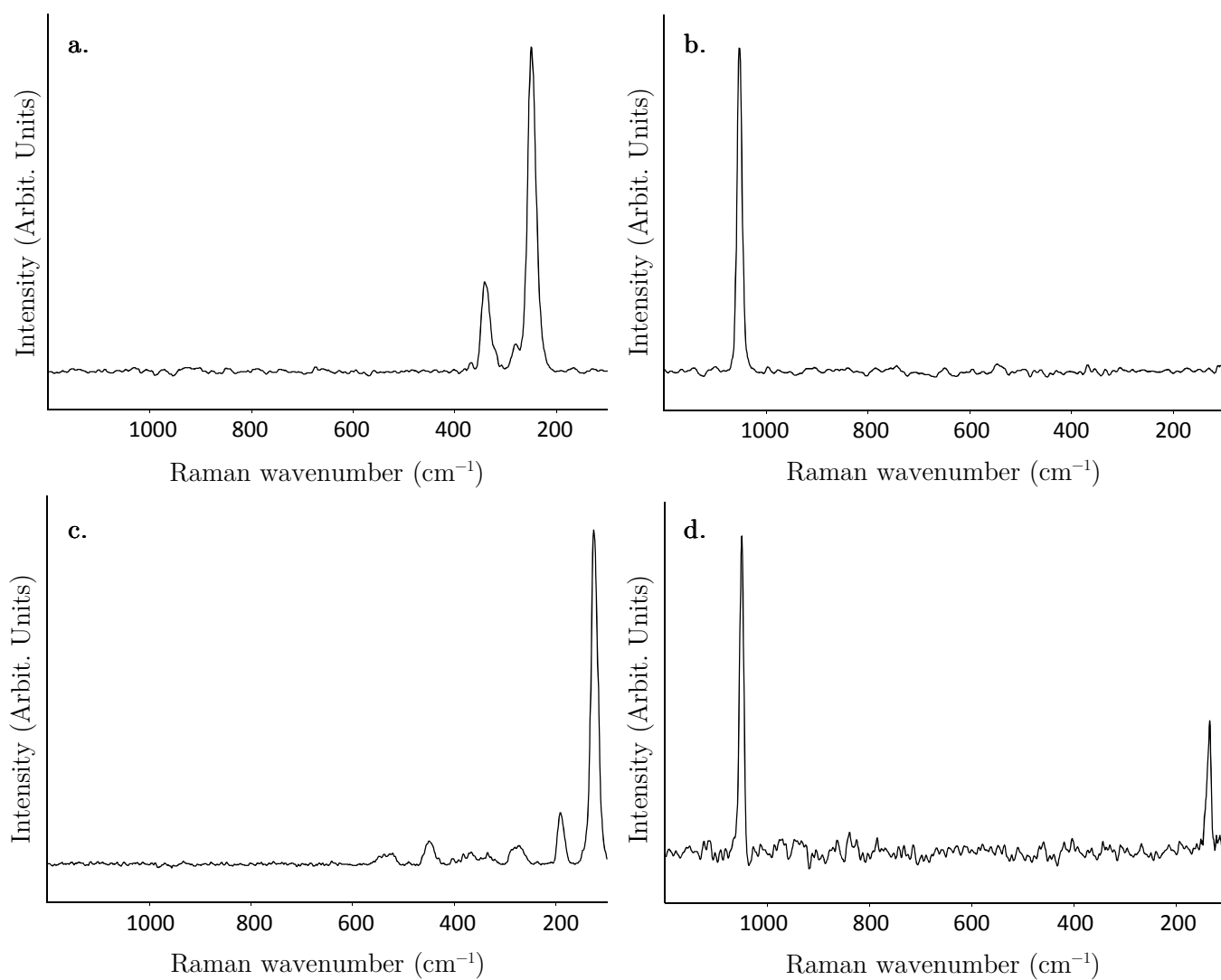
Figure 4.3 Raman spectra are recorded with the 785 nm laser with only 30 s of accumulation time (baseline corrected), from the mediaeval manuscript, *De Civitate Dei*. (a) spectrum of a red area (f22r, border decoration, point 10). Features of vermilion can be recognised; (b) spectrum of a white area (f22r, miniature, point 15) which can be assigned to lead white; (c) spectrum of a yellow area (f22r, miniature, point 16) with features of lead-tin yellow type I; (d) spectrum of the incarnation (f22r, miniature, point 27), which is a mixture of lead white and lead-tin yellow type I.
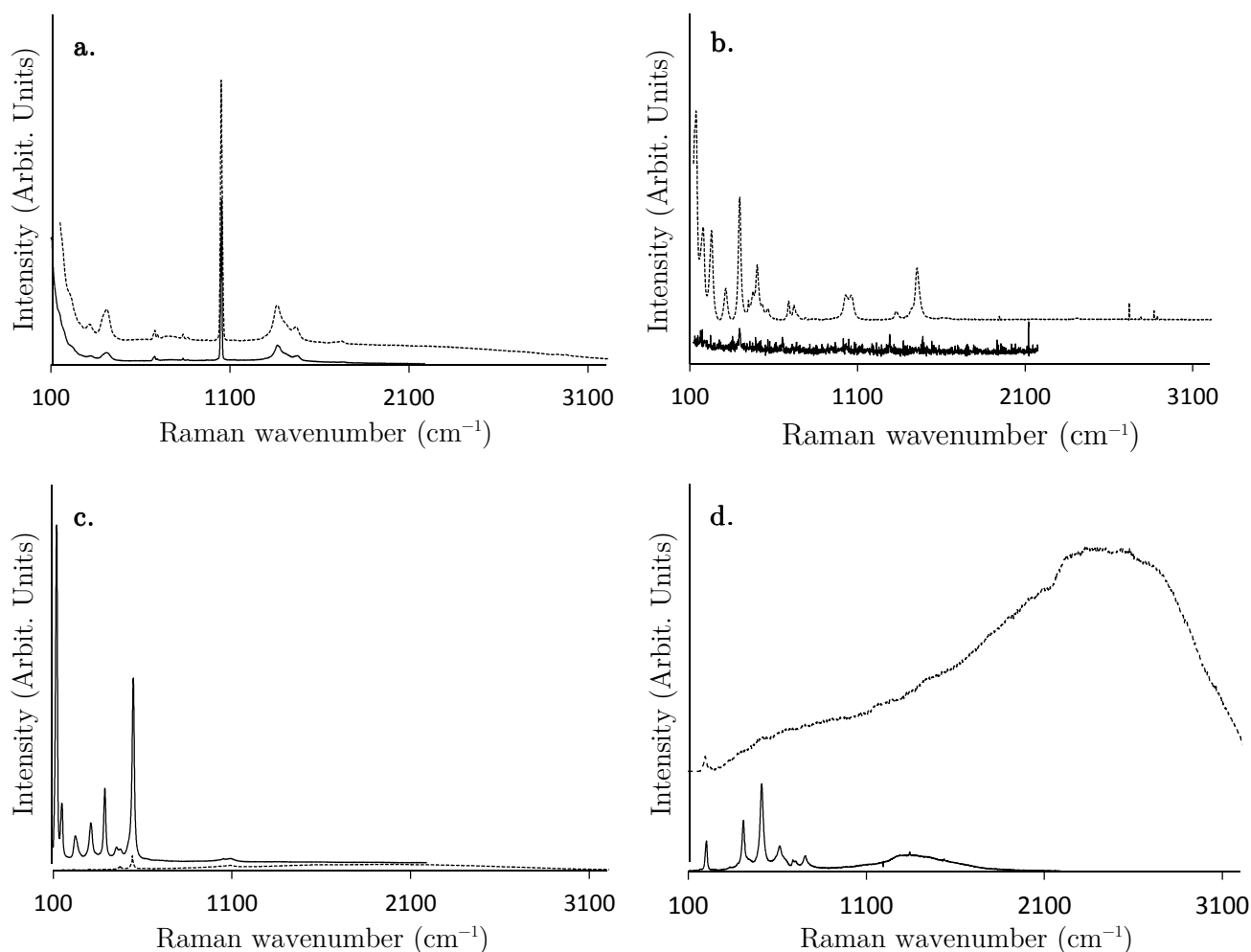
Figure 4.4 Raman spectra are recorded with the 785nm laser (full line) and the 532 nm laser (striped line) (a) Raman spectrum of lead white (λ=785 nm: 2x2 s, 129 mW; λ=532 nm: 2x2 s, 21 mW); (b) Raman spectrum of atacamite (λ=785 nm: 60x10 s, 10 mW; λ=532 nm: 10x5 s, 8 mW); (c) Raman spectrum of red lead (λ=785 nm: 2x2 s, 70mW; λ=532 nm: 10x5 s, 0.9 mW) (d) Raman spectrum of cobalt blue (λ=785 nm: 10x5 s, 129 mW; λ=532 nm: 10x5 s, 20 mW).

To prove this concept, the instrument was tested on the manuscript: the blue area of the decorated initial (f22r, point 11) was analysed with both lasers. The spectra were recorded with a total measured time of 150 s, using the STD lens. Although both spectra are noisy, the SNR is much better for the green laser than for the red laser (Figure 4.5). Studying the detected band position, the blue pigment used for the illumination could be identified as azurite ($Cu_3(CO_3)_2(OH)_2$). Azurite was an important blue mineral in the middle ages and has characteristic Raman bands at 405 (vs) and 1093 (s) cm^{-1}, due to Cu-O stretching vibration and the symmetrical stretch vibration of the carbonate ion,

respectively. The intensity of the bands can differ, depending on the orientation, because azurite is anisotropic: the spectrum is strongly orientation-dependent [36].
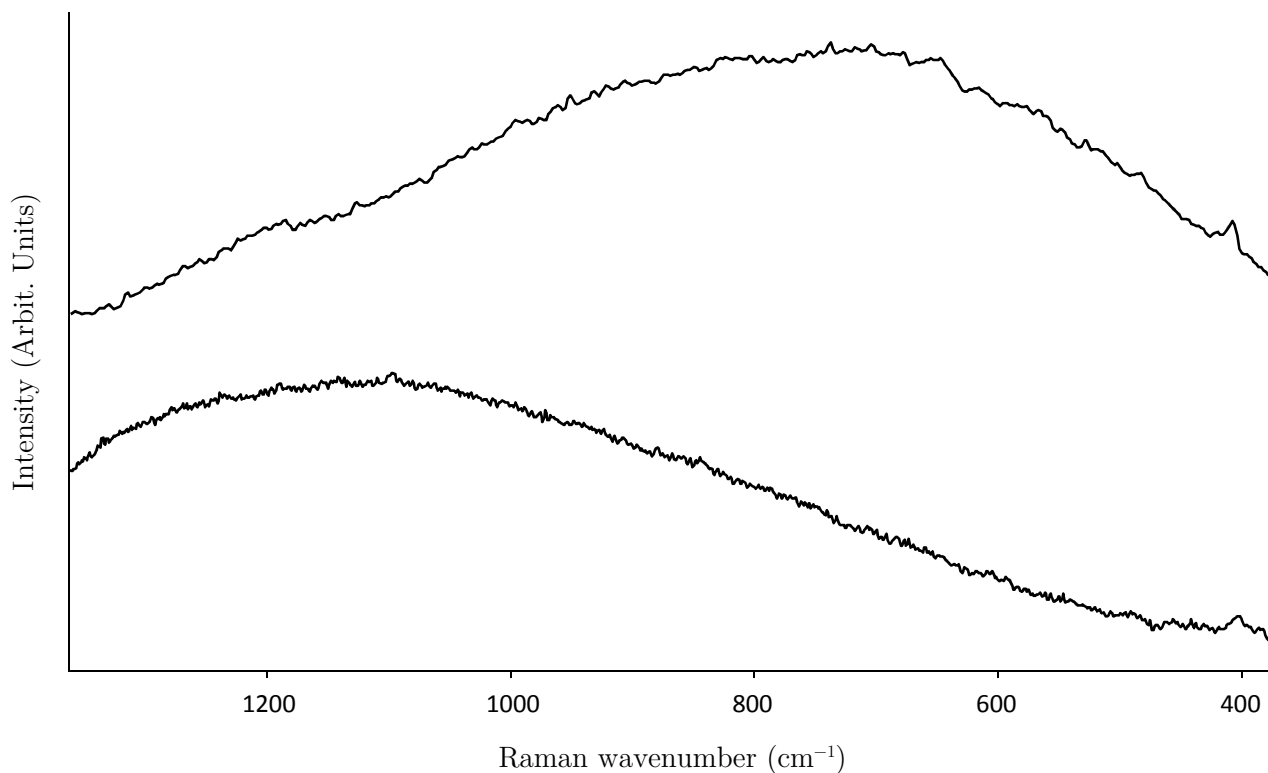
Figure 4.5 Raman spectra (30x2s, STD lens, 70mW, External power source) of: <u>top</u>: Raman spectrum of the unknown blue colour recorded with the 532 nm laser, identified as azurite ($Cu_3(CO_3)_2(OH)_2$); <u>bottom</u>: Raman spectrum of the unknown blue colour recorded with the 785 nm laser, identified as azurite ($Cu_3(CO_3)_2(OH)_2$).

4.3.2. Pigment identification of the De Civitate Dei manuscript

The different colours were examined using the Enwave Raman spectrometer, in the border illumination (f22r), a decorated initial (f22r), fleuronée-initials, more specific litterae duplex (f1r and f22r) and the miniature (f22r), ascribed to Willem Vrelant. The litterae duplex, in both folios, was written by using a combination of red and blue ink [37]. For both initials, vermilion (HgS) was used as a pigment in the red ink. Unfortunately, the composition of the blue ink could not be determined (Table 4.1) due to very strong fluorescence: this may arise from the binding agent [38–40]. The decorated initial, on the other hand, was painted with four pigments: an unknown red

(probably organic) pigment, azurite ($Cu_3(CO_3)_2(OH)_2$) for the blue colour and malachite ($Cu_2CO_3(OH)_2$) for the green colour (Table 4.1). In this latter zone also, lead-tin yellow type I (Pb_2SnO_4) was detected: it was used to create a lighter hue in some areas.

The selected regions of the border decoration and miniature contain blue, white, green, yellow, black, brown, grey, orange, gold and different red paints (Table 4.1). When investigating the green leaf of the border decoration, a remarkable identification was carried out: an exact match was found with chrome yellow ($PbCrO_4$, bands at 840 and 358 cm^{-1}) (Figure 4.6a). On the basis of microscopic evaluation, it is difficult to say whether the green colour was obtained by a mixture of a blue pigment and a yellow pigment or if a green pigment was used in combination with the yellow pigment to soften the colour. The reason why we were not able to detect the additional Raman bands of the green or blue pigment, lies in the fact that these pigments are weak Raman scatters. It is likely that these bands are masked by the strong scatterer lead chromate. Chrome yellow is an artists' pigment that was commonly used after the mid of the 19th century [41]. This proves that this pigment could not be used in the original colour palette and thus points out a probable restoration of the manuscript during the 19th century. It is known that in 2006 a restoration was executed by *BVBA De Zilveren Passer*. During this intervention, mainly the structural elements were stabilised. It is not clear if interventions were also made on the illuminated parts of the manuscript.
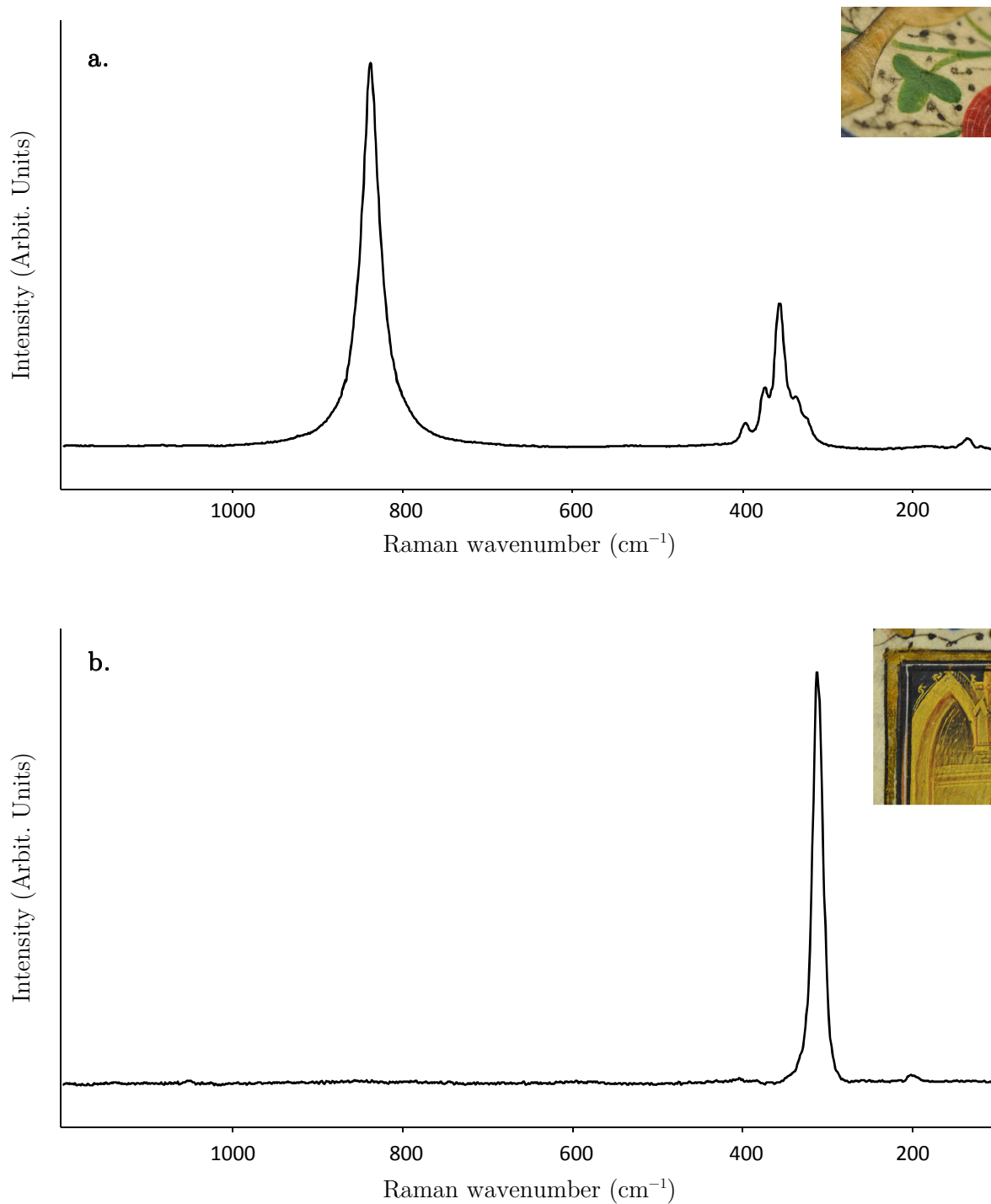
Figure 4.6 Baseline corrected Raman spectra (λ=785 nm, 30x5 s, STD lens, 70mW, External power source) of: (a) Raman spectrum of the unknown green colour in the border decoration, with bands at 840 and 358 cm^{-1} that can be assigned to chrome yellow (PbCrO$_4$); (b) Raman spectrum of the unknown gold colour in the miniature with characteristic band at 313 cm^{-1} that can be assigned to mosaic gold (SnS$_2$).

Table 4.1 Overview of the identified pigments used for the illumination of the miniature, border decoration and initials present in the *De Civitate Dei* (Ms.106).

Ms.106: Folio	Colour and number of measured point (Figure 4.1)	Laser (nm)	Pigment Identification	Chemical Formula
f1r	Red (2)	785	Vermilion	HgS
	Blue (1)	532	/	
f22r, text	Blue (3)	532	/	
	Red (4)	785	Vermilion	HgS
f22r, initial	Red (13)	785	/	
	Blue (11)	532	Azurite	$Cu_3(CO_3)_2(OH)_2$
	Green (12)	785	Lead tin yellow type I	Pb_2SnO_4
			Malachite	$Cu_2CO_3(OH)_2$
f22r, decoration	Yellow/gold (5, 6)	785	/ (probably gold leaf)	
	Red (strawberries) (7)	785	Vermilion	HgS
			Lead white	$2PbCO_3 \cdot Pb(OH)_2$
	Red (flower) (9)	785	/	
	Red (hat) (10)	785	Vermilion	HgS
	Green (8)	785	Chrome yellow	$PbCrO_4$
f22r, miniature	White (14,15)	785	Lead white	$2PbCO_3 \cdot Pb(OH)_2$
	Yellow (16)	785	Lead tin yellow type I	Pb_2SnO_4
			Lead white	$2PbCO_3 \cdot Pb(OH)_2$
	Yellow/gold (17, 18)	785	Mosaic gold	SnS_2
	Red (19)	532	/	
	Orange/red (20)	785	Minium	Pb_3O_4
	Purple (21)	785	Lead white, ?	$2PbCO_3 \cdot Pb(OH)_2$
	Green hills (23)	785	Lead tin yellow type I	Pb_2SnO_4
	Green mantle (22)	532 and 785	/	
	Blue (24)	532	Azurite	$Cu_3(CO_3)_2(OH)_2$
	Brown (29)	785	/	
	Grey (26)	785	Lead white	$2PbCO_3 \cdot Pb(OH)_2$
	Black (25)	785	Carbon black	
	Incarnation (27, 28)	785	Lead white	$2PbCO_3 \cdot Pb(OH)_2$
			Lead tin yellow type I	Pb_2SnO_4

Another important colour in the investigation of the border decoration and miniature is the gilding. The question arises if the gilding is actual gold or mosaic gold, i.e. tin sulphide (SnS_2) [42]. On the basis of visual investigation, the golden colour has been painted, not gilded [9]. The analysis showed that in the border decoration, probably metallic gold was used because of the absence of Raman bands and the presence of a high fluorescence signal. In the miniature, on the other hand, on several illuminations, the characteristic Raman band of mosaic gold (SnS_2) at 313 cm^{-1}, corresponding to ν(SnS) symmetric stretching, was detected (Figure 4.6b) [43]. However, its production and use in the middle ages has been described repeatedly [44,45], the identification of mosaic gold in mediaeval manuscripts is rather rare [46]. Probably its use was suppressed by other easily obtainable yellow pigments [47].

On the basis of these results, one can conclude that the Raman spectrometer was a helpful instrument in the identification of the materials used. However, it must be mentioned that there are still pigments unidentified such as, amongst others, the yellow in the border decoration. Complementary, *in situ* techniques (such as XRF and FTIR reflectance) exist to support the obtained results and enrich the information. Because of limited access to the manuscript, these experiments could not be performed. Also micro-sampling techniques (e.g. Q-tip method) exist, but due to the preciousness of the manuscript, sampling was not allowed.

4.4 Conclusions

It can be concluded that the Raman spectrometer, EZRaman-I-Dual Raman system, is well suited for the identification of pigments in mediaeval manuscripts. It is discussed how the availability of two lasers, leads to a more successful identification of pigments and what is the importance of stable positioning. In addition, it is proven that the introduced Raman spectrometer is highly performant to allow pigment identification in a short time. Finally, the research was completed with an *in situ* test by characterising the pigments in the mediaeval manuscript *De Civitate Dei* (Ms.106). This resulted in the identification of pigments, which is in agreement with the mediaeval artists' palette. However, the identification of chrome yellow, suggests a modern (post 1800) restoration.

This research was the starting point for the investigation of other interesting mediaeval manuscripts. As it was confirmed that the equipment is an ideal tool for pigment identification, two additional projects were undertaken, contributing to the material research of two master thesis topics [48,49]. In comparison to the illustrated example, it was preferred in these cases to obtain excellent quality spectra of a selection of paint colours to solve the research questions. In a first project two manuscripts of the Chronicles of Flanders (Ms. 437 (public library Biekorf, Bruges) and Ms. 13073-74 (Royal library, Brussels) were compared to understand if they were manufactured by the same person (as assumed by Dogaer [50]) (cf. Master thesis "De Kronieken van Vlaenderen ontleed" (2013-2014), Ine Craenhals, UA). The second case study contained the visual and technical investigation of 4 Cistercian manuscripts (Ms. 27, Ms. 101, Ms. 140, Ms. 142 (public library Biekorf, Bruges)) in order to obtain more knowledge about the manuscripts and to try to assign them to the abbeys *Ten Duinen* or *Ter Doest* (cf. Master thesis "Verluchtingen Ten Duinen en Ter Doest belicht" (2014-2015), Jitske Groenland, UA).

As pigment identification is not the only application of Raman spectroscopy in art analysis, another type of material has been investigated to prove the success of the dual laser portable Raman spectrometer. In the next chapter, a collection of glyptics, belonging to the collection of the museum 'Quinta das Cruzes' in Funchal (Madeira, Portugal), is examined to illustrate the advantage of the two lasers in one set-up.

In addition, the investigation of the mediaeval manuscripts has shown that the use of a single technique is sometimes not sufficiently satisfactory. Raman spectroscopy has the disadvantage of being a weak effect and can be masked by a high fluorescence signal, leading to missing pigment identification. A combined approach of two techniques can overcome this problem. The following chapter demonstrates the benefit of using multiple, complementary techniques, portable Raman spectroscopy and handheld XRF, for *in situ* analysis.

4.5 References

[1] P. Dhamelincourt, P. Bisson, Principe et réalisation d'un microscope optique utilisant l'effet Raman, Microsc. Acta. 79 (1977) 267–276.

[2] R.J.H. Clark, Pigment identification by spectroscopic means: an arts/science interface, Comptes Rendus Chim. 5 (2002) 7–20.

[3] B. Guineau, Analyse non destructive des pigments par microsonde Raman laser : exemples de l'azurite et de la malachite, Stud. Conserv. 29 (1984) 35–41.

[4] A. Jurado-López, O. Demko, R.J.H. Clark, D. Jacobs, Analysis of the palette of a precious 16th century illuminated Turkish manuscript by Raman microscopy, J. Raman Spectrosc. 35 (2004) 119–124. doi:10.1002/jrs.1115.

[5] B. Wehling, P. Vandenabeele, L. Moens, R. Klockenkämper, A. von Bohlen, G. Van Hooydonk, et al., Investigation of pigments in medieval manuscripts by micro Raman spectroscopy and total-reflection X-ray fluorescence spectrometry, Mikrochim. Acta. 130 (1999) 253–260. ISI:000079727500005.

[6] A. Deneckere, M. De Reu, M.P.J. Martens, K. De Coene, B. Vekemans, L. Vincze, et al., The use of a multi-method approach to identify the pigments in the 12th century manuscript Liber Floridus., Spectrochim. Acta. A. Mol. Biomol. Spectrosc. 80 (2011) 125–132. doi:10.1016/j.saa.2011.03.005.

[7] V. Košařová, D. Hradil, I. Němec, P. Bezdička, V. Kanický, Microanalysis of clay-based pigments in painted artworks by the means of Raman spectroscopy, J. Raman Spectrosc. (2013). doi:10.1002/jrs.4381.

[8] R.J.H. Clark, P.J. Gibbs, Analysis of 16th century Qazwini Manuscripts by Raman Microscopy and Remote Laser Raman Microscopy, J. Archaeol. Sci. 25 (1998) 621–629.

[9] L. Burgio, D.A. Ciomartan, R.J.H. Clark, Raman Microscopy Study of the Pigments on Three Illuminated Mediaeval Latin Manuscripts, J. Raman. 28 (1997) 79–83.

[10] L. Burgio, D.A. Ciomartan, R.J.H. Clark, Pigment identification on medieval manuscripts, paintings and other artefacts by Raman microscopy: applications to the study of three German manuscripts, J. Mol. Struct. 405 (1997) 1–11. doi:10.1016/S0022-2860(96)09422-7.

[11] S.P. Best, R.J.H. Clark, M. Daniels, C.A. Porter, R. Withnall, Identification by Raman microscopy and visible reflectance spectroscopy of pigments on an Icelandic manuscript, Stud. Conserv. 40 (1995) 31. doi:10.1179/sic.1995.40.1.31.

[12] S. Pessanha, M. Manso, M.L. Carvalho, Application of spectroscopic techniques to the study of illuminated manuscripts: A survey, Spectrochim. Acta Part B At. Spectrosc. 71-72 (2012) 54–61. doi:10.1016/j.sab.2012.05.014.

[13] S. Bruni, F. Cariati, F. Casadio, V. Guglielmi, Micro-Raman identification of the palette of a precious XVI century illuminated Persian codex, J. Cult. Herit. 2 (2001) 291–296. doi:10.1016/S1296-2074(01)01131-1.

[14] L. Burgio, R.J.H. Clark, S.F. Muralha, T. Stanley, Pigment analysis by Raman microscopy of the non-figurative illumination in 16th to 18th-century Islamic manuscripts, J. Raman Spectrosc. 39 (2008) 1482–1493. doi:10.1002/jrs.

[15] K. Trentelman, N. Turner, Investigation of the painting materials and techniques of the late-15th century manuscript illuminator Jean Bourdichon, J. Raman Spectrosc. 40 (2009) 577–584. ISI:000266611900016.

[16] M. Aceto, a Agostino, G. Fenoglio, P. Baraldi, P. Zannini, C. Hofmann, et al., First analytical evidences of precious colourants on Mediterranean illuminated manuscripts., Spectrochim. Acta. A. Mol. Biomol. Spectrosc. 95 (2012) 235–245. doi:10.1016/j.saa.2012.04.103.

[17] S. Bruni, V. Guglielmi, Applications of a Compact Portable Raman Spectrometer for the Field Analysis of Pigments in Works of Art, in: Lasers Conserv. Artworks, 2007: 407–414.

[18] P. Vandenabeele, B. Wehling, L. Moens, B. Dekeyzer, Pigment investigation of a late-medieval manuscript with total-reflection X-ray fluorescence and micro-Raman spectroscopy, Analyst. 124 (1999) 169–172.

[19] S.P. Best, R.J.H. Clark, R. Withnall, Non-destructive pigment analysis of artefacts by Raman microscopy, Ende. 16 (1992) 66–73.

[20] L. Burgio, R.J.H. Clark, R.R. Harck, Raman microscopy and x-ray fluorescence analysis of pigments on medieval and Renaissance Italian manuscript cuttings, PNAS. 107 (2012) 5726–5731.

[21] A. Deneckere, M. Leeflang, M. Bloem, C. Chavannes-Mazel, B. Vekemans, L. Vincze, et al., The use of mobile Raman spectroscopy to compare three full-page miniatures from the Breviary of Arnold of Egmond., Spectrochim. Acta. A. Mol. Biomol. Spectrosc. 83 (2011) 194–199. doi:10.1016/j.saa.2011.08.016.

[22] D. Bersani, P. Lottici, F. Vignali, G. Zanichelli, A study of medieval illuminated manuscripts by means of portable Raman equipments, J. Raman Spectrosc. 37 (2006) 1012–1018. ISI:000241209500008.

[23] P. Vítek, E.M. a Ali, H.G.M. Edwards, J. Jehlička, R. Cox, K. Page, Evaluation of portable Raman spectrometer with 1064 nm excitation for geological and forensic applications., Spectrochim. Acta. A. Mol. Biomol. Spectrosc. 86 (2012) 320–327. doi:10.1016/j.saa.2011.10.043.

[24] P. Vandenabeele, Practical Raman spectroscopy: An introduction, john Wiley & Sons, Ltd., 2013.

[25] R.L. McCreery, Raman spectroscopy for chemical analysis. Chapter 1: introduction and scope., John Willey & Sons, New York, 200AD.

[26] D. Lauwers, A.G. Hutado, V. Tanevska, L. Moens, D. Bersani, P. Vandenabeele, Characterisation of a portable Raman spectrometer for *in situ* analysis of art objects., Spectrochim. Acta. A. Mol. Biomol. Spectrosc. 118 (2013) 294–301. doi:10.1016/j.saa.2013.08.088.

[27] P. Vandenabeele, H.G.M. Edwards, J. Jehlička, The role of mobile instrumentation in novel applications of Raman spectrsocopy: archaeometry, geosciences, and forensics, Chem. Soc. Rev. 43 (2014) 2628-2649. doi:10.1039/C3CS60263J.

[28] G. Bousmanne, Guillaume Wielant of Willem Vrelant: Miniaturist aan het Bourgondische Hof in de 15de eeuw, 1997.

[29] F. Lyna, Onbekende handschriften verlucht door Willem Vrelant en zijn atelier", Gentse Bijdrage tot de Kunstgeschiedenis, 1943.

[30] http://cabrio.bibliotheek.brugge.be/browse/webgaleries/MS106/index.html, (n.d.).

[31] W. et. al. Le Loup, Vlaamse kunst op perkament: handschriften en miniaturen te Brugge van de 12de tot de 16de eeuw, Brugge, 1981.

[32] A. Derolez, De wereld van het middeleeuwse boek: een codicologische benadering, in: Besloten Wereld, Open Boeken Middeleeuwse Handschriften Dialoog Met Actuele Kunst, 2002: 109–128.

[33] P. Vandenabeele, K. Castro, M. M.Hargreaves, L. Moens, J.. Madariaga, H.G.M. Edwards, Comparative study of mobile Raman instrumentation for art analysis, Anal. Chim. Acta. (2007).

[34] P. Vandenabeele, T.L. Weis, E.R. Grant, L.J. Moens, A new instrument adapted to *in situ* Raman analysis of objects of art, Anal. Bioanal. Chem. 379 (2004) 137–142. ISI:000222116300025.

[35] R.T. Downs, 19th General meeting of the international mineralogical association, Kobe, Japan, 2006.

[36] P. Vandenabeele, L. Moens, Non-destructive microanalysis of cultural heritage materials, in: K. Janssens, R. Van Grieken (Eds.), XLII, Comprehensive Analytical Chemistry XL, Antwerp, 2004: 635–662.

[37] A. Derolez, The Palaeography of gothic manuscript books: from the twelfth to the early sixteenth century, 2006.

[38] H.H. Willard, L.L. Meritt, Instrumental methods of analysis, Wadsworth Publishing Company, Belmont (California), 1981.

[39] J.R. Wigelsworth, Science and technology in medieval european life, Greenwood Press, Westport, 2006.

[40] L. Arvin, Scribes, script and books: the Book Arts from Antiquity to the Renaissance, American Library Association, Chicago, 1991.

[41] H.G.M. Edwards, D.W. Farwell, C.J. Brooke, Raman spectroscopic study of a post-medieval wall painting in need of conservation., Anal. Bioanal. Chem. 383 (2005) 312–321. doi:10.1007/s00216-005-0012-y.

[42] D.V. Thompson, The materials and techniques of mediaeval painting, Dover Publications, Inc., New York, 1956.

[43] H.G.M. Edwards, D.W. Farwell, E.M. Newton, F.R. Perez, S.J. Villar, Raman spectroscopic studies of a 13th century polychrome statue : identification of a " forgotten " pigment, J. Raman Spectrosc. 31 (2000) 407–413.

[44] H.G.M. Edwards, E.L. Dixon, I.J. Scowen, F.R. Perez, Lead-tin mirror formation from mixtures of red lead and tin sulphide, Spectrochim. Acta Part A-Molecular Biomol. Spectrosc. 59 (2003) 2291–2299. ISI:000185038100012.

[45] D. Gulotta, S. Goidanich, M. Bertoldi, S. Bortolotto, L. Toniolo, Gildings and False Gildings of the Baroque Age: Characterization and Conservation Problems, Archaeometry. 54 (2012) 940–954. doi:10.1111/j.1475-4754.2011.00658.x.

[46] J.L. Ross, Maney Publishing A Note on the Use of Mosaic Gold, Stud. Conserv. 18 (1973) 174–176.

[47] M. Merrifield, Original treatises dating from the XIIth to the XVIIIth centuries on the art of painting, John Muray, London, 1849.

[48] I. Craenhals, De *Kronieken van Vlaenderen o*ntleed: Een comparatieve materiaal-technische studie van Ms.437 en Ms.13073-74, getoetst aan de historische context en een stijlkritische analyse van beide handschriften, Master thesis University of Antwerp (2013-2014).

[46] J. Van groenland, Verluchtingen Ten Duinen en Ter Doest belicht: Een codicologische studie van de vier cisterciënzermanuscripten Ms.27, Ms.101, Ms.140 en Ms.142 die ca. 1200 werden vervaardigd, Master thesis University of Antwerp (2014-2015).

[50] G. Dogaer, Flemish Miniature Painting in the 15th and 16th Centuries, B.M.Israel BV, Amsterdam, 1987.

Chapter 5

Evaluation of portable Raman spectroscopy and handheld X-ray fluorescence analysis (hXRF) for the direct analysis of glyptics

Portable Raman spectroscopy is known for its successful application for the pigment examination of art objects, as illustrated in chapter 4. However, the use of the method is not limited to this purpose: several other applications are known such as the investigation of rock materials, minerals, etc. To prove the appropriateness of the EZRaman-I-Dual spectrometer for applications other than pigment identification, a set of 64 glyptics (42 Roman glass specimens and 22 modern ones), belonging to the collection of the museum 'Quinta das Cruzes' in Funchal (Madeira, Portugal), is examined. The advantage of having two lasers in one set-up is described.

Moreover, in previous chapters we have concentrated on the use of a single method for art analysis. However, the application of only one technique is not always sufficient to answer the research question. In the case of Raman spectroscopy, the weak Raman signal can sometimes be masked by fluorescence, which leads to missing results. Additionally, this qualitative method is not always the best to use: quantitative techniques are more suitable for provenance studies.

To gain a maximum of information, complementary techniques can be applied. Here, we demonstrate the advantage of using portable Raman spectroscopy and handheld X-ray fluorescence spectroscopy for analysing engraved gemstones or glass materials (i.e. glyptics). Raman analysis results in molecular information, whereas XRF can deliver information on the main elemental composition of the material and, where possible,

illustrate differences between samples. These techniques were also used to confirm the gemmological identification of these precious objects and they can give extra information about the glass composition.

5.1 Introduction

In archaeometry, several studies have been published demonstrating the advantages of using Raman spectroscopy combined with X-ray fluorescence (XRF) spectroscopy such as when analysing paintings, manuscripts, tiles, etc. [1–3]. Despite the complementary use of these techniques, lithic material, like stones and gemstones, is usually only studied by one of these methods [4–6].

Classically, lithic material is examined by a gemmological approach which consists of measurement of the material's physical properties (e.g. specific gravity, refractive index, thermal conductivity) and microscopic characteristics [7,8]. However, spectroscopic research provides specific information about the (elemental or molecular) composition of the material and thus results in a more complete identification [9,10]. When applying analytical methods for the characterisation of museum artefacts − in this particular case lithic material − it should be taken into account that some objects are immovable due to their size or preciousness. To avoid extensively high costs for transportation or insurance of a collection, the use of *in situ* instrumentation is a good alternative in archaeometrical research of museum artefacts [11–13].

Recently, *in situ* analysis of these precious materials, gained interest: several publications are found where *in situ* Raman or XRF spectroscopy is used for the identification of natural gems and imitations [10,14–18]. Nowadays, also the complementary use of XRF and Raman spectroscopy for these types of samples turns to be an interesting topic. Barone et al. describe a case study by using both instruments, portable Raman spectroscopy and handheld XRF spectroscopy [19]. The aim of their study was to validate the results obtained by portable Raman spectroscopy with lab instrumentation, and using XRF for the discrimination between synthetic and neutral sapphires.

In this study, we demonstrate for the first time the advantage of using both, portable Raman spectroscopy and handheld XRF spectroscopy for analysing engraved gemstones or glass materials (i.e. glyptics). Via these spectroscopic methods, a confirmation of the gemmological identification (based on visual appearance and expert gemmological knowledge) was obtained for a set of 64 glyptics (42 Roman pieces and 22 modern artefacts) which belongs to the collection of the museum 'Quinta das Cruzes' in Funchal (Madeira, Portugal) [20]. Next to this, this section aims to describe the advantages of using handheld XRF spectroscopy as well as portable Raman spectroscopy with different lasers. Moreover, next to purely identifying the materials, this methodology can also serve to discriminate between Roman glass materials and modern ones.

5.2 Experimental

5.2.1. The collection of glyptics in the museum 'Quinta das Cruzes', Funchal (Madeira, Portugal)

In this work, a collection of 64 glyptics was analysed by using different non-destructive techniques. All objects belong to the collection of the museum 'Quinta das Cruzes' in Funchal (Madeira, Portugal): it contains 112 glyptics, of which 64 pieces are displayed (Figure 5.1). Glyptics are engraved gemstones or glass objects; they consist sometimes of different layered materials. The word glyptic is derived from the Greek verb γλιπτω, a verb indicating engraving or carving on hard stones. Glyptics were originally used as stamps, to identify the owner, for instance on letters, but also on wine amphora. Later, they were also used as ornaments or as a talisman to protect the owner. The objects in the current collection, donated to the museum by César Filipe Gomes, seem to be brought together based on aesthetic aspects. The collection contains antique Roman objects (3rd century BC – 4th century AD), as well as more modern artefacts (16–19th century AD). The gemmological identification of these precious objects was based on visual analysis of the artefacts. In most of the cases, our findings confirm this identification.

Figure 5.1 <u>Top</u>: Overview of the glyptics collection at display in the museum 'Quinta das Cruzes' in Funchal (Madeira, Portugal). <u>Bottom</u>: Images of some glyphs in the collection. Numbers indicate the assigned number in the collection display case.

5.2.2. Handheld X-ray fluorescence analysis (hXRF)

All specimens in the collection were analysed by using handheld X-ray fluorescence analysis (hXRF). It is a non-destructive technique which delivers an elemental fingerprint of the material being investigated. More information about the principle can be found in the literature [21,22]. XRF spectroscopy was executed using a Bruker Tracer III-SD

spectrometer with a silicon-drift (SDD) detector (XFlash ®) and a Rh-target delivering a polychromatic X-ray beam of 3 × 3 mm for the excitation of the analysed areas. The XRF spectrometer can operate at two different settings. In this work, 74 XRF spectra were recorded: each glyptic is measured once, except when we were dealing with 'doublet' assembled gemstones. Each specimen was analysed with setting I corresponding with following conditions: tube voltage of 40 kV, tube current 30 µA, without filter and measuring time of 60 s (life time). This setting delivers information about main, side and trace elements (like Pb or Sn). Spectra were recorded with a spectral resolution of 145 eV. The X-ray source was connected to a portable PC, which allowed remotely controlling and monitoring the XRF measurements. Spectra were acquired using S1PXRF software (Bruker, version 3.8.30) and deconvoluted using the software Artax (Bruker) in order to obtain semi-quantitative data.

For this study, the instrument was positioned in a stand and the object was placed on top of the instrument (Figure 5.2a). To avoid any scattered X-rays accidentally reaching the operator or bystanders, the sample and the nozzle of the device were covered by a metal cap. The instrument was operated from a distance through USB connection with a laptop computer (Figure 5.2b). Because the analysis was performed in a museum setting, access time was limited. Therefore only one spectrum per glyptic could be recorded, except if the sample was composed of two layers of material, i.e. a 'doublet' assembled gem (e.g. Figure 5.1, glyptic 60). As a consequence, performing multivariate data analysis is limited due to the small dataset and lack of repetitive measurements.

5.2.3. Portable Raman spectroscopy

The glyptic collection was analysed by using an EZRaman-I-Dual portable Raman spectrometer of which the technical characteristics are explained in chapter 2. The laser power was reduced to ca. 50% of the maximal laser power. In the museum, we had access to 230 V AC power, so it was not needed to use the built-in batteries. During this intense measurement campaign, 290 Raman spectra were recorded using the contact lens, with typical measuring times ranging from 20 s to 120 s. All measurements were performed using contact lenses and manually holding the probes in contact with the different zones

of the glyptics (Figure 5.2c-d). A detailed characterisation of the instrument is presented elsewhere [23].

Figure 5.2 Overview of the experimental set-up during the analysis of the glyptics. a-b: Handheld XRF experiments (hXRF). c-d: portable Raman spectroscopy.

5.3 Results and discussion

5.3.1. Handheld X-ray fluorescence analysis (hXRF)

hXRF was used to evaluate whether the antique Roman glass specimens can be discriminated from the modern ones, based on the elemental composition of the glass. It is known that Roman glass, typically contains high concentrations of Na. In Roman times, natron was used as a flux, to lower the melting temperature. Therefore, it would be interesting to check the results based on this concentration. Unfortunately, the

instrumentation is limited to the detection of elements with Z > 11. Therefore, other correlations of elements were evaluated. Interesting results are found by the relationship between Pb and Sn values, both normalised to the Rh-K line (source signal) (Figure 5.3): a clear distinction can be made between lead-based glasses and non-lead-based ones (i.e. often soda-limeglasses). Lead glasses are produced in the same way as ancient glasses but a proportion of potash or natron is substituted by lead oxide [24]. Based on Figure 5.3, they are characterised by a high amount of lead and tin. It seems also that both elements are correlated with each other.
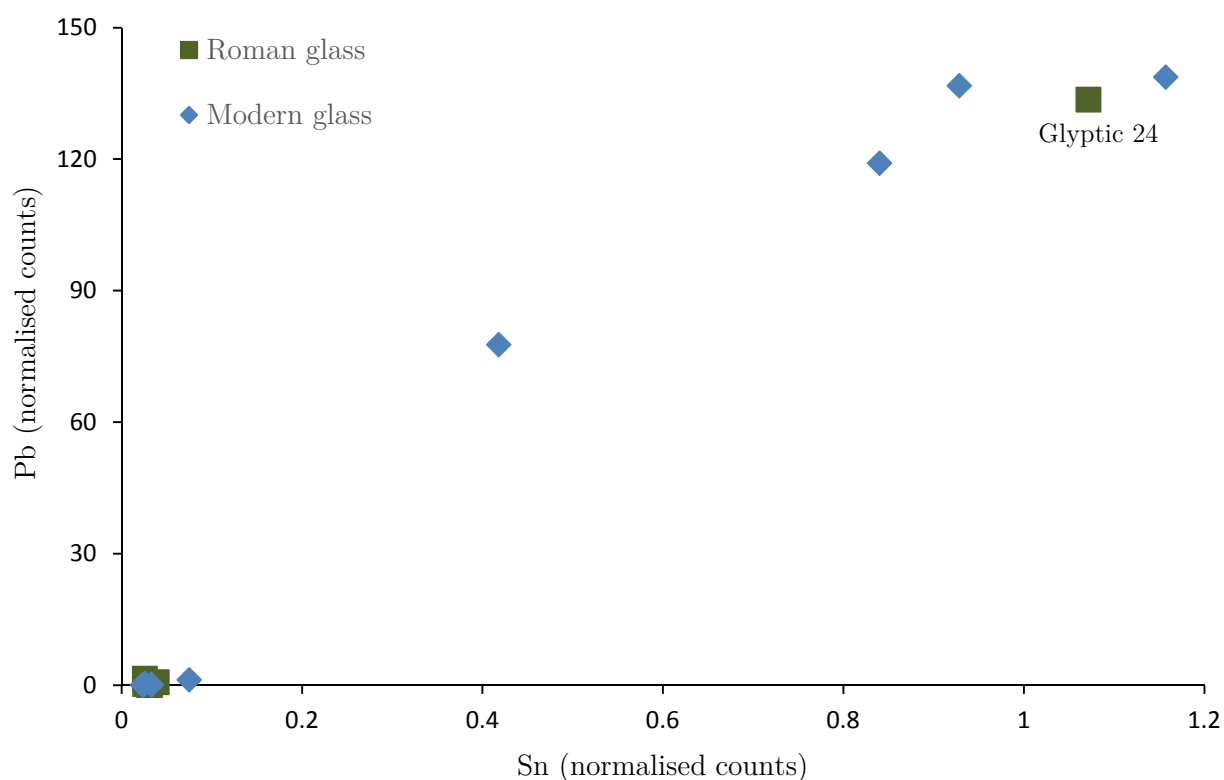
Figure 5.3 Elemental evaluation of the glyptics made out of glass: discrimination between modern and Roman samples. Relationship between lead and tin (both normalised to rhodium) showing a clear separation of lead- and non-lead-based glasses. Roman glasses are characterised by a low amount of Pb and Sn.

When taking a closer look at the graph, we see that the collection of modern glass samples is divided into two groups: lead-based samples and non-lead-based specimens. On the other hand, the Roman glass samples form a group and are characterised by a low amount of Pb and Sn. Lead glass was invented in the 17th century and thus explains

the low concentration of lead in the Roman samples [24]. Note that one outlier is observed, glyptic 24, which groups together with the lead-based, modern glasses. We suspect that by visual inspection this sample was misclassified and probably belongs to a modern production batch.

However, it should be noted that quantification of the elements in these artefacts is not straightforward, and the quantification table as produced by the handheld XRF instrument should be handled with care. At least two important reasons need to be considered. On the one hand, the sampling volume is not precisely determined and the objects may be inhomogeneous on the scale of the analysis. For handheld XRF instruments, the diameter of the X-ray bundle is typically more than 0.5 cm; the penetration depth is highly dependent on the matrix and is difficult to estimate. This inconvenience between the beam size and the sample inhomogeneity is illustrated when looking at object 60 (Figure 5.1), which seems to consist of two different materials. On the other hand, also matrix effects hamper the quantification procedure. Absorption of primary and secondary X-rays by the matrix result in a quantification that is offset. As the matrix is different for various glyptics, the extent of this effect is difficult to predict. Moreover, especially in the group of modern glasses, some lead-glasses are present, which strongly absorb the X-rays. Fortunately, the differences between antique and modern glasses are rather extreme, so these can be distinguished on qualitative grounds.

5.3.2. Portable Raman spectroscopy

On site molecular analysis of these precious artefacts was performed by using portable Raman spectroscopy. This approach is often used as analytical technique for the analysis of different minerals and gemstones. Provided the laser power is kept sufficiently low, the objects are not damaged. Moreover, the obtained spectrum contains information on the molecular composition as well as on the crystalline phases that are present. Being a molecular spectroscopic method, the technique is able to reveal the inorganic as well as the organic composition of the specimen. Although on-site Raman spectroscopic measurements are feasible, they are more complicated than measurements

carried out in the laboratory. Difficulties in orientation of the sample/the probehead and the inability to clean the mineral surface, can hamper the analysis [25].
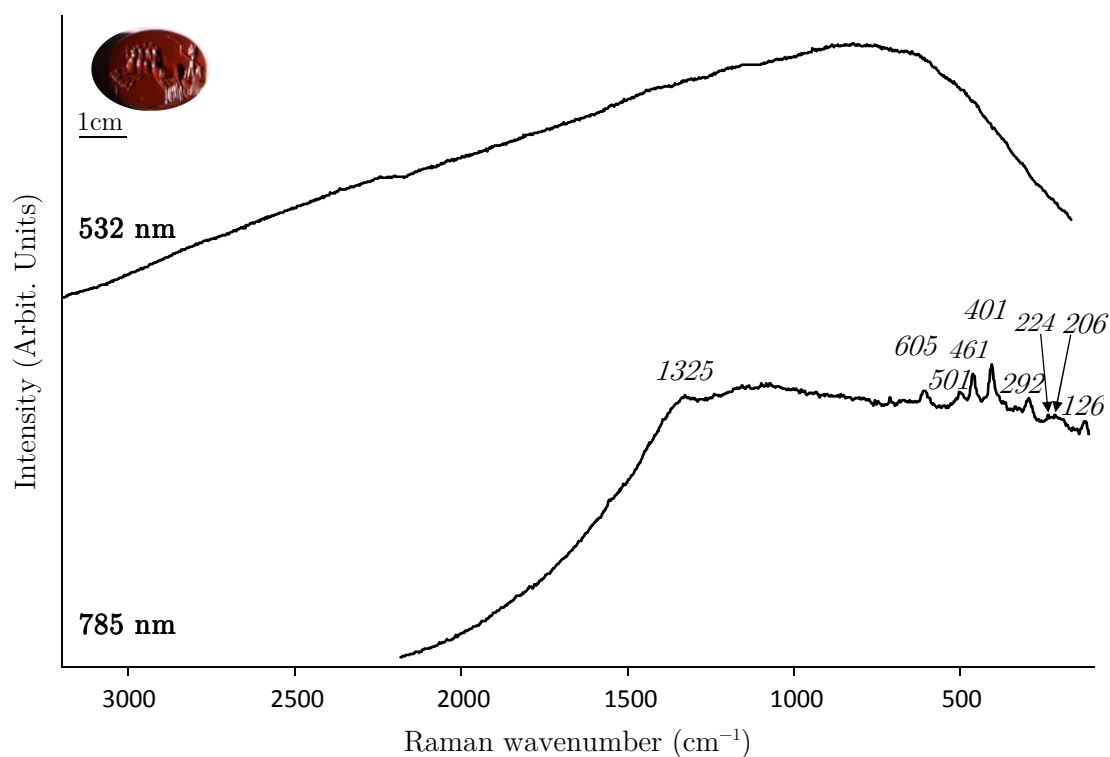
Figure 5.4 Raman spectra of glyptic 9. The spectrum recorded with the red 785 nm laser is dominated by the Raman bands of haematite (α-Fe$_2$O$_3$: 224, 292, 401, 500, 605 and 1325 cm^{-1}), α-quartz (SiO$_2$: 126, 206, 461 cm^{-1}) and a small amount of moganite (monoclinic SiO$_2$: 501 cm^{-1}); when using the green 532 nm laser only a high fluorescence signal is obtained.

A particular advantage of using the Enwave EZRaman-I-Dual portable Raman spectrometer is the availability of two different lasers. Therefore, if fluorescence overwhelms a Raman spectrum recorded with one laser wavelength, it is possible to record a spectrum by using the other laser. Figure 5.4 represents the Raman spectra, recorded for glyptic 9 using both lasers. The spectrum recorded with the red 785 nm laser is dominated by the Raman bands of haematite (α-Fe$_2$O$_3$: 224, 292, 401, 500, 605 and 1325 cm^{-1}), α-quartz (trigonal SiO$_2$: 126, 206, 461 cm^{-1}) and a small amount of moganite (monoclinic SiO$_2$: 501 cm^{-1}). When using the green 532 nm laser, only a high fluorescence signal is obtained. This can be explained by the fact that haematite strongly absorbs incoming radiation with a wavelength shorter than its optical absorption edge

(570 nm) [26]. The detection of haematite, α-quartz and moganite is in strong relationship with the gemmological identification: the visual inspection declares that glyptic 9 can be identified as the gem jasper. Jasper is an impure, opaque variety of microcrystalline silica, usually red, yellow, green or brown [27]. It is known to contain a high amount of iron oxide, mainly haematite [28].
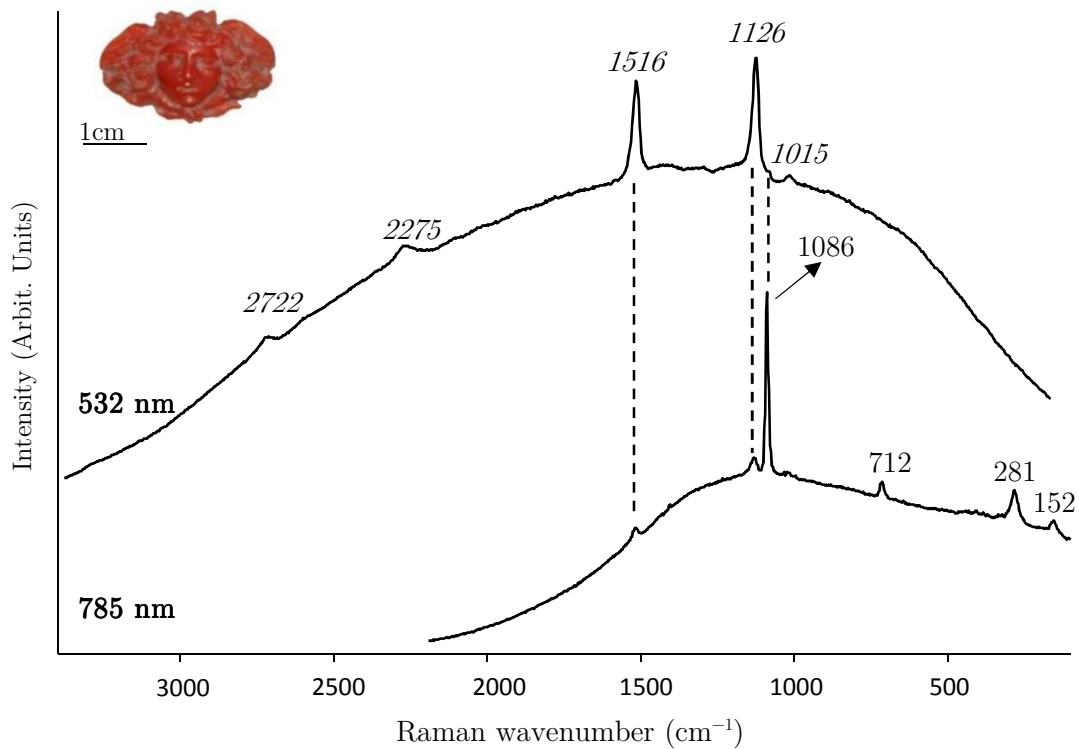
Figure 5.5 Raman spectra of glyptic 61. The spectrum recorded with the red 785 nm laser is dominated by the Raman bands of calcite; when using the green 532 nm laser a resonance Raman spectrum is recorded of the polyenes in the coral. (Band positions are indicated in italics).

Another example of the advantage of having access to two different lasers is illustrated when analysing glyptic 61, displaying a human face carved in an orange lithic material. Two Raman spectra were recorded, by using the different lasers that are available (Figure 5.5). When using the 785 nm laser, a spectrum is recorded in the wavenumber range from 100 till 2200 cm⁻¹, while when using the 532 nm laser, the recorded spectrum ranges between 165 and 3370 cm⁻¹. The spectrum as recorded with the red laser is dominated by the intense band at 1086 cm⁻¹, which together with the medium to weak bands at 712, 281, and 152 cm⁻¹ can be assigned to the presence of

calcite ($CaCO_3$). Note that although these spectra are recorded with a portable instrument, based on the Raman band positions it is straightforward to discriminate between the calcite and aragonite polymorphs of $CaCO_3$ [29]. In this spectrum, the bands at 1516 and 1126 cm^{-1} are rather weak. However, when recording a spectrum of the same object with the green laser, the latter two bands are very strong. Carotenoids and polyenes are well-known to show resonance enhancement when irradiated with a 532 nm laser. These bands are assigned to the in-phase v_1(C=C) and v_2(C–C) stretching vibrations [30,31]. The exact band positions can be related to the length of the polyene chain [32]. Although it is difficult to assign these bands to a specific molecule, as band positions may shift slightly due to matrix effects and the folding of the chain [33,34], the v(C–C) band position seems more likely to correspond to a non-methylated polyene than to a carotenoid, that typically shows this band at ca. 1155 cm^{-1} [35]. Our observed band positions are similar to those reported for the coral species Coenaculum secundum (514 nm laser: 1520, 1130, 1088 cm^{-1}) [36], Leptogorgia punicea (632 nm laser: 1512, 1126, 1090, 1020 cm^{-1}), and Lespedeza violacea (632 nm laser: 1510, 1125, 1090, 1020 cm^{-1}) [35]. Not only the bands at 1126 and 1512 cm^{-1} are of interest, also the overtone bands at 2265 cm^{-1} (2 v_2) and 2642 cm^{-1} (v_1+v_2) have a significant value to the identification polyenes or carotenoids [37–40]. This proves again that the presence of two lasers is of great advantage: the red laser has a low quantum efficiency of the CCD-detector at higher wavenumbers, which is not the case for the green laser [41].

5.3.3. Confirmation of gemmological identification

After the demonstration of the beneficial use of both instruments, we want to illustrate the advantage of using both complementary techniques for the identification of the materials of the glyptic collection. Based on the gemmological identification, five main materials can be found in the assemblage: the collection mainly consists of chalcedony (most often carnelian), jasper, coral, glass and porcelain glyptics. All these materials, except coral, are silicates. Therefore, Si is an interesting element for investigation. As mentioned, XRF and Raman spectroscopy are applied to confirm the existing identification and to give additional information. In a first step, hXRF is used to discriminate the different types of samples based on their elemental composition.

When evaluating the correlation of the peak intensities of Fe and Si – normalised to Rh-K – (Figure 5.6), the jasper samples can clearly be distinguished from the other materials. Jasper is known to be analogues of low-temperature, hydrothermal iron deposits [27,42]. It is an opaque rock that owes its colour to the mineral content of the original sediment or ash, mainly iron oxides, and are commonly associated with massive sulphide deposits [43]. This can explain the high iron signal in the elemental fingerprint and thus results in the separation of jasper in the plot. Additionally, Raman spectroscopy (Figure 5.4) has proven that the jasper samples of the collection are composed of micro-crystalline quartz with a high amount of iron oxide, mainly haematite.

Not only jasper has a red colour in the museum collection as this applies also to the carnelians. This type is mainly composed of silica, as well as the jasper samples, is characterised by translucency, and has a hue from yellowish orange to orange and from deep red to brownish red. But why are they not showing a significant amount of iron in their elemental composition? An explanation can be found in the treatment of the gem, before its use. It is known that this type of gems were dyed or heated to improve their optical appearance or to enhance their colour [44]. So it can be suggested that the original carnelian was probably less intense in colour. Consequently, the impurities, which are responsible for the hue such as iron, are less represented and thus a low amount is detected. Carnelian belongs to the general group of chalcedony gems which are characterised by the presence of micro- or crypto-crystalline varieties of silica. The main component of chalcedony is α-quartz; it also contains minor component moganite and a lot of opacifying and colouring impurities [45,46]. The Raman spectra of all varieties of chalcedony samples – carnelian, agate, amethyst, nicolo, sard, plasma – show the same bands. A representative example is given in Figure 5.7a: the bands observed at 123 (E), 201 (A_1), 462 (A_1), 802 (E_{LO}), 1067 (E_{TO}), 1154 ($E_{(LO+TO)}$) cm^{-1} are corresponding to α-quartz; the one at 500 cm^{-1} (v(Si–O–Si) symmetric stretching mode) can be assigned to moganite [47,48]. Some of the Raman spectra also have bands at 1147, 1227, 1282 cm^{-1} that probably correspond to an organic red dye. This supports the assumption made for the low presence of iron. As a drawback, it can be said that Raman spectroscopy can only be used to identify the general type 'chalcedony'. To determine the subgroup, complementary micro and macroscopic investigation is needed. The XRF data-analysis

was able to distinguish this type of glyptic from the others (Figure 5.6), characterised by a high amount of silicon and a low amount of iron.
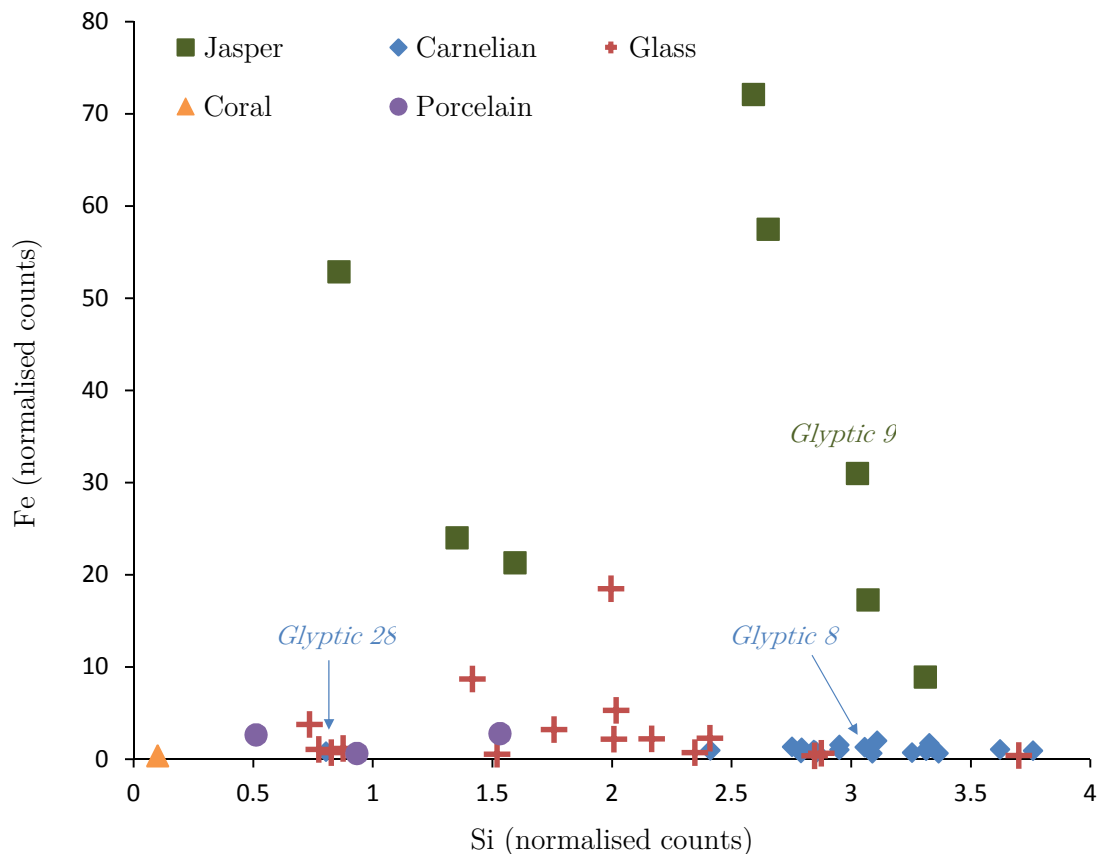
Figure 5.6 Elemental evaluation of the glyptics: discrimination between the five major types of sample within the collection. Relationship between iron and silicon (both normalised to rhodium) showing a clear grouping of coral, carnelian samples and jasper samples. As expected, the porcelain objects cannot be distinguished from the glass artefacts.

However, when taking a closer look at the graph, one outlier is observed (glyptic 28): it seems that this sample belongs to the group of glass objects instead of the carnelian artefacts. In a situation like this, Raman spectroscopy is of great help to give more insight on why this sample is not belonging to the carnelian group. Figure 5.7b represents the Raman spectrum obtained for this sample. The lack of sharp bands and the general shape of the Raman spectrum suggest the identification as a glassy silicate. However, the bands are detected at higher wavenumbers than usual aluminosilicates.

When evaluating the spectrum, three bands are observed on top of the high fluorescence signal: 1336, 1236 and 1146 cm^{-1}. Because they are detected at higher wavenumbers than the ones characteristic for general aluminosilicates [49–51], probably we are dealing with an other type of silicate. However, due to the lack of the more intense Raman bands at lower wavenumbers only an assumption can be made of the composition. Literature supports the idea that maybe the glyptic is composed of a borosilicate glass [52–54]. Modification of the connectivity of the (SiO_4) polymeric network due to the presence of boron oxide gives a characteristic band at 1336 cm^{-1} that corresponds to B–O stretching vibration of non-bounded BO_3 in the silicate network. More specifically, lead based borosilicate is thought to be identified. The XRF results support this observation: a significant amount of lead is detected. Due to the low atomic number of B, this element could not be detected. The high frequency band should occur at 1350 cm^{-1} but the presence of a concentration of PbO attributes to a shift towards a lower Raman position [55,56]. The band at 1236 cm^{-1} and 1146 cm^{-1} can be assigned to B–O stretching vibration of pyroborate and to Si–O vibration, respectively [57]. It needs to be noted that this detected Raman spectrum corresponds with some of the other Raman spectra of the modern glass materials in the collection. Figure 5.6 shows that the glass materials can be separated from the other artefacts in the collection, except from the porcelain samples, and show an intermediate amount of Si and low amount of Fe. However, different types of glasses (soda-limeglasses, lead glasses etc.) cannot be observed in this graph. Nevertheless, as described in section 5.3.1 it was possible to make a distinction between lead based glasses and non-lead based ones (Figure 5.3). More specifically, it has been concluded that the lead based glasses belong to the modern samples and the Roman glasses are characterised by a low amount of lead. The difference in elemental fingerprint of a lead based, modern glass (glyptic 57) and a Roman fragment (glyptic 5), is represented in Figure 5.8.

Finally, the coral sample seems to be characterised by a low amount of Fe and Si. The Raman results have shown that the sample is mainly composed of calcium carbonate and polyene (based on the Raman results, Figure 5.5). However, no clear conclusion about coral objects can be drawn, as we are dealing with only one sample..
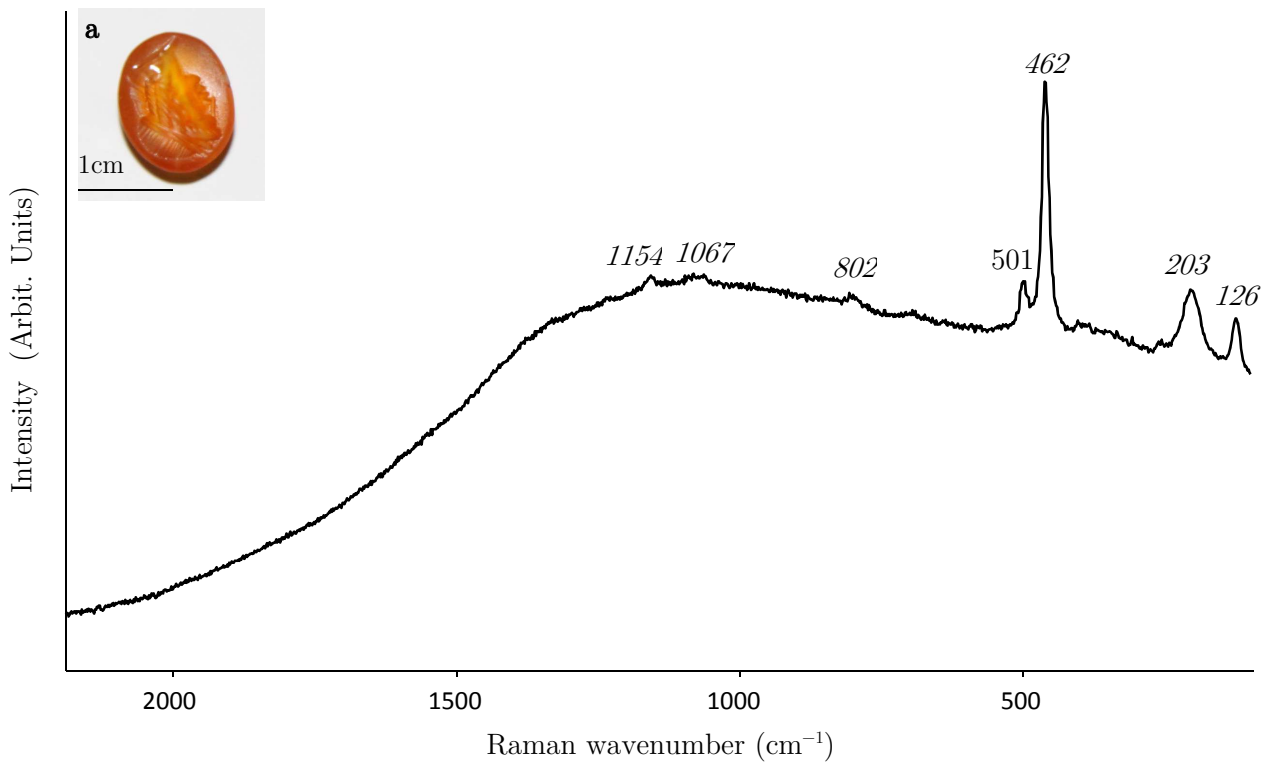
Figure 5.7 (a) Raman spectrum of glyptic 8 recorded with 785 nm laser for 30x4 s. Characteristic bands of chalcedony are detected: bands of α-quartz (band positions are indicated in italics) and moganite are found.
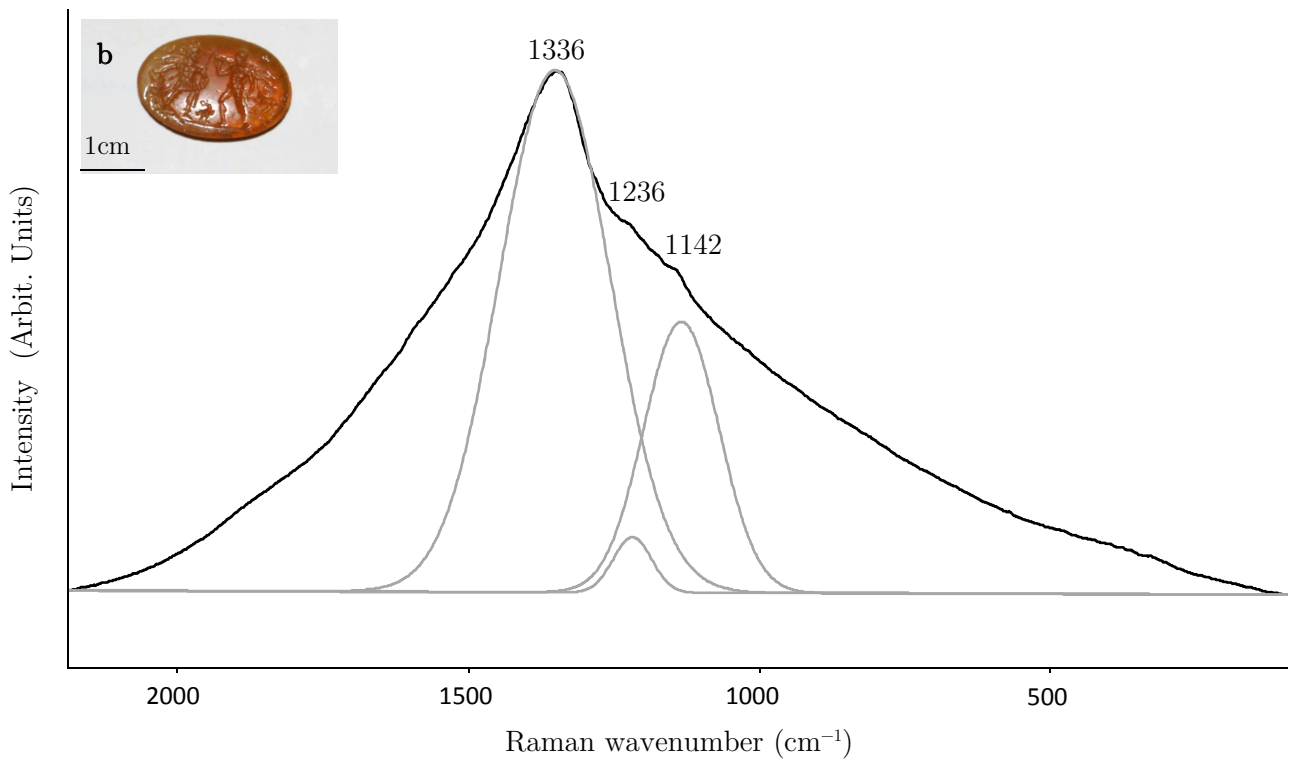
Figure 5.7 (b) Raman spectrum of glass (glyptic 28) recorded with 785nm laser for 30x4 s. The bands can be assigned to a borosilicate glass.
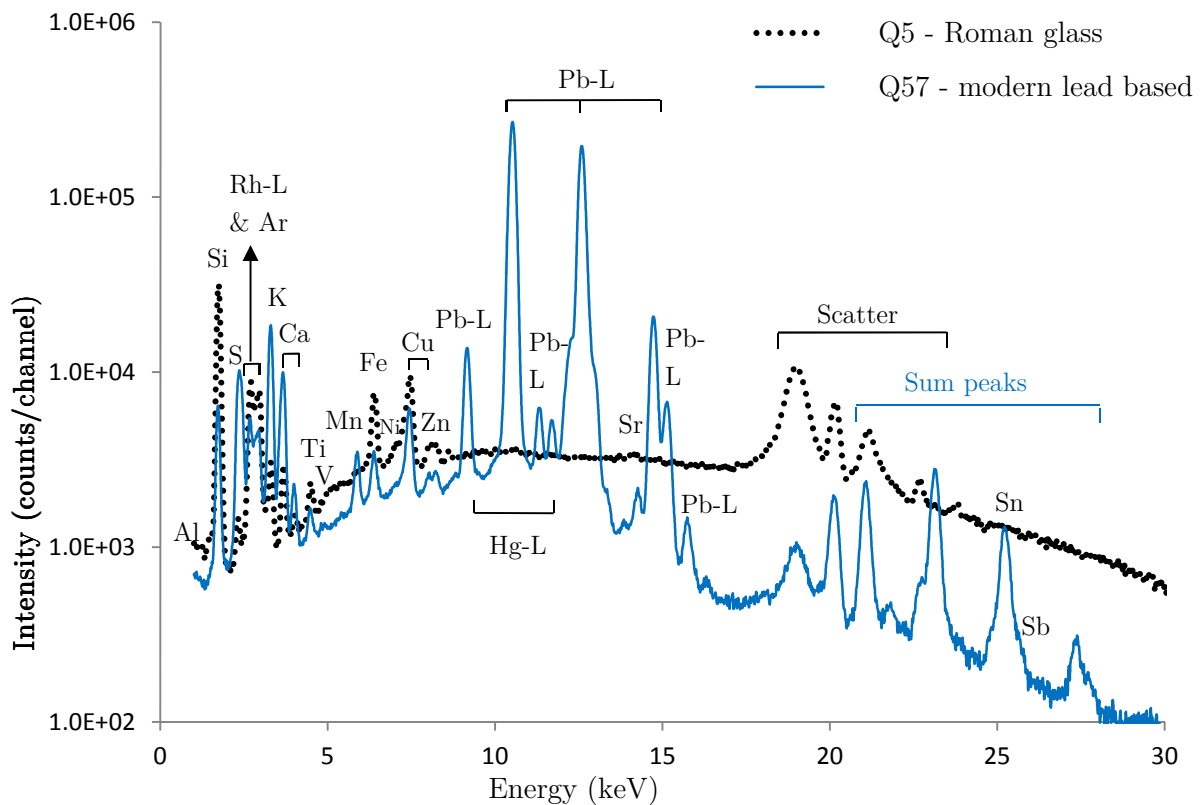
Figure 5.8 Stacked XRF spectra of a lead based, modern glass (glyptic 57) and a Roman fragment (glyptic 5), illustrating the difference in elemental fingerprint.

5.4 Conclusions

This case study has confirmed that both techniques, portable Raman spectroscopy and handheld X-ray fluorescence spectroscopy, are well suited for the analysis of glyptics. The combined use of Raman spectroscopy and XRF spectroscopy leading to more successful identification of the material used have been discussed. Finally, the research was completed with a confirmation of the gemmological identification. Information about the molecular composition as well as the crystalline phases is obtained. The XRF analysis results in a clear distinction between the different types of material, present in the collection. Additionally, more information is gained about the glass materials used in Roman and modern times.

Moreover, it should be stressed that during *in situ* analysis some problems always need to be considered. A general issue is the time constraint for the research. When more measurement time would be available, more measurements can be performed. This can lead to more data and repetitive results, inducing the possibility to perform statistical data treatment to visualise significant differences between different types of samples. In the case of X-ray fluorescence spectroscopy, quantification of should be considered. Raman spectroscopy on the other hand, has the practical issues that crystal orientation and the inability to clean the mineral surfaces can hamper the results. Despite these issues, both techniques are well suited for the analysis of engraved gemstones.

In this chapter, it was explained that the combined use of Raman spectroscopy and XRF spectroscopy is beneficial for art analysis. Both methods have their advantages and disadvantages but they can support each other: where one technique fails, the other one can give interesting results. In addition, a combination of results can lead to better conclusions. Nevertheless, as the focus of the PhD mainly lies on the application of mobile Raman spectroscopy an extra note has to be made. Until now, we were able to figure out characteristics which are of importance for the optimal use of the EZRaman-I-Dual portable Raman spectrometer for art analysis, based on the case studies of pigment analysis (chapter 4) and the investigation of gemstones (chapter 5). This knowledge can be used for future applications to work more efficiently and rapidly and can serve as a starting point for further optimisation. However, this instrument is not the only one available on the market. In the next chapter, the properties of this instrument are compared to other mobile spectrometers on the market, including a Raman spectrometer that is equipped with a longer wavelength (1064 nm).

5.5 References

[1] L. Van De Voorde, J. Van Pevenage, K. De Langhe, R. De Wolf, B. Vekemans, L. Vincze, et al., Non-destructive *in situ* study of "mad Meg" by Pieter Bruegel the Elder using mobile X-ray fluorescence, X-ray diffraction and Raman spectrometers, Spectrochim. Acta Part B At. Spectrosc. 97 (2014) 1–6. doi:10.1016/ j.sab.2014.04.006.

[2] L. Van de Voorde, M. Vandevijvere, B. Vekemans, J. Van Pevenage, J. Caen, P. Vandenabeele, et al., Study of a unique 16th century Antwerp majolica floor in the Rameyenhof castle's chapel by means of X-ray fluorescence and portable Raman analytical instrumentation, Spectrochim. Acta Part B At. Spectrosc. 102 (2014) 28–35. doi:10.1016/j.sab.2014.10.007.

[3] A. Duran, M.L. Franquelo, M.A. Centeno, T. Espejo, J.L. Perez-Rodriguez, Forgery detection on an Arabic illuminated manuscript by micro-Raman and X-ray fluorescence spectroscopy, J. Raman Spectrosc. 42 (2011) 48–55. doi:10.1002/ jrs.2644.

[4] J. Dong, Y. Han, J. Ye, Q. Li, S. Liu, D. Gu, *In situ* identification of gemstone beads excavated from tombs of the Han Dynasties in Hepu county, Guangxi Province, China using a portable Raman spectrometer, J. Raman Spectrosc. 45 (2014) 596–602. doi:10.1002/jrs.4501.

[5] T. Katsaros, T. Ganetsos, Raman Characterization of Gemstones from the Collection of the Byzantine & Christian Museum, Archaeology. 1 (2012) 7–14. doi:10.5923/j.archaeology.20120102.01.

[6] O. Williams-Thorpe, P.J. Potts, P.C. Webb, Field-portable non-destructive analysis of lithic archaeological samples by x-ray fluorescence instrumentation using a mercury iodide detector: comparison with wavelength-dispersive XRF and a case study in British stone axe provenancing, J. Archaeol. Sci. 26 (1999) 215–237. doi:10.1006/jasc.1998.0323.

[7] J.E. Shigley, A Review of Current Challenges for the Identification of Gemstones, Geologija. 50 (2008) 227–236.

[8]   J.I. Koivula, R.C. Kammerling, D. DeGhionno, I. Reinitz, E. Fritsch, M.L. Johnson, Gemological Investigation of a New Type of Russian Hydrothermal Synthetic Emerald, Gems Gemol. 32 (2008) 32–39. doi:10.5741/GEMS.32.1.32.

[9]   D. Bersani, P.P. Lottici, Applications of Raman spectroscopy to gemology, Anal. Bioanal. Chem. 397 (2010) 2631–2646. doi:10.1007/s00216-010-3700-1.

[10]   Z. Petrová, J. Jehlička, T. Čapoun, R. Hanus, T. Trojek, V. Goliáš, Gemstones and noble metals adorning the sceptre of the faculty of science of charles university in prague: Integrated analysis by Raman and XRF handheld instruments, J. Raman Spectrosc. 43 (2012) 1275–1280. doi:10.1002/jrs.4043.

[11]   A.G. Karydas, D. Kotzamani, R. Bernard, J.N. Barrandon, C. Zarkadas, A compositional study of a museum jewellery collection (7th-1st BC) by means of a portable XRF spectrometer, Nucl. Instruments Methods Phys. Res. Sect. B Beam Interact. with Mater. Atoms. 226 (2004) 15–28. doi:10.1016/j.nimb.2004.02.034.

[12]   H.G.M. Edwards, P. Vandenabeele, Overview: Raman Spectroscopy of Artefacts, in: Raman Spectrosc. Archaeol. Art Hist., Royal Society of Chemistry, 2005: 174.

[13]   G. Van der Snickt, C. Miliani, K. Janssens, B.G. Brunetti, A. Romani, F. Rosi, et al., Material analyses of "Christ with singing and music-making Angels", a late 15th-C panel painting attributed to Hans Memling and assistants: Part I- non-invasive *in situ* investigations, J. Anal. At. Spectrom. 26 (2011) 2216–2229. doi:10.1039/c1ja10073d.

[14]   L. Pappalardo, A.G. Karydas, N. Kotzamani, G. Pappalardo, F.P. Romano, C. Zarkadas, Complementary use of PIXE-alpha and XRF portable systems for the non-destructive and *in situ* characterization of gemstones in museums, Nucl. Instruments Methods Phys. Res. Sect. B Beam Interact. with Mater. Atoms. 239 (2005) 114–121. doi:10.1016/j.nimb.2005.06.184.

[15]   I. Liritzis, N. Zacharias, Chapter 6: Portable XRF of archaeological artifacts: current research, potentials and limiations, in: M.S. Shackley (Ed.), X-Ray Fluoresc. Spectrom. Geoarchaeology, Springer science, 2011: pp. 109–142. doi:10.1007/978-1-4419-6886-9_6.

[16] L.L. Reiche I., Pages-Camagna S., *In situ* Raman spectroscopic investigations of the adorning gemstones on the reliquary Heinrich's Cross from the treasury of Basel Cathedral, J. Raman Spectrosc. 35 (2004) 719–725. ISI:000223113600019.

[17] K. Osterrothová, L. Minaříková, A. Culka, J. Kuntoš, J. Jehlička, *In situ* study of stones adorning a silver Torah shield using portable Raman spectrometers, J. Raman Spectrosc. 45 (2014) 830–837. doi:10.1002/jrs.4541.

[18] G. Barone, D. Bersani, J. Jehlička, P.P. Lottici, P. Mazzoleni, S. Raneri, et al., Non-destructive investigation on the 17-18th centuries Sicilian jewelry collection at the Messina regional museum using mobile Raman equipment, J. Raman Spectrosc. (2015). doi:10.1002/jrs.4649.

[19] G. Barone, D. Bersani, V. Crupi, F. Longo, U. Longobardo, P.P. Lottici, et al., A portable versus micro-Raman equipment comparison for gemmological purposes: the case of sapphires and their imitations, J. Raman Spectrosc. 45 (2014) 1309–1317. doi:10.1002/jrs.4555.

[20] Glyptic Collection, (n.d.). http://mqc.gov-madeira.pt/en-GB/Coleccoes_ing/joalharia_ing/ContentDetail.aspx?id=333 (accessed June 4, 2015).

[21] B. Beckhoff, B. Kanngieß, N. Langhoff, R. Wedell, H. Wolff, Handbook of Practical X-Ray fluorescence analysis, Springer Berlin Heidelberg, 2006.

[22] R. Van Grieken, A. Markowicz, Handbook of X-Ray Spectrometry, 2nd edition, Crc Press, 2001.

[23] D. Lauwers, A.G. Hutado, V. Tanevska, L. Moens, D. Bersani, P. Vandenabeele, Characterisation of a portable Raman spectrometer for *in situ* analysis of art objects, Spectrochim. Acta. A. Mol. Biomol. Spectrosc. 118 (2013) 294–301. doi:10.1016/j.saa.2013.08.088.

[24] S. Davison, R.G. Newton, Conservation and restoration of Glass, 2nd edition, Elsevier Science Ltd, 2003.

[25] P. Vandenabeele, H.G.M. Edwards, J. Jehlička, The role of mobile instrumentation in novel applications of Raman spectroscopy: archaeometry, geosciences, and forensics, Chem. Soc. Rev. 43 (2014) 2628–2649. doi:10.1039/c3cs60263j.

[26] J. Wang, W.B. White, J.H. Adair, Optical properties of hydrothermally synthesized hematite particulate pigments, J. Am. Ceram. Soc. 88 (2005) 3449–3454. doi:10.1111/j.1551-2916.2005.00643.x.

[27] J. Zöldföldi, Gemstones at Qaṭna Royal Tomb : Preliminary Report, in: P. Pfälzner (Ed.), Interdiszip. Stud. Zur Königsgruft Qatna, 1st ed., Harrassowitz Verlag, 2011: pp. 234–248.

[28] C.T.S. Little, S.E.J. Glynn, R.A. Mills, Four-Hundred-and-Ninety-Million-Year Record of Bacteriogenic Iron Oxide Precipitation at Sea-Floor Hydrothermal Vents, Geomicrobiol. J. 21 (2004) 415–429. doi:10.1080/01490450490485845.

[29]   H.G.M. Edwards, S. Villar, J. Jehlicka, T. Munshi, FT-Raman spectroscopic study of calcium-rich and magnesium-rich carbonate minerals, Spectrochim. Acta Part A-Molecular Biomol. Spectrosc. 61 (2005) 2273–2280. ISI:000231027600002.

[30] J.C. Merlin, Resonance Raman spectroscopy of carotenoids and carotenoid-containing systems, Pure Appl. Chem. 57 (1985) 785–792. doi:10.1351/pac198557050785.

[31] I. Agalidis, T. Mattioli, F. Reiss-Husson, Spirilloxanthin is released by detergent from Rubrivivax gelatinosus reaction center as an aggregate with unusual spectral properties, Photosynth. Res. 62 (1999) 31–42. doi:10.1023/A:1006384113191.

[32] L. Brambilla, M. Tommasini, G. Zerbi, R. Stradi, Raman spectroscopy of polyconjugated molecules with electronic and mechanical confinement: The spectrum of Corallium rubrum, J. Raman Spectrosc. 43 (2012) 1449–1458. doi:10.1002/jrs.4057.

[33] V.E. de Oliveira, H.V. Castro, H.G.M. Edwards, L.F.C. de Oliveira, Carotenes and carotenoids in natural biological samples: A Raman spectroscopic analysis, J. Raman Spectrosc. 41 (2010) 642–650. doi:10.1002/jrs.2493.

[34] J. Jehlička, A. Oren, Use of a handheld Raman spectrometer for fast screening of microbial pigments in cultures of halophilic microorganisms and in microbial communities in hypersaline environments in nature, J. Raman Spectrosc. 44 (2013) 1285–1291. doi:10.1002/jrs.4362.

[35] L.F. Maia, B.G. Fleury, B.G. Lages, J.P. Barbosa, À.C. Pinto, H. V. Castro, et al., Identification of reddish pigments in octocorals by Raman spectroscopy, J. Raman Spectrosc. 42 (2011) 653–658. doi:10.1002/jrs.2758.

[36] S. Karampelas, E. Fritsch, B. Rondeau, A. Andouche, B. Métivier, Identification of the endangered pink-to-red stylaster corals by Raman spectroscopy, Gems Gemol. 45 (2009) 48–52.

[37] M. Tommasini, G. Longhi, S. Abbate, G. Zerbi, Theoretical investigation and computational evaluation of overtone and combination features in resonance Raman spectra of polyenes and carotenoids, J. Raman Spectrosc. 45 (2014) 89–96. doi:10.1002/jrs.4415.

[38] Y.-Z. Chen, S. Li, M. Zhou, Z.-W. Li, C.-L. Sun, A polyene chain of canthaxanthin investigated by temperature-dependent resonance Raman spectra and density functional theory (DFT) calculations, Chinese Phys. B. 22 (2013) 083301. doi:10.1088/1674-1056/22/8/083301.

[39] J. Urmos, S.K. Sharma, F.T. Mackenzie, Characterization of some biogenic carbonates with Raman spectroscopy, Am. Mineral. 76 (1991) 641–646.

[40] T. Kupka, H.M. Lin, L. Stobiński, C.H. Chen, W.J. Liou, R. Wrzalik, et al., Experimental and theoretical studies on corals. I. Toward understanding the origin of color in precious red corals from Raman and IR spectroscopies and DFT calculations, J. Raman Spectrosc. 41 (2010) 651–658. doi:10.1002/jrs.2502.

[41] P. Vandenabeele, Practical Raman Spectroscopy: An introduction, John Wiley & Sons, Ltd., 2013.

[42] M. Halbach, P. Halbach, V. Lüders, Sulfide-impregnated and pure silica precipitates of hydrothermal origin from the Central Indian Ocean, Chem. Geol. 182 (2002) 357–375. doi:10.1016/S0009-2541(01)00323-0.

[43] T. Grenne, J.F. Slack, Bedded jaspers of the Ordovician Lokken ophiolite, Norway: Seafloor deposition and diagenetic maturation of hydrothermal plume-derived silica-iron gels, Miner. Depos. 38 (2003) 625–639. doi:10.1007/s00126-003-0346-3.

[44] F.H. Pough, R.T. Peterson, J. Scovil, Rocks and minerals, Houghton Mifflin Harcourt, 1995.

[45] W. Schumann, Gemstones of the world, Sterling Publishing Company, 2009.

[46] D. Pop, C. Constantina, D. Tătar, W. Kiefer, Raman spectroscopy on gem-quality microcrystalline and amorphous silica varieties from romania, Geologia. XLIX (2004) 41–52.

[47] P.F. MacMillan, A.S. Hess, Ab Initio Valence Force Field Calculations for Quartz, Phys. Chem. Miner. 17 (1990) 97–107.

[48] A.C. Prieto, O. Martinez, J. Souto, M. Avella, A. Guedes, Study of a tabernacle with a remarkable architectural structure: *In situ* examination using Raman spectroscopy, J. Raman Spectrosc. 44 (2013) 1156–1162. doi:10.1002/jrs.4346.

[49] D.A. McKeown, F.L. Galeener, G.E. Brown, Raman studies of Al coordination in silica-rich sodium aluminosilicate glasses and some related minerals, J. Non. Cryst. Solids. 68 (1984) 361–378. doi:10.1016/0022-3093(84)90017-6.

[50] P. Colomban, Polymerization degree and Raman identification of ancient glasses used for jewelry, ceramic enamels and mosaics, J. Non. Cryst. Solids. 323 (2003) 180–187. doi:10.1016/S0022-3093(03)00303-X.

[51] P. Colomban, On-site Raman identification and dating of ancient glasses: A review of procedures and tools, J. Cult. Herit. 9 (2008) e55–e60. doi:10.1016/j.culher.2008.06.005.

[52] S.V. Stefanovsky, K.M. Fox, J.C. Marra, Infrared and Raman Spectroscopic Study of Glasses in the Al2O3-B2O3-Fe2O3-Na2O-SiO2 System, MRS Proc. 1518 (2013) 53–58. doi:10.1557/opl.2013.143.

[53] D. Manara, A. Grandjean, D.R. Neuville, Advances in understanding the structure of borosilicate glasses: A raman spectroscopy study, Am. Mineral. 94 (2009) 777–784. doi:10.2138/am.2009.3027.

[54] P. Colomban, F. Treppoz, Identification and differentiation of ancient and modern European porcelains by Raman macro- and micro-spectroscopy, J. Raman Spectrosc. 32 (2001) 93–102. doi:10.1002/jrs.678.

[55] B.N. Meera, A.K. Sood, N. Chandrabhas, J. Ramakrishna, Raman study of lead borate glasses, J. Non. Cryst. Solids. 126 (1990) 224–230. doi:10.1016/0022-3093(90)90823-5.

[56] B.N. Meera, J. Ramakrishna, Raman spectral studies of borate glasses, J. Non. Cryst. Solids. 159 (1993) 1–21. doi:10.1016/0022-3093(93)91277-A.

[57] R.K. Brow, D.R. Tallant, G.L. Turner, Polyhedral Arrangements in Lanthanum Aluminoborate Glasses, J. Am. Soc. 80 (1997) 1239–1244. doi:10.1111/j.1151-2916.1997.tb02970.x.

Chapter 6

Non-destructive Raman investigations on wall paintings at Sala Vaccarini in Catania (Sicily)

A wide variety of analytical techniques can be applied in cultural heritage. As illustrated in chapter 5, the use of complementary techniques for art analysis can result in a complete characterisation of the investigated material. Various methods result in complementary information but within a single method, diverse instrumentation can deliver different or similar results. This will be illustrated in more detail for portable Raman spectroscopy, as it is the general topic of this thesis.

Recently, an increasing number of mobile Raman spectrometers have become available and are designed for a broad range of applications. When selecting a suitable Raman spectrometer, different characteristics (spectroscopic and in situ related issues) need to be considered as described in chapter 3. However, the selection of the excitation source is still a topic that needs amplification. Spectrometers with different excitation sources are available (i.e. different laser wavelength) and it is useful to evaluate which excitation wavelength is of greater interest for art analysis. In this chapter, the EZRaman-I-Dual spectrometer, equipped with a 785 and 532 nm laser, is compared with a 1064 nm Raman equipment for its suitability. The examination is executed during the study of 17th century Sicilian wall paintings (Catania) that was acquired to provide an in situ diagnostic analysis of the paintings (in terms of colourants and preparation layer) and to support the conservators in the framework of the ongoing restoration.

6.1 Introduction

After the well-known earthquake in 1693, the southeastern Sicilian towns experienced a lively architectonic and artistic season. The earthquake destroyed, partially or entirely, approximately fifty urban centers and intensive reconstruction work then started. In this framework, the Baroque architectural style flourished and the majority of the newly constructed monuments exhibited standards of beauty devoted to emphasize volumes and voids. The new artistic rules were applied in the buildings from outside to inside: painters revoked from the entire island decorated the rebuilt private and public buildings, cathedrals, and churches with exquisite frescoes on the walls and on the vaults. The town of Catania was widely reconstructed and new monumental buildings were also established in the urban center. Among the protagonists and the financiers of the restoration and construction works, the Benedictine Monasteries of San Nicolò stand out. They decided to take advantage of the earthquake to transfer their monastery to the urban center of Catania, where they built a huge Benedictine Monastery following the coeval artistic style. A large number of architects were invited to work at this project and numerous painters were mobilised in order to marvelously adorn the buildings.

The Monastery is nowadays considered the second in the world for relevance and extension [1] and has been included since 2002 in the UNESCO Heritage List. Due to its relevance, the Monastery has therefore to be preserved and conserved. The preservation of such structures is quite complex, due to the association of different materials and parts (*i.e.*: masonry, substrate, wall paintings, etc.). Regarding wall paintings, numerous agents (external ones as well as those which are strictly related to the standing buildings) can affect their integrity and only appropriate restoration works can assure the maintenance of these object of art without damaging risks. In this sense, the planning of preliminary diagnostic campaigns is always highly recommended; archaeometric analyses can in fact help conservators, and provide art historians with precise information about techniques and materials employed by the artists.

Among the paintings decorating the buildings of the Benedictine Monastery, the 17th century wall paintings on the vaults of the *Sala Vaccarini* Library are really fascinating. Several attempts of restoration were performed during the 19th century, mainly carried out in invasive way and without the support of appropriate diagnostic activities. For these reasons, part of the scenes was evidently damaged and, in 2014, a new restoration work was started with the aim to bring the frescoes to a more coherent appearance. This was an excellent opportunity to examine the artworks in order to establish an *in situ* diagnostic analysis of the wall paintings (in terms of colourants and preparation layer) and to support the conservators in the framework of the ongoing restoration. Of course, in consideration of the preciosity of the paintings, the application of non-invasive and non-destructive methodologies was required; among them, Raman spectroscopy has recently assessed as particularly suitable tool for the diagnosis of art-objects, especially for paintings, plasters and mortars [2-5]. The method allows in fact the quick, non-destructive, and contactless characterisation and identification of inorganic and organic materials, widely employed in art and archaeometry. Additionally, the development of mobile instruments designed for *in situ* archaeometrical research, brought this analytical method back to the top, especially in the case of unmovable artworks.

Therefore, in this study, an approach based on portable Raman spectroscopic analysis has been applied to the paintings decorating the Sala Vaccarini Library with the aim to characterise (a) the pigments used by the painter; (b) the artistic technique employed; (c) the possible presence of overpaint and (d) the state of preservation of frescoes, including eventual degradation products and/or alteration of pigments.

6.2 Materials and method

6.2.1. Studied wall paintings

The investigated wall paintings are located on the vaults of the *Sala Vaccarini*, one of the exquisite Libraries part of the 16th century monumental complex of Benedictine

Monastery in Catania (Sicily, Italy). The construction of the Library, which would host the rich manuscript collections harvested by the Monasteries over the time, was directed by the architect Giovanni Battista Vaccarini. Finished in 1773, the Library currently preserves its original structural arrangement and numerous volumes collected by the Monastery as well as precious manuscripts. Besides the book collections, the wall paintings on the vaults represent one of the most fascinating aspects of the Library. They were realised in 17th century by the Sicilian painter Giovanni Battista Piparo using the fresco technique (according to bibliographic sources) and exhibit medallions with symbolic representation of Virtues, Arts and Sciences.

Among the medallions, four scenes have been selected for Raman spectroscopic analysis (Figure 6.1), being representative of the "artist's palette" and exhibiting several conservation issues as well as degraded areas.
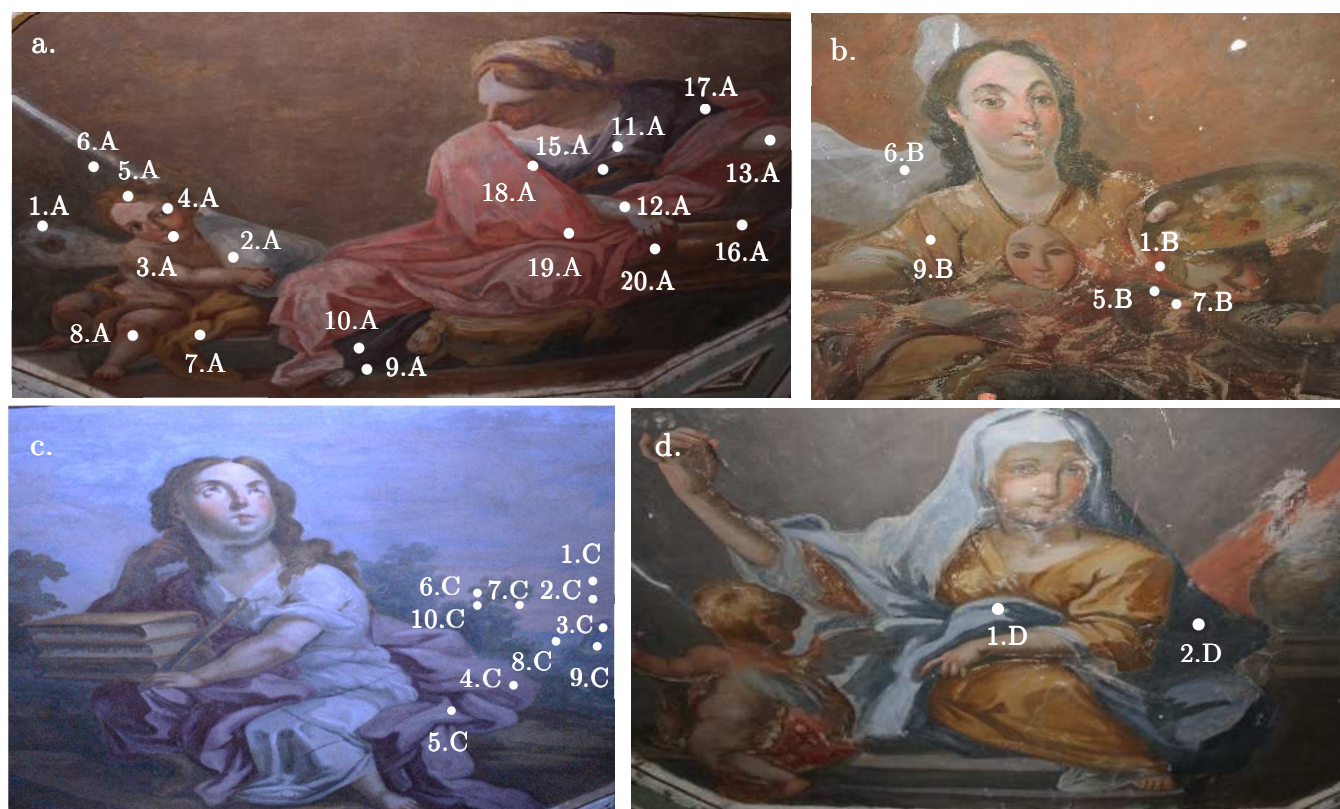
Figure 6.1 Pictures of the studied medallions and measurement points. Symbolic representation of (a) "*The Alchemy*", (b) "*The Literature*" (c) "*The Art Painting*" and (d) "*The Medicine*"

6.2.2. Raman equipment

Two portable Raman instruments equipped with different wavelength excitation sources have been used for the investigations: a portable EZRAMAN-I-DUAL Raman spectrometer (TSI Inc., Irvine CA, USA) and an i-Raman® EX (Madatec S.r.l., Milan). Specifications of the The EZRAMAN-I-DUAL Raman system can be found in chapter 2. For this investigation, the 785 nm line has been used with a spectral range/spectral resolution of 100-2350 cm^{-1}/7 cm^{-1}. The selected laser power for these analyses was adjusted at about 30 mW. The i-Raman® EX is a portable BWTek Raman system equipped with a 1064 nm line. Using a high sensitivity thermoelectrically cooled InGaAs array detector with a wide and high dynamic range, this portable Raman spectrometer delivers a high signal to noise ratio without inducing auto-fluorescence. The system provides spectral resolution as fine as 9.5 cm^{-1} and a spectral coverage range from 175 to 2500 cm^{-1}. It uses a fibre optic probe with an laser power adjustable up to 450 mW. A laptop is connected to the spectrometer.

Both spectrometers were calibrated before each experimental session. All spectra, from both instruments were recorded with a total measurement time of 2 to 10 accumulations of 3 to 60 seconds each. The Raman probes were held a few millimeters from the front of the object, corresponding to the focal distance of the lens. In the chosen configurations, the laser spot was c.a. 0.1 millimeter in diameter, allowing the achievement of a real spatial resolution in the range of few microns. Due to the relatively large spot size, the laser power density was too weak to induce any undesired effect or damage, even on organic or photosensitive materials, with both laser lines. The instrument output lenses were shielded with a black cloth in order to minimise spectral interference from ambient light. Referring to the data processing, the Raman spectra acquired by the 1064 nm line have not been subjected to any data manipulation or processing techniques and are reported generally as collected, being characterised by a very low fluorescence background. In contrast, for spectra collected with 785 excitation, a baseline correction has been applied in order to better visualise the Raman signal. In general, during the measurement campaign, as both instruments were connected via a USB cable to a laptop, Raman spectra have been simultaneously visualised, allowing a

real time identification of materials. Of course, the final identification was accomplished by comparison with reference spectra present in the libraries of the authors and with published literature.

6.3 Results

6.3.1. Painted layers

<u>Reddish hues</u>

Red-orange, pink and yellow hues were investigated in the medallions representing "The Alchemy" and "The Art Painting". In the Alchemy medallion, measurements were carried out by using both excitation sources, namely 785 nm (Figure 6.2a-c) and 1064 nm (Figure 6.2d). In detail, the pinkish colour was measured on the skin of both the women (points 12.A and 13.A) and angel (point 8.A). The obtained results suggest the use of a mixture of haematite (Fe_2O_3; Raman bands at 620 and 412 cm^{-1} [6]) and lead white ($2PbCO_3 \cdot Pb(OH)_2$; Raman band at 1052 cm^{-1} [7]). Additionally, the 785 nm laser detected the presence of red lead (Pb_3O_4) (band at 548 cm^{-1}). Different tones of the woman's vest were analysed in order to characterise the pigmenting agents employed for obtaining the reddish hues. Measurements collected on bright red areas (point 18.A) reveal the use of pure vermilion (HgS; typical Raman bands at 343, 282, 252 cm^{-1} [8]), which seems to be mixed with haematite (main bands at 411 and 292 cm^{-1}) and carbon-based black pigments (typical Raman features of amorphous carbon centered at 1588 and 1320 cm^{-1} [8]) for attaining bright shades of red (point 20.A). As far as the yellow hues present on the vase, the woman's belt (points 15.A and 16.A) and the angel's vest (point 7.A), the Raman spectra collected using both excitation sources exhibit the typical peak of goethite (α-FeO(OH); Raman band at about 403 cm^{-1} [9]). Finally, it should be noted that the presence of Pb-sulphates (anglesite, $PbSO_4$) might indicate that the ongoing lead compound alteration process has occered due to atmospheric SO_2 [10-13]. It is not possible to determine which pigment, red lead or lead white, is degraded. However, as is evident from recent researches [14–16], sucha secondary phase is

occasionally detected on discoloured red lead [17], even if this soluble lead salt may be often leached out during ageing in humid conditions.
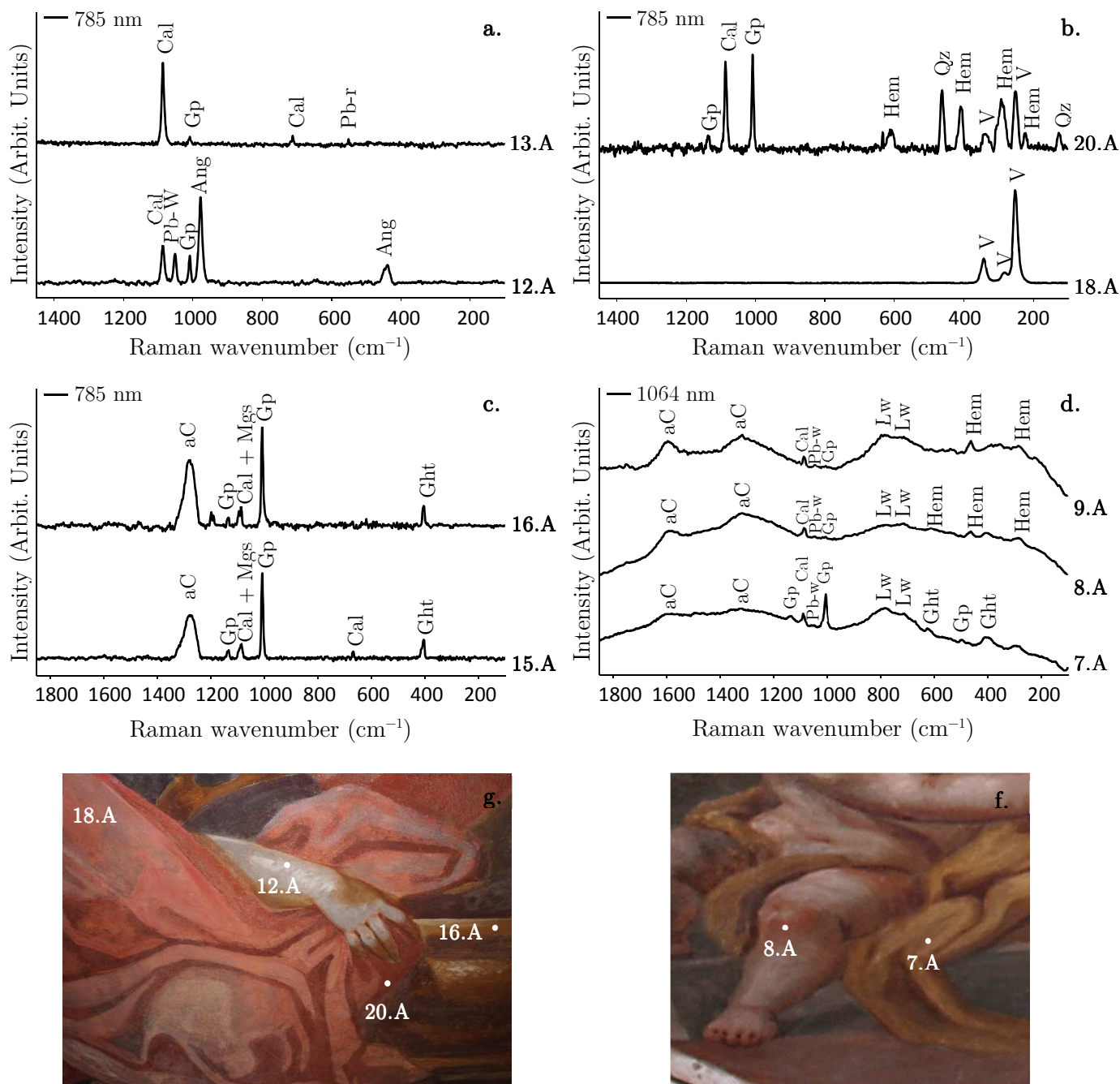
Figure 6.2 Raman spectra collected from the medallion representing "The Alchemy" on (a) incarnate, (b) red and (c) yellow layers by using 785 nm line (baseline correction applied) and (d) incarnate, red and yellow layers by using 1064 nm line; (e-f) detail of the layers. Symbols: aC: amorphous carbon; Ang: anglesite; Cal: calcite; Gth: goethite; Gp: gypsum; Hem: haematite; Lw: limewash; Mgs: magnesite; Pb-r: red lead; Pb-w: lead white; Qz: quartz; V: vermilion.

Considering the "The Art Painting" medallion, measurements have been performed using the 1064 nm line on different red tones of the vest (points 9.B and 1.B) as well as on the angel skin (point 8.B). The analysis of the collected Raman spectra (Figure 6.3) suggests, also in this case, the use of vermilion (HgS; Raman bands detected at 345, 280, 252 cm^{-1}) in the reddish-orange areas. Haematite seems to be used in order to obtain dark and light red hues, also mixed with carbon-based pigments (presence of bands related to amorphous carbon). Finally, the use of a haematite and carbon mixture has been observed in the darker areas of the angel's skin.
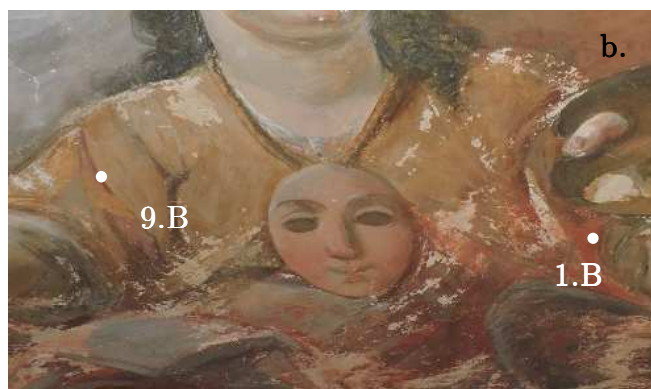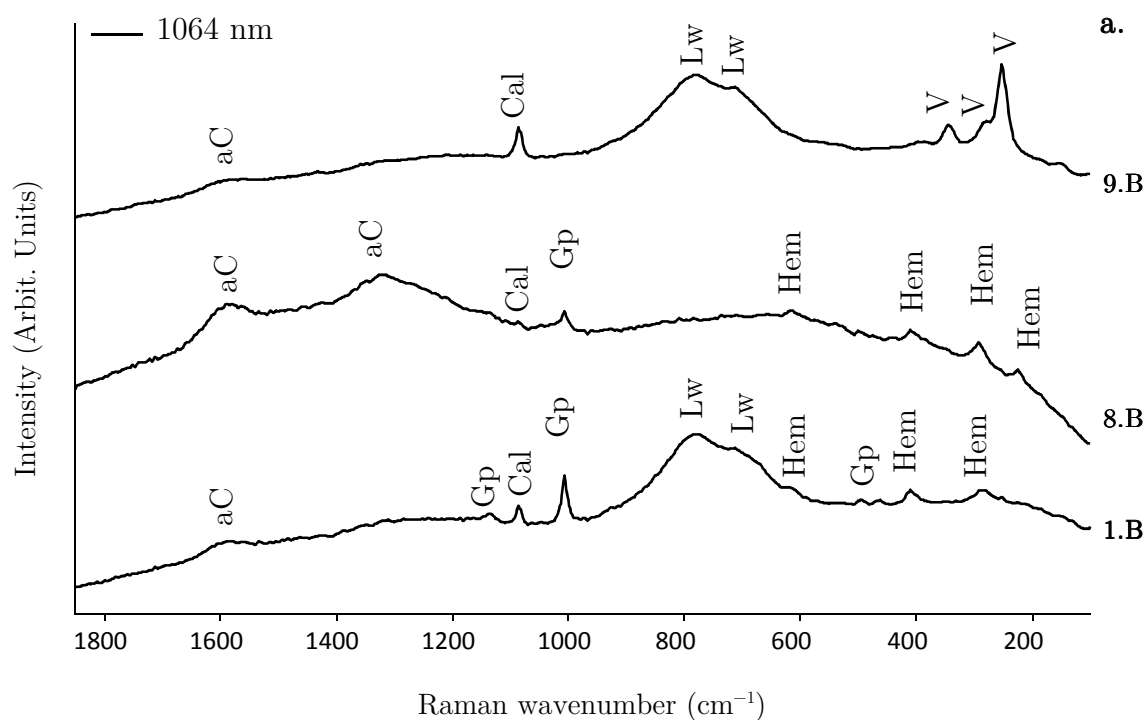
Figure 6.3 Raman spectra collected on the medallion representing "The Art Painting" by using 1064 nm line on (a) incarnate (point 8.B) and reddish layers (points 1.B and 9.B) and (b) a detail of the investigated layers, as examples. Symbols: aC: amorphous carbon; Cal: calcite; Gp: gypsum; Hem: haematite; Lw: limewash; V: vermilion.

Greyish and black hues

The interpretation of the collected Raman spectra on greyish and black layers reveals the prevalent use of amorphous carbon as a pigmenting agent (Raman features centered at 1588 and 1350 cm^{-1}), mixed with lead white (main Raman band detected at about 1052 cm^{-1}). Such mixtures were detected at the measurement points established on the woman's vest (point 17.A), angel's wing (point 11.A) and ampoule (point 14.A) in the Alchemy medallion (Figure 6.4.a) and on the woman's voile (point 6.B) and angel's workbook (point 5.B) in the Art Painting (Figure 6.4.b). It is noteworthy that the mixture of carbon-based black pigment and lead white seems to be employed also in order to obtain a greyish-purple hue in some parts of the woman's vest represented in the Alchemy allegoric frescoes. In detail, the purple tone has been obtained by adding haematite to the mixture (see point 17.A in Figure 6.4.a). The presence of lead-based pigments suggests, also in this case, the occurrence of degradation products. In fact, because of the use of the 785 nm laser, anglesite (PbSO$_4$; Raman features at 978, 453 and 437 cm^{-1}), has been detected in several greyish areas (see point 11.A in Figure 6.4.a, for example). The missing lead white signal in the Raman spectrum can be explained by the fact that the residual concentration, after degradation, is less than the LOD of the Raman spectrometer.

Green and blue hues

In the medallions representing "The Literature" (Figure 6.5a-b) and "The Medicine"(Figure 6.5c-d) green and blue hues prevail. Globally, the analyses performed on different representative areas of the paintings did not allow the identification of the pigmenting agents responsible for these colours, as only Raman features attributable to lead white and carbon black were detected by using the 1064 nm line (Figure 6.5a). The latter maybe used in order to obtain darker tones. However, the employment of the 785 nm line has given some interesting results in comparison with the 1064 nm excitation source, supporting some additional hypotheses. In particular, spectra collected on green areas show the presence of weak Raman bands at about 125 and 846 cm^{-1} (Figure 6.5b) that could be related to the Cu-O vibration or hydroxyl
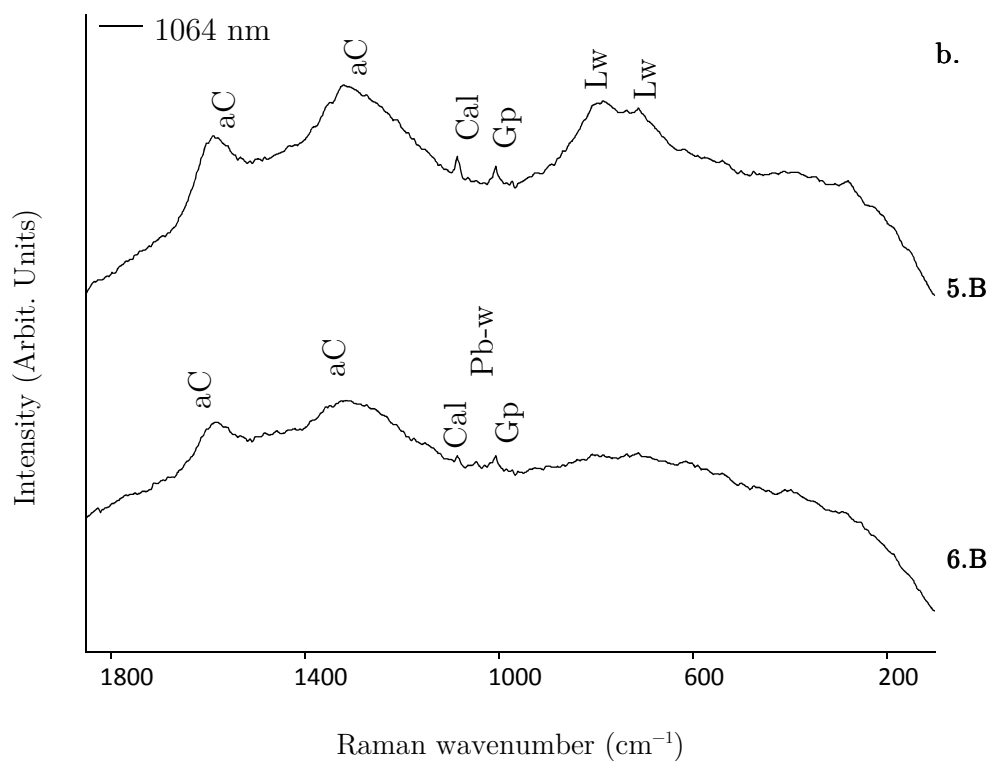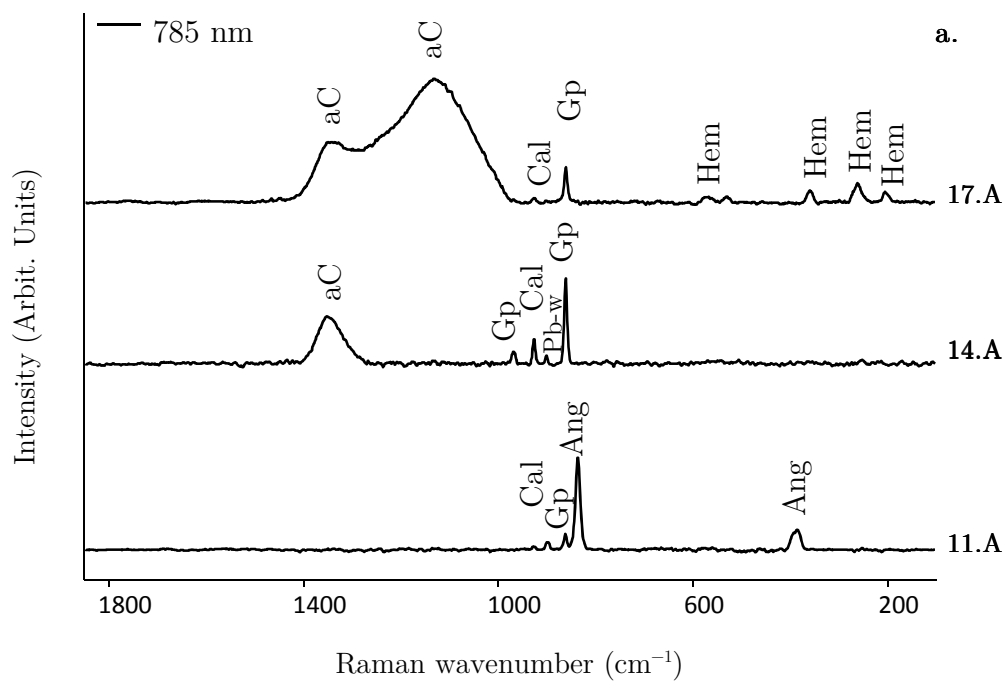
Figure 6.4 Raman spectra collected on greyish layers: (a) measurement points (11.A, 14.A and 17.A) on "The Alchemy" medallion by using 785 nm line and (b) measurements points (5.B. and 6.B) on "The Art Painting" medallion by using 1064 nm line. Symbols: aC: amorphous carbon; Ang: anglesite; Cal: calcite; Gp: gypsum; Hem: haematite; Lw: limewash; Pb-w: lead white.

deformation in copper-chloride minerals (such as atacamite and paratacamite; $Cu_2Cl(OH)_3$), frequently found in pigments of ancient paintings as result of malachite and azurite degradation [18,19].

In contrast, no pigments have been identified in the blue areas mainly investigated in "The Medicine" medallion. Notwithstanding this the detection of Raman bands attributed to the calcium oxalate whewellite ($CaC_2O_4 \cdot H_2O$; main Raman band at 1464 cm^{-1}) could deny the use of copper salts as blue pigments (Figure 6.5c). In fact, even if oxalates were largely detected as deterioration products due to lichen attach in works of art, especially in paintings, blue surfaces achieved by using copper pigments are usually preserved as the Cu-ions inhibit the growth of microorganisms [20]. Finally, worthy of note is the evidence of a recent restoration campaign (PB15 and anatase; see Figure 6.5b point 8.C) in the light-blue background area of "The Literature" medallion scene.

6.3.2. Substrate preparation

Beside the Raman signals attributable to pigments, in all the spectra acquired by both excitation sources, a sequence of bands characteristic of calcite ($CaCO_3$) was detected (main Raman band at 1086 cm^{-1}, usually associated with weak bands at 709 and 281 cm^{-1}). This suggests a lime-based preparation layer and supports the bibliographic sources about the fresco technique used in the realisation of the medallions. Indeed, the use of lime and its derivative for the preparation of surfaces to aid adhesion of pigments is widely attested over time, especially from the Roman to the Renaissance period. Along with calcite, a band at 464 cm^{-1} reveals in some spectra the presence of quartz. This informs us about the use of sand mixed with pigments or used in the wall preparation (see Figure 6.2b). As its occurrence varies significantly with sampling position, it could be an indication of variable composition of the mortar used in the wall preparation. In addition, a more detailed inspection of the acquired spectra can provide additional information about the sourcing of materials, the methodologies of the wall painting preparation and the deterioration products.
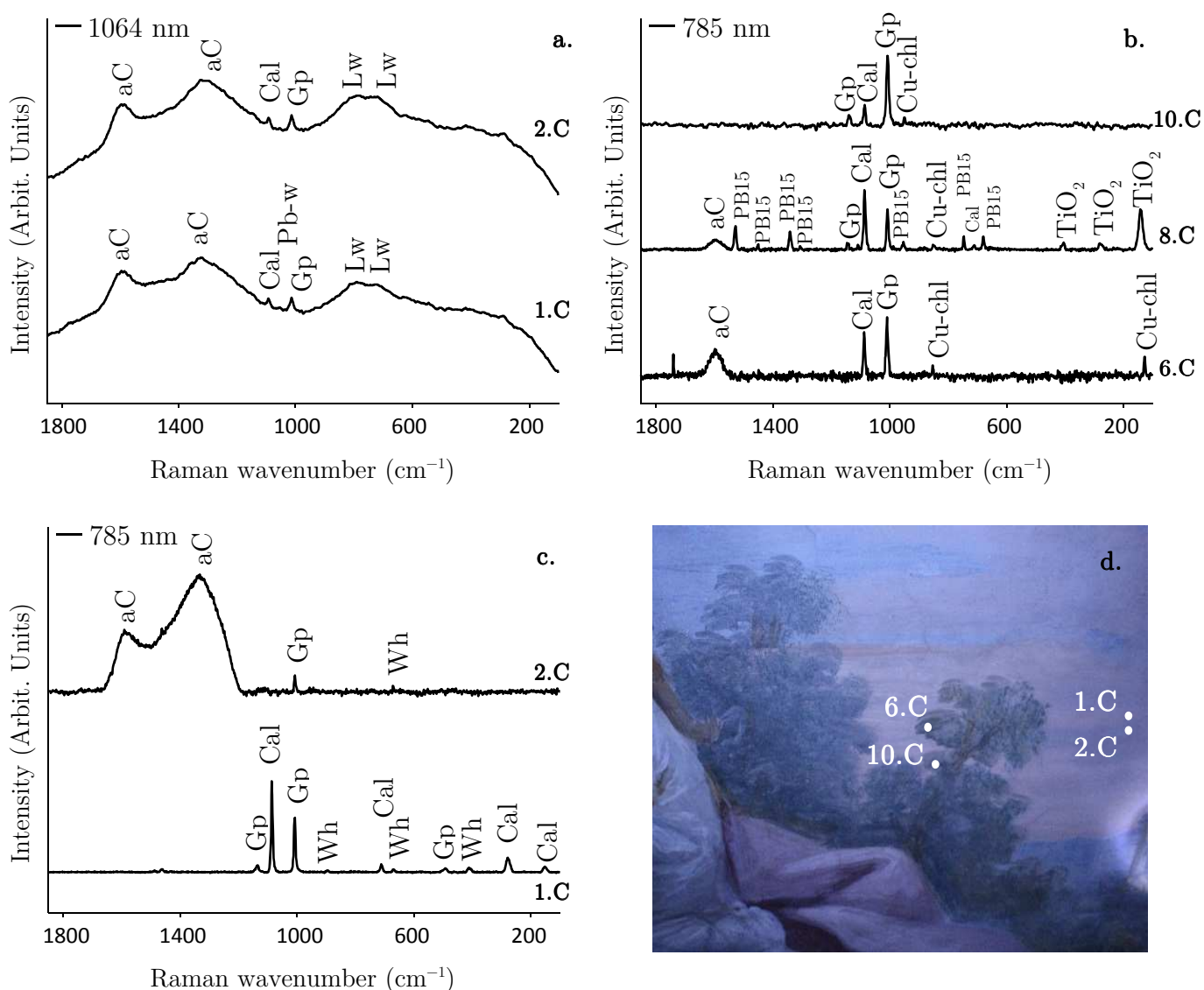
Figure 6.5 Raman spectra collected on the medallion representing "The Literature" on greenish layers by using (a) 1064 nm line and (b) 785 nm line; (c) Raman spectra collected on "The Medicine" medallion on blue layers by using 785 nm line; (d) detail of the investigated layers, as examples. Symbols: aC: amorphous carbon; Cal: calcite; Cu-chl: copper-chloride; Gp: gypsum; Lw: limewash; Pb-w: lead white; TiO$_2$: anatase; PB15: PB15; Wh: whewellite.

The first interesting aspect is the concomitant presence of calcite and gypsum signals, characterised by the main Raman bands at about 1086 and 1008 cm^{-1}, respectively (Figure 6.6.a). Usually, the presence of gypsum can be ascribed to the attack of sulfur dioxide from atmospheric pollution upon lime-based surfaces. However, in this case, because of the indoor location of the wall painting and the high intensity of both

calcite and gypsum signals, it is possible to hypothesize the use of a transitional approach for the substrate preparation, widely attested in literature, for which the two components are mixed together [21]. In addition, the presence of a broad feature in the form of an ill-resolved doublet at about 790 and 710 cm^{-1} (Figure 6.6.b) in the spectra acquired with the 1064 nm line, is of great interest. Numerous researches, also performed on lime-wash/calcite wall paintings, have attributed this Raman feature to calcium hydroxides [22,23] and it has not been observed with lower wavelength excitation [24]. It may seem surprising that the conversion of limewash to calcium carbonate by reaction with atmospheric carbon dioxide is a relatively slow process and unconverted calcium hydroxide can persist for decades on wall painting substrates [21]. Based on this interpretation, we can suppose that, also in this case, the presence of the Raman bands attributable to slaked lime could be the evidence of an incomplete conversion of lime to calcium carbonate.

Another interesting aspect, widely studied in ancient wall paintings, is related to the calcium carbonate source used for calcination; overall, the results obtained by the analysis of the collected spectra suggest the use of common limestone in the form of $CaCO_3$. However, some spectra collected by using the 785 nm excitation line reveal a weak band at about 1092 cm^{-1} (see Figure 6.2c) attributable to magnesite $MgCO_3$ or dolomite $CaMg(CO_3)_2$ [25], suggesting an interesting hypothesis on the probable use of dolomitic limestone [26].
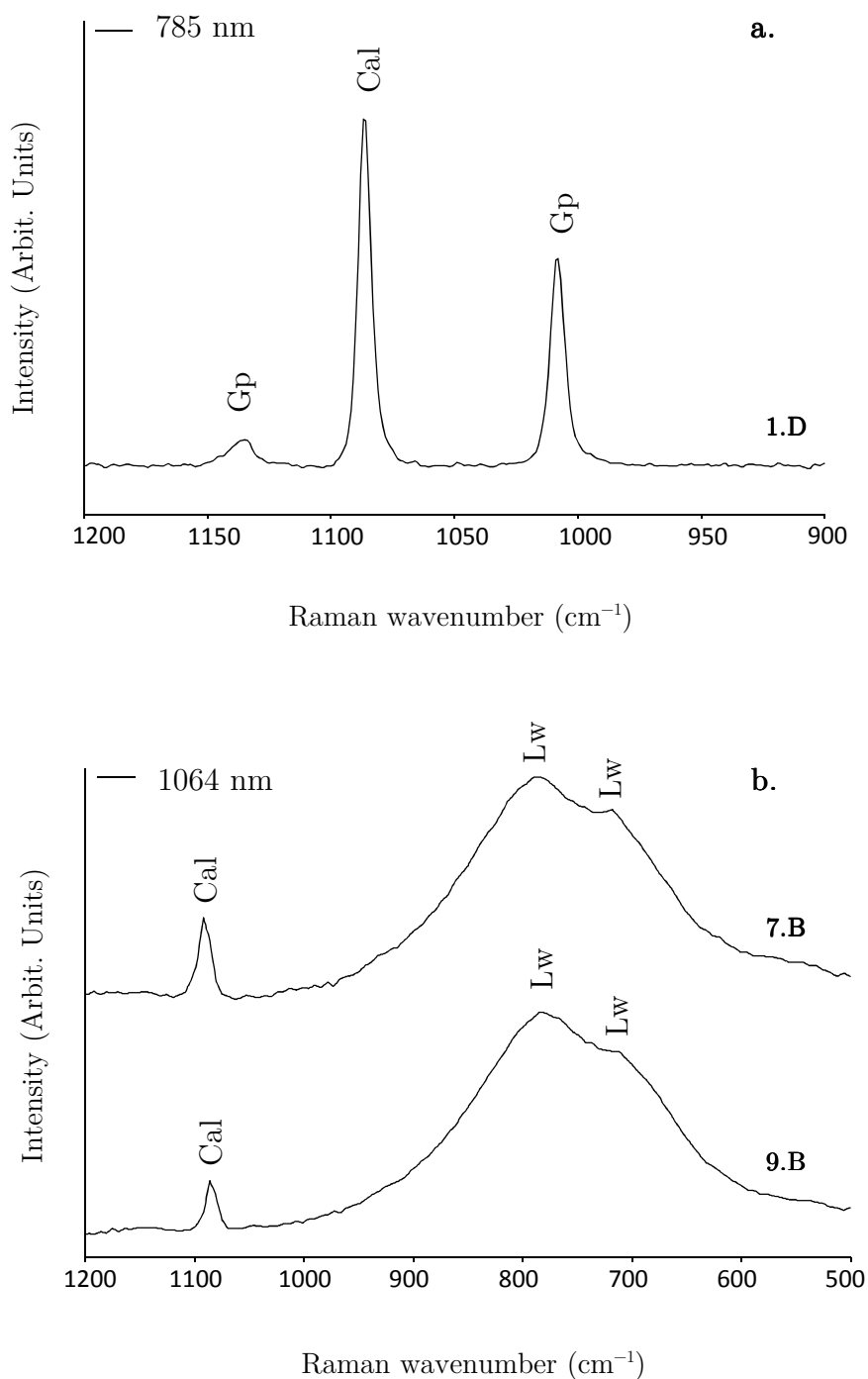
Figure 6.6 Raman spectra collected on the studied wall painting representative of (a) the concomitant presence of calcite (Cal) and gypsum (Gp) suggesting a transitional approach for substrate preparation and (b) the presence of calcite (1086, 713 cm^{-1}) with a greater relative proportion of unconverted limewash (Lw), as testified by the broad features centered at about 780 cm^{-1}.

6.4 Discussion and conclusions

The overview of the Raman spectra collected on the wall paintings (see Table 6.1) allows us to infer the following observations. As far as coloring agents, red hues were mainly obtained by using vermilion, mixed with lead white and carbon-based black pigments in order to represent lighter and darker shades. However, the painter seemed to use also red lead and haematite, the latter usually mixed with white pigments for the restitution of the incarnate. Black and grey colours were achieved by using carbon-based pigments, also mixed with white ones for making lighter tones. In the case of blue and green colours, no evidence for specific pigmenting agents could be collected, even if the hypothesis on the use of copper salts for greenish hues could be proposed.

Referring to the preparation layer (in terms of composition, source materials and technique), the detection of bands related to calcium carbonate confirms the use of a lime-based preparation by employing the secco or fresco technique. Bibliographic sources refer to the use of a fresco technique in the manufacture of the medallions. However, pigments such as lead white, red lead, vermilion are not compatible with this painting technique and points to the use of a secco technique [28,29]. Unfortunately, portable Raman spectroscopy could not contribute a solution to this issue. Therefore, cross-sectional analysis is needed to characterise the stratigraphy and provide information on the painting technique. The systematic association of calcite with high intensity bands attributable to gypsum, strongly supports the idea of the application of a transitional approach between Romanesque and Renaissance Art methods, in which both components were mixed together in the wall preparation. The occurrence of magnesium-containing carbonates could provide information on possible marine carbonate sources. Finally, the presence of calcium oxide/hydroxide (band at 790 cm^{-1}, only detectable with the 1064 nm laser), together with calcium carbonate (1086 cm^{-1}) can provide information on the degree of calcination. In this case, the relative intensity of these two bands suggests an incomplete process has occurred probably due to the indoor conditions.

The campaign offered also the possibility to compare the performances of the two portable Raman spectrometers that were used as well as to study the suitability of the

different laser lines. In fact, the EZRaman-I-Dual Raman spectrometer has a wider spectral window (starting from 100 cm^{-1}) in comparison to the i-Raman® EX (which ranges from 175 to 2500 cm^{-1}), allowing the detection of compounds characterised by low wavenumber Raman bands, such as lead-containing pigments, chloride minerals and Pb-sulphate alteration products. At the same time, by working at 785 nm, the identification of the minerals was made easier by the higher intensity of the Raman signal. On the other hand, as expected, a lower fluorescence background was observed by using the 1064 nm line, allowing the detection of compounds such as calcium oxide/hydroxide and carbon-based black pigments, characterised by broad Raman features. Apart from the aforementioned aspects, the use of the two instruments, equipped with different excitation wavelengths, produced in the majority of cases very similar results. In conclusion, this study has allowed us to achieve a complete characterisation of the pigments and technique used in the paintings of the vaults, supplying fundamental information to the conservators, useful for planning appropriate conservation and preservation actions.

In general, both spectrometers are ideal tools for the investigation of artefacts. However, each laser wavelength has specific strengths and weaknesses. Instruments equipped with a laser of a short wavelength (785 nm and 532 nm) are more suitable for inorganic material detection, which has characteristic Raman bands at low wavenumbers (in this case until 100 cm^{-1}). On the other hand, the competition between the fluorescence signal and the Raman effect is larger in comparison to a long laser wavelength (1064 nm), causing a higher background signal in the Raman spectrum. Furthermore, for a 532 nm and a 785 nm laser a CCD-detector can be used as detection system and shows an optimum response in the visible range ($400 - 750$ nm) and the NIR range ($750 - 1050$ nm), respectively. However, this type of detector is not sensitive when using a 1064 nm laser and thus another detector, InGaAs, needs to be used which is less efficient [27].

Due to these reasons, the EZRaman-I-Dual Raman spectrometer is preferred to the i-Raman® EX (1064 nm) as the focus of the research lays on art analysis and thus identification of inorganic compounds is of great interest. It is also noteworthy that an instrument provided with two excitation sources, as our Raman spectrometer, is more

beneficial for purchase. Not every compound is Raman active for the chosen laser wavelength. Therefore, when an additional laser is present, there is a better change to identify the unknown material in addition to the minimsaion of problems of interference such as absorption and fluorescence.

Recapitulating the conclusions of the earlier chapters, the success of a Raman instrument is dependent upon the research question and can be evaluated based upon different parameters such as practical limitations, spectroscopic characteristics, measurement time, suitability of the type of laser, etc. So far, only painted objects with a simple paint structure have been examined. When considering complex painted materials, such as oil paintings, *in situ* Raman analysis becomes more complicated. Chapter 5 has already illustrated that sometimes the use of a single technique is not satisfactory. Hence, chapter 7 will discuss the difficulties of *in situ* research performed on oil paintings and will explain the benefit of using complementary methods for these complex samples. Additionally, it will be described how the applied analytical methods are optimised to obtain the best results.

Table 6.1 For each medallion, measurement point IDs, colour, main Raman bands (in cm⁻¹) detected by using both wavelength (namely 785 nm and 1064 nm) and attribution are reported.

	Analysis point ID	Colour	Raman bands (cm⁻¹)	Attribution
Medallion A: symbolic representation of "The Alchemy"				
1064 nm	1.A	light grey	1590, 1320, 1086, 1007, 790, 710, 280	amorphous carbon, calcite, limewash, gypsum
	2.A	grey	1590, 1320, 1086, 1047, 1007, 790, 713, 280	amorphous carbon, calcite, limewash, lead white, gypsum
	3.A	incarnate	1590, 1320, 1086, 1047, 1007, 790, 713, 620, 490, 411, 280	amorphous carbon, calcite, limewash, lead white, gypsum, haematite
	4.A	dark-grey	1590, 1320 1086, 1047, 1007, 790, 280	amorphous carbon, lead white, calcite, limewash, gypsum
	5.A	dark-orange	1590, 1320, 1086, 1007, 713, 613, 411	amorphous carbon, calcite, gypsum, haematite
	6.A	dark background	1590, 1320	amorphous carbon
	7.A	yellow	1590, 1320, 1136, 1086, 1007, 790, 713, 620, 495, 404	amorphous carbon, calcite, limewash, gypsum, goethite
	8.A	incarnate	1590, 1320, 1136, 1086, 1047, 1007, 620, 498, 411, 292, 226	amorphous carbon, calcite, lead white, gypsum, haematite
	9.A	greyish-purple	1590, 1320, 1086, 1047, 1007, 790, 713, 460, 226	amorphous carbon, calcite, limewash, lead white, gypsum, haematite
	10.A	greyish-purple	1590, 1320, 1007	amorphous carbon, gypsum
785 nm	11.A	grey	1598, 1056, 1086, 1050, 1008, 978, 453, 437	anglesite, gypsum, lead white, calcite
	12.A	incarnate	1084, 1054, 1049, 1008, 978, 447, 437, 280	anglesite, gypsum, calcite, lead white
	13.A	incarnate	1086, 1008, 710, 673, 549, 411, 280	calcite, gypsum, red lead
	14.A	grey	1590, 1134, 1086, 1054, 1008, 668	amorphous carbon, lead white, calcite, gypsum
	15.A	yellow	1269, 1136, 1086, 1008, 668, 404	goethite, magnesite, calcite, gypsum
	16.A	yellow	1274, 1197, 1136, 1096, 1086, 1008, 403	goethite, magnesite, calcite, gypsum
	17.A	dark grey	1590, 1330, 1008, 610, 411, 293	amorphous carbon, gypsum, haematite
	18.A	bright red	1086, 340, 281, 251	vermilion, calcite
	19.A	light red	1086, 1009, 712, 604, 463, 404, 383, 343, 336, 289, 283, 250, 151	vermilion, haematite, calcite, gypsum, quartz
	20.A	dark red	1590, 1134, 1084, 1006, 848, 633, 604, 462, 406, 342, 290, 250, 221	amorphous carbon, vermilion, haematite, calcite, gypsum, quartz

Medallion B: symbolic representation of "The Art Painting"				
1064 nm	1.B	light red	1136, 1086, 1007, 790, 713, 615, 496, 411, 292	calcite, limewash, gypsum, haematite
	2.B	red	1136, 1086, 1007, 790, 713, 615, 495, 411, 292, 225	calcite, limewash, gypsum, haematite
	3.B	light red	1086, 1007, 790, 713, 411, 280	calcite, limewash, gypsum, haematite
	4.B	dark grey	1590, 1320	amorphous carbon
	5.B	grey	1590, 1320, 1086, 1047, 1007	amorphous carbon, lead white, calcite, gypsum
	6.B	grey	1590, 1320, 1086, 1007, 790, 713, 280	amorphous carbon, calcite, limewash, gypsum
	7.B	absence of pigment layer	1086, 790, 710, 280	calcite, limewash
	8.B	incarnate	1590, 1320, 1086, 1007, 615, 411, 292, 225	amorphous carbon, calcite, gypsum, haematite
	9.B	reddish-orange	1086, 790, 713, 345, 280, 252	calcite, limewash, vermilion
	10.B	black	1590, 1320	amorphous carbon
Medallion C: symbolic representation of "The Literature"				
1064 nm	1.C	light blue	1590, 1320, 1086, 1047, 1007, 790, 713, 280	amorphous carbon, lead white, calcite, limewash, gypsum
	2.C	dark blue	1590, 1320, 1086, 1047, 1007, 790, 713, 280	amorphous carbon, lead white, calcite, limewash, gypsum
	3.C	blue	1590, 1320, 1086, 1047, 1007, 790, 713, 280	amorphous carbon, lead white, calcite, limewash, gypsum
	4.C	light purple	1590, 1086, 790, 713, 411, 280, 225, 157	amorphous carbon, calcite, gypsum, haematite
	5.C	dark purple	1136, 1086, 1007, 615, 493, 411, 292, 225	calcite, gypsum, haematite
785 nm	6.C	green	1739, 1590, 1084, 1006, 851, 129, 125	amorphous carbon, calcite, gypsum, copper chloride
	7.C	green	1600, 1086, 1007, 895, 851	amorphous carbon, calcite, gypsum, copper chloride
	8.C	light blue	1600, 1528, 1449, 1340, 1305, 1285, 1144, 1130, 1108, 1086, 1008, 987, 951, 850, 746, 709, 679, 591, 401, 281, 142	amorphous carbon, calcite, gypsum, , copper chloride, anatase, PB15
	9.C	light blue	1600, 1136, 1086, 895, 711, 670, 490, 411, 279, 154	amorphous carbon, calcite, gypsum
	10.C	green	1600, 1140, 1086, 1006, 950	amorphous carbon, calcite, gypsum, copper chloride
Medallion D: symbolic representation of "The Medicine"				
785 nm	1.D	light blue	1597, 1487, 1462, 1432, 1134, 1084, 1008, 895, 710, 669, 503, 491, 410, 278, 150	amorphous carbon, calcite, gypsum, whewellite
	2.D	dark blue	1600, 1462, 1320, 1006, 670	amorphous carbon, gypsum, whewellite

6.5 References

[1]   V. Librando, Quattro progetti per il Monastero di S. Nicolo L'Arena, Catania, 1988.

[2]   A. Perardi, L. Appolonia, P. Mirti, Non-destructive *in situ* determination of pigments in 15th century wall paintings by Raman microscopy, Anal. Chim. Acta. 480 (2003) 317–325. doi:10.1016/S0003-2670(02)01660-4.

[3]   P. Vandenabeele, Raman spectroscopy in art and archaeology, J. Raman Spectrosc. 35 (2004) 963–965. doi:10.1002/jrs.2008.

[4]   A. Deneckere, W. Schudel, M. Van Bos, H. Wouters, A. Bergmans, P. Vandenabeele, et al., *In situ* investigations of vault paintings in the Antwerp cathedral., Spectrochim. Acta. A. Mol. Biomol. Spectrosc. 75 (2010) 511–519. doi:10.1016/j.saa.2009.10.032.

[5]   N. Buzgar, A. Buzatu, A.-I. Apopei, V. Cotiugă, *In situ* Raman spectroscopy at the Voroneţ Monastery (16th century, Romania): New results for green and blue pigments, Vib. Spectrosc. 72 (2014) 142–148. doi:10.1016/j.vibspec.2014.03.008.

[6]   A. Zoppi, C. Lofrumento, E.M. Castellucci, P. Sciau, Recent Advances in linear and nonlinear Raman spectroscopy I, J. Raman Spectrosc. 39 (2008) 40–46. Doi:10.1002/jrs.1811.

[7]   A.M. Correia, M.J.V. Oliveira, R.J.H. Clark, M.I. Ribeiro, M.L. Duarte, Characterization of Pousão pigments and extenders by micro-X-ray diffractometry and infrared and Raman microspectroscopy, Anal. Chem. 80 (2008) 1482–1492. doi:10.1021/ac701887p.

[8]   L. Burgio, R.J.H. Clark, Library of FT-Raman spectra of pigments, minerals, pigment media and varnishes, and supplement to existing library of Raman spectra of pigments with visible excitation, Spectrochim. Acta Part A-Molecular Biomol. Spectrosc. 57 (2001) 1491–1521. http://www.ncbi.nlm.nih.gov/pubmed/11446703.

[9]   S. Daniilia, D. Bikiaris, L. Burgio, P. Gavala, R.J.H. Clark, Y. Chryssoulakis, An extensive non-destructive and micro-spectroscopic study of two post-Byzantine overpainted icons of the 16th century, J. Raman Spectrosc. 33 (2002) 807–814. doi:10.1002/jrs.907.

[10] M. Perez-Alonso, K. Castro, I. Martinez-Arkarazo, M. Angulo, M.A. Olazabal, J.M. Madariaga, Analysis of bulk and inorganic degradation products of stones, mortars and wall paintings by portable Raman microprobe spectroscopy, Anal. Bioanal. Chem. 379 (2004) 42–50. doi:10.1007/s00216-004-2496-2.

[11] J.L. Perez-Rodriguez, C. Maqueda, M.C. Jimenez De Haro and P. Rodriguez-Rubio, Effect of pollution on polychromed ceramic statues, Atmosperic environment 32(6) (1998) 993-998.

[12] M.J. Campos-Sunol, M.J. De la Torre-Lopez, M.J. Ayora-Canada and A. Dominguez-Vidal, Analytical study of polychromy on exterior sculpted stone, J. Raman Spectrosc. 40 (2009) 2104-2110.

[13] S.M. Lussier, An examination of lead white discoloration and the impact of treatment on paper artifacts: a summary of experimental testing, Book & Paper group session, AIC 34th annual meeting, Rhode Island (2008).

[14] S. Aze, J.M. Vallet, A. Baronnet, O. Grauby, The fading of red lead pigment in wall paintings: Tracking the physico-chemical transformations by means of complementary micro-analysis techniques, Eur. J. Mineral. 18 (2006) 835–843.

[15] S. Aze, J.M. Vallet, A. Baronnet, O. Grauby, Chromatic alterations of red lead pigments in artworks: A review, Phase Transit. 81 (2008) 145–154.

[16] S. Daniilia, E. Minopoulou, D. Demosthenous, G. Karagiannis, A comparative study of wall paintings at the Cypriot monastery of Christ Antiphonitis: one artist or two?, J. Archaeol. Sci. 35 (2008) 1695–1707. doi:10.1016/j.jas.2007.11.011.

[17] E. Kotulanová, P. Bezdička, D. Hradil, J. Hradilová, S. Švarcová, T. Grygar, Degradation of lead-based pigments by salt solutions, J. Cult. Herit. 10 (2009) 367–378. doi:10.1016/j.culher.2008.11.001.

[18] G. Bertolotti, D. Bersani, P. Lottici, Micro-Raman study of copper hydroxychlorides and other corrosion products of bronze samples mimicking archaeological coins, Anal. Bioanal. Chem. 402 (2012) 1451. http://link.springer.com/article/10.1007/s00216-011-5268-9 (accessed September 11, 2015).

[19] R.L. Frost, W. Martens, J.T. Kloprogge, P.A. Williams, Raman spectroscopy of the basic copper chloride minerals atacamite and paratacamite: implications for the study of copper, brass and bronze objects of archaeological significance, J. Raman Spectrosc. 33 (2002) 801–806. doi:10.1002/jrs.921.

[20] R.L. Frost, M.L. Weier, J.T. Kloprogge, Raman spectroscopy of some natural hydrotalcites with sulphate and carbonate in the interlayer, J. Raman Spectrosc. 34 (2003) 760–768. doi:10.1002/jrs.1050.

[21] H.G.. Edwards, D.W. Farwell, The conservational heritage of wall paintings and buildings : an FT-Raman spectroscopic study of prehistoric, Roman, mediaeval and Renaissance lime substrates and mortars, J. Raman Spectrosc. 39 (2008) 985–992. doi:10.1002/jrs.1917.

[22] D. Chiriu, P.C. Ricci, A. Polcaro, P. Braconi, D. Lanzi, D. Nadali, Raman study on Pompeii potteries: the role of calcium hydroxide on the surface treatment , J. Spectrosc. 14 (2014) 10.

[23] H.G.M. Edwards, D.W. Farwell, D.L.A.D. Faria, A.M.F. Monteiro, M.C. Afonso, P. DeBlasis, et al., Raman spectroscopic study of 3000-year-old human skeletal remains from a sambaqui , Santa Catarina , J. Raman Spectrosc. 32 (2001) 17–22. doi:10.1002/1097-4555(200101)32:1<17::AID-JRS658>3.0.CO;2-1.

[24] A. Aminzadeh, Fluorescence bands in the FT-Raman spectra of some calcium minerals, Spectrochim. Acta Part A-Molecular Biomol. Spectrosc. 53 (1997) 693–697. ISI:A1997XF62200007.

[25] H.G.M. Edwards, S.E.J. Villar, J. Jehlicka, T. Munshi, FT-Raman spectroscopic study of calcium-rich and magnesium-rich carbonate minerals, Spectrochim. Acta Part A-Molecular Biomol. Spectrosc. 61 (2005) 2273–2280. ISI:000231027600002.

[26] S. Bruni, F. Cariati, P. Fermo, A. Pozzi, L. Toniolo, Characterization of ancient magnesian mortars coming from northern Italy, Thermochim. Acta. 321 (1998) 1 61–165. doi:10.1016/S0040-6031(98)00455-9.

[27] J.M. Chalmers, H.G.M. Edwards, M.D. Hargreaves, Introduction and scope, in: Infrared Raman Spectrosc. Forensic Sci., John Wiley & Sons Ltd, 2012: 24.

[28] C. Cennini, The craftsman's handbook, Courier corporation, 1954.

[29] G.W.R. Ward, The grove encyclopedia of materials and techniques in art, Oxfrod university press, 2008.

Chapter 7

Direct analysis of the Ghent Altarpiece

In the previous chapters, a description was given about how to decide which portable Raman spectrometer is the most suitable for answering research questions in archaeometry. The evaluation is based on different parameters such as practical limitations, spectroscopic characteristics, measurement time, suitability of the type of laser, etc. In the cases previously described, objects with a simple paint structure were investigated.

When dealing with complex painted materials, more specifically oil paintings, in situ Raman analyses are not straightforward. Interferences of varnish or glaze overwhelming the Raman spectrum and masking weak Raman scatterers are commonly observed. Therefore, sometimes cross-sections need to be taken for lab analysis. However, this has the disadvantage that the results are only of specific (limited) areas and this causes damage to the artwork.

Moreover, cross-sections are not the only solution to obtain better results. Complementary techniques can provide a more complete characterisation of the investigated material as well. Therefore, in this next part, we want to expand the investigation of mediaeval oil paintings resolving specific research questions supporting restoration and conservation with the aid of only in situ equipment. The opportunity was given to perform analyses on one of the most famous artworks of the Flemish Primitives i.e. the Ghent Altarpiece. The concerted research actions (GOA) program financially supported the archaeometrical study of the Ghent Altarpiece. This program forms a network between scientists, art historians and conservators for which close collaboration is of high importance. This scientific research represents only a small contribution to the total work package and is one of the three items which the Raman spectroscopy research group is working on. This research group is mainly dealing with (i)

the optimisation of XRF techniques for the study of oil paintings; (ii) the conservation study of the exposed silver foils of the frames and (iii) the optimisation of mobile Raman spectroscopy for the study of art objects (i.e. the topic of this PhD thesis).

In this section, the used in situ analytical methods are described, followed by how the analysis can be optimised to obtain as complete information as possible.

7.1 Introduction

In the 15th and early 16th century, the Low Countries saw a major breakthrough in the art of painting with the introduction of a group of painters, now known as the Flemish Primitives. They are well known for their refined oil painting technique and represent themes related to realism, naturalism and religion [1]. The brothers Hubert and Jan Van Eyck are considered to be some of the greatest contributors to this flourishing period and it was believed that Jan was the "inventor" of the technique of oil painting. However, in the last centuries, this has been refuted and it is now believed that probably oil as a medium was already used before their time [2] and thus a new assumption is made: the brothers Van Eyck can be considered as the masters who improved substantially the application of oil as a painting medium [3].

Hubert and Jan Van Eyck created one of the most important paintings of the 15th century, the Ghent Altarpiece (Figure 7.1) (1426- 1432), which has an enormous cultural and arthistorical impact [4]. It is a large oil painting with oak support, made for and still displayed in the Saint Bavo Cathedral (Ghent). Its impressive dimensions are 3.5 x 4.6 m in open view (closed: 3.5 x 2.3 m). During its history, the panel painting was not continuously exhibited in the Cathedral. Over time, the individual oak panels have been repeatedly separated from each other for long periods, and groups of panels were subjected to distinctly different climatic conditions and restoration treatments [5]. In the 18th century, the three top centre panels were removed from their original frames and cropped at the top. The wing panels retained their frames, however, only two panels, Adam and Eve, still have their original shapes. The other six wing panels were bought by Willem III of Prussian in the 19th century and displayed in the Gemäldegalerie, Berlin.

To exhibit all painted surfaces side by side, the panels were split lengthwise and the 12 resulting panels were cradled at the back. [6]

Due to its bad condition, related to its complex material history, the polyptych has been in conservation treatment from October 2012 which will last until at least October 2019 by the Royal Institute for Cultural Heritage (KIK-IRPA). This scheduled conservation campaign has provided a unique opportunity to examine this precious painting.

The conservation and restoration treatment is undertaken in the Museum of Fine Arts in Ghent and is divided into three phases (Figure 7.1): imvolving one third of the panels at a time, the other parts of the altarpiece remain in the Cathedral. It is important to devise separate treatment protocols for the panels due to their different material history. The previous (partial) treatment took place in 1950-51 (Coremans 1953) [7]. Before the current conservation project started, the panels underwent a preliminary examination and conservation in 2010, coordinated by Prof. A. Van Grevenstein (University of Amsterdam), consisting of 5 phases: (i) preparation of condition reports of the panels; (ii) consolidation securing flaking paint; (iii) conservation treatment of the copy of the Just Judges; (iv) report and advice for a complete conservation treatment of the Ghent Altarpiece, and (v) documentation of all panels in digital high resolution visual photography, infrared photography and infrared reflectography [6]. It is important to mention that the examinations were primarily in the function of the advisory report and thus the scientific interests were not considered at that time.

With our research, we want to provide information on the painters' technique and knowledge and also support the ongoing conservation, by analysing the materials used on the frames and painting to: (i) detect misidentified pigments during previous restoration campaigns; (ii) reveal overpainted areas and retouching. The project illustrates how several complementary, non-destructive approaches can be implemented in archaeometrical research and conservation science. Additionally, it is explained how the use of current spectroscopic techniques is optimised, from which the archaeometrical study of the Ghent Altarpiece benefits directly.

Phase III: Open altarpiece

Phase II: Open altarpiece

Phase I: Closed altarpiece
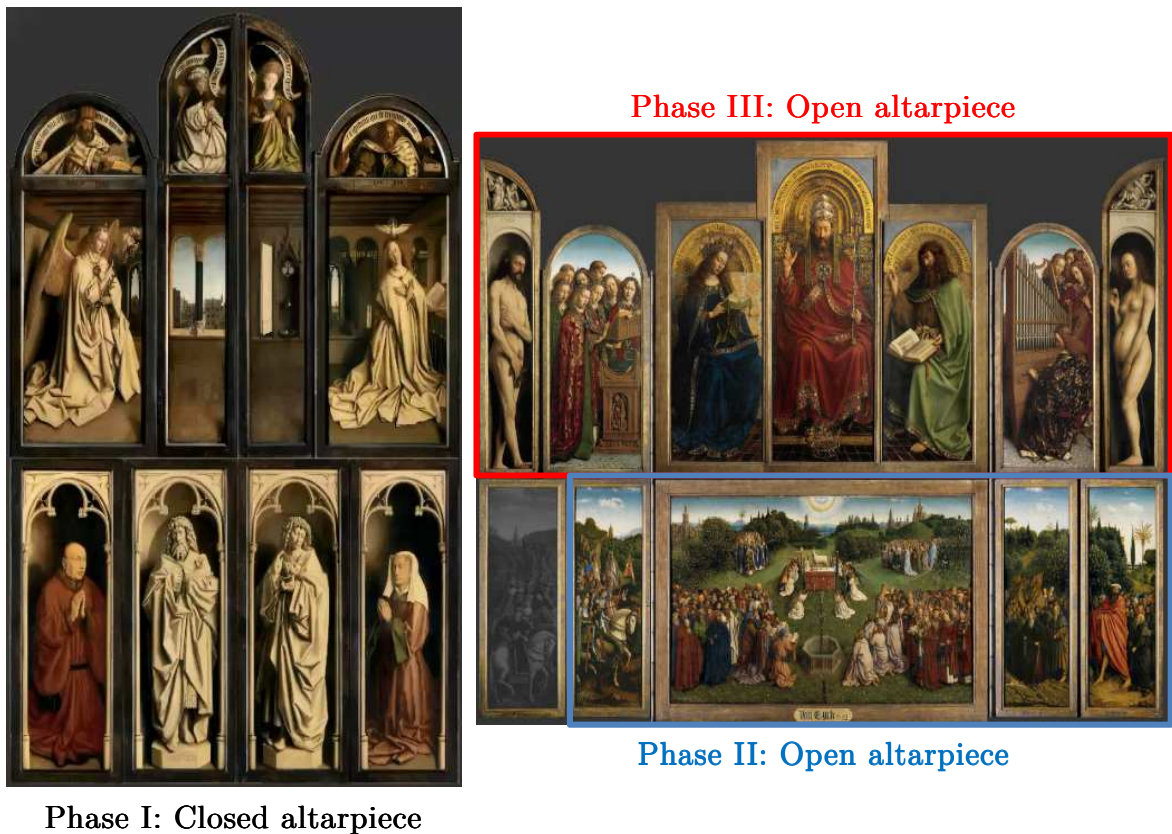
Figure 7.1 Ghent Altarpiece, created by Hubert and Jan Van Eyck. It is under conservation and restoration (2012-2019) by the Royal Institute for Cultural Heritage and the restoration campaign is divided in 3 phases. *© Sint-Baafskathedraal Gent, copyright Lukasweb.be - Art in Flanders VZW, photo KIK-IRPA.*

7.2 Cross-disciplinary project

Different scientific projects including the development of mathematical tools based on wavelets for automated image analysis of the Eyckian painting, were conducted on the Ghent Altarpiece during this conservation campaign. We, the Raman spectroscopy research group, focussed on two aspects within the research: (i) support the identification of the paint material, original and overpaint; (ii) protection of the exposed silver foils of the frames, which is important for the conservation. As mentioned, this first item was the focal point of this thesis. Via the implementation of a non-destructive, *in situ* study, we created a quick method to identify the paint material and its authenticity without damaging the painting (i.e. taking cross-sections). These analytical data were essential to determine the state of conservation and reveal earlier restoration campaigns.

However, the spectroscopic work is only successful when it is embedded in a complementary way with the achievements of the other partners (UGent, KIK-IRPA, UA), as shown in Figure 7.2. The network for this cross-disciplinary project consists of art historians, scientists and conservators. Close collaboration between these research groups results in the adequate interpretation and contextualisation of the Ghent Altarpiece. This includes information concerning the execution of the painting, the painting technique & materials and restoration history. Close collaboration in multi-disciplinary/multi-institutional projects is of high importance to obtain a complete documentation about the mediaeval painting. This is, however, not straightforward and is influenced by several factors. Colleagues of different disciplines have various backgrounds, which can cause communication problems. It is important to find a common way to report findings and explain them in a clear language. In addition, timing is crucial: conservation takes precedence over all other investigations. For example, Raman measurements are preferably executed when the varnish is removed. Yet, the restoration must proceed which limits the measurement time and thus measurement points need to be selected wisely. Moreover, parameters such as politics and commercial aspects may not be forgotten, as the Ghent altarpiece is an important piece of art.

7.3 Analytical techniques for the paint analysis

In science, different *in situ* methods exist for the analysis of cultural heritage, each with their advantages and disadvantages. For the direct, non-destructive pigment analysis of the Ghent Altarpiece, three methods were available in our laboratory: handheld X-ray fluorescence spectroscopy (hXRF), high resolution digital microscopy and portable Raman spectroscopy. By using a combination of these complementary methods, optimal information can be obtained. However, to achieve the best results/interpretation, it is crucial to have a close cooperation and interaction with colleagues from different disciplines.
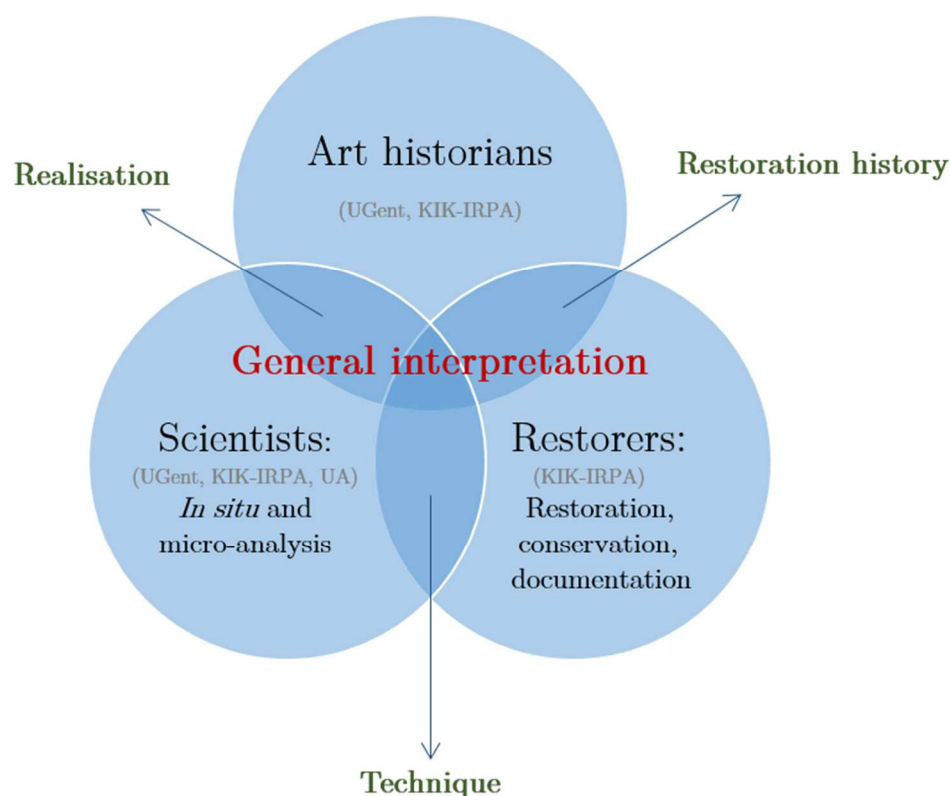
Figure 7.2 Schematic overview of the interdisciplinary collaboration for the best interpretation and contextualisation of the scientific results. [8]

As one can imagine, the interpretation of the data obtained is not simple. As the structure of oil paintings is complex (as illustrated in chapter 1, section 1.2), it is essential to know from which layer the information is retrieved. Table 7.1 gives an overview of the applied methods with some of their important instrumental and methodological characteristics. All these techniques are very useful to investigate the artists' palette. Hirox microscopy can deliver information about distribution, colour and morphology of pigment particles; crack patterns; etc., whilst Raman spectroscopy is a good tool to obtain molecular information. To secure high quality results, it is better to perform measurements after varnish removal. This is a very delicate process and is therefore performed by the conservation team [9]. Finally, hXRF can provide information on the elemental composition of the paint. Although, it helps to exclude possible pigments that were used, we need to be aware that simultaneous information is obtained from several layers. This makes it harder to draw clear conclusions on the paint composition.

Table 7.1 Overview of the applied methods with some of their important instrumental and methodological characteristics.

Method	Instrumentation	Information	Penetration depth	Remarks
High resolution digital microscopy	**Hirox microscope MXG–2500REZ lens** Source: White light Magnification 35-2500x, depending on the selected objective (low, mid or high range) Working distance : 10 mm	Microscopic: Information about distribution, crack patterns and colour and morphology of pigment particles;	"As deep as you can see": Depending on thickness, homogeneity and transparency of layer	Stable set-up needed due to vibrations
Portable Raman spectroscopy	**EZRaman-I-Dual Raman spectrometer** Source: 785 nm and 532 nm laser low laser power is selected. (See also Chapter 2 and 3)	Molecular	"As deep as you can see": Depending on the upper-most layer	Varnish can be a problem Working in the dark
hXRF	**Olympus InnovX Delta** Source: Rh X-ray tube (40 keV, 79 μA) Spot size: 5 mm^2 SDD detector, 300 s LT measurement time	Multi-elemental	Penetrates over several layers	Information from different paint layers simultaneously

7.4 Results and discussion

The direct analysis of the precious panel painting Ghent Altarpiece is a valuable tool for the conservation and restoration of the painting. The techniques used are non-destructive, fast and their application can reduce the necessity of sampling. Only when information on the stratigraphy needs to be retrieved, cross-sections have to be taken in the areas of interest. To be able to answer the research questions about overpaint, retouchings and misidentified pigments (during previous restoration campaigns), a good selection of instrumentation is required to obtain complementary information. Afterwards, their set-up needs to be optimised for the analysis in the conservation studio at the Museum of Fine Arts (Ghent).

As mentioned, 3 techniques — portable Raman spectroscopy, hXRF and Hirox microscopy — were selected and measurements were performed once a week. Consequently, the equipment needs to be transported to the museum and back to the lab, on the same day. In order to optimise the set-up, some practical parameters need to be taken into account. Aforementioned research (i.e. previous chapters) performed, with the portable Raman spectrometer, apply an articulating arm (chapter 4) or a clamp (for holding the probeheads) mounted on perpendicular optical rails with slides (introduced in chapter 3). Because sometimes both XRF and Raman spectroscopy were used on the same day for the analysis of Ghent Altarpiece, it was more convenient to utilise the same stage for both instrumentation so the latter set-up has been preferred (Figure 7.3). Therefore, a special holder for the hXRF spectrometer has been developed [10]. Also, this construction has the advantage of being compact and lightweight for travelling. Additionally, to secure the safety for the visitors and conservators, all measurements were performed in a black tent to preserve the safety zone. At the same time, this has the benefit to darken the area, so no interference from the environmental light would hamper the Raman signal.

The confined measurement space in the Museum of Fine Arts (Ghent) is not the most optimal region to perform microscopic analysis with the Hirox instrumentation due to the lack of space. So another suitable area is required within the conservation room.

As for all analytical techniques, some issues need to be considered: it is desired to keep vibrations (caused by visitors and research people) and manipulation of the paintings to a minimum. For this reason, an aluminum table was created (HIROX Europe, including JAAP Enterprise for art scientific research, Amsterdam (JE)) which is equipped with wheels and shock absorbers (Figure 7.3c).

Once these issues are solved, the analytical investigation of the different panels can be executed in their optimal condition.
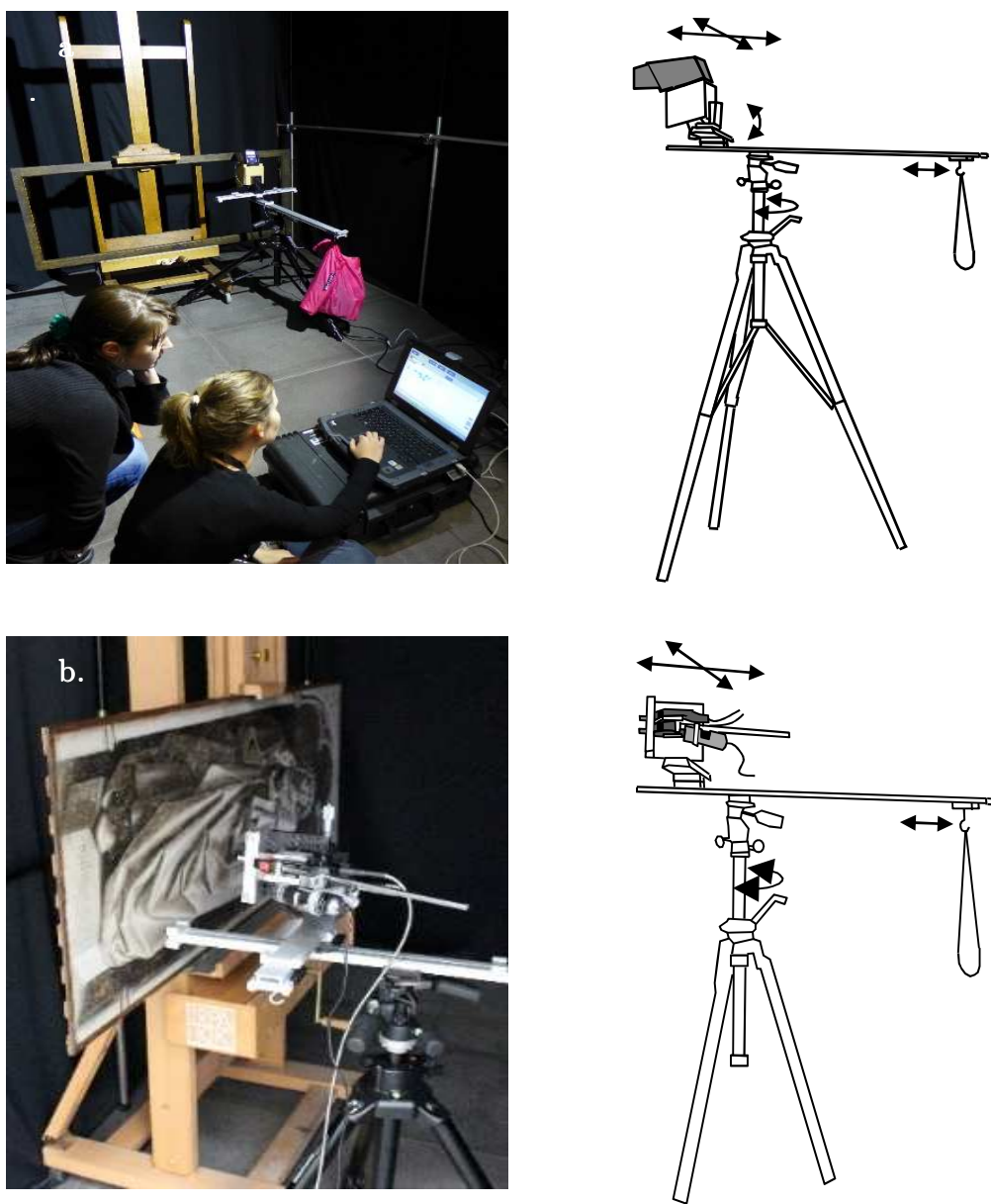
Figure 7.3 Set up of the 3 applied non-destructive techniques handheld X-ray fluorescence spectroscopy (a), mobile Raman spectroscopy (b) and High resolution digital microscopy (c).
© Sint-Baafskathedraal Gent, copyright Lukasweb.be - Art in Flanders VZW, photo UGent.
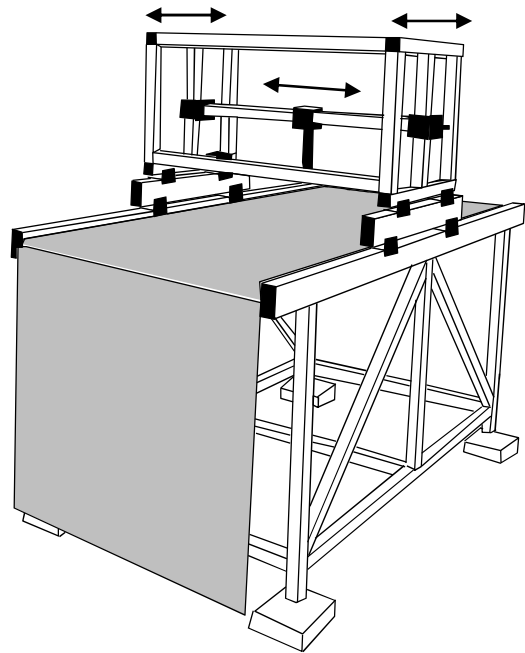
Figure 7.3 Set up of the 3 applied non-destructive techniques handheld X-ray fluorescence spectroscopy (a), mobile Raman spectroscopy (b) and High resolution digital microscopy (c). *© Sint-Baafskathedraal Gent, copyright Lukasweb.be - Art in Flanders VZW, photo UGent.*

7.4.1. Insert of Raman spectroscopy and hXRF

In a first step, the non-destructive methods Raman spectroscopy and hXRF are applied, performing point measurements. Two examples of examinations conducted using these techniques are presented here.

Pigment comparison of the polychrome decoration of the frames

During the previous conservation campaign (1950-51), the scientific research was mainly focused on the analysis of the painted surface. However, the original frames also make an important contribution to the visual aspect of the total altarpiece. In the report of the preliminary examination and conservation campaign of 2010, it was described that the polychrome decoration of the frames is overpainted and their condition is bad; in some cases, the paint shows some blisters [7]. Within the present conservation campaign, more information needs to be retrieved on the materials used for both the original paint and overpaint, in order to assemble a more complete documentation. The question needs to be answered whether during the different interventions in the past the same materials as the original ones were used.
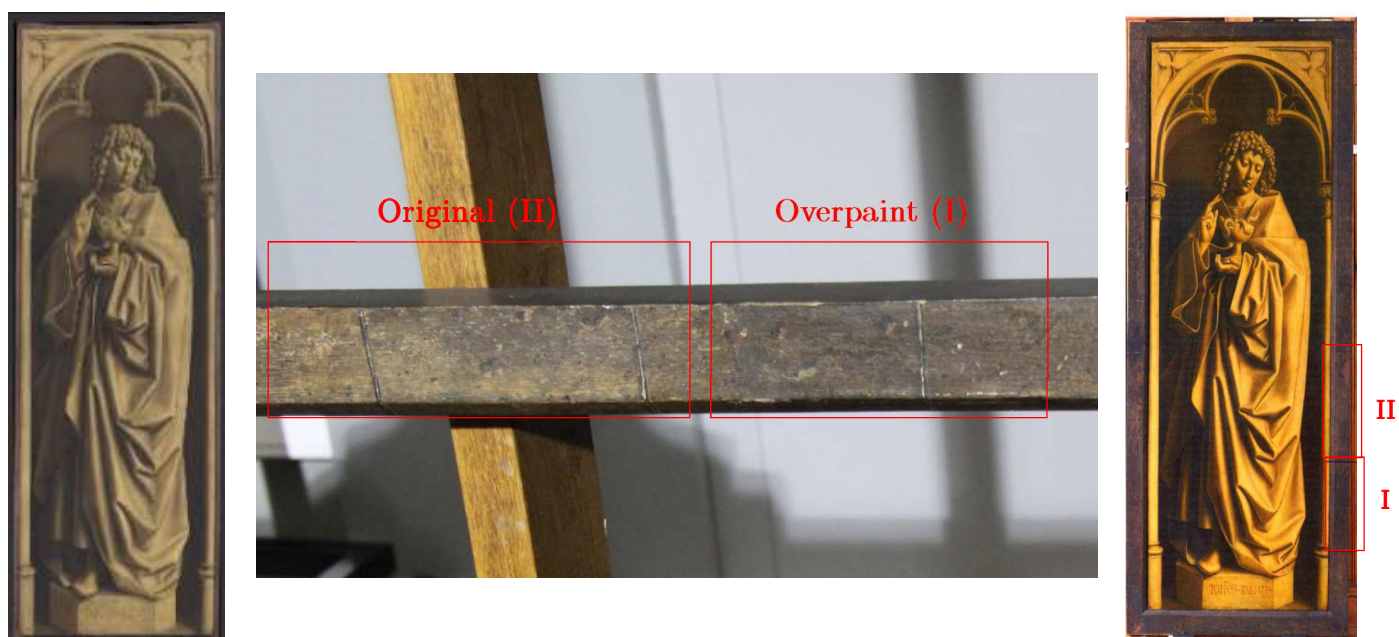
Figure 7.4 XRF and Raman analysis area of the Frame of Johannes the Evangelist. Information about the original paint layers and overpainting is requried. *© Sint-Baafskathedraal Gent, copyright Lukasweb.be - Art in Flanders VZW, photo KIK-IRPA and UGent.*

The frame of *Johannes the Evangelist* is selected for this research (Figure 7.4): the investigation focuses on the highighted pink areas. Before the start of the analysis, part of the frame was cleaned, enabling the investigation of the original paint and overpaint to be carried out.

In a first approach, hXRF was used to provide a fast indication of the used material. XRF detects information from the pigment but also from the support: it is important to figure out which elemental signal is significant for the pigment. For this reason, blank spots were searched to record a fingerprint of the carrier. This is compared with the signal recorded at the pink spots, to facilitate the interpretation of the XRF-spectra (Figure 7.5a-c). The restored blank area is characterised by a significant amount of Cu, Zn, Mn and Sn in comparison to the original blank area. This can be explained by the fact that there is a continuous layer of paint on top of the wooden support. After subtracting the blank, it is found that both, restored and original, pink areas are characterised by a significant Hg peak. This suggests the use of vermilion (HgS), probably mixed with a white pigment, given the pale hue.

To support this assumption Raman spectroscopy was applied (Figure 7.6). During the measurements, it has been discovered that the cloth of the dark tent was not sufficiently thick, causing interference due to the environment. A new fabric was purchased to solve this issue. Even though this problem occurred, it was possible to obtain clear Raman spectra. As suggested, it is confirmed that vermilion is used in both regions. Moreover, the Raman spectra prove the application of lead white ($2PbCO_3.Pb(OH)_2$) and calcite ($CaCO_3$) in the original and overpainted areas, respectively, mixed with vermilion. This indicates that the conservators at the time of intervention, only focused on the visual imitation instead of the chemical similarity.

Figure 7.5 XRF spectrum of the restored pink spot compared to the restored blank area (a) and the spectrum of the original pink spot compared to the original blank area (b). A significant amount of Hg is detected in both cases.

a. Restored pink vs restored blank

b. Original pink vs original blank
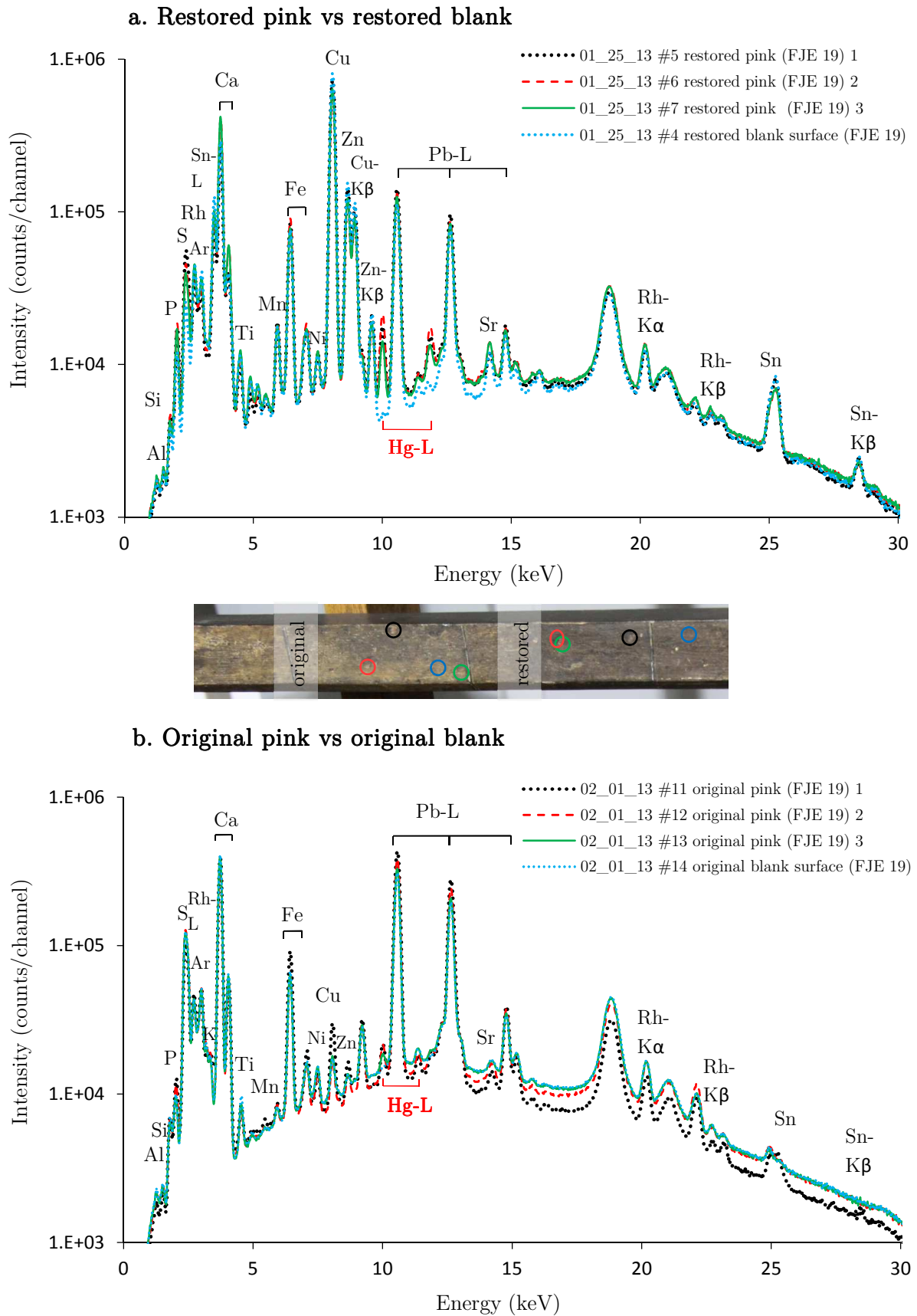
c. Restored pink and orignal pink (blank substraction)
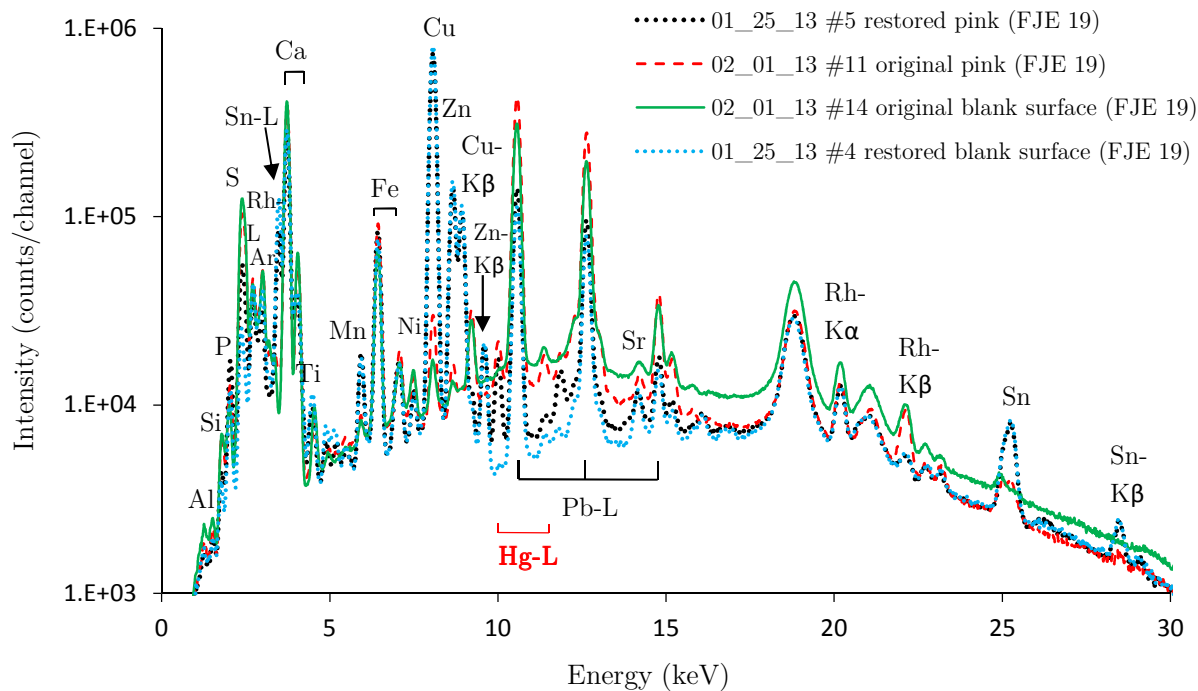
Figure 7.5c XRF spectrum of the restored pink spot compared to the restored blank area. A significant amount of Hg is detected.
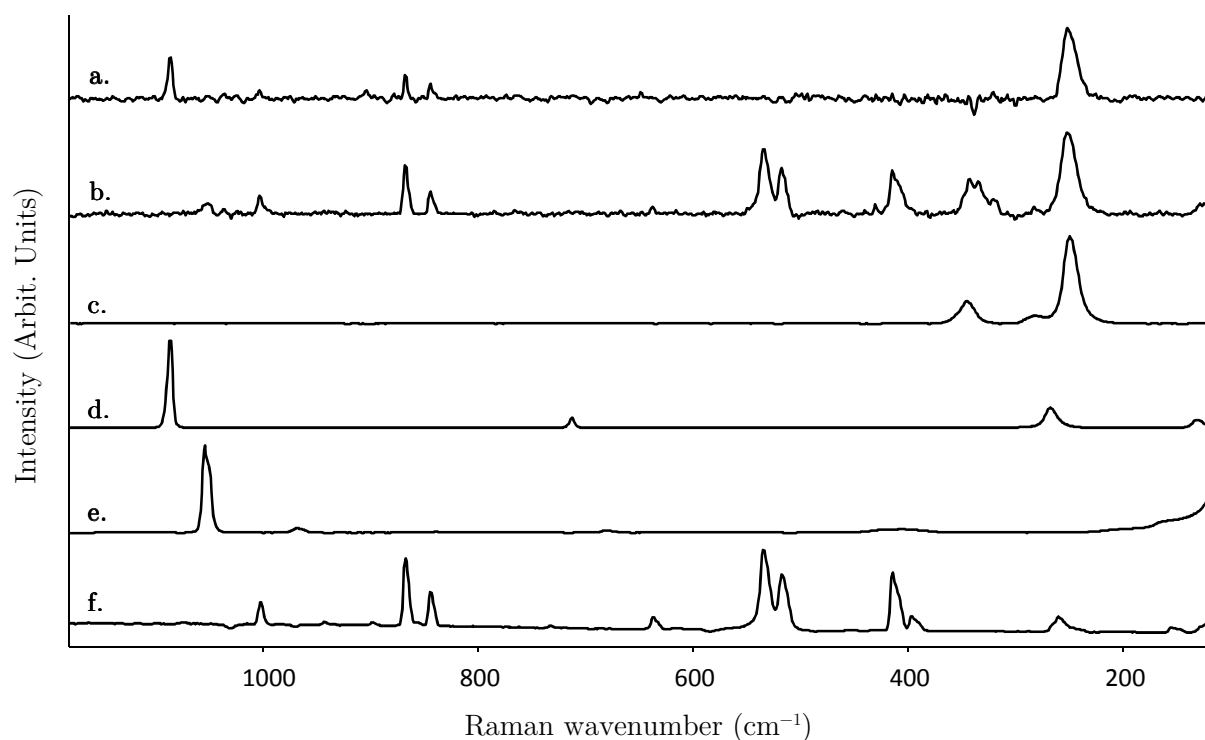
Figure 7.6 Raman spectra (λ=785 nm, 30x15 s, STD lens, 0.06mW, External power source, baseline corrected) of: (a) the restored pink spots, with Raman bands at 252 cm^{-1} (vermilion) and 1086 cm^{-1} (calcite); (b) the original pink spots, with Raman bands at 252, 283, 340 cm^{-1} (vermilion) and 1053 cm^{-1} (lead white); Reference spectrum of (c) vermilion, (d) calcite, (e) lead white; (f) spectrum of the environmental signal.

<u>Questions concerning original paint and retouching in a column of the painting Elisabeth Borluut.</u>

Both the frames and the panel paintings have been retouched. During the current conservation campaign a problem was observed in the panel representing *Elisabeth Borluut*, which needed to be clarified by spectroscopic analysis.

The conservator, Marie Postec, observed via macrophotography and X-ray radiography some issues in the base of the left column of *Elisabeth Borluut*. Although, the pillar is homogeneous in colour and *craquelure*, the X-ray images of that area show some inhomogeneities (Figure 7.7). Our research group has taken additional microscopic images of the region of interest with a Dino-lite camera (Premier AD7013MT), revealing indeed the presence of depressions (i.e. lacunaes) in the panel surface, filled with retouching pigment (Figure 7.7). To complete the documentation, it is of interest to determine which pigments are used for the original paint and retouching. For this reason, hXRF and Raman analysis are performed. It is noteworthy that the examination with hXRF was not straightforward. The retouched lacunaes are smaller than the spot size of the hXRF instrument (5 mm^2) and its positioning is not trivial. The detected signal is thus coming from the retouched areas as well as from the original paint (including all underlying layers). So a proper interpretation of the results cannot be made.

Three retouched areas and one original one were investigated (Figure 7.8a). In all cases, a high amount of lead is detected and a high amount of calcium, which fluctuates between the different retouchings and the original paint (Ca>Ca=Ca>Ca) (Figure 7.8b-d; colours refer to different areas). These elemental data suggest that calcite and/or a lead containing pigment (such as lead white) is used.
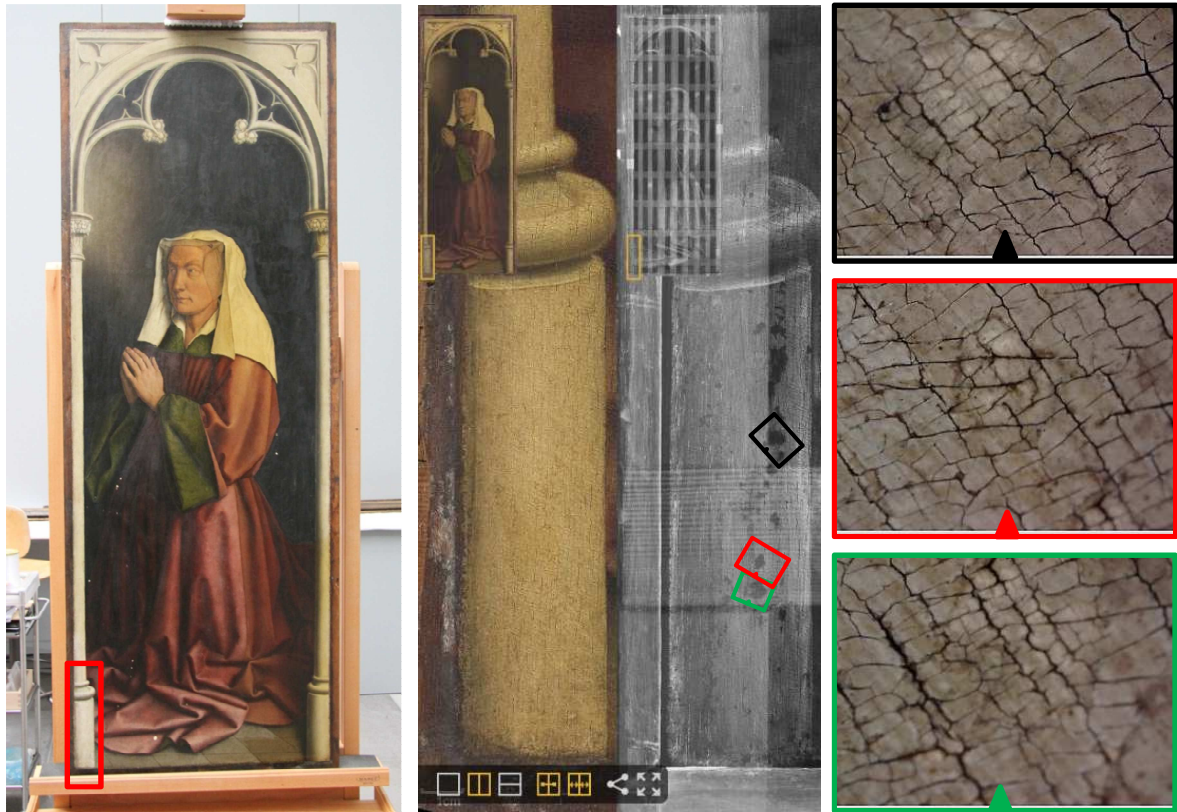
Figure 7.7 Overview of the problems (lacunaes) observed via macrophotography and X-ray radiography in the base of the left column of the painting *Elisabeth Borluut*. (colour codes correspond to Figure 7.8a) *© Sint-Baafskathedraal Gent, copyright Lukasweb.be - Art in Flanders VZW, photo KIK-IRPA and UGent.*

© KIK-IRPA, Brussels
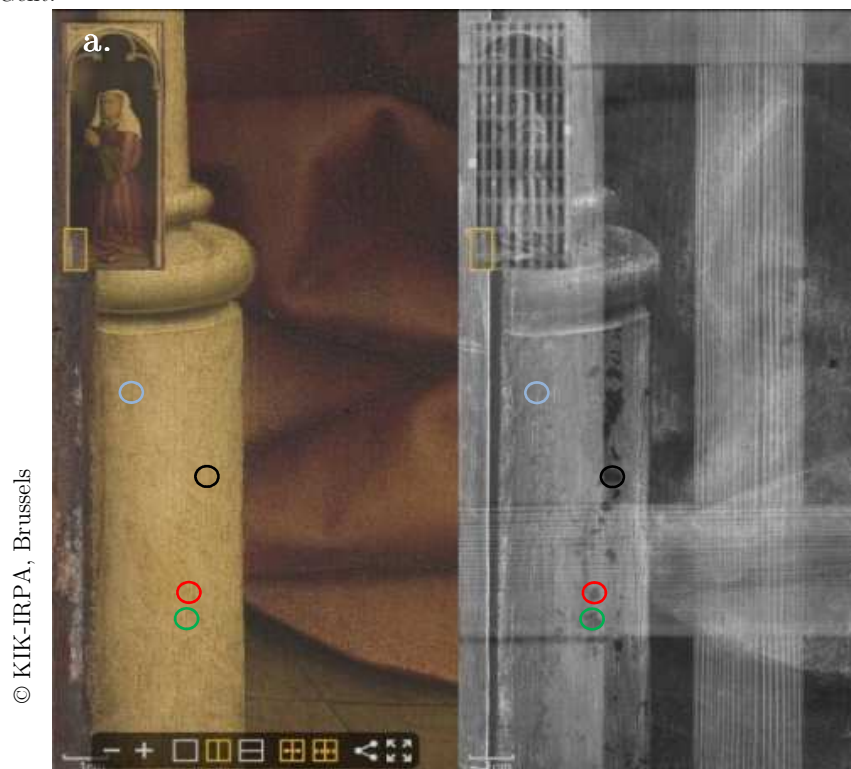
Figure 7.8 (a) Overview of the measured areas: Three retouched spots (black, red, green) and one original spot (blue). *© Sint-Baafskathedraal Gent, copyright Lukasweb.be - Art in Flanders VZW, photo KIK-IRPA and UGent.*

Figure 7.8 (b-d) XRF spectra of the retouched lacunaes compared to the original white areas. (Colour codes correspond to Figure 7.8a)

b. Painting Elisabeth Borluut: old white retouching point 1 vs white painting (original)

c. Painting Elisabeth Borluut: old white retouching point 2 vs white painting (original)

Figure 7.8 (b-d) XRF spectra of the retouched lacunaes compared to the original white areas. (Colour codes correspond to Figure 7.8a)

d. Painting Elisabeth Borluut: old white retouching point 3 vs white painting (original)
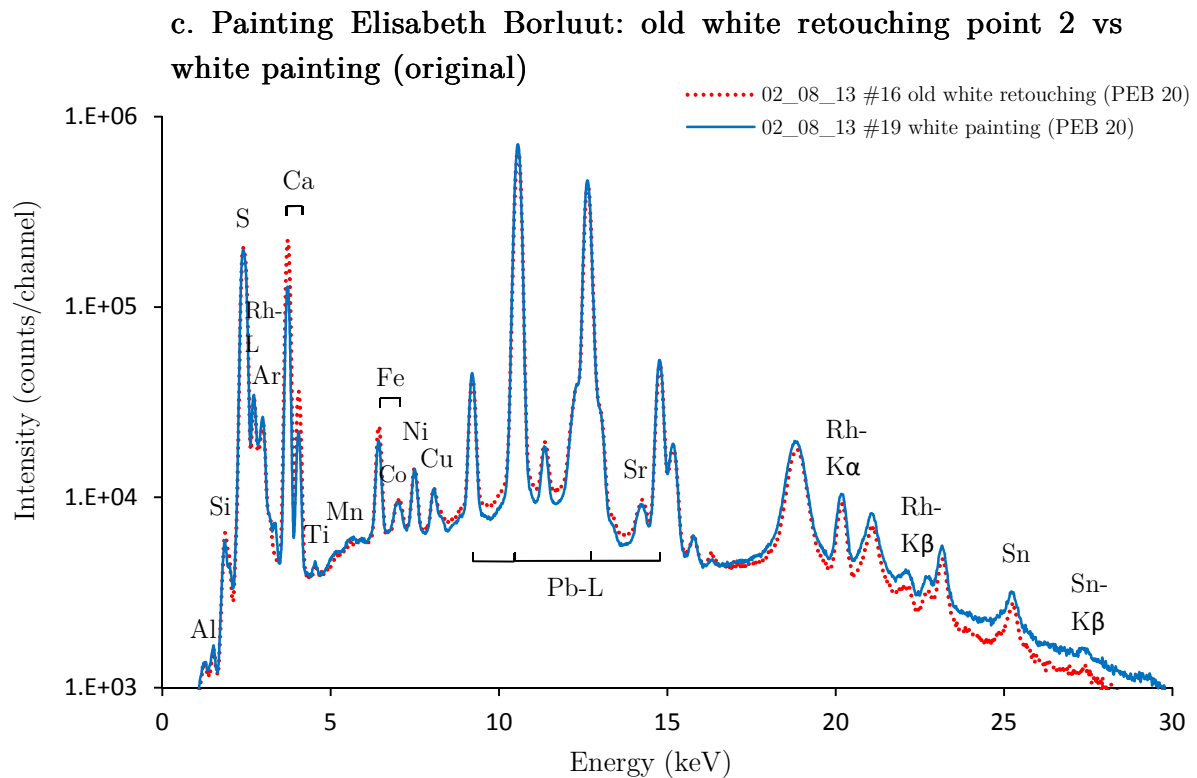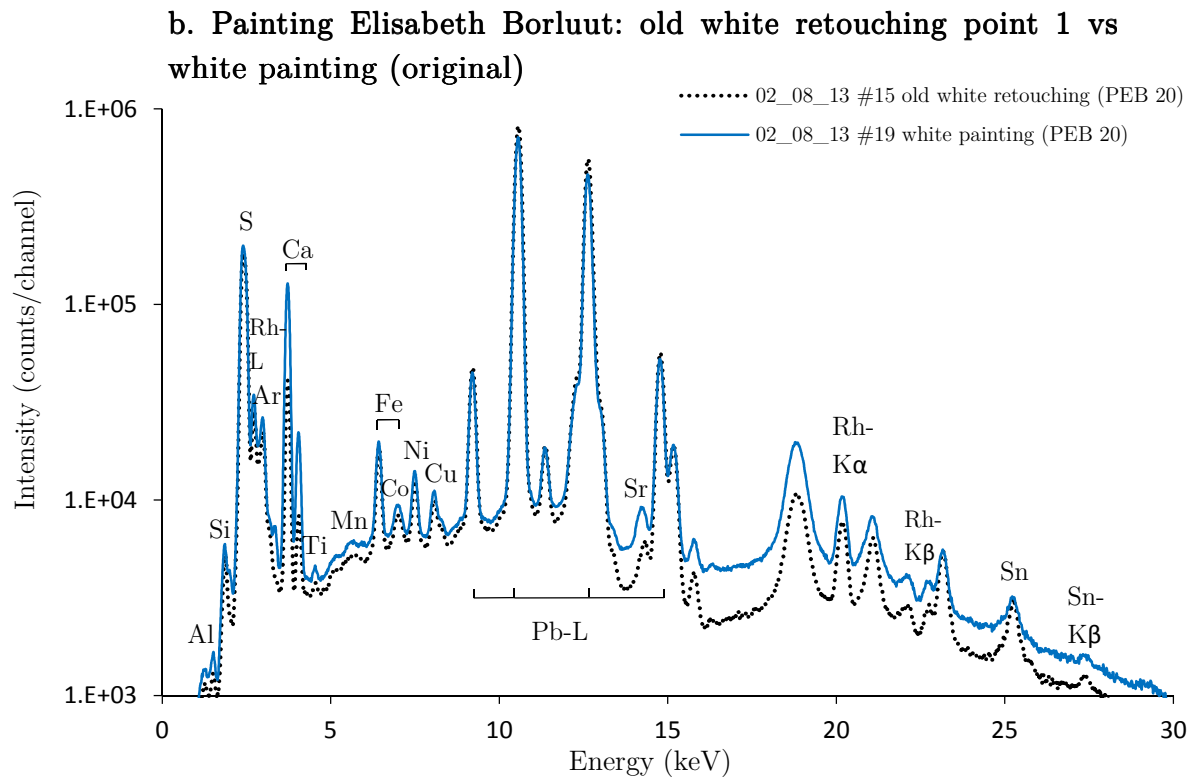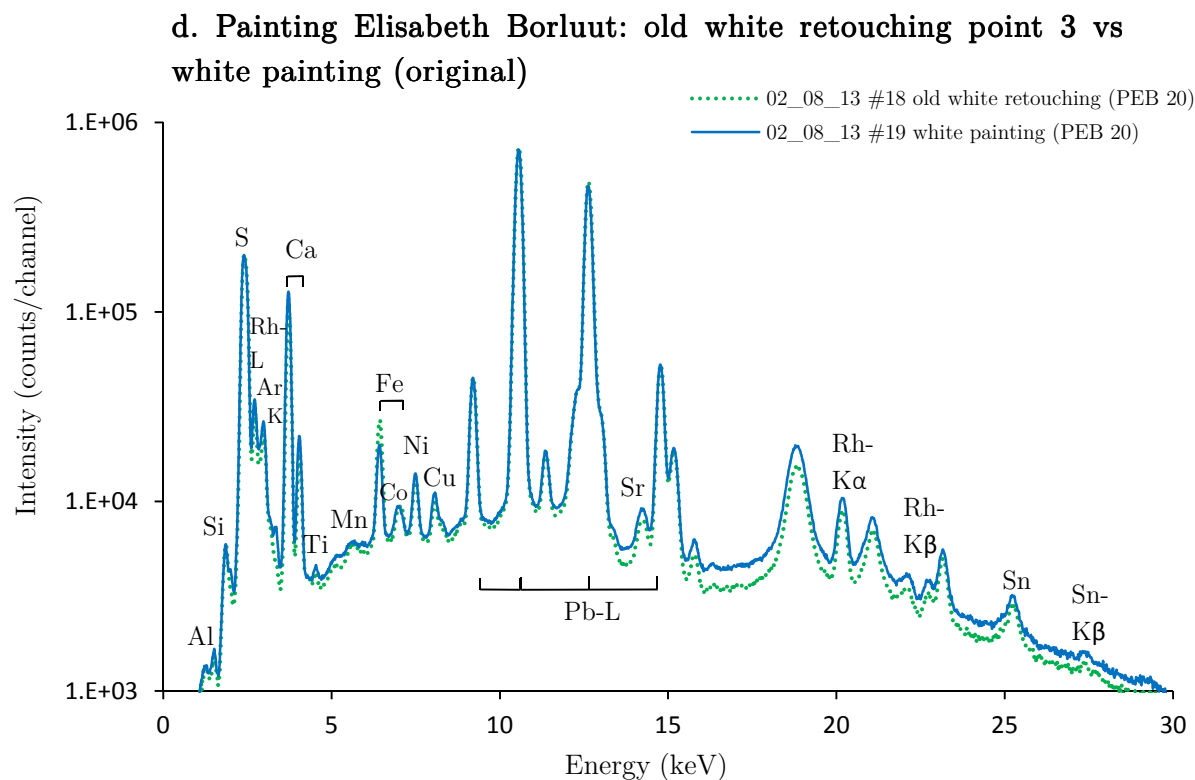
A clearer interpretation can now be given, based on the Raman results of the same areas (Figure 7.9). It has been detected that in both cases, for both the retouched as original paints, calcite is used in the paint material. Furthermore, the original paint layer consists of a mixture of lead white and calcite, except in the highlighted area (Figure 7.10). There is a difference noticeable in conservation of the pure and mixed lead white: the characteristic Raman band around 1050 cm^{-1} has different shapes. The single pigment seems to be altered − probably caused by the formation of a degradation product (possibly the presence of a mixture of new carbonate species mixed with unreacted lead white) due to the activity of H_2S − while the calcite may have acted as a protection for the lead based pigment [11].
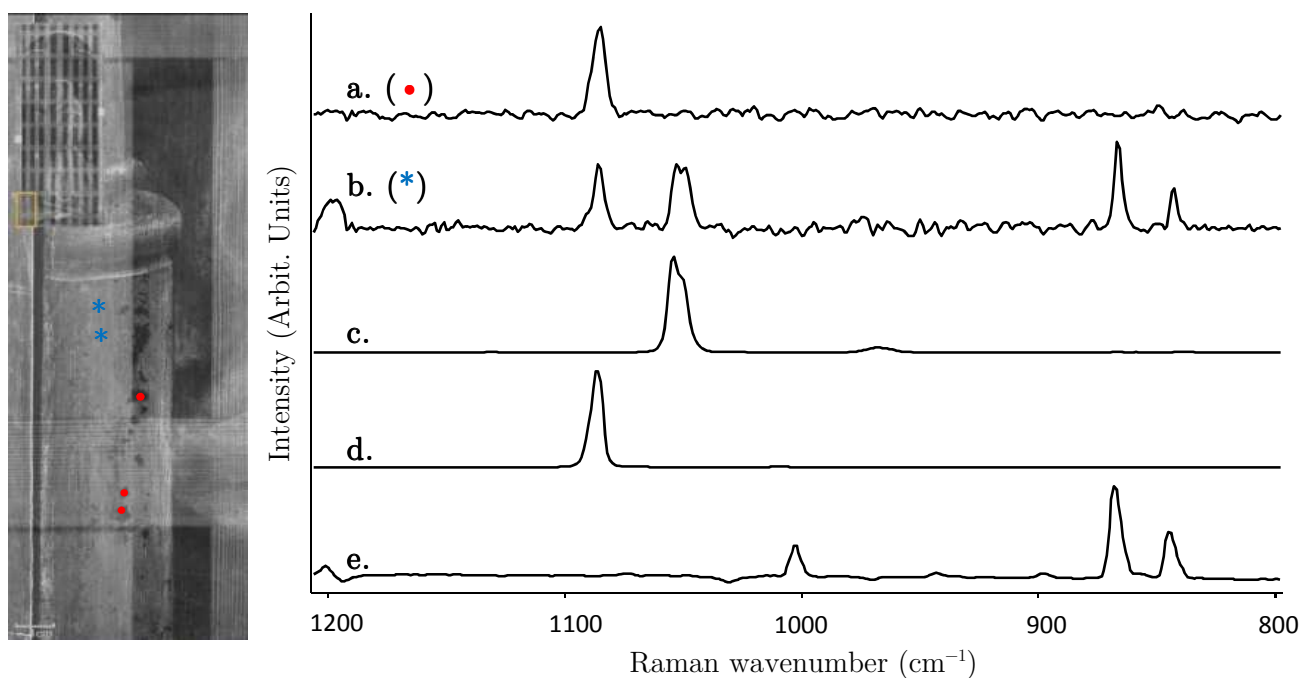
Figure 7.9 Average Raman spectra (λ=785 nm, 5x10 s, STD lens, 35.03 mW, External power source, baseline corrected) of: (a) the retouched lacunaes, marked with • , with a characteristic Raman band at 1086 cm⁻¹ (calcite); (b) the original white paint layer, marked with *, with Raman bands at 1054, 1050 cm⁻¹ (lead white) and 1086 cm⁻¹ (calcite); Reference spectrum of lead white (c), calcite (d); (e) Raman spectrum of the environmental signal.
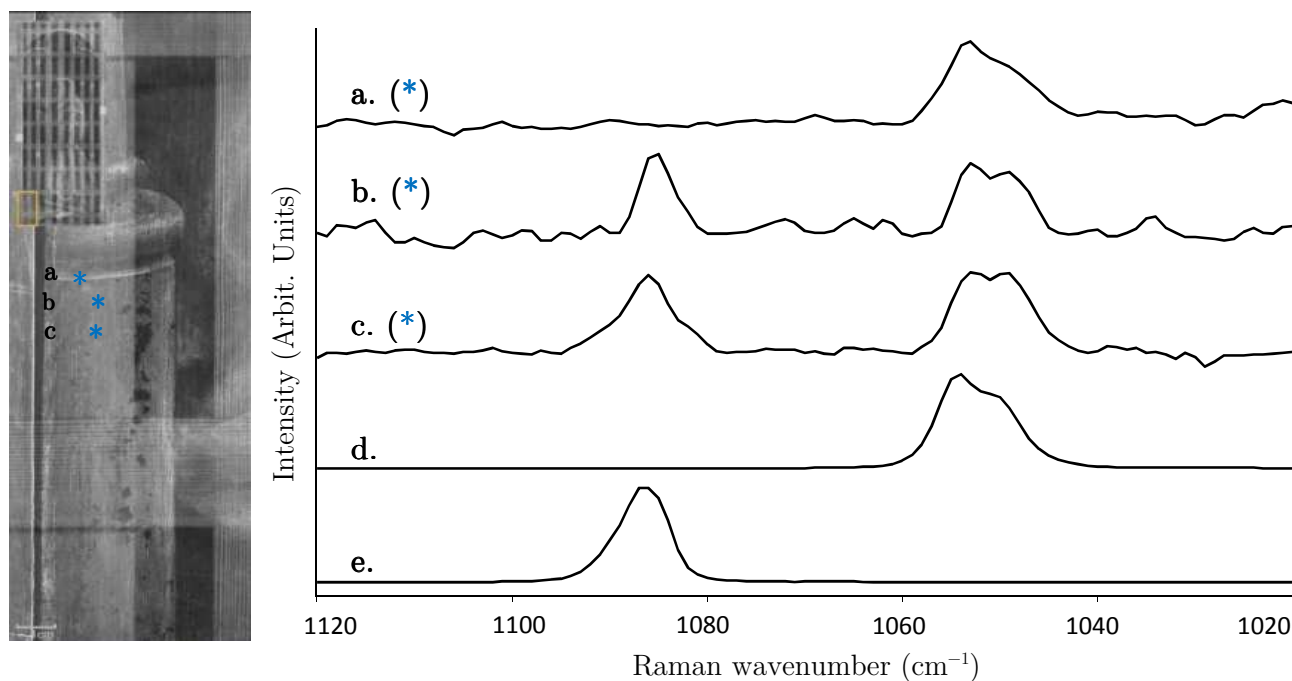
Figure 7.10 Raman spectra (λ=785 nm, 5x10 s, STD lens, 35.03 mW, External power source, baseline corrected) of the original white paint layer, marked with *, with Raman bands at 1054, 1050 cm⁻¹ (lead white) and 1086 cm⁻¹ (calcite) (a-c); Reference Raman spectrum of lead white (d) and calcite (e).

When combining these results with the expertise of the conservators, it was concluded that the detection of calcite in the original oil paint layer is unexpected. Two possible explanations can be given: (i) calcite is added to the oil painting as an extender and to provide the desired consistency of the paint. It makes no contribution to the colour as it becomes transparent in the medium. (ii) it can be a marker for the detection of an overpaint but this seems, at first sight, rather unlikely. In order to exclude one of these assumptions, the conservation team and other partners performed further investigations. The examinations included macroscopic and microscopic observations (using Hirox microscopy) and macro-XRF imaging. In this later stage of the conservation, our assumption about the presence of an overpaint, proved to be correct. This first proof of overpainting was also the trigger for a more intensive investigation of the oil painting, leading to the remarkable conclusion that 70% of the panels were overpainted.

General conclusions based on the given examples

The *in situ*, non-destructive methods proved to be successful to reveal the presence of overpainting in an early phase of conservation. However, not all measurements were satisfactory to answer the conservators' questions, especially with respect to the XRF measurements: the signal is obtained from different layers and often the spot size of the instrument was too large for the concerned area. In addition, it delivers mostly similar information as the Raman analyses. Consequently, it has been decided to complement the measurements with microscopic investigation of the paint material using Hirox microscopy.

7.4.2. Combination of Raman spectroscopy and Hirox microscopy

The combined use of Raman spectroscopy and Hirox microscopy is a new approach for the direct analysis of oil paintings. To use this combination in an effective way, a protocol had to be developed in order to have an optimal approach.

It has been decided to apply Hirox measurements prior to the Raman analysis as the set-up does not allow one to record images and a Raman spectrum sequentially. Unfortunately, the table of the Hirox instrumentation does not fit in the dark tent where

Raman examinations need to be carried out. As a consequence, Hirox and Raman investigations cannot be performed on exactly the same spot and thus it is preferred to execute first a good documentation using Hirox microscopy, before moving the painting for Raman investigations. This proposal makes it possible to first determine and capture the status together with the conservators and to choose the best regions for the molecular investigation. Some parameters need to be kept in mind when selecting measurement areas: (i) the varnish layer should be absent (or as thin as possible); (ii) the selected area may not be smaller than the laser spot size (80 µm), to avoid interference of the surrounding paint; (iii) the location of the measurement spot should be easy to retrieve. The latter requirement is not as simple as it first seems as some details are barely visible with the naked eye. A solution is found by documenting the coordinates of the region of interest to relocate the are more precisely.

As an example, the panel painting *Johannes the Evangelist* is examined with this protocol. In the painting some interesting areas of retouching and yellow details were found and documented with Hirox microscopy. This thesis focuses on the investigation of these yellow details as they were often misidentified in the previous conservation campaign (1950-51, Coremans) as massicot (PbO). The yellow pigment was found in the highlights of the robe and hands but also in the inscription on the soccle of the grisaille (Figure 7.11). Raman positioning was not always easy due to the issues mentioned above. Nevertheless, in all cases it is proven that the yellow pigment used by Van Eyck was not massicot, but lead tin yellow type I (Pb_2SnO_4) (Figure 7.11). A distinction between lead tin yellow type I (Pb_2SnO_4) and II ($Pb(Sn_{1-x}Si_x)O_3$) can be made due to the good spectral resolution of the Raman instrumentation. Both the images and the pigment identification were helpful to complete the documentation on the artist' palette and technique. However, this approach can still be improved, to make it an excellent qualitative method.
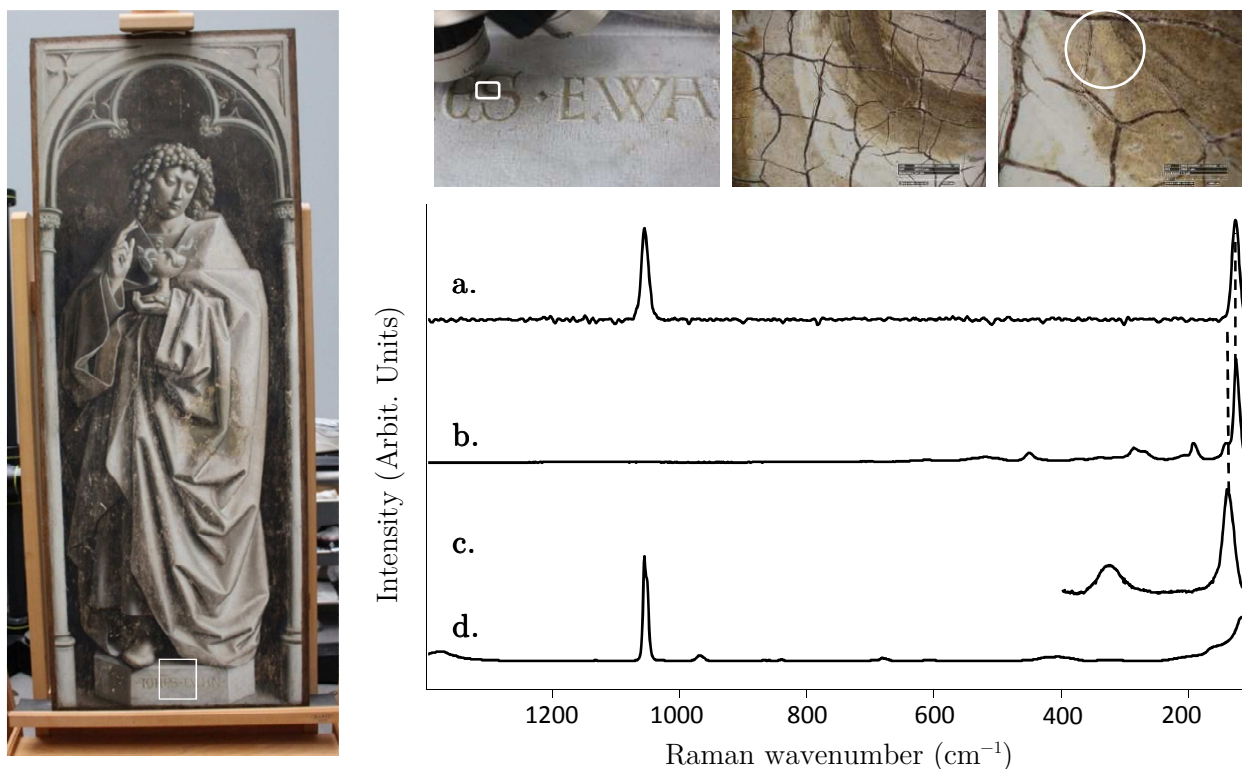
Figure 7.11 Examination of the panel *John the Evangelist* with Hirox microscopy and Raman spectroscopy. At the top, the recorded Hirox images are illustrated which are important for the documentation. Next to this, the Raman spectrum (λ=785 nm, 10x30 s, STD lens, 20 mW, External power source, baseline corrected) of the analysed yellow area is displayed with characteristic Raman bands at 129 cm⁻¹ (Lead tin yellow type I) and 1052 cm⁻¹ (Lead white) (a); Reference Raman spectrum of lead tin yellow type I (b), lead tin yellow type II (c) and lead white (d). *© Sint-Baafskathedraal Gent, copyright Lukasweb.be - Art in Flanders VZW, photo KIK-IRPA and UGent.*

7.5   Conclusions

This chapter has illustrated how several complementary, non-destructive, *in situ* approaches can be implemented in archaeometrical research and conservation science. More specifically, it is explained how the techniques hXRF, portable Raman spectroscopy and Hirox microscopy are optimised from which the conservation of Ghent Altarpiece benefits directly.

Even though the approaches were successful, the method of application can still be improved. Until now, only point measurements were performed with both hXRF and

portable Raman spectroscopy. Recently, M. Alfeld et al. have developed an *in situ* scanning macro-XRF scanning system to create elemental distribution images [12]. In a next step of our research, it would be beneficial to automate the positioning system of the portable Raman spectrometer and develop a method that makes chemical imaging possible.

In addition to the improvement made in the application of the single techniques the combined use of Raman spectroscopy and Hirox microscopy can be expanded in this direction. So far, the approach consists of two steps: firstly, the microscopic imaging is carried out, followed by Raman point measurements. To bring it to the next level, merging the microscopic imaging and the chemical imaging system would be of added value. For this, the set-up of the Hirox microscope and the portable Raman spectrometer should be combined in order to accomplish an *in situ* mapping system with high spatial resolution.

To summarise, so far a complete characterisation of the portable Raman spectrometer for *in situ* art analysis, is discussed, including its beneficial combination with other techniques. For all the analyses, only point measurements were executed. In the next part of this thesis we want to take the applicability of portable Raman spectroscopy to a higher level and steps are undertaken to create an automated, molecular, *in situ* imaging system. Chapter 9 discusses a first step towards this chemical imaging concept where the challenges of the development are explained. The focus of the chapter mainly is on the data-treatment, which is important for the creation of a Raman map, but also hardware and software will be discussed, as a suitable set-up and software are essential for the *in situ* Raman mapping system.

7.6   References

[1]   J. Koldeweij, A. Hermesdorf, P. Huvenne, De schilderkunst der Lage Landen: Deel 1- Middeleeuwen en de zestiende eeuw,Amsterdam University press, 2006.

[2]   E. Effmann, Theories about the Eyckian painting medium from the late-eighteen to the mid-twentieth centuries, Rev. Conserv. 7 (2006) 17–26.

[3]   P. Brinkman, Het geheim van Van Eyck, WBooks, 1993.

[4]   C. Harbison, Jan Van Eyck: The Play Of Realism, Reaktion books, London, 1991.

[5]   A. Born, M. Martens, Het Lam Gods ont(k)leed!, Provincie Oost-Vlaanderen, 2013.

[6]   Anne van Grevenstein-Kruse et al., Conservatie en materieel onderzoek van het Retabel van het Lam Gods Gent, Sint-Baafskathedraal (2011), http://closertovaneyck.kikirpa.be/

[7]   P. Coremans, Les Primitifs Flamands: III. Contributions a L'etude Des Primitifs Flamands, No. 2: L'Agneau Mystique Au Laboratoire, Examen et Traitemant, De Sikkel, 1953.

[8]   http://closertovaneyck.kikirpa.be/

[9]   E. Carretti, I. Natali, C. Matarrese, P. Bracco, R.G. Weiss, P. Baglioni, et al., A new family of high viscosity polymeric dispersions for cleaning easel paintings, J. Cult. Herit. 11 (2010) 373–380. doi:10.1016/j.culher.2010.04.002.

[10]   L.Van de Voorde, J. Van Pevenage, K. De Langhe, R. DeWolf, B. Vekemans, L. Vincze, P. Vandenabeele, M.P.J. Martens, Non-destructive in situ study of "Mad Meg" by Pieter Bruegel the Elder using mobile X-ray fluorescence, X-ray diffraction and Raman spectrometers, Spectrochim. Acta Part B 97 (2014) 1–6. http://dx.doi.org/10.1016/j.sab.2014.04.006

[11]   G.D. Smith, R.J.H. Clark, The role of H_2S in pigment blackening, J. Cult. Herit. 3 (2002) 101–105. doi:10.1016/S1296-2074(02)01173-1.

[12]   M. Alfeld, J.V. Pedroso, M. van Eikema Hommes, G. Van der Snickt, G. Tauber, J. Blaas, M. Haschke,K. Erler, J. Dik and K. Janssens. A mobile instrument for in situ scanning macro-XRF investigation of historical paintings, J. Anal. At. Spectrom. 28 (2013) 760-767. doi:10.1039/c3ja30341a.

Chapter 8

In situ Raman mapping of art objects

In the previous chapters, an intensive evaluation of the portable Raman spectrometer for in situ art analysis has been described. This included a discussion of the important characteristics for selecting an appropriate spectrometer as well as parameters which need to be taken into account for in situ analysis. Additionally, it has been pointed out that the use of complementary, non-destructive techniques is ideal to obtain more complete results. However, the individual Raman spectrometer as well as the combined use of different methods can still be improved.

Until now, portable Raman spectroscopy fails in the reconstruction of the chemical distribution of a compound because only point measurements are performed. Laboratory Raman mapping experiments of paint cross-sections have several times proven their success of constructing chemical images with high spatial resolution. Why would we not implement this advantage on a bigger scale and develop an in situ Raman mapping system. This story was already achieved with success in the world of X-ray fluorescence spectroscopy: M. Alfed et al. developed recently an in situ scanning macro-XRF scanning system to create elemental distribution images [1].

Therefore, in this chapter a first step towards an automated in situ Raman mapping system is made. The focus mainly lays on the data-treatment which is important for the creation of a Raman map, but also hard- and software will be discussed, as a suitable set-up and software are essential for the in situ Raman mapping system.

8.1 Introduction

Archaeometrical research has grown significantly during recent decades and a trend can be observed to minimise sampling, for ethical reasons. Due to the development of more sensitive equipment, sample size could be reduced. Moreover, recently, the wide development of non-destructive approaches using, mobile instrumentation (Raman spectrometers, infrared devices, X-ray fluorescence equipment, etc.), allowing for *in situ* investigations makes sampling often unnecessary [1,2]. As the interest in archaeometrical science is still increasing, innovative approaches are needed.

In situ methods are indispensable in cultural heritage research. Raman spectroscopy is a molecular spectroscopic approach that has many advantageous properties for the study of cultural heritage objects. These positive features include an excellent spatial resolution and the ability to perform *in situ* studies. Several publications can be found relevant to the on-site, molecular examination of mediaeval wall paintings, museum objects, geo-biological samples, etc. [3–7]. In these cases, point measurements are performed on the objects. This punctual analysis has some limitations that need to be taken into account. One of the main problems is the failure to represent the heterogeneity, complexity of materials or potential degradation phenomena present on the surface of art objects [8]. Until now, only laboratory micro-Raman mapping systems have been shown to be very useful for resolving these problems. Quaranta et al. [9] have shown that a Raman mapping system can be useful to represent the heterogeneity of corroded high-leaded bronzes. Not only is the investigation of degradation processes, using mapping experiments, of interest, also the study of pigment materials is an important research topic [10]. It has been demonstrated how impurities can be linked to their spatial distribution in historical zinc-based white pigments using laboratory instruments [11]. As for the complexity of materials, Raman maps with high spatial resolution were able to provide information of pigment distribution in painting cross-sections [12,13]. However this sampling method has a major drawback in that only information of limited areas of a total panel painting is obtained. Therefore, we aim to combine the excellent spatial resolution of the approach with its ability to be applied *in situ*, allowing for a virtually unlimited size of the art object.

In all cases mentioned here it has been shown that laboratory Raman mapping systems are an ideal tool for imaging molecular distributions. However, these experiments also have their constraints [12,14,15]. As the object being investigated moved step by step under the microscope using an XYZ stage, the main limitation is the restriction of the sample size: the object has to fit under the microscope and should be sufficiently flat, even if an autofocus system is present [14]. In this project, we want to implement this approach for use outside the laboratory and for its use *in situ*. Challenges for the development of an *in situ* Raman mapping system are discussed. Although the focus of this paper mainly concentrates on the data-treatment which is important for the creation of a Raman map, also hardware and software will be explained, as a suitable set-up and software are both essential for the *in situ* Raman mapping system.

8.2 Experimental

8.2.1. Raman instrumentation

For the development of an *in situ* Raman mapping system, the portable Raman spectrometer, EZRAMAN-I-DUAL Raman system is modified. For a correct positioning, in the current experiments, the LWD lens is selected, which has a focal distance of 15 mm. In order to map accurately a region of interest, good positioning equipment is necessary. The set-up used for the direct analysis is shown in Figure 8.1. The probeheads are mounted on an articulating arm [16] using an clamp developed in-house [6]. Micro-positioning of the probeheads can be performed by changing the position of the XYZ mounting stage by means of program controlled step motors, introduced by Vandenabeele et al. [16].
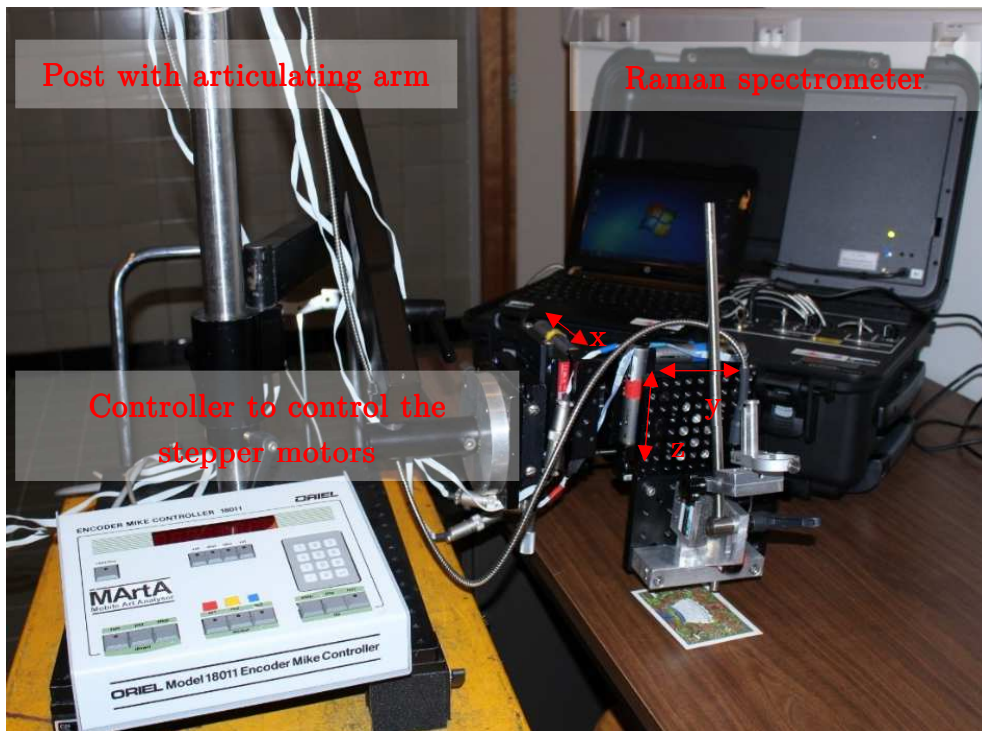
Figure 8.1 *In situ* Raman mapping set-up, developed in-house. The porcelain card is horizontally positioned on a table, the system is focused and the probehead can move in a horizontal plane above the artefact.

8.2.2. Samples

Objects with irregular surfaces are difficult to map and pose a problem for the correct focusing of the system. To avoid this issue during this phase of development, 19th century porcelain cards are used (Figure 8.2), as these are flat. Porcelain cards were used as publicity cards or for announcements in the 19th century. They consist of a card board that is first covered with a layer of lead white and then decorated by hand using pigments such as vermilion, chrome yellow, red lead, lead white, Prussian blue, etc.. Historical details of these cards are described elsewhere [17].

Figure 8.2 19th century porcelain cards, used for the test-measurements of the *in situ* Raman mapping system.

8.3 Results and discussion

8.3.1. Development of a Raman mapping system

The development of a Raman mapping system is not straightforward. Several critical parameters are of importance: (i) focusing; (ii) stable positioning system; (iii) software for controlling the movements and data-acquisition; (iv) data-processing procedures to create the Raman map.

The first factor 'focusing' is critical, as a defocused laser beam does not yield high-quality Raman spectra. Raman scattering is inherently weak: misfocusing leads to low SNR Raman spectra and thus characteristic Raman bands can be masked by the noise [18]. The laser beam is focused on the surface of the artefact by changing the distance between the probehead and the object of art. Different approaches can be used, such as the measurement of the distance towards the surface (profilometry) [19], or by evaluating the spectral response. It needs to be mentioned that not only the defocused beam is a major issue in the Raman analysis of art objects. Samples such as oil paintings have a problem in that they are covered by a varnish layer. The approaches mentioned here can lead to a focusing being made on this top layer instead of the layer of interest. Nevertheless, using objective lenses with a relatively large depth of focus, the influence

of focusing can be reduced [20]. The focusing problem when performing Raman mapping has been well-described by Davies (2015) [21]. However, solving this problem is currently out of the scope of our research, and therefore, to avoid this problem, porcelain cards are appropriate test-cases for the current work because of their flat surface.

To be able to perform Raman mapping, an accurate and stable positioning system needs to be created. In cultural heritage research, many of the analysed objects are fragile, difficult to manipulate or too large to handle and therefore, it is easier to move the instrument probehead relative to the artefact, instead of moving the art object. Due to the beneficial use of the fiber-optic probeheads, a system can be developed such that these can be moved relative to the object, in a horizontal or vertical way. To make this operation feasible, a stable motorized stage is designed (Figure 8.1). Thus, the (flat) porcelain card is horizontally positioned on a table, the system is focused and the probehead can move in a horizontal plane above the artefact.

The set-up can be operated by the in-house developed software which permits the control on the one hand the movements of the stepper motors (for stable and reliable positioning) and on the other hand the data acquisition. Both functions need to be well-coordinated, to be sure that the data recording of each spectrum is properly positioned. When performing a mapping experiment, typically a large number of spectra is recorded consecutively, and the measurement time per spectrum is kept as low as possible (in these experiments, typically 3 accumulations of 5 seconds). Moreover, the software also allows for the correct spectral calibration of the spectral data [22].

The large number of spectra in a Raman map has not only an influence on the data acquisition, but also on the post-measurement data processing. A Raman map typically is composed of hundreds to thousands of spectra and manual examination of every spectrum is impossible. Therefore, a well-structured data-processing protocol is needed.

8.3.2. Protocol for the creation of a Raman map

Our data processing protocol consists of 4 essential steps: (i) importing the data in the software; (ii) visualisation of the dataset; (iii) extraction of variables of interest and (iv) creation of a Raman image.

Correctly importing the spectra into the software (Matlab) is evidently a crucial step: the spectra need to be accurately read and linked to their x, y coordinates to create the appropriate Raman map. In a second step, it is convenient to be able to visualize the spectral data. Thus, the analyst is able to see the spectral quality, and to observe the different types of spectra that are present, to assist in selecting the variables of interest. Spectra can be plotted in a 3D plot, the average spectrum can be plotted or one can examine all the spectra separately (Figure 8.3). Creating an average spectrum can be useful when degradation phenomena are investigated: a direct evaluation can be made whether degradation processes occurred. It has to be remarked that making a 3D-plot is not always the best option when dealing with large datasets, as creating such a plot requires quite some computing time and small details are not easily observed in the large plot containing many spectra.
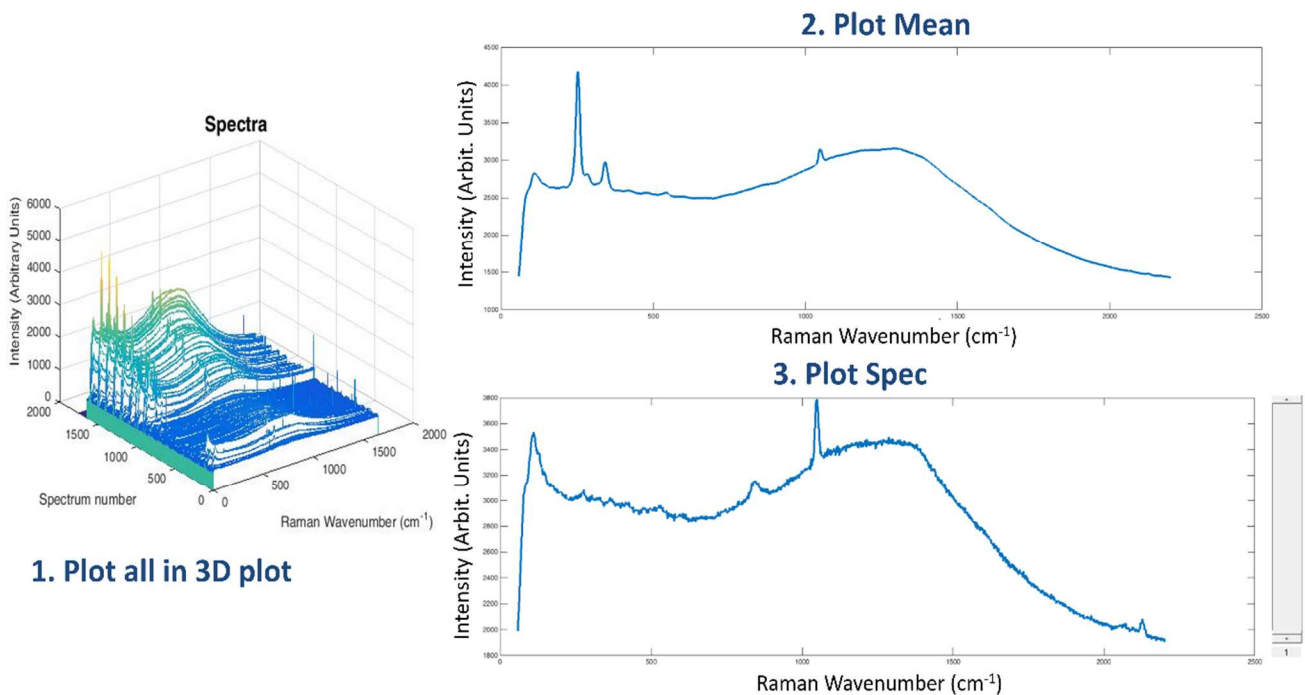
Figure 8.3 Visualisation methods to easily select the variables of interest.

Before extracting the variables of interest, sometimes a spectral pretreatment can be useful, as the spectral signal may originate from different processes (Raman scattering, cosmic rays, fluorescence, etc.). Moreover, because of the large number of spectra, they are typically recorded using short measurement times, the spectral quality (signal-to-noise ratio) is often rather poor. Preprocessing functions, such as baseline correction, smoothing, or taking the derivative can assist in avoiding these interferences.

After visualization of the spectra and appropriate spectral preprocessing, the data for Raman mapping can be selected. It is possible to select univariate processing if spectral regions of interest are known. On the other hand, when using multivariate methods, the whole spectrum is used for the data extraction.

<u>Univariate analysis</u> monitors one variable per spectrum. Different extraction methods are illustrated in Figure 8.4a. The selection of the method depends on the research question. In most of the cases, the selected variable corresponds to the Raman band intensity at a specific wavenumber. This approach can eventually be fine-tuned or modified by performing a (local) baseline correction, or by selecting the maximum or average intensity over a small window (to diminish the influence of slight shifts in the Raman spectrum). For other applications, it can be of interest to study the exact Raman band positions, as these can eventually indicate some degradation phenomena (e.g. photodegradation of realgar) or stress factors (e.g. in polymers used in contemporary art). The functions *EPos* or *ENpos* determine a specific Raman wavenumber within the region of interest and can result in important information about the ongoing degradation. To demonstrate the success of univariate extractions, a Raman mapping experiment has been performed on a 1.2 x 1 cm region on one of the porcelain cards. The characteristic band of lead white ($2PbCO_3 \cdot Pb(OH)_2$) at 1050 cm^{-1} has been selected for the processing to be able to create the Raman map. Figure 8.4b represents the result of different extraction methods. The approaches are illustrated in Figure 8.4a and they are described in more detail in Table 8.1. It seems that in this particular case the functions *ENet* and *ENArea* deliver the best results.

Table 8.1 Overview of the different extraction methods of a single variable.

Extraction method	Description
Evalue	Extraction of the Raman intensity at a fixed Raman wavenumber
EMean	For the characteristic wavenumber range, the average Raman intensity is calculated
EMax	Determination of the maximum Raman intensity within the wavenumber region of interest
ENet	Determination of the net Raman intensity within the wavenumber region of interest
EArea	Calculation of the total band area (including net and background intensity) within the region of interest
ENArea	Calculation of the net Raman band area within the region of interest
EPos	A specific Raman wavenumber is saved of which its Raman intensity (sum of net and background intensity), within the selected Raman wavenumber range, is the highest
ENPos	A specific Raman wavenumber is saved of which its net Raman intensity, within the selected Raman wavenumber range, is the highest.

Multivariate processing takes the entire spectrum into account instead of a single value. This approach can be of interest if many low quality spectra are present, for instance, when very short measuring times per spectrum were used. If the signal-to-noise ratio (SNR) is low, but sufficient to discriminate between different types of spectra/ materials, cluster analysis can be used to group similar spectra. Once good classification is achieved, representative spectra of each group can be examined and identified. It is even possible to average all the spectra of the same cluster, to obtain a better signal-to-noise ratio, as thus the influence of shot noise is reduced.
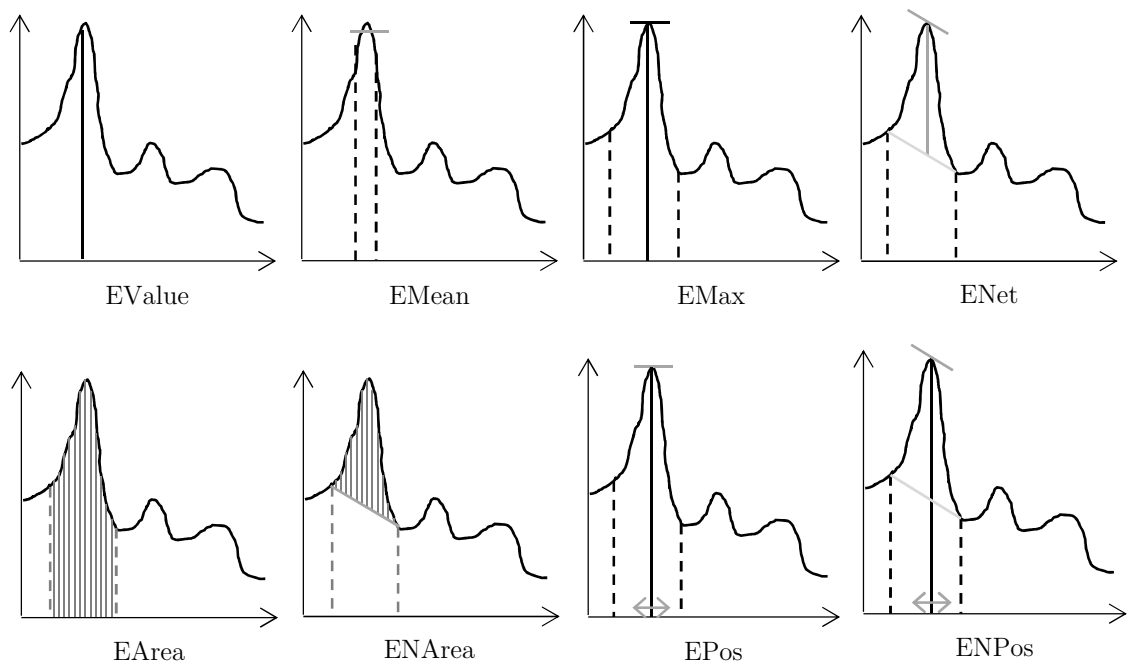
Figure 8.4a Univariate extraction methods for specific variables.
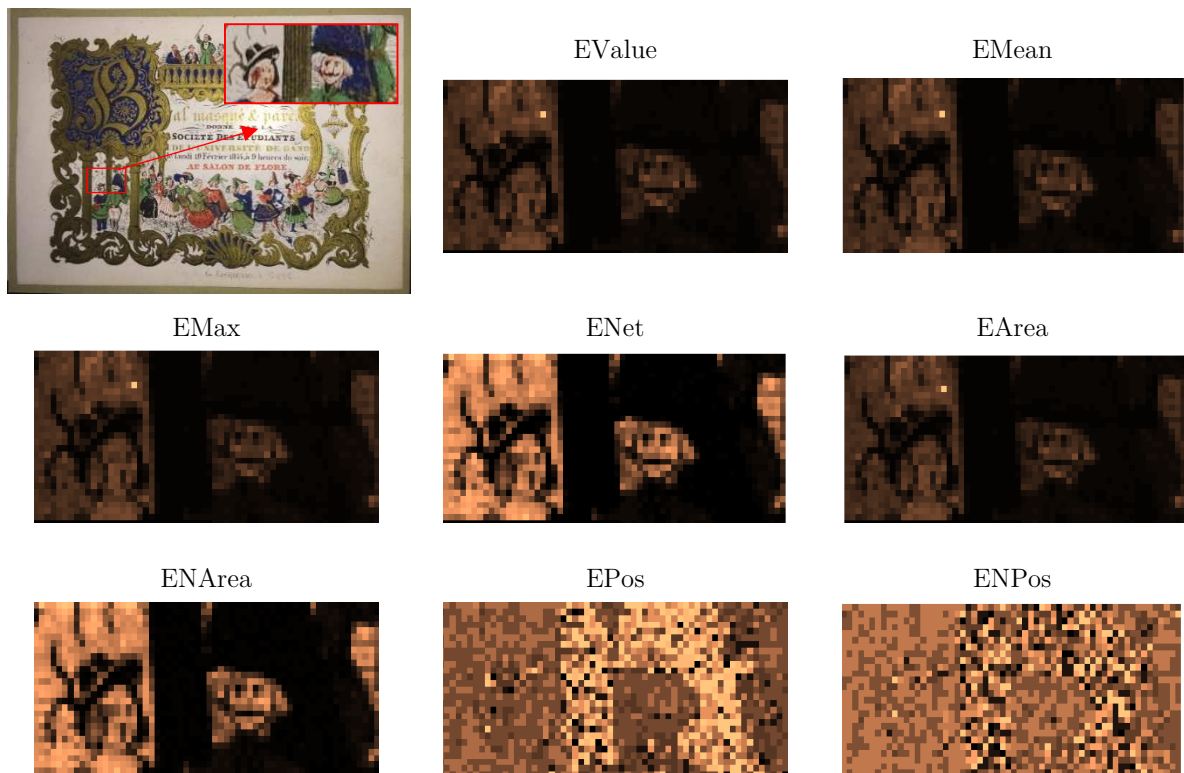
Figure 8.4b Application of the univariate extraction methods for the illustration of the distribution of lead white (characteristic band at 1050 cm^{-1}) on the porcelain card.

The possibility of multivariate analysis in this work is based on K-Means clustering. In contrast to hierarchical methods, the number of clusters needs to be defined beforehand. The clustering calculates the city block distance (i.e. the sum of absolute differences, Equation (4)) between the centroid and the individual spectra [23,24]. By using the K-Means clustering algorithm, each spectrum is assigned to one of the clusters, and the selected variable corresponds to the number of the cluster.

$$d(x, c) = \sum_{j=1}^{p} |x_j - c_j| \tag{4}$$

The last step in data-treatment is the actual creation of the Raman map. This basically corresponds to colour-coding the selected variable and plotting it according to the coordinates on the map. For this, a function is created to simply map the data series in a 2D plot using these extracted data. A Raman map can be constructed by a single variable or visualising multiple variables in one map. For demonstration, on a porcelain card, an area of 60 x 20 steps is mapped using the 785 nm laser with a measurement time of 9s at each point. Three characteristic Raman bands are considered for further investigation and extracted with the *ENet* function: (i) 262 cm^{-1} of vermilion (HgS); (ii) 1050 cm^{-1} of lead white ($2PbCO_3 \cdot Pb(OH)_2$) and (iii) 536 cm^{-1} of Prussian blue ($Fe_4[Fe(CN)_6]$).

As mentioned, different maps (single or multiple variables) can be produced. Figure 8.5a represents the Raman map of a single variable illustrating the distribution of the characteristic Raman band of vermilion (262 cm^{-1}). A good image can be obtained for a single variable but also for multiple ones, as shown in Figure 8.5b.

Figure 8.5 (a) Map of a single variable illustrating the distribution of the characteristic Raman band of vermilion (262 cm^{-1}); (b) Map of a multiple variables illustrating the distribution of the characteristic Raman band of vermilion (262 cm^{-1}), lead white (1050 cm^{-1}) and Prussian blue (536 cm^{-1}). Bands in both images are extracted with the ENet extraction function.

It is clear that the proposed mapping processing method is very successful. When an *in situ* Raman mapping system is considered, not only the processing of this large dataset is of importance and it can be expected that the measurement area of interest (on an art object) can be large in size. As the access to the material is often limited, it needs to verify that in short acquisition time good Raman images can be obtained. For this purpose, an area of 50 x 30 points, where both vermilion and Prussian blue are present, is mapped with the 785 nm laser. This area is analysed twice, once with a measurement time of 3 accumulations of 3 s each and once with a single accumulation of 1 s (Figure 8.6). Both the single variable Raman images of both compounds as the multivariate results, reveal that the 1 x 1 s measurement is too short for the proper identification of Prussian blue. It appears that the large difference in scattering efficiency between vermilion and Prussian blue seems significant. When dealing with weak Raman scatterers, a good quality image is rarely obtained for a single scan. On the other hand, it is proven that while measuring for only 9 s on each point, a relatively good image can be acquired. To achieve these results, the total measurement time is also largely

influenced by the system repositioning time since at each spot the system needs to repositioned which requires valuable set-up.
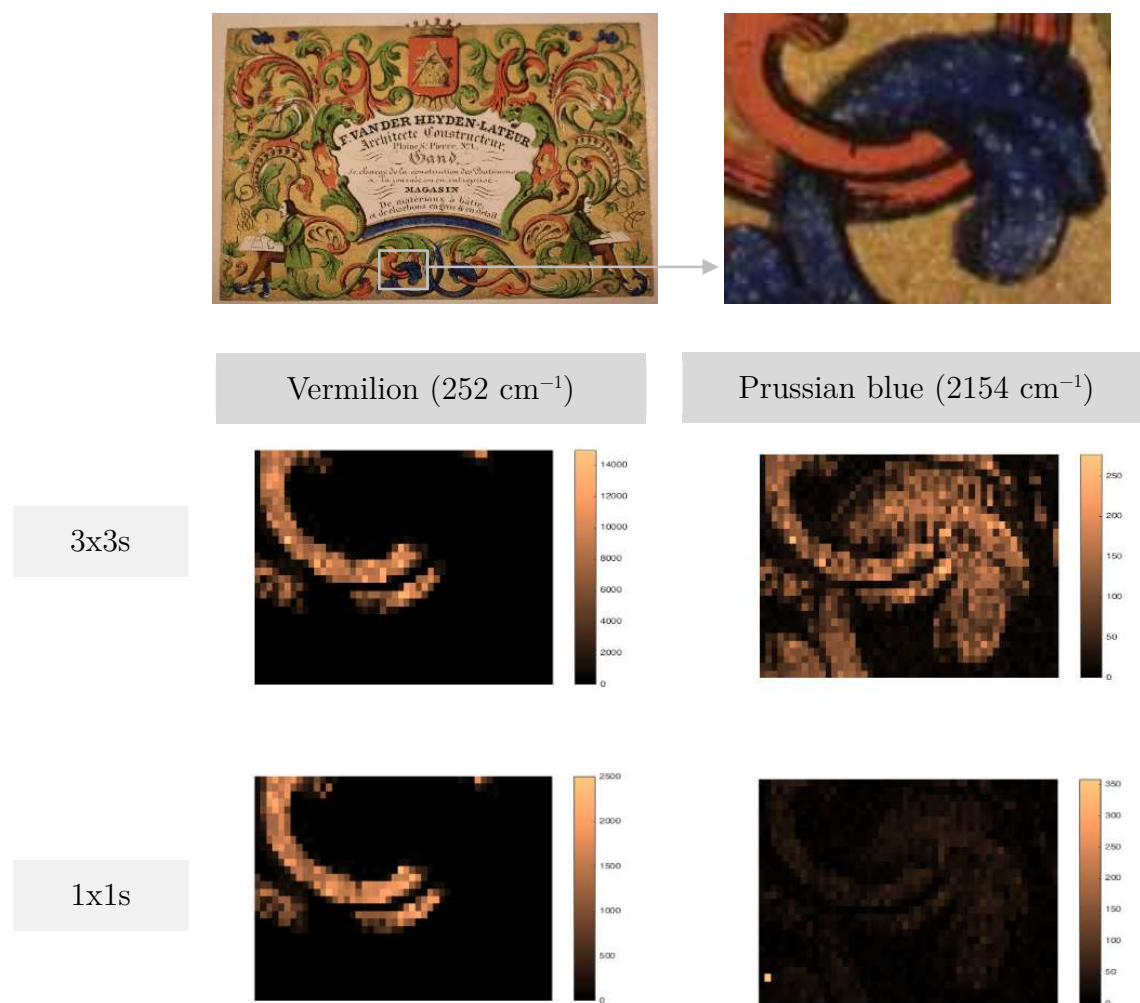
Figure 8.6 Raman maps obtained, with the 785 nm laser, of single variable extraction using the ENet function, illustrating the distribution of vermilion and Prussian blue using different acquisition times.

8.4 Conclusions and perspectives

Although the development is a challenging task, the first steps towards an *in situ* Raman mapping system seems to be very promising. The challenges of focusing, system positioning, software development and data-processing are well-discussed. As the positioning needs to be accurate and as sometimes the samples are too large and fragile

to be moved, a motorized stage was developed, operated with the in-house software, to move the probeheads of the instrument. In addition, the crucial steps for the creation of a Raman map, such as visualisation and extraction are described, based on the Raman analysis of a porcelain card. The extraction of variables can be performed in a univariate (monitoring one variable per spectrum) or multivariate way. The latter proved to be helpful when dealing with low quality spectra.

At this stage, the system still requires improvement before being applicable in the field. Issues such as autofocus, roughness and complexity of a sample still need to be evaluated. In a later phase, the *in situ* Raman mapping system can be tested and optimised for applications other than to art objects. Questions concerning homogeneity, complexity of composition, degradation phenomena, occur not exclusively in cultural heritage applications but also in the pharmaceutical sector, gemmology, astrobiology, etc. So further tests on different materials will be required to reach a final improvement of the system.

In the world of Raman analysis of art objects, point measurements have been so far the only possible way to investigate samples in situ. Despite the fact that the development of an in situ Raman mapping system is still in its preliminary phase, the results obtained are positive results and support further development. As real world samples are often more complicated, this chapter was only a starting point for a complete development. Criteria such as autofocus, larger positioning system, etc. still need to be treated. One of the first optimisation steps towards the applicability in the field concerns the merging of microscopic information with molecular distribution. At this time, only chemical images are created during the in situ Raman mapping and it would be of great interest to be able to relate a microscopic image with the obtained molecular image. For this purpose, in the next chapter we try to merge the portable Raman mapping system with the Hirox microscope system involving the Hirox microscope set-up and this will be discussed in the next chapter.

8.5 References

[1] M. Alfeld, J.V. Pedroso, M. van Eikema Hommes, G. Van der Snickt, G. Tauber, J. Blaas, M. Haschke,K. Erler, J. Dik and K. Janssens. A mobile instrument for in situ scanning macro-XRF investigation of historical paintings, J. Anal. At. Spectrom. 28 (2013) 760-767. doi:10.1039/c3ja30341a.

[2] P. Vandenabeele, M.K. Donais, Mobile Spectroscopic Instrumentation in Archaeometry Research, Appl. Spectrosc. 70 (2016) 27–41. doi:10.1177/0003702815611063.

[3] B. Brunetti, C. Miliani, F. Rosi, B. Doherty, L. Monico, A. Romani, et al., Non-invasive Investigations of Paintings by Portable Instrumentation: The MOLAB Experience, Top. Curr. Chem. 374 (2016) 10. doi:10.1007/s41061-015-0008-9.

[4] M.J.. Pérez-Alonso M., Castro K., Investigation of degradation mechanisms by portable Raman spectroscopy and thermodynamic speciation: The wall painting of Santa Maria de Lemoniz (Basque Country, North of Spain), Anal. Chim. Acta. 571 (2006) 121–128. doi:10.1016/j.aca.2006.04.049.

[5] L.L. Reiche I., Pages-Camagna S., In situ Raman spectroscopic investigations of the adorning gemstones on the reliquary Heinrich's Cross from the treasury of Basel Cathedral, J. Raman Spectrosc. 35 (2004) 719–725. doi:10.1002/jrs.1197.

[6] D. Lauwers, V. Cattersel, L. Vandamme, A. Van Eester, K. De Langhe, L. Moens, et al., Pigment identification of an illuminated mediaeval manuscript *De Civitate Dei* by means of a portable Raman equipment, J. Raman Spectrosc. 45 (2014) 1266–1271. doi:10.1002/jrs.4500.

[7] G. Barone, D. Bersani, J. Jehlička, P.P. Lottici, P. Mazzoleni, S. Raneri, et al., Non-destructive investigation on the 17-18th centuries Sicilian jewelry collection at the Messina regional museum using mobile Raman equipment, J. Raman Spectrosc. 46 (2015) 989–995. doi:10.1002/jrs.4649.

[8] A. Brambilla, I. Osticioli, A. Nevin, D. Comelli, C. Dandrea, C. Lofrumento, et al., A remote scanning Raman spectrometer for in situ measurements of works of art, Rev. Sci. Instrum. 82 (2011) 1–8. doi:10.1063/1.3600565.

[9] M. Quaranta, E. Catelli, S. Prati, G. Sciutto, R. Mazzeo, Chinese archaeological artefacts: Microstructure and corrosion behaviour of high-leaded bronzes, J. Cult. Herit. 15 (2014) 283–291. doi:10.1016/j.culher.2013.07.007.

[10] C. Conti, I. Aliatis, C. Colombo, M. Greco, E. Possenti, M. Realini, et al., micro-Raman mapping to study calcium oxalate historical films, J. Raman Spectrosc. 43 (2012) 1604–1611. doi:10.1002/jrs.4072.

[11] V. Capogrosso, F. Gabrieli, S. Bellei, L. Cartechini, A. Cesaratto, N. Trcera, et al., An integrated approach based on micro mapping analytical techniques for the detection of impurities in historical Zn-based white pigments, J. Anal. At. Spectrom. 30 (2015) 828–838. doi:10.1039/C4JA00385C.

[12] D. Lau, C. Villis, S. Furman, M. Livett, Multispectral and hyperspectral image analysis of elemental and micro-Raman maps of cross-sections from a 16th century painting, Anal. Chim. Acta. 610 (2008) 15–24. doi:10.1016/j.aca.2007.12.043.

[13] J.M. Madariaga, Raman spectroscopy in art and archaeology, J. Raman Spectrosc. 41 (2010) 1389–1393. doi:10.1002/jrs.2850.

[14] P. Ropret, C. Miliani, S. a. Centeno, Č. Tavzes, F. Rosi, Advances in Raman mapping of works of art, J. Raman Spectrosc. 41 (2010) 1462–1467. doi:10.1002/jrs.2733.

[15] K.C. Gordon, C.M. McGoverin, Raman mapping of pharmaceuticals, Int. J. Pharm. 417 (2011) 151–162. doi:10.1016/j.ijpharm.2010.12.030.

[16] P. Vandenabeele, T.L. Weis, E.R. Grant, L.J. Moens, A new instrument adapted to in situ Raman analysis of objects of art, Anal. Bioanal. Chem. 379 (2004) 137–142. doi:10.1007/s00216-004-2551-z.

[17] P. Vandenabeele, P. De Paepe, L. Moens, Study of the 19th century porcelain cards with direct Raman analysis, J. Raman Spectrosc. 39 (2008) 1099–1103. doi:10.1002/jrs.

[18] J.R. Ferraro, K. Nakamoto, C.W. Brown, Introductory Raman spectroscopy, 2nd edition, Academic Press, 2003.

[19] B. Bissonnette, L. Courard, A. Garbacz, Concrete Surface engineering, Crc Press, 2015.

[20] R.L. McCreery, Raman spectroscopy for chemical analysis, John Wiley & Sons, 2000.

[21] A.N. Davies, Raman imaging of difficult surfaces, Spectrosc. Eur. 27 (2015) 16–17.

[22] D. Lauwers, A.G. Hutado, V. Tanevska, L. Moens, D. Bersani, P. Vandenabeele, Characterisation of a portable Raman spectrometer for in situ analysis of art objects., Spectrochim. Acta. A. Mol. Biomol. Spectrosc. 118 (2013) 294–301. doi:10.1016/j.saa.2013.08.088.

[23] M. Blowers, W. Williams, Machine learning applied to cyber operations, in: R.E. Pino (Ed.), Netw. Sci. Cybersecurity, SPRINGER, New York, 2014: 160–163. doi:10.1007/978-1-4614-7597-2.

[24] R. Nisbet, G. Miner, J. Elder, Handbook of Statistical Analysis and Data Mining Applications, Academic press, 2009.

Chapter 9

In situ combination of microscopic and molecular imaging: proof-of-concept

In situ Raman point analyses have extensively proven their success in different applications. In this thesis, a portable Raman spectrometer was introduced and applied for the examination of art objects. The equipment has been shown to be an excellent tool in this field (Chapter 4-7) after an extended characterisation and optimisation (Chapter 3). In a second stage (Chapter 8), this Raman spectrometer was modified further for the creation of an in situ Raman mapping system.

When sampling is limited or not allowed, non-invasive Raman mapping may provide useful information on the composition and distribution of materials present at the artwork's surface. In laboratory applications, Raman mapping systems have to face the restriction of sample size: the object needs to fit under the microscope and needs to be movable by operation of the stage. So, as introduced in previous chapter, the creation of an in situ Raman mapping system can overcome this problem. It was described which challenges are of importance during the first steps of the development phase. This includes issues relevant to the positioning system, software development and data processing.

When using the in situ Raman mapping system (Chapter 8), an image is obtained of the distribution of (pigment) molecules over the surface. However, it would help the interpretation significantly if the obtained molecular distribution could be linked to the visual (microscopic) image. Therefore, in this chapter, we try to couple the mobile Raman instrument with a high-resolution 3D microscope. The latter instrument provides high-quality digital images of paint surfaces and is already frequently used in conservation practice.

9.1 Introduction

Innovation in archaeometrical science is a necessity as the interest in non-destructive methods is increased intensively. Chemical characterisation by Raman spectroscopy already has made a big step forward in its applicability in this field. This is noticeable by the large number of portable Raman spectrometers which are now available on the market. However, automatisation of these *in situ* instruments is still a working point.

Micro-Raman spectrometers, developed for laboratory experiments, are often equipped with an automated system. In this way, the analyst is able to apply a Raman mapping or Raman imaging method. Mapping records a sequence of micro-Raman spectra where the position of the excitation laser is changed between sequential measurements [1]. During the raster scanning, the relative positions of the excitation beam are recorded along with the Raman spectra, which allows us to spatially address each Raman spectrum and then create chemical maps of the sample. The principle of Raman imaging consists of the illumination of a larger area, using a defocused beam, followed by the selection of a small spectral range (depending on the Raman band of interest), utilising filters, to image the area [2]. In the field of art analysis, it is preferred to perform Raman mapping experiments, as often the composition of the material is unknown before the analysis. Full spectra are obtained and one then has the option to decide which variable is of interest to map in the post-processing step, for instance band positions, Raman band intensities, etc [2].

When sampling is allowed the Raman mapping method can be used to gain insight into the composition of artworks' multilayered structures, such as paintings. On the other hand, when sampling is not possible, information can be retrieved on the composition and distribution of materials present at the artwork's surface. The problem within laboratory applications is the restriction of the sample size, as it needs to be able to fit under the microscope objective and be small enough to be moved by the stage [3], unless the probehead is moved over the object.

Lauwers et al. [4] described a first step towards the development of an *in situ* Raman mapping system. In this process, sampling is not required anymore and it can be utilised to map larger objects. The established system still requires improvement in different aspects such as autofocus, complexity of samples and combining the set-up with microscopic imaging of the object. Here, a first attempt concerning the optimisation of the set-up is undertaken. As a proof-of-concept, it is demonstrated how the coupling of the portable Raman spectrometer, the EZRAMAN-I-DUAL Raman system, with a high resolution digital microscope, Hirox microscope, is accomplished in order to combine chemical and microscopic information.

9.2 Experimental

In this work, it is aimed to combine The EZRAMAN-I-DUAL Raman system (TSI Inc., Irvine CA, USA) with the High-resolution digital microscopy (Hirox Europe). Details of both instruments have already been described in previous chapters. Experiments have been undertaken on 19th century porcelain cards (introduced in chapter 8), using the 785 nm laser and the STD lens of the Raman spectrometer (focal length of 7 mm) and the MXG-2500REZ lens, with a working distance of 10 mm, of the Hirox microscope. In order to retrieve qualitative information, including knowledge about pigment distribution, the high magnification objective is selected for further the development.

9.3 Results and discussion

A Raman mapping system consists of several features such as stable equipment, controlling software for the set-up and recording the data, etc. In general, the working principle of performing a mapping is composed of the following steps: (i) image the area of interest; (ii) select the area you want to map and write observations/remarks; (iii) perform scanning and (iv) finalise with the creation of a chemical image and compare it to the microscopic image.

If we want to implement this approach in the field, an additional step to the creation of the *in situ* Raman mapping system (described in chapter 8) is needed. Until now, a basic motorised set-up has been designed but there is still room for improvement. As explained, the first important action in performing a Raman mapping experiment is the visualisation of the region of interest. At this moment the experimental arrangement does not have a camera/microscope to monitor the surface of the object. The implementation of a microscopic camera supports the observation of the area and can be used in the future for the development of an autofocus system.

The experiment is based on the integration of an optical microscope, Hirox microscope, with the Raman mapping set-up in order to compare the microscopic image with the chemical distribution. In an ideal case, a region of interest is first scanned in microscopic view, with selected step sizes in the x- and y-direction. After the image is recorded, the same region is mapped in dark view (i.e. a Raman mapping). In this way, at each coordinate an image and chemical data are obtained which can be combined using post-processing software. However, the merging of the portable EZRaman-I-Dual Raman system with the Hirox microscope is not straightforward. Firstly, a solution needs to be found to guide the excitation beam via the microscope onto the sample. When a good pathway has been achieved, it is important to check the yield of the Raman signal and to ascertain whether or not the SNR is good. These issues will be discussed in this session.

9.3.1. Combining the portable Raman spectrometer and the Hirox microscope

Combining the two set-ups is not straightforward, as different constrains are encountered. Firstly, it was necessary to determine from which side the Hirox microscope could be approached without damaging the instrumentation. Figure 9.1a (standard illumination) represents a schematic overview of the Hirox microscope, where two possible access points can be considered, namely, access from the top or from the side, where the white light source enters the microscope. The first access point, however, is too dangerous because we do not want to jeopardize the microscope. The other access seems to be feasible after repositioning the fibre bunch at the other possible holder and after unmounting the part that contains the illumination optics (Figure 9.1a). Considering this access point, we first had to determine if the microscope objective was
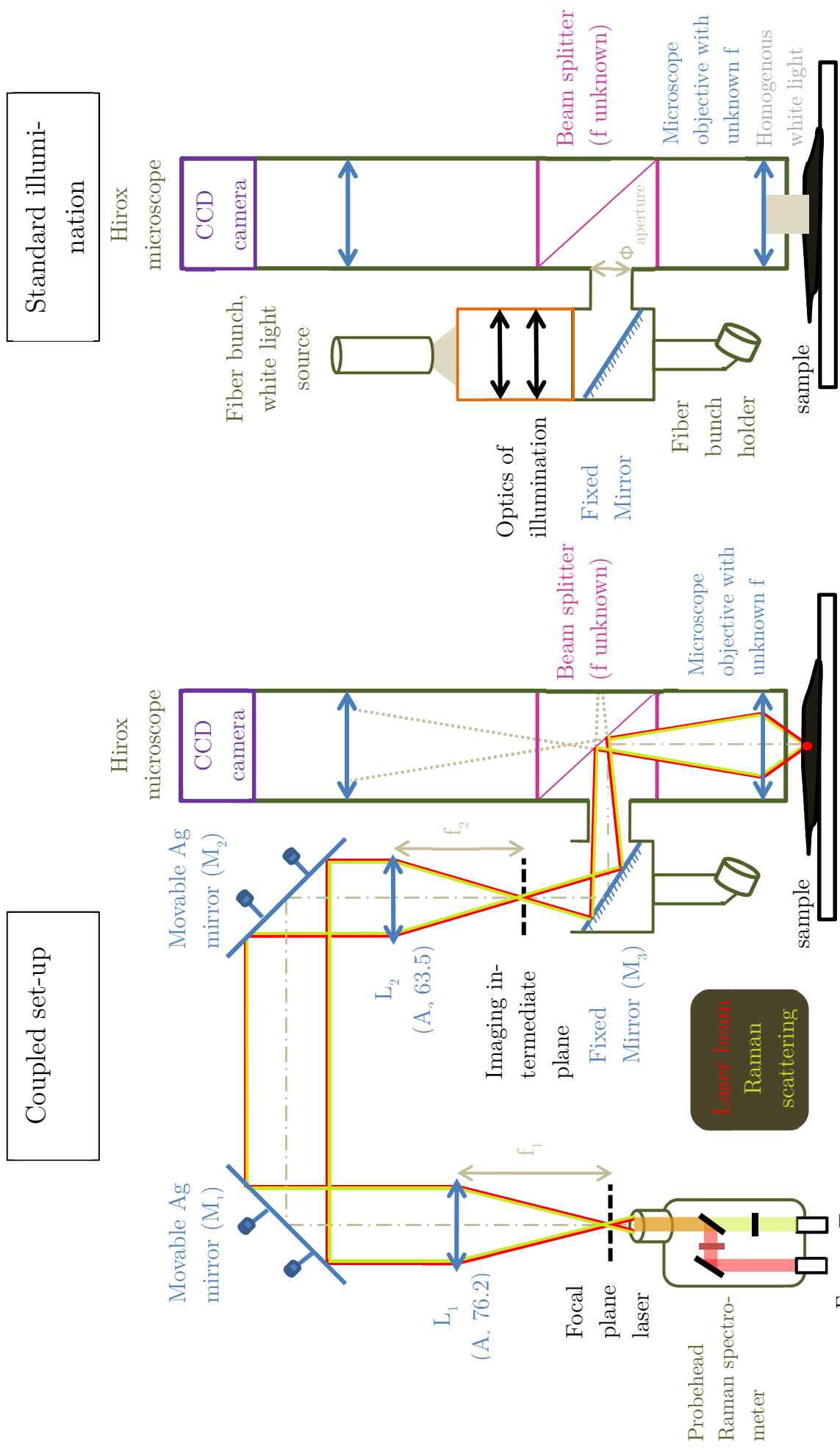
Figure 9.1a Schematic overview of the combined set-up of the EZRaman-I-Dual Raman system and the Hirox microscope.

corrected at infinity, using a collimated beam, in order to calculate whether additional lenses are needed. Tests have shown that the spot size on the sample was too large, which means that the objective is not infinity corrected. Consequently, additional lenses were needed to obtain a focused beam.
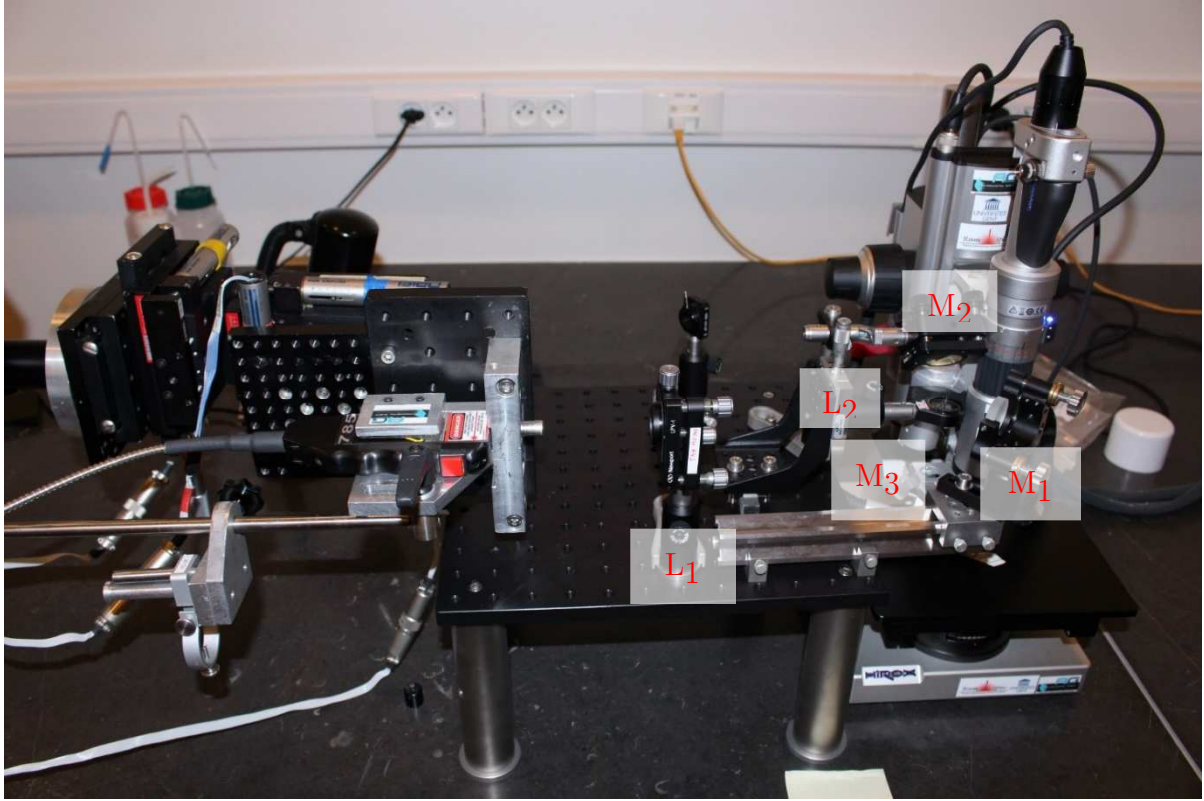
Figure 9.1b Picture of the merged set-up of the EZRaman-I-Dual Raman system and the Hirox microscope.

From a more technical point of view, a way needs to be found to image the light field at F_{laser} onto the sample (Figure 9.1a). At this point, a second constraint had to be considered. The laser light should pass through the fixed aperture of the Hirox microscope (with a diameter $\varphi_{aperture}$) without losing laser intensity. The beam divergence was optimised at the intermediate imaging plane in order to fill the entire pupil of the Hirox microscope objective, i.e. optimising the étendue at the intermediate plane (Equation (4)).

$$\text{Etendue} = S \times \Omega$$

(5)

with S, the area of the entrance pupil and Ω, the solid angle

In addition, the alignment of the set-up is of great importance to avoid energy loss. Taking these remarks into account and with grateful assistance from Prof. Dr. Nicolas Le Thomas (UGent, Faculty of Engineering and Architecture, Department of Information Technology (INTEC), Photonics Research group), the portable Raman spectrometer and the Hirox microscope were combined successfully (Figure 9.1a-b). In this combination, the incident laser beam is directed along a collimator (L_1, A_1 76.2) to create a parallel beam and is then guided via two movable silver mirrors (M_1, M_2). The beam is again focused with the aid of a lens (L_2, A_2 63.5) and then directed onto the sample via the fixed mirror (M_3), passing a beam splitter, both internal parts of the Hirox microscope, through the microscope objective.

After the construction modification, the quality of the Raman signal was evaluated. For this experiment, the reference product lead white ($2PbCO_3 \cdot Pb(OH)_2$) was selected, which is a good Raman scatterer. The EZRAMAN-I-DUAL Raman system as a single instrument is often applied *in situ* with a fixed laser power of 50% (31.33 mW). This condition is proved to give relatively good Raman results and there is no risk posed of damage to the art object. Using the same output power in the combined set-up, no Raman signal was observed. To illustrate the output difference between the single spectrometer and the combined construction, the laser power was increased to a value of 63% (103 mW). For both cases, the recorded Raman spectra are shown in Figure 9.2. Although this figure clearly demonstrates the loss in Raman signal, the SNR was significant for the application of subsequent data treatment that is included in the *in situ* Raman mapping system (chapter 8). The observed weak signal could be the consequence of several factors: It might be caused by a small misalignment or, more likely, it might be explained by the energy loss of at least 50% at the beam splitter. To retrieve better SNR the power can be increased but this may lead to possible damage of the optics.
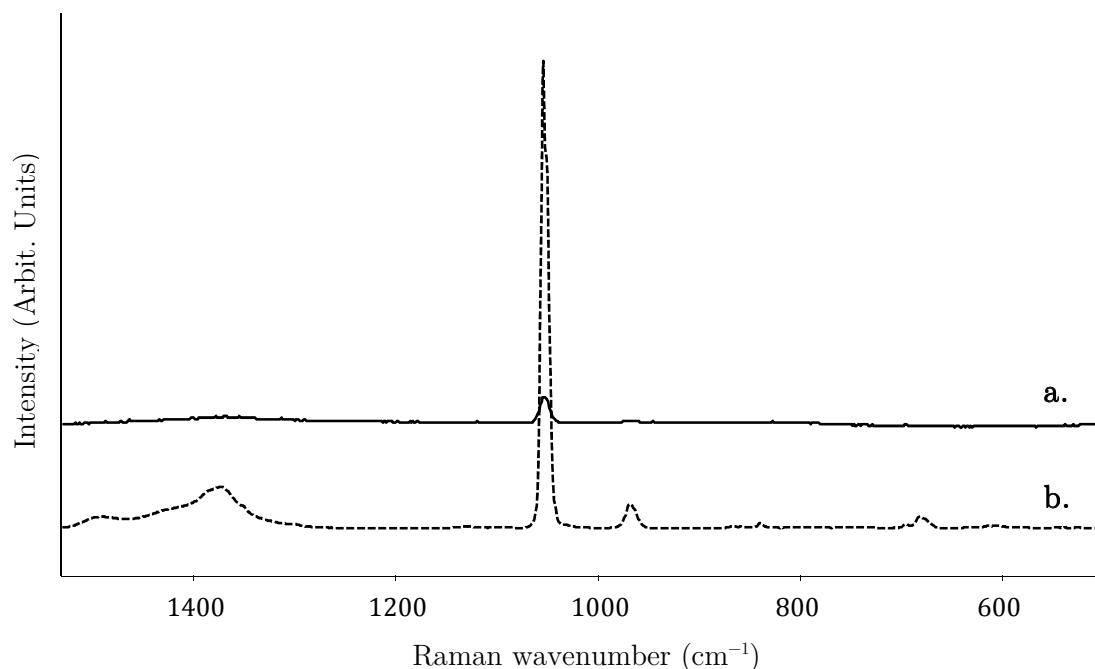
Figure 9.2 Raman spectra (λ = 785 nm, STD lens, 30 x 3 s, ext. power source) of the reference product lead white recorded with a set laser power of 63% by (a) the combined construction of the EZRAMAN-I-DUAL Raman sytem and Hirox microsope and (b) the single Raman spectrometer as used before.

9.3.2. Mapping experiment

The combination of both instruments proved to be successful to record a Raman spectrum. In a second step, we wanted to find out if it is essential to focus the laser beam at the centre point of the microscopic image. If in one microscopic image multiple interesting areas are observed, it would be beneficial to be able to analyse them by only moving the probehead of the Raman spectrometer. At the same time, a first estimation of the spot size could now be obtained.

In order to evaluate this research question, a Raman mapping experiment was performed to analyse the Raman spectral quality, recorded at different areas in one microscopic image. Figure 9.3a-c illustrates the microscopic images, taken by the Hirox microscope of the mapped area. In this region, only good Raman scatterers (vermilion and lead white) were present. In this way, we were sure that the Raman signals would be detectable. Before initiating the Raman map, the microscopic image is recorded and

afterwards the light of the microscope was turned off because of interference with the Raman spectra.
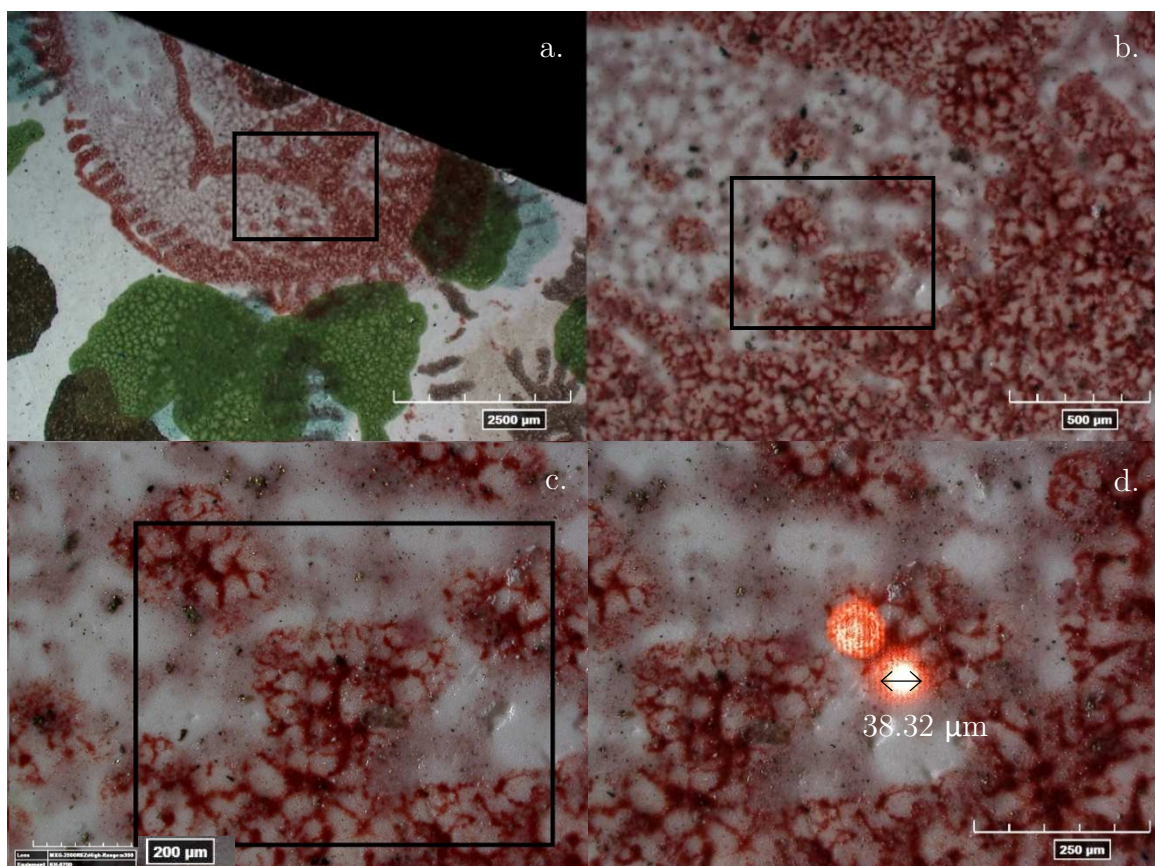
Figure 9.3 Microscopic images taken with the Hirox microscope of a piece of a 19th century porcelain card. In figure (a)-(c) the mapped area is marked. Figure (d) illustrates the spot size of the 785 nm laser after coupling the EZRaman-I-Dual Raman system and the Hirox microscope.

When determining the conditions for the measurement such as the step size of the mapping, it is important to estimate the spot size of the laser. For the adapted set-up, the spot size of the 785 nm laser measures 38.32 μm (Figure 9.3d), using the measurement tool of the Hirox software. The exact spot size determination should be made by a laser profile, using a mirror as substrate. However, it can already be said that the spot is at least half the size of the original beam (i.e. 0.074 ± 0.002 mm [5]), although it can vary depending on the scattering of the sample and laser power. In Figure 9.3d a second spot is visible as a result of internal reflection (possibly ascribed to a ghost image from the beam splitter) and could not be avoided. Fortunately, this reflection beam is weak and has no influence on the Raman results.

After spot size determination, a Raman mapping could be executed with a measurement condition of 3 accumulations with a measurement time of 60 s for each spot. Shorter analysis time would result in poor quality Raman spectra, as the Raman signal is already weak due to the low laser power (illustrated in Figure 9.2). Therefore, a limited amount of measurement points (20 x 20 points) was selected to keep the total measurement time reasonable. The data were processed via the univariate extraction method ENArea [4] for the specific variable of vermilion (the Raman band at 252 cm^{-1}) and lead white (Raman band at 1050 cm^{-1}) of which a Raman map is created (Figure 9.4). A good Raman map was obtained of the region of interest. Lead white was dispersed over the total region, as expected. However, the representation of the distribution of vermilion is missing at the border of the microscopic image. This could be a consequence of signal loss due to misalignment, an improper focusing or the intensity of Raman signal being lower than the detection limit. Based on our current observations, no clear answer can be given whether it is necessary to position the laser beam exactly to the centre point of the image. A better calibration with a homogenous sample is necessary, in order to correct the profile of the intensity map. To avoid this issue, the combined set-up can be improved by fixing the Raman probehead, the Hirox microscope and the intermediate optical system as one ensemble and move it as a whole.
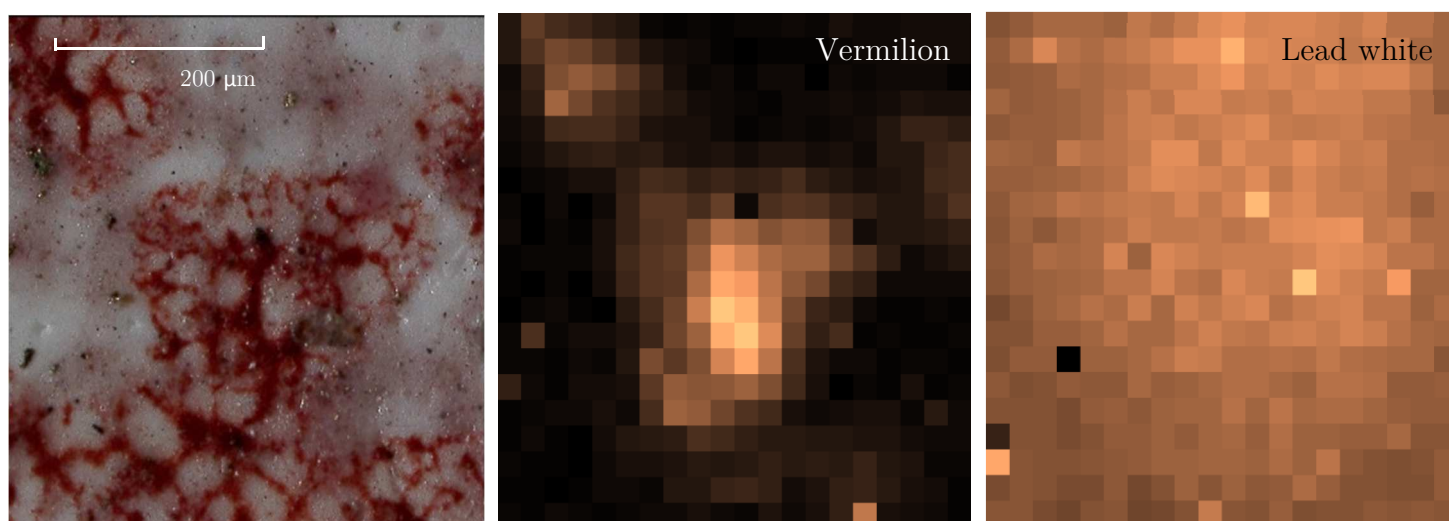
Figure 9.4 Raman map obtained, with the 785 nm laser, of single variable extraction using the ENArea function, illustrating the distribution of vermilion and lead white.

9.4 Conclusions

A proof-of-concept study was performed in order to merge microscopic images with chemical images for *in situ* application. The challenging attempt to combine High-resolution digital microscopy, the Hirox microscope, with portable Raman spectroscopy, applying the EZRaman-I-Dual Raman system, proved to have a successful outcome. The junction was accomplished by implementing different optics, resulting in some signal loss. In addition, information about the spot size and the scanning area, within one image, was obtained.

It was possible to determine whether the coupling of the two set-ups was possible and a reasonable Raman signal could be retrieved. However, the experiments were performed with a good Raman scattterer, lead white, for which a relatively poor signal yield was obtained. This observation indicates possible problems could arise when investigating weak scatterers. So far, only the Raman probehead is moveable via the step motors, which limits the accessible field of view at the sample. As we want to apply the modified instrument for *in situ* analysis, it needs to be improved for larger objects such as paintings, but this is outside the scope of this proof-of-concept study. This improvement could be achieved by rigidly combining the Raman probehead with the Hirox microscope and the intermediate optical system and moving this entire ensemble simultaneously over the object. In this manner, large samples can be investigated with a high spatial and spectral resolution. However, in the case of time restrictions, it is probably better to depict regions of interest and investigate them with high spatial and spectral resolution.

In general, it was proven that it is possible to couple a portable Raman system with a High-resolution digital microscope, which has a lot of potential for art analysis. Still, several optimisation steps need to be executed to have an optimal tool for this purpose. The following three steps for improvement can be considered: (i) adjustment of the system to make it more user-friendly; (ii) improvement the data-treatment; (iii) enhancement of the speed of analysis. Usability is a key parameter in method development. For this reason, the implementation of an autofocus and automatic adjustment

of the set-up will advance this aspect. The latter includes the improvement of the positioning and implement the possibility to switch between the two lasers. In addition, automatisation of the data-treatment would be of great help and is indirectly linked to the enhancement of the usability. Data-processing algorithms need to be programmed in order to combine the microscopic image with the chemical image. Also, during a Raman mapping measurement a large dataset is recorded and thus the development of an auto-identification software would make it possible to obtain information rapidly about the materials and their distribution.

A third, but no less important, aspect is related to the reduction of the measurement time and this can be achieved in several ways. During a Raman mapping experiment, a matrix of $m \times n$ point analyses is obtained. Consequently, for an m x n mapping, the overall measurement time equals $m \times n \times t$ with t the acquisition time per spectrum), plus the time needed for repositioning of the probehead. A first reduction is based on practical issues and observations with other methods (visual or analytical) can reduce the field of interest A second time reduction can be achieved by the introduction of a fast scan method which can reduce the time by continuously moving the motors and recording the Raman spectra at regular time intervals. A final option is based on recording several Raman data at the same time which can be achieved by adjusting the probehead-design by introducing an extra optical component in the probehead which modifies the laser spot into a linear focused light source. The system is combined with a linear array of fibese, which is carefully aligned and oriented along the linear laser beam. Thus, the Raman signals that hit different fibres originate from different volumes being analysed along the laser beam. The linear fibre bundle is projected along the entrance slit of the spectrometer and the signal of each fibre hits the 2-dimensional (CCD) in a different position, allowing us to record several spectra simultaneously.

However, some limitations of a Raman mapping system cannot be solved and need to be kept in mind while performing experiments. For each Raman mapping spectrum the acquisition time at each coordinate is the same. The fixed measurement condition is set as such to avoid pigment degradation/burning of sample by the laser wavelength and detector saturation. Detector saturation is often an issue when good Raman scatterers are present but has the disadvantage that weak Raman scatterers are not detected.

9.5 References

[1] H.J. Bowley, D.J. Gardiner, D.L. Gerrard, P.R. Graves, J.D. Louden, G. Turrell, Practical Raman spectroscopy, Springer-Verlag Berlin Heidelberg, 2012.

[2] P. Vandenabeele, Practical Raman spectrosopy, John Wiley & Sons, Ltd, 2013.

[3] P. Ropret, C. Miliani, S. A. Centeno, Č. Tavzesa and F. Rosie, Advances in Ramanmapping of works of art, J. Raman Spectrosc. 41 (2010) 1462–1467.

[4] D. Lauwers, P. Brondeel, L. Moens, P. Vandenabeele, In situ Raman mapping of art objects, Philos. Trans. A. accepted (2016).

[5] D. Lauwers, A.G. Hutado, V. Tanevska, L. Moens, D. Bersani, P. Vandenabeele, Characterisation of a portable Raman spectrometer for *in situ* analysis of art objects., Spectrochim. Acta. A. Mol. Biomol. Spectrosc. 118 (2013) 294–301. doi:10.1016/j.saa.2013.08.088.

Chapter 10

Conclusions and future prospects

Preservation of cultural heritage is considered important as this reflects the historical and present culture. For many years, non-destructive, *in situ* scientific research on historical and archaeological objects was not possible but this is now gaining more and more interest. The study of these materials supports restoration/conservation processes and, at the same time, historical and visual examination assists in the interpretation of scientific data. Close collaboration between different research areas is very important for cultural heritage research. In this PhD thesis, we wanted to contribute to the spectroscopic investigation of cultural heritage objects with a focus on painted artefacts.

Through history, many artists have used paint as a medium for expressing their ideas, given its colourful appearance. Paint is a solution, suspension or colloid, and consists of three components: a colourant (i.e. dye, pigment or lake), a binder and a solvent. It is applied in different ways to a range of substrates such as walls, parchment, wooden panels, etc. Pigments are very attractive targets for scientific studies and can be studied using a broad range of analytical techniques, which comprise direct methods as well as approaches that require destructive sampling. Direct investigation of art objects is mostly preferred as it is assumed to be non-destructive. The demand for non-destructive, mobile methods has increased significantly; therefore, we have concentrated our research on the application of mobile Raman spectroscopy for the investigation of art objects. This PhD thesis can be an informative guideline to help the decision as to whether a specific Raman spectrometer is an ideal instrument for a specific type of research.

In general, we want to improve the possibilities/applicability of portable Raman spectrometers for art analysis. Acquiring full knowledge of the *in situ* approach is

regarded as indispensable to making the technique work as efficiently as possible an to the best of our knowledge, we were the first to write a protocol on how to fully characterise a mobile Raman instrument. The exploration started with delineating which aspects need to be considered when selecting a mobile Raman spectrometer for *in situ* art analysis (Chapter 3). The case was made for the adoption of a dual laser (785 and 532 nm) portable Raman spectrometer, the EZRaman-I-Dual Raman system from which it was deduced that a balance has to be found between different parameters, such as practical limitations and spectroscopic characteristics for the specific case of cultural heritage objects that forms the focus of the research.

The suitability of a Raman spectrometer is not only dependent upon several operational parameters, it is also crucial to examine its versatility of usage as the method should be applicable for various types of art objects with different shapes, sizes and composition. Thus, characteristics that are important for the appropriate *in situ* analysis were evaluated as well. For this reason, the appropriateness of the introduced Raman instrument for different case studies (simple and complex painted materials, gemstones) including testing and optimisation where needed (Chapter 4 and 5). Aspects such as measurement time (relative to the quality of the Raman spectrum), suitability of the type of laser, instrumental stability, beneficial presence of two lasers, etc. were examined. Extensive knowledge of these parameters helps to apply the Raman spectrometer in the most efficient and rapid way. However, each instrument has its limitations and advantages (Chapter 6), so it is always important to define a priori which aspects are relevant for the type of research being undertaken.

Looking back at the suggested protocol, the success of a Raman instrument in these applications is dependent on the research question. However, sometimes the use of a single technique is not satisfactory. In the case of complex painted materials, especially oil paintings, it has been illustrated that *in situ* Raman analysis is not always straightforward. To achieve a more complete characterisation it is often beneficial to use complementary techniques such as X-ray fluorescence spectroscopy (XRF, elemental information) or Hirox microscopy (microscopic images), as illustrated in this thesis

(Chapter 7). It is noteworthy that the complementary use of the Hirox microscope proved its success in improvement of positioning and leading to better interpretation of the data.

During the second part of this thesis, the applicability of portable Raman spectrometers for art analysis was further developed. Hitherto, only point measurements could be performed *in situ*. Here, novel steps were undertaken that included further optimisation of the Raman system set-up. A first step towards the development of *in situ* Raman mapping system was made with main focus on the data-treatment, which is important for the creation of a Raman map (Chapter 8). At this stage it was not possible to relate microscopic information with the molecular distribution of the components. Consequently, in a second step, it was aimed to merge the set-up of the portable Raman spectrometer, the EZRaman-I-Dual Raman system, with a high-resolution digital microscope (Hirox), to solve this issue (Chapter 9). This implementation was not straightforward and still needs improvement but the first development steps were successful.

As a final thought, it can be concluded that this research has made significant steps forward, but still more work needs to be completed before having a fully operational system and protocol. This PhD research has made it clear that no obvious solutions exist for the characterisation and optimisation of portable Raman spectrometers for art analysis. Further development of the *in situ* Raman mapping methodology can only be established through extensive testing of different applications. Therefore, this thesis may not be seen as an end product, but rather as a first step towards several research objectives which can be considered three-fold:

1) <u>Improvement of the positioning system</u>: Aspects such as an autofocus system and fast scanning should be implemented. The latter would create the advantage of reducing measurement time and still create a Raman map of a sufficient quality.

2) <u>Further optimisation of the combination setup using the Hirox-Raman</u>: As mentioned, the set-up is still in a preliminary phase. So far, it has been demonstrated that it is possible to record a Raman signal via a combined set-up. The system can be extended to map larger areas both at microscopic and molecular levels. This can include integration of the portable Raman spectrometer and the High-resolution digital microscope on one stage. Consequently, a more accurate positioning would be achieved.

3) <u>Auto-identification of the data</u>: In this thesis, we have only explained the data-treatment required to create a Raman map, without considering the identification of the molecular components. When performing a Raman mapping experiment, a large dataset is recorded and thus it is very time consuming to identify all the detected material manually. Therefore, if it were possible to implement auto-identification software, information about the materials and their distribution could be obtained more quickly.

The autor is convinced that through extensive further research this *in situ* Raman mapping system can be very successful for different applications and thereby many research questions can be adressed.

Chapter 11

Conclusie en toekomstperspectieven

Behoud en beheer van cultureel erfgoed is een wereldwijd belangrijk aspect omdat het onze geschiedenis en cultuur reflecteert. Sinds enkele jaren vormt niet-destructief, in situ wetenschappelijk onderzoek op kunsthistorische objecten een essentieel onderdeel, ter ondersteuning van conservatiestudies. Hierdoor wordt belangrijke informatie verkregen over de samenstelling van de objecten en terzelfdertijd dragen historisch en visueel onderzoek bij tot de interpretatie van deze wetenschappelijke data. Bijgevolg is een nauwe samenwerking tussen deze verschillende onderzoeksvelden van groot belang. Dit doctoraatswerk situeert zich in deze interdisciplinair context en draagt bij tot het spectroscopisch onderzoek van cutureel erfgoed, voornamelijk tot de analyse van geschilderde objecten.

Doorheen de tijd gebruikten artiesten verf als hulpmiddel om hun ideeën op een kleurrijke manier tot uiting te brengen. Verf bestaat uit drie componenten: de kleurstof (pigmenten, lakken of substraatpigmenten) en het bindmiddel, meestal opgelost in een solvent. Het kan aangebracht worden op verschillende wijze, op verscheidene ondergronden zoals muren, perkament, houten panelen, enzovoort. De kleurende eigenschap van verf wordt hoofdzakelijk bepaald door de gebruikte kleurstoffen. Deze kunnen geanalyseerd worden via een ruim gamma aan analytische technieken, bestaande uit zowel directe analyses als methoden die staalname vereisen. Direct onderzoek op kunstobjecten wordt verondersteld niet-destructief te zijn en wordt veel verkozen boven andere. De laatste jaren steeg de vraag naar niet-destructief, mobiel onderzoek beduidend. Daarom richtte deze thesis zich tot de toepassing van mobiele Ramanspectroscopie voor de studie van kunstobjecten. Dit doctoraatswerk dient als richtlijn om het juiste Ramaninstrument te selecteren, voor een specifieke onderzoeksvraag.

De algemene doelstelling van dit werk omvat de verbetering van de mogelijkheden en toepassing van mobiele Raman spectrometers in kunstanalyse. Het is van essentieel belang om een volledig inzicht te krijgen in deze *in situ* methode om zo efficiënt mogelijk te opereren. Bijgevolg, werd er een protocol ontwikkeld die een volledige omschrijving bevat in hoe een mobiele Ramanspectrometer gekarakteriseerd kan worden. Allereerst, werden aspecten aangekaart die belangrijk zijn voor de selectie van een mobiel Raman-toestel voor *in situ* kunstanalyse (Hoofdstuk 3). Deze parameters werden uitgelegd aan de hand van een draagbare Ramanspectrometer, uitgerust met twee lasers (785 nm en 532 nm), het EZRaman-I-Dual Raman instrument. De studie toonde aan dat er steeds een balans gezocht moet worden tussen verschillende parameters, zoals praktisch beperkingen en spectroscopische karakteristieken.

Niet enkel deze parameters zijn belangrijk voor de ultieme geschiktheid van een Ramanspectrometer. De veelzijdigheid van een Ramaninstrument is ook van belang: de methode moet toegepast kunnen worden op verschillende kunstobjecten met diverse afmetingen, vormen en samenstelling. Karakteristieken die belangrijk zijn hiervoor, met de nadruk op *in situ* analyses, dienen daarom ook onderzocht te worden. Dit omvatte het evalueren van meettijd (ten opzichte van de kwaliteit van het Ramanspectrum), geschiktheid van lasertype, stabiliteit van het toestel, enz. Deze aspecten werden getest, op basis van verschillende case studies (eenvoudige en complexe materialen), om de bekwaamheid na te gaan van de geïntroduceerde Ramanspectrometer en waar nodig werden deze geoptimaliseerd (Hoofdstuk 4, 5 en 6). Maar ieder instrument heeft zijn voordelen en beperkingen; het is dus steeds belangrijk om vooraf de aspecten te definiëren die belangrijk zijn voor het gewenste onderzoek.

Uit bovenstaande analyses, kan er geconcludeerd worden dat het succes van een meetcampagne afhankelijk is van de onderzoeksvraag. Bijkomstig, werd er aangetoond dat soms één analyse techniek niet voldoende was om tot de gewenste resultaten te komen. In het geval van objecten met een complexe samenstelling, zoals olieverfschilderijen, werd het duidelijk dat de interpretatie van *in situ* Raman-spectroscopie niet altijd eenvoudig was. Om een complete karakterisering van materialen te verkrijgen is het vaak voordeliger om daarnaast complementaire technieken aan te

wenden, zoals X-straal fluorescentie spectroscopie (elementaire informatie) of Hirox microscopie (microscopische beelden) (Hoofdstuk 7). De introductie van Hirox microscopie heeft duidelijk zijn meerwaarde aangetoond in de verbetering van positione-ring en interpretatie van data.

In het tweede deel van de doctoraatsthesis, lag de focus op verdere verbetering van de toepasbaarheid van mobiele Ramanspectrometers voor de analyse van kunst. *In situ* analyses waren tot nu toe enkel mogelijk via puntmetingen. In dit werk, werden vernieu-wende stappen ondernomen om de opstelling van de Ramanspectrometer te verbeteren. Een eerste belangrijke stap was de ontwikkeling van een *in situ* Ramanmapping. De focus lag de gegevensverwerking, die belangrijk was voor de creatie van een Ramanmap (Hoofdstuk 8). In deze fase waren we nog niet in staat om microscopische informatie te koppelen met moleculaire verdeling van componenten. Daarom werd er in een volgende stap gestreefd naar een opstelling waarbij de mobiele Raman spectrometer, het EZRaman-I-Dual Raman system, en de hoge resolutie, digitale microscoop (Hirox), ver-enigd werden. Deze koppeling was niet eenvoudig en is nog aan verbetering toe, maar de eerste ontwikkelingen zijn veelbelovend.

Om af te sluiten, kunnen we stellen dat dit onderzoek enorme vooruitgang heeft geboekt maar dat nog verder ontwikkelingen moeten uitgevoerd worden vooraleer we kunnen spreken van een volwaardig, operationeel systeem en protocol. Gedurende de thesis werd het duidelijk dat het karakteriseren en optimaliseren van mobiele Ramanspectrometers voor kunstanalyse, geen simpele taak was. Voortgang in het gehele ontwikkelingsproces van een *in situ* Ramanmapping methodologie, kan enkel verkregen worden door het verder testen op verschillende toepassingen. Daarom beschouwen we deze thesis niet als een eindproduct maar eerder als een vertrekpunt naar verschillende onderzoeksdoeleinden. Toekomstige studies kunnen onderverdeeld worden in drie:

1) <u>Verbetering van positioneringssysteem</u>: Aspecten zoals een autofocus en een *fast scanning* methode zouden geïmplementeerd moeten worden. Deze laatste creëert de mogelijkheid om de meettijd te verkorten maar nog steeds een Ramanmap te verkrijgen van goede kwaliteit.

2) <u>Optimaliseren van de Hirox-Raman opstelling</u>: Zoals eerder vermeld, is deze opstelling slechts in een eerste ontwikkelingsfase. Tot nu toe zijn we erin geslaagd om een Raman signaal te detecteren via de gecombineerde opstelling. Het systeem kan nog uitgebreid worden om grotere regio's te onderzoeken op microscopische en moleculair niveau, door de integratie van beide toestellen in een opstelling. Dit zou leiden tot een betere en meer accurate positionering.

3) <u>Auto-identificatie van de data</u>: Hoewel, de identificatie van de moleculaire componenten een belangrijk aandeel heeft tot de interpretatie van de Raman resultaten, richtte deze doctoraatsthesis zich voornamelijk tot de dataverwerking om een Ramanmap te creëren. In een verdere ontwikkelingsfase zou de aanwezigheid van een auto-identificatie systeem zeker een meerwaarde bieden. Door de grote dataset die gecreëerd wordt tijdens een Ramanmapping, is een manuele identificatie van alle componenten zeer tijdrovend zijn. Deze extra toevoeging kan ervoor zorgen dat terzelfdertijd informatie over de gebruikte materialen en hun distributie wordt verkregen en dit op een snelle manier.

Ik ben er dus van overtuigd dat verder, intensief onderzoek kan leiden tot een succesvolle ontwikkeling van een *in situ* Ramanmapping system die toegepast kan worden in verschillende domeinen en dus resulteren in zeer kwaliteitsvolle analyses.

Dankwoord

Na veel zwoegen ben ik toegekomen aan het schrijven van de laatste eindjes, mijn dankwoord. Je zou denken dat dit het meest eenvoudige onderdeel is van heel het doctoraat maar je wil natuurlijk geen mensen vergeten te bedanken.

In eerste instantie wil ik mijn promotor, Prof. Dr. Luc Moens, en co-promotor Prof. Dr. Peter Vandenabeele bedanken. Zonder hun hulp had ik nooit de gelegenheid gehad om de wereld van onderzoek te ontdekken. Bedankt voor deze leerrijke ervaring en alle kansen die ik gekregen heb om mezelf te ontwikkelen, zoals het ontmoeten van buitenlandse collega's via congressen, meettijden op verplaatsing, etc. Dit was natuurlijk niet mogelijk zonder de financiele steun van het GOA (geconcerteerde onderzoeksactie programma)-project "archaeometrical research of the Ghent Altarpiece". Graag zou ik nog een speciaal dankwoordje willen toewijzen aan Peter. Bedankt, voor uw deur die steeds open stond voor het oplossen van problemen of een gezellige babbel. Ook de kleine duwtjes in de rug die u op de gepaste tijden gaf, waren meer dan welkom.

Een doctoraat voer je vanzelfsprekend niet helemaal in je eentje uit: het zou niet zo vlot en aangenaam verlopen zijn zonder de dagelijkse steun van mijn collega's van de Ramangroep: Alessia, Anastasia, Jolien, Possum, Mafalda en Sylvia. Zij steunden me door een aantal moeilijke perioden en waren altijd in voor een babbeltje, een aperitiefje of samen te lunchen. Een extra bedankje wil ik uiten aan Alessia. We zijn min of meer samen gestart aan ons doctoraat en dit heeft toch direct een band gecreëerd! We hebben samen toffe momenten op conferenties gehad (met aansluitende reisjes) en andere leuke momenten. Je was altijd zo lief om voor me in te vallen waar nodig en te dienen als luisterend oor wanneer ik het nodig had. Na ons doctoraatavontuur hoop ik nog steeds toffe dingen samen te doen, hier of in Italië!

Ook zou ik enkele andere onderzoeksgroepen willen bedanken. Eerst en vooral wil ik alle collega's van S12 (XMI, A&MS en ESA groep) bedanken voor alle toffe momenten op onze departementsactiviteiten en in het bijzonder Tine, Kris en Sylvia. Jullie zijn er

keer op keer in geslaagd om superactiviteiten te organiseren en deze in goede banen te leiden. Daarnaast wil ik ook nog Philip Brondeel en Davy de Pauw bedanken voor hun hulp bij de optimalisatie van de mobiele Ramanspectrometer. Zonder hun had ik de opstelling en het gebruik van de spectrometer niet kunnen verbeteren. Maar ook de medewerking van Nicolas le Thomas (UGent, Faculty of engineering and architecture, department of information technology (INTEC), photonics research group) wordt enorm geapprecieerd. Dankzij hem zijn we er in geslaagd om onze in situ Raman mapping opstelling te koppelen met de Hirox microscoop. Verdere samenwerking kan leiden tot enkele mooie toekomstplannen.

Bijkomstig, wil ik nog enkele collega's van het binnen- en buitenland bedanken. Dankzij volgende mensen had ik de kans om enkele unieke stukken te analyseren en zo tot interessante resultaten te komen. Bedankt Vincent Cattersel (UA, faculteit ontwerp-wetenschappen: Conservatie-restauratie) en Ludo Vandamme (Openbare bibliotheek Biekorf, Brugge) voor de waardevolle en plezante samenwerking. Dankzij jullie hadden we de gelegenheid om enkele bijzondere manuscripten (De Civitate Dei, De kronieken van Vlaanderen, Cisterciënzer manuscripten) te analyseren en zo onze mobiele Ramaninstrumentatie te verbeteren. Daarnaast wil ik Antonio Candeias (University of Evora, Hercules Laboratory) bedanken. Zonder hem hadden we nooit de opportuniteit gehad om bij te dragen tot de belangrijke restauratiecampagne van het 16de eeuwse altaarstuk, dat te bezichtigen is in de kathedraal van Funchal (Madeira). Als ook de mogelijkheid om een spectroscopische bijdrage te leveren omtrent de mooie collectie van glyptieken die tentoongesteld zijn in het museum 'Quinta das Cruzes' (Funchal, Madeira, Portugal). Deze goede collaboratie heeft ervoor gezorgd dat er enkele mooie resultaten konden uit voortvloeien. Natuurlijk wil ik ook Germana Barone en Danilo Bersani (University of Parma) bedanken voor de ondersteuning tijdens de analyses van muur-schilderingen van Sala vaccarani (Catania, Sicilië). Finaal wil ik nog mijn dank betuigen aan Prof. Dr. Howell Edwards. Dankzij zijn inspanning kan ik trots zijn op de kwaliteit van mijn geschreven tekst.

Tenslotte wil ik ook nog de conservators (KIK-IRPA), die instaan voor de restauratie van het Lam Gods, bedanken om ons bij te staan gedurende heel het project. Helene en Bart, bedankt om iedere meetdag ter onze beschikking te staan voor al onze

vragen en ondersteuning, alsook voor de interpretatie van onze data. Ook wil ik de rest van het restauratieteam bedanken voor hun vertrouwen en ondersteuning. Maar dit team is niets zonder de nauwe samenwerking met laboratoria. Dankzij de goede begeleiding en gastvrijheid van Jana Sanyova (KIK, departement labo) hebben we de kans gekregen om analyses te mogen uitvoeren op enkele cross-secties van het Lam Gods. Als ook op leerschool te gaan in het laboratoria van KIK-IRPA.

Ik heb niet alleen enorme steun gehad van mijn collega's. Mijn vier jaar durende doctoraat had ik nooit tot een goed einde kunnen brengen zonder de hulp van mijn vrienden en familie. Zij zorgden steeds voor de nodige afleiding naast de werkuren. Mijn ouders, zus, broers, schoonbroers en schoonzussen, schoonouders, neefjes dank ik voor alle leuke familie-uitstappen, etentjes, etc. Zo'n grote familie, vol met energie, kan niet anders dan plezier betekenen.

Vriendjes van de chemie, super dat we elkaar nog steeds door dik en dun steunen sinds ons eerste jaar unief. Ik zou niet weten wat ik zonder jullie zou doen. De ontspannende en lekkere etentjes, gezellige avondjes uit, lekker kletsen met de meiden, … (noem maar op); mogen we deze traditie nog lang volhouden!

Als laatste maar wel de allerbelangrijkste steun, al voor 6 jaar, is mijn allerliefste partner, Olivier. Je was er altijd om mij thuis op te vangen: goed of slecht gezind (en ik weet dat is niet altijd eenvoudig). Je hebt me altijd door dik en dun gesteund en toverde een lach op mijn gezicht wanneer ik het nodig had. Als ik het minder zag zitten, was jij er om mijn doorzettingsvermogen aan te wakkeren en te zorgen dat ik verder deed op een succesvolle manier! Zeker in de laatste maanden, met alle stress van onze verbouwingen, schrijven van de thesis en het voorbereiden/verwelkomen van onze prachtige dochter Lotte. Er zijn onvoldoende woorden om je te bedanken!!

Finaal wil ik nog even vermelden dat ik de afgelopen vier jaar een enorme levenservaring heb opgedaan en dat ik uitkijk naar de volgende mijlpalen in mijn leven, die me nog staan te wachten staan. OP NAAR HET VOLGENDE AVONTUUR!

Debbie

Publications and Contributions

LIST OF PUBLICATIONS

1. D. Lauwers, A.G. Hutado, V. Tenavska, L. Moens, D. Bersani and P. Vandenabeele (2014). Characterisation of a portable Raman spectrometer for *in situ* analysis of art objects. Spectrochimica Acta A,118:294-301.

2. D. Lauwers, V. Cattersel, L. Vandamme, A. Van Eester, K. De Langhe, L. Moens and P. Vandenabeele (2014). Pigment identification of an illuminated mediaeval manuscript *De Civitate Dei* by means of a portable Raman equipment. Journal of Raman Spectroscopy, 45:1266-1271.

3. D. Lauwers, A. Candeias, A. Coccato, J. Mirao, L. Moens and P. Vandenabeele (2016). Evaluation of portable Raman spectroscopy and hanheld X-ray fluorescence (hXRF) for the direct analysis of glyptics. Spectrochimica Acta Part A: Molecular and Biomolecular Spectroscopy, 157:146-152.

4. G. Barone, D. Bersani, A. Coccato, D. Lauwers, P. Mazzoleni, S. Raneri, P. Vandenabeele, D. Manzini, G. Agostino, N.F. Neri (2016). Non-destructive Raman investigation on wall paintings at Sala Vaccarini in Catania (Sicily). Applied Physics A (Submitted).

5. D. Lauwers, Ph. Brondeel, L. Moens and P. Vandenabeele (2016). *In situ* Raman mapping of art objects. Philosophical Transactions Royal Society A, accepted.

LIST OF CONFERENCE CONTRIBUTIONS

1. D. Lauwers, A.G. Hutado, V. Tenavska, L. Moens, D. Bersani and P. Vandenabeele. Characterisation of a new mobile Raman spectrometer for *in situ* analysis. 7th International Congress on the Application of Raman Spectroscopy in Art and Archeology (RAA), Slovenia, Ljubljana, 2-6 September 2013. (Oral presentation).

2. D. Lauwers, V. Cattersel, L. Vandamme, A. Van Eester, I. Craenhals, J. Van Groenland, L. Moens and P. Vandenabeele. Pigment identification of illuminated mediaeval manuscripts by means of a new, portable Raman equipment. 7th International Congress on the Application of Raman Spectroscopy in Art and Archeology (RAA), Slovenia, Ljubljana, 2-6 September 2013. (Poster presentation).

3. D. Lauwers, A. Coccato, A.E. Candeias, J. Mirão, L. Moens, P. Vandenabeele. Archaeometrical study of the main altarpiece of the cathedral of Funchal (Madeira). The Chemistry Conference for Young Scientists (Chem-Cys), Belgium, Blankenberge, 27-28 February 2014. (Poster presentation).

4. D. Lauwers, A. Coccato, J. Mirao, P. Vandenabeele, A.Candeias. Evaluation of portable Raman spectroscopy and handheld X-ray fluorescence spectroscopy for the analysis of glyptics. Technart, Sicily, Catania, 27-30 April 2015. (Poster presentation).

5. D. Lauwers, Ph. Brondeel, L. Moens and P. Vandenabeele. A novel concept towards in situ Raman mappings using a portable Raman spectrometer. 8th International Congress on the Application of Raman Spectroscopy in Art and Archeology (RAA), Poland, Wroclaw, 1-5 September 2015. (Poster presentation).

6. D. Lauwers, Ph. Brondeel, L. Moens and P. Vandenabeele. A novel concept towards in situ Raman mappings using a portable Raman spectrometer. 2nd International Conference on Innovation in Art Research and Technology (InArt), Belgium, Ghent, 21-25 March 2016. (Oral presentation).

7. G. Barone, D. Bersani, A. Coccato, D. Lauwers, P. Mazzoleni, S. Raneri, P. Vandenabeele, D. Manzini, G. Agostino, N.F. Neri. Non-destructive investigations on wall paintings at Sala Vaccarini in Catania (Sicily). 2nd International Conference on Innovation in Art Research and Technology (InArt), Belgium, Ghent, 21-25 March 2016. (Poster presentation).

8. V. Aldazabal, D. Lauwers, P. Vandenabeele, L. Moens, C. Vazquez. The use of colour on pottery decoration from late Holocene South American hunter gatherers. 2nd International Conference on Innovation in Art Research and Technology (InArt), Belgium, Ghent, 21-25 March 2016. (Poster presentation).

9. S. Gomes, M. Lorena, P. Vandenabeele, D. Lauwers, A. Coccato, S. Valadas and A. Candeias. Green colour in the 16th century Portuguese paintings of the Funchal's Cathedral altarpiece. 2nd International Conference on Innovation in Art Research and Technology (InArt), Belgium, Ghent, 21-25 March 2016. (Poster presentation).

10. F. Rosier, H. Dubois, G. Van der Snickt, J. Sanyova, A. Coudray, C. Glaude, K. Janssens, D. Lauwers, A. Coccato, M. Martens, L. Moens, P. Vandenabeele. Identification of restorations on the Cumean Sibyl of the Van Eyck brothers' Ghent Altarpiece (1432). 4th International Congress Chemistry for Cultural Heritage (CHEMCH), Belgium, Brussels, 6-8 July 2016. (Poster presentation).